# A Comprehensive Experimental Study of the Effects of Adjacent Buildings on Near-Field Pollutant Dispersion

Bodhisatta Hajra

A Thesis

in

The Department

of

Building, Civil and Environmental Engineering

Presented in Partial Fulfilment of the Requirements

For the Degree of Doctor of Philosophy in Building Engineering at

Concordia University, Montreal, Canada

May 2012

**CONCORDIA UNIVERSITY**

**SCHOOL OF GRADUATE STUDIES**

This is to certify that the thesis prepared

By: **Bodhisatta Hajra**

Entitled: **A Comprehensive Experimental Study of the Effects of Adjacent Buildings on Near-Field Pollutant Dispersion**

and submitted in partial fulfillment of the requirements for the degree of

DOCTOR OF PHILOSOPHY (Building Engineering)

complies with the regulations of the University and meets the accepted standards with respect to originality and quality.

Signed by the final examining committee:

_____ Chair
Dr. L. Kadem

_____ External Examiner
Dr. H. Tanaka

_____ External to Program
Dr. A. Dolatabadi

_____ Examiner
Dr. L. Wang

_____ Examiner
Dr. R. Zmeureanu

_____ Thesis Supervisor
Dr. T. Stathopoulos

Approved by _____
Dr. M. Elektorowicz, Graduate Program Director

June 14, 2012

_____
Dr. Robin A.L. Drew, Dean
Faculty of Engineering & Computer Science

## ABSTRACT

**A Comprehensive Experimental Study of the Effects of Adjacent Buildings on Near-Field Pollutant Dispersion**

**Bodhisatta Hajra, Ph.D.**

**Concordia University, 2012**

Pollutants released from rooftop emissions can re-enter the building from which they are released or affect a neighbouring building with intakes or other openings, causing potential health hazards to the building occupants. Most dispersion models do not take into account the turbulence caused by adjacent buildings, which greatly affect the plume structure. Majority of micro-scale pollutant dispersion studies have been limited to isolated buildings which seldom exist in the urban environment. Therefore, it is necessary to accurately estimate effluent concentrations in the presence of adjacent buildings, particularly at distances within the recirculation zone of the source.

This study constitutes of a comprehensive series of tracer gas experiments performed in the Boundary Layer Wind Tunnel of Concordia University. In this connection, building models of various geometries were placed upstream, downstream and on either side of an emitting building. Tracer gas was released from the rooftop of an emitting building and concentrations were measured on various building surfaces. Flow visualisation studies were also performed at the outset to understand the air and pollutant flow within the building recirculation zone. Detailed measurements were then carried out

on various building surfaces for different stack heights, stack location, spacing between buildings, building geometries and exhaust momentum ratios. Results from current dispersion models such as ASHRAE 2007 and ASHRAE 2011 were also compared to wind tunnel findings of the present study.

Results show that a low building lying within the recirculation length of a taller upstream building produced higher rooftop concentrations on the emitting building. A taller building placed on either side of the source increases rooftop concentrations on the emitting building due to plume meandering. In general, spacing between buildings, height and across wind dimension of the adjacent building were found to be critical parameters affecting the plume geometry. Based on this study, guidelines for safe location of intake and stack on various building surfaces were suggested. Also, a relationship was established between dilution estimates for adjacent building configurations and the isolated case for various building surfaces. ASHRAE estimates were found to be overly conservative for all cases examined. A rectified ASHRAE approach which can be used to assess plume dilution on emitting and adjacent buildings was proposed. The rectified ASHRAE model was found to perform well for most cases when compared to results obtained from present and previous studies.

**Acknowledgements**

I would like to thank my supervisor Dr. T. Stathopoulos for his guidance and efforts throughout the study. He has always been a source of inspiration for me. I have learnt a lot from his expertise in wind engineering during my stay at Concordia, for which I am highly grateful to him.

The financial contributions of the Institut de recherche Robert-Sauvé en santé et en sécurité du travail (IRSST), Montreal is gratefully acknowledged. Many thanks to Dr. P.J. Saathoff, Dr. A. Gupta, Dr. I. Zisis, Mr. J. Hrib, Mr. J. Payer and Mr. L. Demers for their help and advice in performing wind tunnel experiments.

I also wish to thank my parents and my elder brother for their support and encouragement for all these years.

# Table of Contents

## List of Figures

## List of Tables

## Nomenclature

| Symbol | Definition | Units |
|---|---|---|
| $A_e$ | Stack area | $m^2$ |
| $A_m$ | Area of the model | $m^2$ |
| $A_o$ | Cross sectional area of the wind tunnel | $m^2$ |
| $B_l$ | Distance dilution parameter | - |
| $B_s$ | Smallest dimension of building face normal to wind | m |
| $B_L$ | Largest dimension of building face normal to wind | m |
| $C_e$ | Exhaust concentration | ppm |
| $C_r$ | Receptor concentration | ppm |
| $D_o$ | Initial dilution | - |
| $D_d$ | Dilution on roof of the downstream building | - |
| $D_{de}$ | Dilution on downwind edge of low building | - |
| $D_{min}$ | Minimum dilution | - |
| $D_{lu}$ | Dilution on leeward wall of the upstream building | - |
| $D_{le}$ | Dilution on the leeward wall of the low building | - |
| $D_r$ | Dilution at roof level | - |
| $(D_r)_s$ | Dilution estimated for a shorter averaging time | - |
| $D_s$ | Dilution downwind of stack | - |
| $D_{normalised}$ | Normalised dilution | - |
| $D_i$ | Dilution on roof of isolated building | - |
| $D_a$ | Dilution on roof of low building for adjacent building configurations | - |
| $D_{wd}$ | Dilution on windward wall of downstream building | - |
| $d_e$ | Stack diameter | m |

| | | |
|---|---|---|
| f1 | Factor which relates roof dilution of isolated and adjacent building configurations | - |
| f2 | Factor which relates dilutions on roof of the downstream and downwind edge of the low building | - |
| f3 | Factor which relates the dilution downwind of stack and the dilution on the leeward wall of upstream building | - |
| f4 | The ratio of the dilution on downwind edge of low building to the dilution on leeward wall of low building | - |
| f5 | Factor which relates dilutions on windward wall of downstream building and downwind edge of low building | - |
| h | Height of the low building | m |
| $h_1$ | Height of the upstream building | m |
| $h_2$ | Height of the downstream building | m |
| $h_d$ | Reduction in plume height | m |
| $h_{plume}$ | Height of plume | m |
| $h_r$ | Plume rise (ASHRAE 2003, 2007) | m |
| $h_x$, $h_f$ | Plume rise (ASHRAE 2011) | m |
| $h_s$ | Stack height | m |
| $h_{small}$ | Smallest plume height | m |
| $h_{top}$ | Height of critical recirculation zone | m |
| $H_c$ | Maximum height of the roof recirculation zone | m |
| $I_u(z)$ | Turbulence intensity at a given height z | - |
| $i_x$, $i_y$, $i_z$ | Turbulence intensities in x, y, z directions | - |
| k | Von Karman constant = 0.4 | - |
| L | Along wind dimension of the low building | m |
| $L_1$ | Along wind dimension of the upstream building | m |
| $L_2$ | Along wind dimension of the downstream building | m |

| | | |
|---|---|---|
| $L_c$ | Length of the roof recirculation zone | m |
| $L_r$ | Length of the building wake recirculation | m |
| $m_i$ | Measured dilution at a given receptor | - |
| M | Exhaust momentum ratio ($V_e$/ $U_H$) | - |
| n | Total number of sampling points (receptors) | - |
| $p_i$ | Predicted dilution at a given receptor | - |
| $Q_e$ | Volumetric flow rate | $m^3/s$ |
| S | Stretched string distance | m |
| $S_1$ | Distance between low building and upstream building | m |
| $S_2$ | Distance between low building and downstream building | m |
| $Sc_t$ | Turbulent Schmidt number | - |
| $t_s$ | Averaging time | minutes |
| $u_*$ | Friction velocity | m/s |
| $U_H$ | Wind velocity at building height | m |
| $V_e$ | Exhaust velocity | m/s |
| V (z) | Velocity of wind at height z | m/s |
| $V_g$ | Gradient velocity | m/s |
| w | Across wind dimension of the low building | m |
| $w_1$ | Across wind dimension of the upstream building | m |
| $w_2$ | Across wind dimension of the downstream building | m |
| x | Receptor distance from upwind edge | m |
| x’ | Receptor distance from edge of downstream building | m |
| $X_s$ | Stack location from upwind edge | m |
| $X_c$ | Distance from the leading edge to $H_c$ | m |
| z | Height above the ground | m |
| $Z_o$ | Roughness length | m |

| | | |
|---|---|---|
| $Z_2$ | High turbulence region | - |
| $Z_3$ | Roof wake boundary | - |
| $Z_g$ | Gradient height | m |

## Greek symbols

| | | |
|---|---|---|
| $\sigma_o$ | Initial source size of the plume | m |
| $\sigma_y$ | Spread parameter (horizontal direction) | m |
| $\sigma_z$ | Spread parameter (vertical direction) | m |
| $\alpha$ | Power law exponent | - |
| $\beta$ | Stack capping factor | - |
| $\beta_j$ | Jet entrainment coefficient | - |
| $\zeta$ | Vertical separation ($h_{plume}$ - $H_c$) | m |
| $\rho_e$ | Density of exhaust | $kg/m^3$ |
| $\rho_a$ | Density of air | $kg/m^3$ |
| $\theta$ | wind azimuth | degrees |

## Acronyms

| | |
|---|---|
| ASHRAE | American Society of Heating Refrigeration and Air conditioning Engineers |
| ADMS | Atmospheric Dispersion Modelling System |
| CFD | Computational Fluid Dynamics |
| EPA | Environmental Protection Agency |
| ESDU | Engineering Science Data Unit |
| GC | Gas Chromatograph |
| ISC | Industrial Source Complex |
| LES | Large Eddy Simulation |
| PRIME | Plume Rise Model Enhancements |
| rmse | root mean square error |
| RTS | Roof Top Structure |

# Chapter 1

# Introduction

## 1.1 General

Air pollution is a major cause for concern especially for the occupants of a laboratory building who are exposed to particulate matter and smoke for long durations which can cause potential health hazards. In the past mortality rates have been linked to short term exposure to air pollution (Schwartz., 1994; Dockery et al., 1993). Estimating pollutant concentrations at distances within the recirculation zone from a source is important for human health and may be critical in urban areas where stacks located on rooftop of buildings emit pollutants (Pasquill, 1961). Effluents released from rooftop stacks within the recirculation zone may not only re-enter the building from which they are released but may also affect an adjacent building in the near-vicinity (Stathopoulos et al., 2008).

Pollutant dispersion problems have gained a lot of significance due to the number of deaths attributed to air quality issues. Most studies related to near-field pollutant dispersion have focussed on isolated buildings (Wilson, 1979; Schulman and Scire, 1991; Cheung and Melbourne, 1995; Khan et al., 2005 etc.) with very few studies on adjacent building effects, which is a more realistic case. Although some studies pertaining to pollutant dispersion within building obstacles were performed by Bentham et al., 2003 and Olvera et al., 2007, no significant research on the effect of buildings within the recirculation zone of the source of pollutants, has been carried out.

A precise definition of near-field or micro-scale dispersion is difficult to generalise as this term has been defined by various researchers in different ways. For instance, studies

carried out by Upadhay et al., 2004 within urban canopy through large group of obstacles and similarly, wind tunnel experiments by Li and Meroney, 1983 have defined the "near-wake" region as $x/H < 5$, where x is the distance of the receptor from the source and H is the height of the building. Wilson et al., 1998 performed water channel studies to assess plume behaviour in the presence of adjacent buildings and defined near-field as a distance within the recirculation region from the source, the calculations of which were based on the windward dimensions of the building.

Some of the most important studies on pollutant dispersion from rooftop stacks of isolated buildings include the models developed by Halitsky, 1963, Wilson and Chui (1985, 1987) and Wilson and Lamb, 1994. The latter two models have also been included in the ASHRAE Fundamentals Handbook, 1997. These models were further modified and included in the various versions of ASHRAE, published in 2003 and subsequently revised in 2007 and 2011 respectively. The flow-structure of the plume is greatly influenced by the building in the near vicinity and local topography as opposed to far-field problems where atmospheric turbulence is greater (Hajra et al., 2010).

Very few studies on the effects of adjacent buildings on near-field pollutant dispersion have been studied. For instance, Stathopoulos et al., 2004 performed field studies at Concordia University, Montreal, and found that an upstream building's presence produced higher effluent concentrations at the rooftop of a low downstream building with stack. Some researchers have also studied the effects of effluent dispersion downwind of a building (Koga et al, 1979, Guenther et al., 1989 and Schulman et al, 1993).

Various dispersion models such as ADMS, SCREEN, CALPUFF etc. and semi-empirical models such as ASHRAE are available, which can be used for assessing effluent concentrations. However, most dispersion models which predict concentrations on ground level and rooftop receptors are unsuitable for near-field dispersion problems. Additionally they assume a uniform concentration profile within the recirculation region formed in the building wake (Riddle et al., 2004). ASHRAE also does not incorporate adjacent building effects in assessing pollutant concentrations and can only be used to estimate rooftop dilution.

Several incidents related to re-ingestion of polluted air have been reported in the past. Unfortunately, the state of the art is not sufficiently advanced to apply appropriate design criteria to help alleviate this issue for existing buildings. Based on a study done by the National Institute of Occupational Health and Safety (NIOHS), it was found that openings within 8 meters of an intake can increase the risk respiratory problems by 140% (http://www.cdc.gov/niosh). Reports of loss in productivity in USA due to the poor indoor environment are estimated to billions of dollars per year (Fisk et al., 2002). The World Health Organization estimates that about 2.4 million people die annually due to asthma and heart diseases which are caused by air pollution (http://www.who.int). This explains the need to have a better understanding of the pollutant dispersion process in the vicinity of the source through detailed experimental studies as discussed further.

### 1.2 Definition of dispersion

When a plume is transported from the source, turbulent eddies generated within the plume with the aid of wind help disperse the effluent. A concentration gradient exists in

the plume due to which effluent concentrations in the centre of the plume are higher than the plume edges. Global and regional air patterns, local topography and terrain conditions largely affect the dispersion of pollutants in the urban environment. In urban areas, wind speed increases with height at a slower rate than in areas where the terrain is less rough. In general, for stable or neutral atmospheric conditions the pollutants released from a stack follow a shape which closely resembles the Normal or Gaussian probability distribution. One of the most widely used models for numerically describing the movement and dispersion of effluent from a point source is the Gaussian plume model. Figure 1.1 shows the coordinate system used to describe a Gaussian plume model.

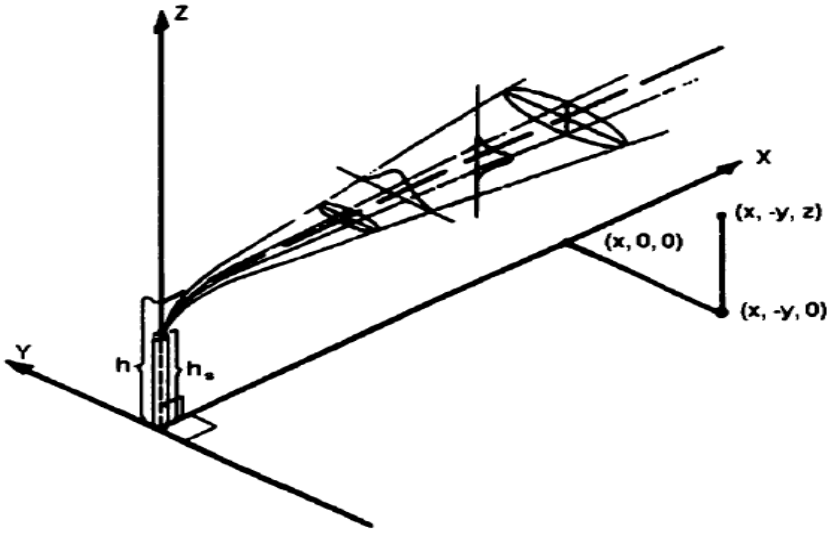


Figure 1.1 Coordinate system showing Gaussian distributions in horizontal and vertical directions (Turner, 1994)

The figure depicts Gaussian (normal) distributions in the vertical and crosswind directions. At the point of release, the concentration of effluents is high near the centreline and reduces rapidly towards the edges. But further downstream, the

distribution of concentration spreads from the centreline. The shapes of the concentration distributions are described in the Gaussian plume model by the standard deviations of the plume in the crosswind (horizontal) ($\sigma_y$) and vertical ($\sigma_z$) directions. Additional information can be found in Turner, 1994.

### 1.3 Objectives

The present study aims at determining the effects of adjacent buildings on near-field pollutant dispersion by performing tracer gas studies at the Boundary Layer Wind Tunnel at Concordia University. Currently, there are very few models such as ASHRAE which can be used to predict near-field plume concentrations for isolated buildings. In the urban environment buildings are mostly found in close proximity to each other. Therefore, the study of adjacent building effects is a more realistic case. This study involved the following tasks:

1.3.1 Four different cases were studied:

a) isolated building (source)

b) building placed upstream of the source

c) building placed downstream of the source

d) a building placed upstream and downstream of the source.

Various parameters which include building dimensions, height and location of stack, exhaust parameters, wind velocity and azimuth; and spacing between the buildings were varied.

1.3.2 Based on the wind tunnel data, the problem of pollutant re-entering the building and affecting an adjacent building was assessed since the behaviour of the plume

from a rooftop stack of an isolated building is markedly different from plumes released in the presence of adjacent buildings.

1.3.3 Design guidelines regarding the placement of stack and intake in the presence of adjacent buildings are suggested since most design guidelines apply only to the isolated case.

1.3.4 An empirical approach to modify ASHRAE estimates for the isolated case as well as to incorporate the effects of adjacent buildings to assess plume dilution on various building surfaces was carried out. The rectified ASHRAE estimates were also validated with experimental results from previous studies.

**1.4 Outline of the thesis**

The thesis has been divided into eight chapters. Following the introduction, Chapter 2 deals with literature review and discusses past numerical and experimental research carried out in the field of pollutant dispersion pertaining to isolated buildings and a few studies involving the effect of adjacent buildings. Chapter 3 discusses the experimental methodology and simulation conditions used in this study. Chapter 4 gives a detailed account of ASHRAE formulations followed by results discussed in Chapter 5. The results of the wind tunnel study have been used to rectify ASHRAE estimates, as discussed in Chapter 6. Design guidelines for safe placement of stack and intakes on building surfaces followed by Conclusions and recommendations for future research have been presented in Chapters 7 and 8 respectively. This is followed by a list of references, which have been used during the study.

# Chapter 2

# Literature review

## 2.1 Introduction

It is very important to study the effects of adjacent buildings on near-field pollutant dispersion. In the past extensive research has been carried out which involve numerical (CFD and Gaussian based models) and experimental studies through wind tunnel, water channel and field studies. Most of the work was initially devoted to the study of isolated buildings; whilst more recently plenty of research on the effects of adjacent building effects has also been carried out. Although, there are plenty of studies involving plume dispersion through an array of obstacles, these do not include studies within the recirculation zone of buildings. This chapter initially focuses on the flow patterns around isolated buildings followed by studies pertaining to the modelling of plume dilution in the presence of adjacent buildings in the built environment.

## 2.2 Flow patterns around an isolated prismatic building

The flow pattern around an isolated building is shown in Figure 2.1. As wind impinges on the wall of the building, airflow separates at the edges causing a zone of recirculation in the wake of the building ($L_r$). Approximately, at the upper one quarter of the building the flow is directed above the roof causing “upwash”. Due to increased wind speeds at the roof compared to the ground, downwash is caused between the lower one half and two thirds of the building. A stagnation zone can exist between the upwash and downwash regions. The size of the recirculation zone depends on the windward wall

dimensions of the building. As seen from Figure 2.1, pollutants released from a flush vent at low exhaust speeds can re-enter the building if the plume gets engulfed within $L_r$.

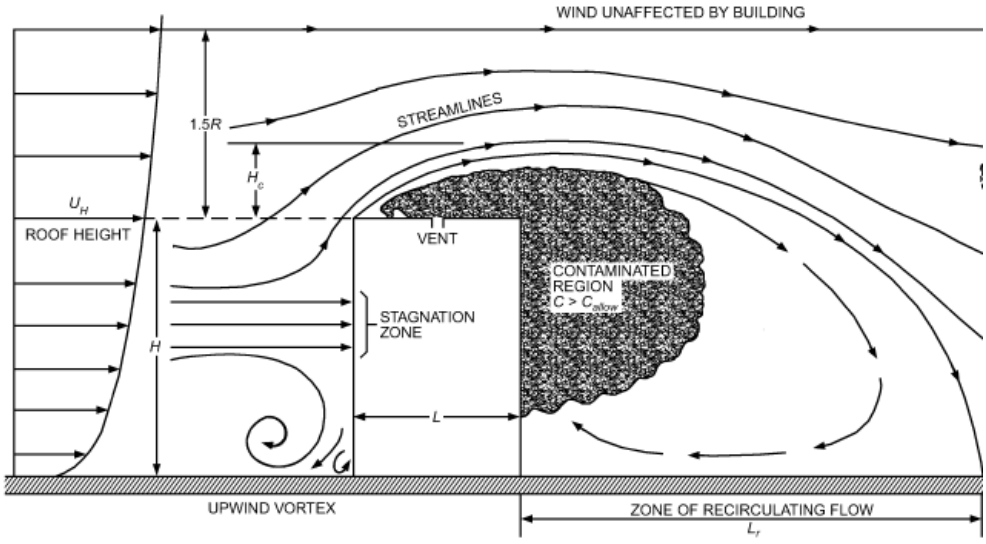


Figure 2.1 Flow patterns around an isolated building (ASHRAE 2005, Chapter 16)

The air and pollutant flow within the recirculation zone of a building is very complex as the turbulence is generated by the building and surrounding topography. Experimental assessment of plume dispersion from isolated rooftop emissions are discussed further.

## 2.3 Experimental studies on plumes released from isolated building

This section focuses on pollutant dispersion studies for plumes released from isolated buildings through wind tunnel, flow visualisation, field and water channel studies. Flow visualisation studies are mostly helpful in determining the flow structure of the plume, but are generally not used to assess plume concentrations (Hoydysh and Dabberdt, 1988).

The near-field pollutant dispersion models developed by Wilson and Chui (1985, 1987), Wilson and Lamb, 1994 and Halitsky, 1963 were used extensively in the development of ASHRAE 1997.

One of the most important wind tunnel studies on plume dispersion from rooftop stack of isolated buildings was carried out by Halitsky in 1962 at New York University. Through extensive studies he was able to show that a recirculation length exists in the wake of the building which is very critical for near-field pollutant dispersion studies. Figure 2.2 shows flow patterns of wind and airborne pollutants around the isolated building. He also found that the size of the primary wake was dependent on the surface of separation formed at the upwind edge of the building. Through his studies he was able to show that a "return flow" in the building wake could bring back the pollutants towards the leeward wall of the building.

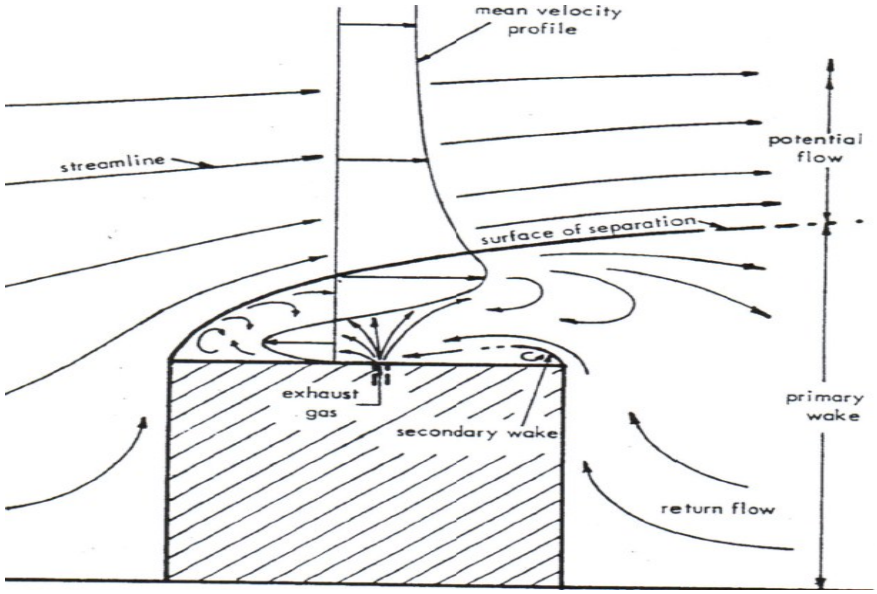


Figure 2.2 Typical flow patterns around a cube with one face normal to wind (from Halitsky, 1962)

Later, based on this experimental data Halitsky, 1963 developed an empirical model to estimate minimum dilution:

$$D_{\min} = [\psi + 0.11(1 + 0.2\psi)S / A_e^{0.5}]^2 \qquad (2.1)$$

Where "S" is the distance from the source, "$A_e$" is the exhaust area and "ψ" is the parameter that depends on building shape, momentum ratio and building orientation. This was one of the most important studies in near-field plume dispersion since prior to this not many studies had focussed on air flow and effluent transport close to the building. However, Wilson, 1979 showed that the results obtained from the Halitsky model were conservative. Although, Equation 2.1 was used in ASHRAE 1999, studies by Stathopoulos et al., 1999 have also shown that results generated by equation 2.1 were too conservative. This was possibly because Halitsky's study was based on wind tunnel data for a suburban area and could not be generalised for any terrain.

In order to study downwash effects downwind of a nuclear reactor, Martin, 1965 performed wind tunnel studies at the University of Michigan and compared them to field data. He found that field and wind tunnel data compared well whilst the plume was affected by building downwash. It is worth noting that Martin performed his simulations in a boundary layer wind tunnel and compared them with field data as opposed to earlier works of Halitsky that were in a uniform flow tunnel.

Most investigations in the early sixties were restricted to stable or neutral stability conditions; also changes in wind direction were not studied. Meroney and Yang, 1970 performed wind tunnel studies on plumes released from flush vent of isolated buildings. The studies were performed for different stability conditions in a thermally stratified wind tunnel located at Colorado State University, for different wind angles. They found that for a given building orientation pollutant dispersion was less affected irrespective of stack location. However, as the building orientation changed a slightly different concentration distribution was found especially in the cavity and near wake region

because of the amount of effluent that was carried in the wake due to convective motions. They also reported that at a distance of x/H (where 'x' is the distance from source to receptor and 'H' is the height of the building) greater than 5 (defined as "far-wake" by the authors) the plume escapes the recirculation cavity formed in the building wake. An increase in concentration of effluents by about 8 % in inversion stratification than neutral stratification was observed by the authors. This study was a good attempt to study the dispersion characteristics around isolated cube particularly for different stability conditions. Additionally, the definition of near-wake and far-wake was also introduced for the first time, which clearly tried to distinguish between the existence and non existence of building generated turbulence.

Castro and Robins, 1977 also investigated building downwash effects from an isolated cubical building in a wind tunnel. Although, most previous studies were involved in assessing plume characteristics from rooftop of isolated building, downwash phenomenon which is mainly caused at low exhaust speeds were not well understood. Their experiments were conducted for various stack heights and wind directions. They showed that there was greater downwash for a wind direction of 45°, resulting in increased pollutant concentrations compared to normal wind. Although, the study did not try to describe the dilution process using empirical or modified Gaussian approaches, the effects of $45^{o}$ wind causing high rooftop concentrations was observed for low stacks.

Dispersion of plumes from isolated rooftop vents was further studied by Wilson, 1977 in a wind tunnel for various vent locations on the roof of two isolated rectangular-shaped models. The experiments were carried out in an urban terrain. Based on his experiments he proposed an empirical relationship:

$$D = 0.11\phi^2 \tag{2.2}$$

where

$\phi^2 = (U_H x^2)/Q_e$

$D$ is the dilution which is the ratio of the exhaust to receptor concentrations,

$U_H$ is the wind speed at building height (m),

$x$ is the distance from source to receptor (m),

$Q_e$ is the volumetric flow rate ($m^3/s$)

According to Wilson, 1977 equation 2.2 gave much better estimates of dilution compared to equation 2.1 suggested by Halitsky, 1963. From the study it was concluded that if the vent was located closer to the upwind face of the building then due to atmospheric turbulence the pollutants had a tendency to undergo downwash which lead to higher concentrations in the wake. Gradually when the location of the vent was shifted towards the centre of the roof the dispersion of the plume increased, although this could not be generalised since this could change with building dimension and terrain characteristics. One of the major differences between Wilson and Halitsky's study was that the former was performed in turbulent boundary layer as opposed to the latter's study in a uniform, non-turbulent approach flow.

One of the most important studies in near-field pollutant dispersion from rooftop stacks of isolated building was carried out by Wilson, 1979. He performed a series of experiments on several cubical building models for different stack locations and exhaust speeds in a water channel. Based on his study he defined three zones which form on rooftop of the building as shown in Figure 2.3.

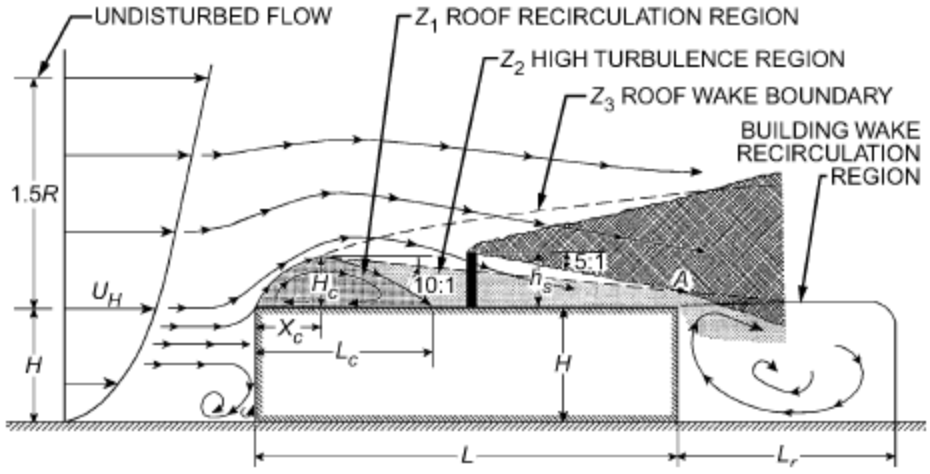


Figure 2.3. Design procedure for required stack height to avoid contamination (from Wilson, 1979)

A roof recirculation region ($Z_1$) forms at the upwind edge of the building, where the flow separates and some portion of the gas may get trapped in this region (especially at very low exhaust speeds). Gradually away from this zone lies a high turbulence zone ($Z_2$) where the turbulence due to the stack exists; concentrations of gas are generally found to be higher in this region. The roof wake boundary ($Z_3$) was defined as a region where pollutants released at low speeds may undergo downwash and get trapped in the building wake. He also found that a recirculation region forms on the roof (depicted as '$L_c$' in Figure 2.3) which is formed due to large along-wind dimension of the building and is responsible for keeping the plume closer to the roof. He further suggested that a plume released from rooftop stack is of triangular shape with the sides at 5:1 away from the centreline. In order to avoid pollutant re-entrainment (building wake recirculation region) the plume rise and stack height must be sufficiently high. Validation studies of the proposed model of Wilson, 1979 were carried out by Wilson and Winkel, 1982; Wilson

and Britter, 1982 and Wilson, 1983 for various isolated buildings. Later the findings of this study were used in ASHRAE 1999 and in subsequent versions published in 2003, 2007 and 2011. Wilson, 1979 also extended his study to wind angles at 45 degrees, as shown in Figure 2.4.

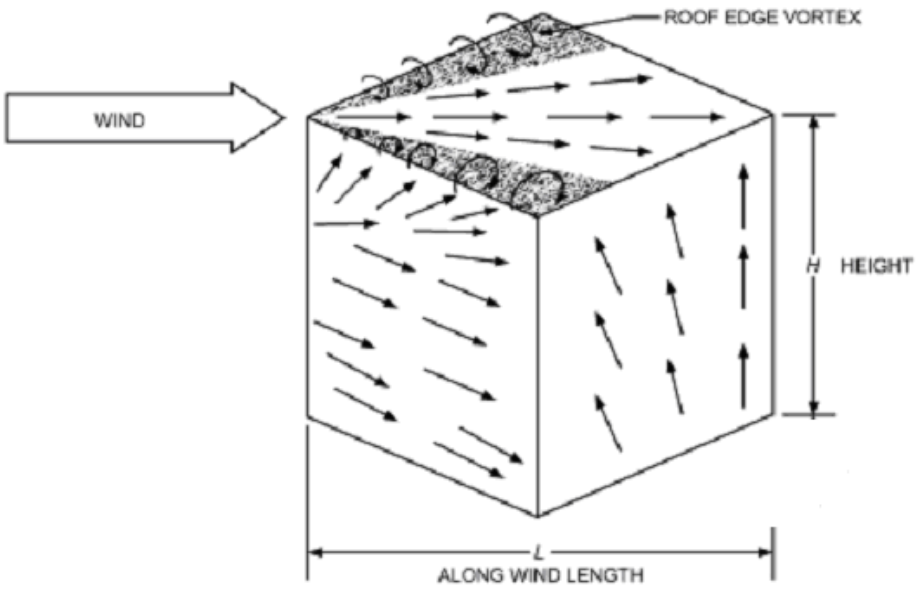


Figure 2.4 Surface flow patterns for wind angle at 45$^{o}$ (from Wilson, 1979)

Wilson showed that although the flow-structure is different at 45$^{o}$, the recirculation length formed on the roof tries to bring the plume closer to the roof surface, though this phenomenon is gradually reduced with higher exhaust momentum ratios (M) which is the ratio of exhaust speed ($V_e$) to wind speed at the building height ($U_H$). The roof edge vortices formed at the sides of the building encourage pollutants to remain closer to the surface of the roof.

Similar studies were performed later by Li and Meroney, 1983 in a wind-tunnel study of concentration fluctuations in the near-wake region ($1.0 < x/H < 5.0$) of a cubical model building in a simulated, neutrally stratified shear layer. Contaminants were released at a

central roof vent for buildings with $0^o$ and $45^o$ orientations, and at a downwind roof vent for a building with $0^o$ orientation. At 45 degrees, maximum ground concentrations were found at x/H = 2.5; the high concentrations were attributed to downwash effects.

While most studies were focussed on wind tunnel measurements, very few studies were focussed on field measurements primarily because of increased cost and time involved in the latter. Ogawa et al., 1983 performed field and wind tunnel studies on the flow and diffusion around an isolated cube. Their study included five different wind angles ranging from 0 to 45 degrees and four different terrain conditions. One of the major contributions of this study was to make field measurements for tracers released from an isolated building located in an open field since most other studies were focussed on wind tunnel or water channel measurements. Tracer gas was released from the centre of the cube at low exhaust speeds and receptors were located on the rooftop. They found at small wind angles (less than 20 degrees) a "reverse flow" phenomenon occurring on the rooftop of the cube which decreased with an increase in upwind turbulence. They also reported that at wind angles less than 20 degrees the size of the recirculation zone on the roof was more influenced by upwind turbulence than at larger angles. Field and wind tunnel data compared well for most cases; however, wind tunnel data did not show signs of "reverse flow" as reported in field measurements. The authors felt that this could be because the turbulence in the field was not modelled accurately in the wind tunnel and due to the sensitivity of instruments used in the experimentation. Although, the authors did not propose a model based on their study, the diffusion and flow characteristics around a cube were well described.

Fackrell, 1984 carried out a wind tunnel study to determine the near-wake dispersion characteristics for different building shapes in varying terrain conditions. In particular, the recirculation length and the time for the concentration of the pollutant within the building wake (residence time) were measured. This study showed that these parameters could be used to estimate the average near-wake concentration. Through a limited number of studies Fackrell found that by changing the spacing between two buildings, the residence time of the pollutant was greatly affected.

Hunt and Castro, 1984 used light scattering technique to measure the residence time of tracer gas within the wake of different building models in a boundary layer wind tunnel. They concluded that turbulent diffusion is the dominant mechanism of tracer dispersion, even for vortex-dominated wakes. They also reported that available empirical models which correlate residence time and model geometry were valid only for wind angle perpendicular to the building face.

Most studies were actually used to assess the plume behaviour on the surface of the isolated building. The models initially defined by Halitsky, 1963 were only applicable for rooftop vents. However, by performing extensive wind tunnel experimentation on isolated buildings, Wilson and Chui (1985, 1987) suggested the following expression for the minimum dilution along the plume centre line:

$$D_{\min} = (D_o^{0.5} + D_d^{0.5})^2 \qquad (2.3)$$

Where "$D_o$" is the initial dilution at the exhaust location and "$D_d$" is the distance dilution which is produced by atmospheric and building generated turbulence. The ASHRAE 1993 formulations have also been derived from the above expressions.

In a separate study Halitsky, 1990 proposed a "jet-plume" model and compared it to equation 2.1 which was proposed by him previously in 1963. He felt that Gaussian dispersion models described in Turner, 1970, had certain deficiencies namely:

a) The equations did not consider an initial plume rise,

b) The growth of the plume less than 100 m was not described using the dispersion parameters ($\sigma_y$ and $\sigma_z$) and it did not take account of building generated turbulence. Therefore, to investigate the matter, Halitsky used the wind tunnel data of Petersen and Wilson, 1989 and proposed the following equation:

$$D = (2\sigma_y\sigma_z)/(f^2 M)[e^{\frac{-(z-h_s)^2}{2\sigma_z^2}} + e^{\frac{-(z+h_s)^2}{2\sigma_z^2}}] \qquad (2.4)$$

where

$z$ is the location of the receptor from rooftop (m),

$\sigma_y$ and $\sigma_z$ are plume dimensions in vertical and lateral directions (perpendicular to plume centreline) estimated for different stability classes (m),

$f$ is the radius of the stack (m),

$h_s$ is the stack height (m)

He also suggested a separate set of curves to estimate the values of $\sigma_y$ and $\sigma_z$ depending on the stability of the atmosphere and found good agreement between the model and wind tunnel data from Petersen and Wilson, 1989.

Schulman and Scire, 1991 performed wind tunnel tests on a rectangular building with varying stack height and exhaust momentum ratio's (M) for wind angle of 0 and 45 degrees. They performed experiments in a boundary layer wind tunnel with a suburban terrain using a building model that was 30 inches square in plan and 6 inches tall at a scale of 1:100. They found that in general an increase in stack height resulted in reduced

concentrations in the wake, though this was more pronounced with lower M. Their results showed that for an increase in M from 0.75 to 5 the concentrations reduced rapidly on the roof, while in the wall and near-wake region this was less pronounced. In the far wake region as the effect of building generated turbulence reduces an increase in M from 0.75 to about 3 does not have a significant effect. Unlike most researchers like Wilson and Halitsky who mostly used formulations described in Wilson, 1979 to assess length of recirculation zone ($L_r$), Schulman and Scire used the following equation by Fackrell, 1984:

$$L_r = 1.8W/[(L/H)^{0.3}(1.0+0.24W/H)] \qquad (2.5)$$

where

L is the along wind dimension of the building (m),

W is the across wind dimension of the building (m),

H is the height of the building (m).

In general, they found a consistent increase in concentrations at the transition from near-wake to far-wake. This study also revealed higher plume concentrations on the roof due to counter rotating vortices for low stack height and lower exhaust speeds similar to the observations made by Li and Meroney, 1983. Unlike previous studies where the concentrations were only restricted to rooftop and ground level receptors, this study also focussed on leeward wall and showed that recirculation lengths estimated by Wilson, 1979 were markedly different which proved the need for further investigation of these formulations.

Most studies were performed for a particular isolated building block in the wind tunnel. However, Wilson and Chui, 1994 investigated the effects of different building

size on rooftop dispersion of exhaust gases. They tested 11 models at six different values of 'M' in the wind tunnel using pure helium tracer gas released from flush vent. According to the authors, earlier models considered the plume spread (σ) independent of building size (frontal area- 'A') and linearly dependent on source to receptor distance (r). From their studies they concluded that by considering 'σ' to be proportional to $A^{0.125}r^{0.75}$ a better representation of rooftop dilutions were possible.

In the following year, Wilson and Lamb, 1994 developed a model based on field studies carried out by Lamb and Cronn, 1986 at the Washington State University (WSU), USA. This was one of the most important field studies carried out in this area in which the buildings had problems of re-ingestion of pollutants due to the surrounding environment causing health problems to the inmates (for details see- Lamb and Cronn, 1986). Wilson and Chui simulated the field study in a wind tunnel. Based on their study they suggested that upstream turbulence to assess plume dilution need to be taken into account through an additional term called "distance dilution parameter" ($B_1$):

$$B_1 = 0.027 + 0.021\sigma_\theta \qquad (2.6)$$

where

$\sigma_\theta$ is the standard deviation of wind direction fluctuation in degrees, varying from $0^o$ to $30^o$

$D_d$ is then calculated as:

$$D_d = (B_1 x^2)/(MA_e) \qquad (2.7)$$

where

$A_e$ is the area of the stack ($m^2$).

The calculations for dilution remain unchanged and are estimated using equation 2.3. The model proposed by Wilson and Lamb, 1994 was considered to be a better approach than the model proposed by Halitsky, 1963 and Wilson and Chui, 1985, 1987. Equations 2.3 along with 2.6 and 2.7 were used in ASHRAE 1999. However, the validity of these formulations has been questioned by Saathoff and Stathopoulos, 1997. They found discrepancies between the field and wind tunnel data of the WSU study by repeating the tests in the boundary layer wind tunnel at Concordia University. According to the authors "*dilution data in the various tests were significantly affected by other factors such as stack height, exhaust momentum and the building geometry"*. Therefore, they felt that considering the dependence of $B_1$ on upstream turbulence was debatable.

Field tracer studies were carried out by Higson et al., 1994 with a stack at varying distances upwind of a small movable building. These results were also simulated in a boundary layer wind tunnel. Results show that wind tunnel predictions were generally higher than field measurements, indicating that the wind tunnel plume was narrower than the field plume. The authors attributed this discrepancy to the absence of large scale turbulence in the wind tunnel.

Later additional wind tunnel studies were performed by Higson et al., 1995 on pollutant dispersion around an isolated building, emphasising on the fluctuating components of dispersion. They found that in near-neutral atmospheric conditions, concentration fluctuation intensities occurring in the field were larger than those measured in the wind tunnel, except in the near-wake region.

Field studies on isolated buildings are generally difficult to perform because in the urban environment they seldom exist especially in densely populated cities. Oikawa and

Meng, 1997 performed field tests to investigate the plume dispersion around a building in an open terrain in Japan. During the test tracer gas ($SF_6$) was released from a central flush vent of the test house. They performed these tests for varying wind directions. A comparison was also made with the test data available from Ogawa et al., 1983 described previously. The concentrations in the field were generally lower than wind tunnel data. They extended their investigations to determine a relationship between the instantaneous concentrations and instantaneous velocity and found tracer concentrations upwind of the flush vent due to reverse flow.

Wind tunnel experiments were carried out by Saathoff et al., 1998 at the Boundary Layer Wind Tunnel at Concordia University to investigate the effect of atmospheric turbulence on plumes released from rooftop of a laboratory building. The results of the wind tunnel study were also compared with ASHRAE 1993 formulations. The study showed that plume dilution in an urban terrain was almost twice as much as in an open terrain due to higher turbulence in an urban exposure. Good comparisons between ASHRAE 1993 and wind tunnel data were obtained for the urban exposure data for 4 m tall stacks. The dilution estimates by ASHRAE 1993 were found to be higher than wind tunnel data for the 4 m stack in an open country, based on which the authors concluded that the ASHRAE formulations did not incorporate the effects of changing terrain.

Law et al., 2004 investigated the re-entrainment of pollutants around a low-rise industrial building under opposing cross winds in a boundary layer wind tunnel using two scaled models of the building. They used Particle image velocimetry technique to calculate the planar velocity measurements. The concentration assessment technique was somewhat different compared to previous studies which generally used a gas

chromatograph to estimate plume concentrations. Their study reported that the maximum re-entrainment occurred at the ends of the building, where the effluents had a tendency to flow around the ends than over the roof. Based on their results, a re-entrainment index was proposed to assess pollutant re-entrainment for a given building configuration.

Santos et al., 2005 investigated the turbulent flow and dispersion of atmospheric contaminants in the vicinity of an isolated building. The main focus of this study was to measure plume concentrations through field studies on a complex-shaped building for different atmospheric stabilities. The results showed that the stability of the atmosphere affected the plume concentrations on the external walls with the exception of the windward wall. Additionally, the buildings width and height affected the concentration values obtained on the building walls.

The subsequent section discusses the numerical modelling of near-field pollutant dispersion for plumes released from isolated buildings.

### 2.4 Numerical modelling of pollutant dispersion from isolated buildings

Most studies in the past were focussed on wind tunnel and field studies. However, with increased costs and time associated with experimental work, many studies have focussed on numerical based research. Numerical modelling can be based on pollutant dispersion models which actually solve Gaussian based equations using a computer or by using Computational Fluid Dynamics (CFD). Although there are plenty of Gaussian based models available in literature, only a few models that include: ADMS, PRIME and ASHRAE are described, since these models are well validated and have been used for near-field dispersion problems (Stathopoulos et al., 2008; Hajra et al., 2010). CFD

models are mostly restricted to k-ε based models with very few studies applying Large Eddy Simulation (LES) owing to the increased computational time associated with the latter, for near-field pollutant dispersion (Chavez et al., 2011). For a comprehensive review of other available models- see Canepa, 2004; Holmes and Morawska, 2006 and Ramsdell and Fosmire, 1998. The subsequent section describes some of the Gaussian based dispersion models.

### 2.4.1 Application of dispersion models

Dispersion models are Gaussian based models which are used to assess plume dilution from various emission sources (isolated stack/rooftop emissions). The models generally assume the plume structure to follow a Gaussian probability distribution curve (bell shaped). A computer is generally employed to solve the equations to estimate plume concentrations at a given receptor. This section describes the widely used ADMS, PRIME and ASHRAE models.

#### 2.4.1.1 ADMS

Atmospheric Dispersion Modelling System (ADMS) is a dispersion model which was developed in the UK in collaboration with the Cambridge Environmental Research Consultants (CERC), University of Surrey and the UK Meteorological office. It is based on the model developed by Hunt and Robins, 1982 and calculates plume concentrations from isolated stacks and stacks placed on rooftop of buildings. The input consist of flow parameters such as wind velocity, exhaust speed, building and stack dimension and meteorological conditions. Building and stack downwash effects can also be modelled

(ADMS User Guide, 2004). The various stages in its development are shown in Figure 2.5.

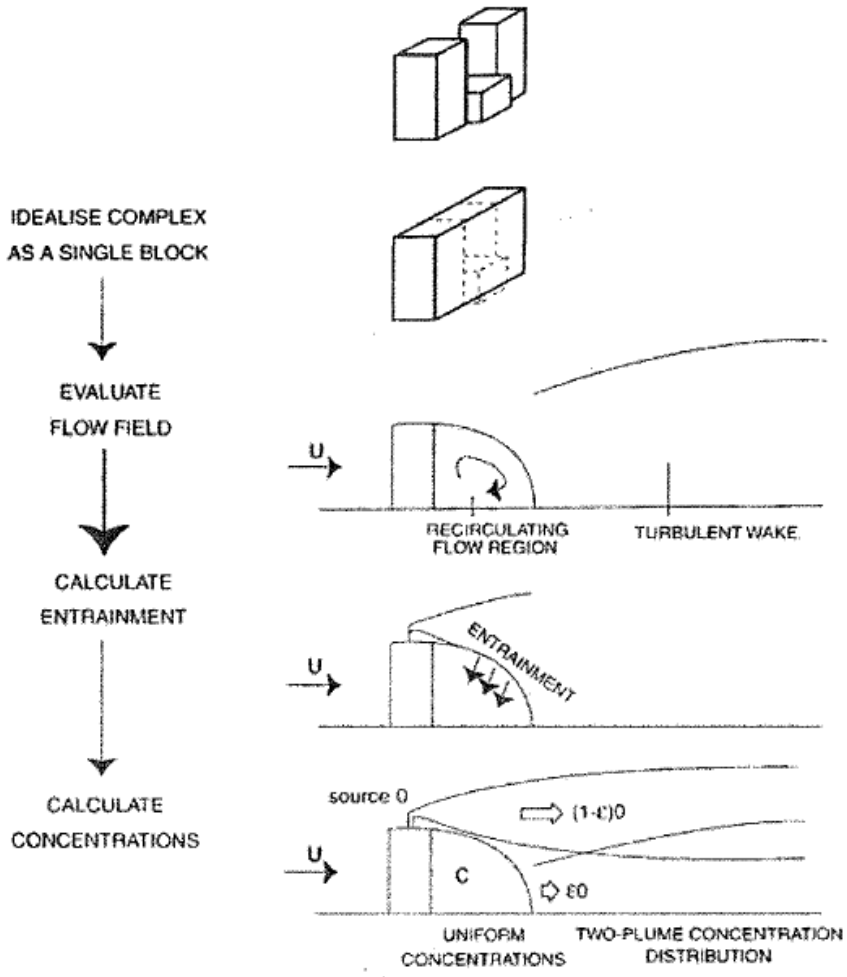


Figure 2.5. Stages in the analysis of the ADMS building effects module (from Carruthers et al., 1994).

However, in case of multiple building complexes the model combines them into a single building. It is capable of simulating the influence on turbulent and mean velocity fields of an extensive downstream wake besides change in wind direction. The model also incorporates the effects of plume rise, wet and dry deposition and variable roughness

terrains (Carruthers et al., 1994). Concentrations may be found as a contour plot or at specific locations desired by the user.

The model has been validated with wind tunnel studies by Carruthers et al., 1999 and field studies by Hanna et al., 2001; the studies mostly pertain to far-field dispersion problems. However, recent studies carried out by Hajra et al., 2010 have reported that the model generated higher concentrations than wind tunnel data for isolated building with rooftop stack; it was also unable to model the effect of rooftop structures. One of the main reasons is that it assumes a uniform flow field within the recirculation region although in reality the flow structure is complex and non uniform (Hajra et al., 2011).

#### 2.4.1.2 PRIME

PRIME which is a Gaussian based model developed by Schulman et al., 2000, stands for Plume Rise Model Enhancements. It incorporates building and stack downwash effects, thus being more suited for near-field dispersion problems. The model is capable of differentiating between the flow of pollutants released from an isolated stack and rooftop stack as shown in Figure 2.6. The study reported that the turbulence generated by the building and stack were markedly different.

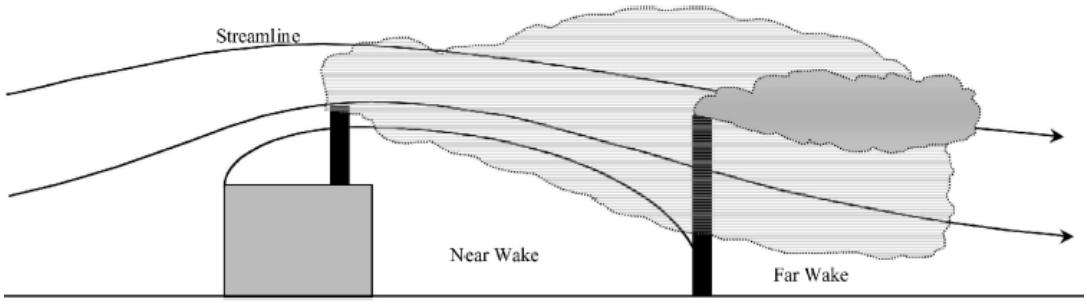


Figure 2.6. Schematic representation of two identical emission sources showing the dependence of plume dispersion on stack proximity to a structure (from Schulman et al., 2000).

The model development was sponsored by the US Electric Power Research Institute. The overall comparison of streamlines between PRIME and wind tunnel for an isolated cube were found to be good as shown in Figure 2.7.

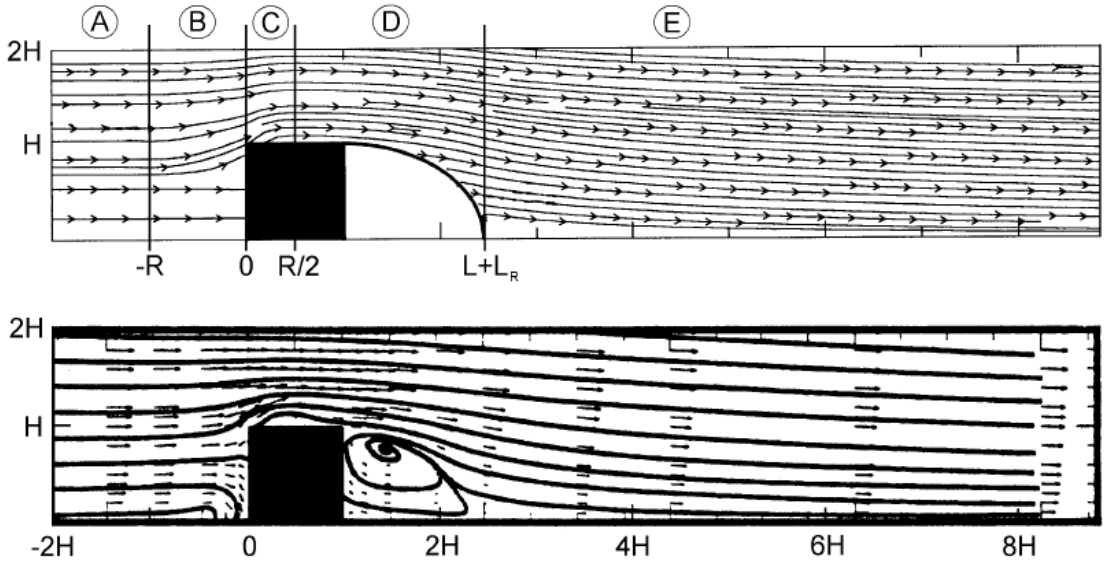


Figure 2.7 Comparison of streamlines predicted by PRIME with those observed in wind tunnel simulations of a cubic building (from Schulman et al., 2000)

PRIME is based on the ISC 3 code that was initially developed by Schulman et al., 1997. The model assumes low plume rise and higher plume dispersion coefficients in the wake of a building.

The location of the stack on building roof is used to estimate plume trajectory near the building. To check the validity of the model, results obtained from PRIME have been compared to experimental data for plumes released from isolated and rooftop stacks (Paine et al., 1998; Petersen, 2001).

#### 2.4.1.3 ASHRAE dispersion model

ASHRAE model underwent several changes since its introduction in 1989 which was based on the model of Halitsky, 1963 described previously. Although this model was in use for some time to estimate plume dilutions from isolated buildings, the results were found to be very conservative as reported by Stathopoulos et al., 1999. In 2003 a new model based on the works of Wilson, 1979 was introduced which also assumed a Gaussian plume. A modified version of the 2003 model was subsequently published in 2007. Recently, ASHRAE 2011 has been published which has undergone significant changes compared to previous versions as discussed in detail in Chapter 4. The accuracy of these models was evaluated for cases involving stack on isolated buildings and rooftop structures; the models were found to be useful only for some cases (Stathopoulos et al., 2008). ASHRAE 2003 and 2007 provide quantitative estimates of plume dispersion and a geometric method to predict the likelihood of a plume making contact with a critical rooftop receptor. ASHRAE 2007 underwent a few changes in calculating plume dilutions compared to the 2003 version. These changes lead to the prediction of low dilution at a given receptor leading to overly conservative design, as discussed in Hajra et al., 2010 and Hajra et al., 2011.

### 2.4.2 Other models and validation studies

There were also some Gaussian based models other than ASHRAE and EPA models, which were developed by other researchers. For instance, Ramsdell and Fosmire, 1990 developed a modified Gaussian dispersion model for predicting ground level centreline concentrations in the wake of buildings for exhausts released downwind of the building.

This model predicted concentrations reasonably well in comparison to the other building wake models, but was found unsuitable for low wind speeds as the predictions were significantly over-estimated. Later, Ramsdell and Fosmire, 1998 modified their previous model and developed a new micro-scale dispersion model, which incorporated these effects thus correcting the deficiencies in the previous model. The authors also compared their model with other models such as Wilson and Chui, 1994 and Wilson and Lamb, 1994 and found that the performance of the new model was significantly better than that of the previous model. A detailed review of non-Gaussian based models can be found in Sharan and Gopalakrishnan, 2003.

Some of the other validations of dispersion models include those by Dunkerley et al., 2000 who compared AERMOD, ADMS and ISC models and concluded that these models use different methods to account for the effect of terrain on dispersion which generate correspondingly diverse results. Air Quality guidelines and standards are often formulated in terms of percentile statistics. The implication of the model results for regulatory purposes is that the location and value of the maximum concentrations predicted by each of the models over a given period is likely to be significantly different. This is borne out by comparative calculations for the entire year.

Petersen et al., 2002 also compared the ISC3 and wind tunnel results. The statistical evaluation showed that ISC3 tends to over predict and PRIME tends to under predict results when compared to the wind tunnel observed concentrations. The study also showed that both models agree well with wind tunnel observations for certain building arrangements and show less favourable agreement in other cases. Although the PRIME model is vastly superior to the ISC3 model from a theoretical standpoint, the results of

this study show that further improvements can be made. The subsequent parts of this section describe CFD simulations of pollutant transport in the urban environment.

### 2.4.3 Application of CFD models to isolated buildings

Initially the use of CFD was only restricted to the k-ε based models with a gradual inclination towards the use of Large Eddy Simulation (LES). Some of the main studies pertaining to CFD simulations of plume dispersion from isolated buildings are presented.

Zhang et al., 1996 performed numerical simulations using k-ε model (TEMPEST) under stable atmospheric conditions for an isolated building with flush vent. TEMPEST stands for "Transient Energy Momentum and Pressure Equations Solution in Three-dimensions". It is a three-dimensional, time-dependent, non hydrostatic model used for engineering problems (see- Trent and Eyler, 1989). They compared their results with available experimental data and found that numerical and experimental data predict an increase in cavity length especially when Froude number < 3. The aim of their study was to assess the effects of changes in the stratification and found that when Froude number > 6 the flow structure is independent of stratification. A general conclusion based on their study on isolated buildings is that stability is not a major factor influencing the flow structure in the near-vicinity of a building.

Li and Stathopoulos, 1998 performed numerical simulation of plume released from cubic and rectangular buildings by using the standard k-ε turbulence model. Their study was focused on comparisons with experimental data obtained from the wind tunnel. The discretisation error was evaluated by a two grid system. The flow-field was estimated using TWIST (Turbulent Wind Simulation Technique), a finite difference code based on

control volume concept, developed at Concordia University, followed by assessment of concentration field with the hybrid scheme and error analysis arising from discretisation and iteration non-convergence. Their simulations showed that wind tunnel data predicted low ground level concentrations at the leeward wall of the building compared to CFD. In general, the discretisation errors were found to be about 15% less for ground-level plume concentrations than for rooftop receptors.

Olvera and Choudhuri, 2006 did CFD simulations for hydrogen and methane in the near vicinity of a cubical building model using standard k-ε model and also compared them with experimental data using a commercial CFD code STAR-CD, which is based on the finite volume method (see Versteeg and Malalasekera, 1995). The k-ε model was chosen because of earlier validation studies and its ability to handle buoyancy effects (Rodi, 1979). In this connection the effects of Froude number was also assessed by the authors to check the effects of stability. They found that independent of the thermal stratification condition and the gas (hydrogen/methane) the effect of the surroundings was much more significant when plumes were released upwind. They also reported that the effect of hydrogen on the building and its surrounding locations were much more than methane irrespective of the stability of the atmosphere owing to the lower molecular weight of hydrogen compared to methane.

Recently, Blocken et al., 2008 performed near-field pollutant dispersion studies using the Reynolds Stress Model (RSM) for two separate cases. Firstly, the field measurement performed at Concordia University (see Stathopoulos et al., 2004 for a detailed description of field measurements), were simulated for a Turbulent Schmidt number ($Sc_t$) of 0.3. Secondly, the experimental data obtained by Li and Meroney, 1983 for a cube

with flush vent were simulated using RSM and compared to ASHRAE 1999. Their study reported that at low exhaust speeds plume dispersion from a rooftop vent within the recirculation could be simulated only to some extent, while downwind and lateral plume dispersions were underestimated. They further noted that the turbulent kinetic energy profiles had unintended stream-wise gradients in the computational domain, leading to computational error.

A few studies are available in literature pertaining to the applications of Large Eddy Simulation (LES) in simulating plume dispersion from isolated buildings. For instance Sada and Sato, 2002 used LES to study pollutant dispersion from a rooftop stack of an isolated building. In their simulations the Smagorinsky-type model for the subgrid scale, i.e. an eddy viscosity-type assumption (for details see Smagorinsky, 1963), was used to set up the flow field. To predict the concentration field a conservation equation was used by the authors considering a $Sc_t$ of 0.5 which was solved using the Finite difference method. They used a "puff method" where the plume is considered as a collection of several small masses of gas (called puffs). A detailed study is available in Sykes and Henn, 1992 and Sada and Sato, 2000. These results were compared to wind tunnel data from Sada and Sato, 1999. One of the major drawbacks of using LES is the amount of computational time associated with them (Tominaga and Stathopoulos, 2011).

### 2.5 Effects of adjacent buildings on near-field pollutant dispersion

In the recent times some research has been carried out by considering the effects of building obstacles that lie in the vicinity of the source. These include the use of CFD,

wind tunnel and field experiments. Several publications in refereed journals have been quoted from in this context, as summarised in this section.

### 2.5.1 Experimental studies

Davidson et al., 1995 carried out the dispersion of a neutrally buoyant plume released upwind of an array of cubes. The aim of their study was to assess plume behaviour through flow visualisations and tracer gas measurements in the wind tunnel. Results showed that obstacle arrays do not change cross sectional profiles and the decay along the centre line significantly, although mean vertical extent of the plume increased by 40-50%.

Davidson et al., 1996 extended the study carried out previously in 1995 and presented the results of two wind-tunnel simulations of dispersion from upwind point sources through a large group of obstacles, and compared them with an associated field study. Detailed flow-field and plume concentration data were obtained from simulations at scales of 1:20 and 1:200. Measurements and flow visualisation of the flow-field further confirmed that there were a number of mechanisms influencing the behaviour of a plume as it passes through an obstacle array: in particular the divergence and convergence of streamlines and changes to the structure of the turbulence within the array. However, although the turbulence within the array was shown to be of greater strength and smaller scale than at corresponding locations outside the obstacle array, it was found that there was little change in the transverse diffusivity and therefore in the lateral plume width.

Macdonald et al., 1997 investigated the effect of plan area density on the near-field dispersion of pollutant plumes in built-up areas. Tracer gas was released from elevated

stacks placed upstream of arrays of cubes of varying plan area density. The results showed that the concentration profiles were Gaussian in all cases for both urban and open terrains.

Wilson et al., 1998 performed studies on adjacent building effects using water channel experiments at the University of Alberta, Canada. They found that high stacks and higher exit velocities which otherwise help in dispersing effluents may not be effective in the presence of adjacent buildings. They were able to show the structure of the plume in the presence of a taller upstream building, which was considered to be an important finding since previously no work was able to reveal the geometry of the plume for upstream configurations. Figure 2.8 shows the plume geometry in the presence of the upstream building and also the formation of the recirculation cavity immediately downstream of the building.

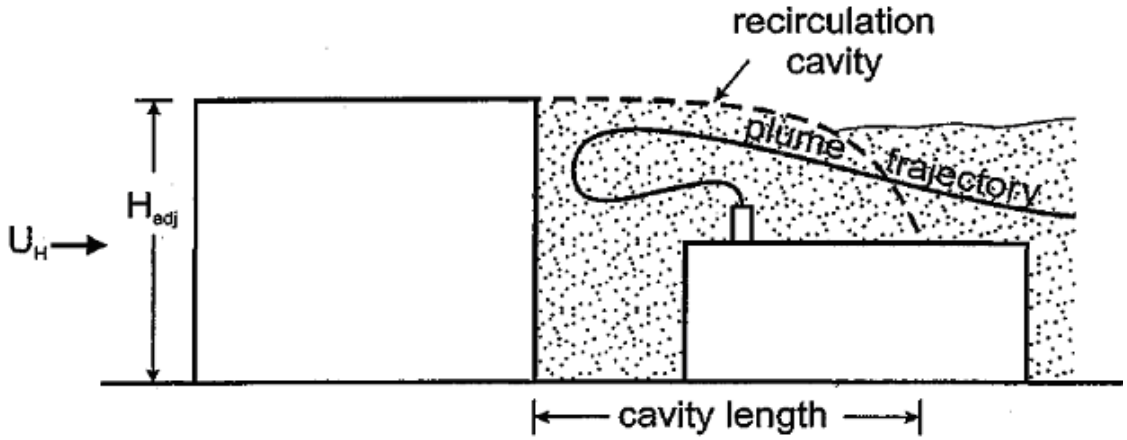


Figure 2.8 Recirculation cavity for a taller upstream building (from Wilson et al., 1998)

The cavity length shown in Figure 2.8 was found to be dependent on the height of the upstream building. Additionally, the authors had also tested the effect of a taller downstream building and were able to predict the approximate shape of the plume as

shown in Figure 2.9. Their study showed that when pollutants were released form rooftop stacks in the presence of taller downstream buildings a major part of the plume escaped through "side-leakage" phenomenon.

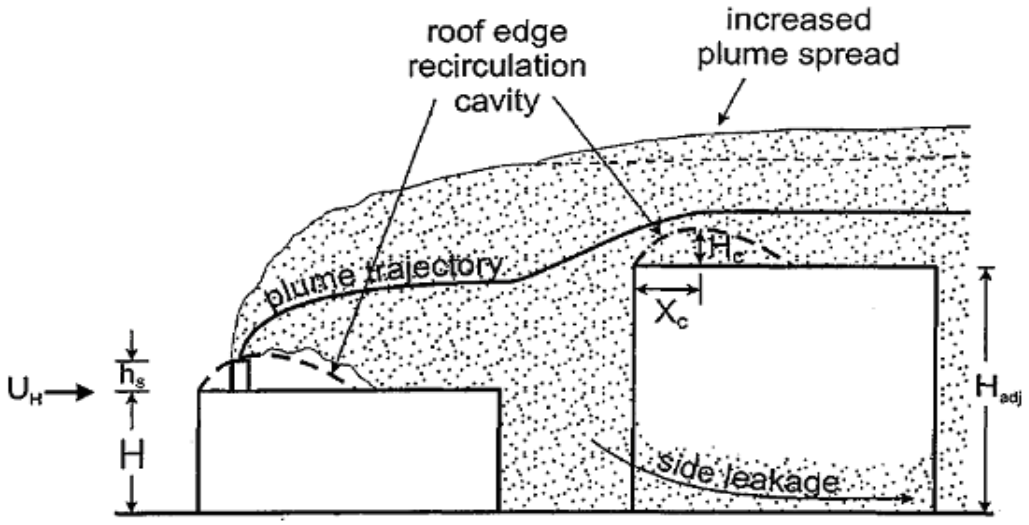


Figure 2.9 Side leakage phenomenon for taller downstream building (from Wilson et al., 1998)

The authors concluded that in general the gap between the low building and adjacent building had negligible effect on plume dilution except for the case of a building with rooftop stack with a higher downwind adjacent building.

Mavroidis et al., 1999 studied the re-entrainment of effluents through a building wake for different atmospheric stability conditions. Tracer was released from a 2 m cube building model at $0^o$ and $45^o$ wind azimuth. Tracer gas was entrained into the wake from a source located at short distance upwind of the cube; the gas was released continuously for a limited period. The residence time was found to be independent of atmospheric stability and was in very good agreement with values calculated using empirical formulae derived from wind tunnel experiments.

Tracer studies in the wind tunnel were carried out by Griffiths et al., 2001 in the near-wake of isolated obstacles to assess plume entrainment. The obstacles represented an urban area in the field at a nominal scale between 1/10 and 1/20. The source of pollutant was located upwind of obstacles. The results revealed that, the plume concentrations in the wake of different obstacles depended on the size of the recirculation zone formed in the wake of the obstacle. Comparisons with field studies showed higher plume concentrations in the wind tunnel compared to field data.

Mavroidis and Griffiths, 2001 examined the dispersion of airborne particles in a boundary layer wind tunnel within building arrays. The objective of their study was to assess the flow and dispersion of effluents in the vicinity of individual obstacles. They found that due to the enhanced mixing and dispersion within the array, differences in pollutant concentrations were measured in the wake of obstacles.

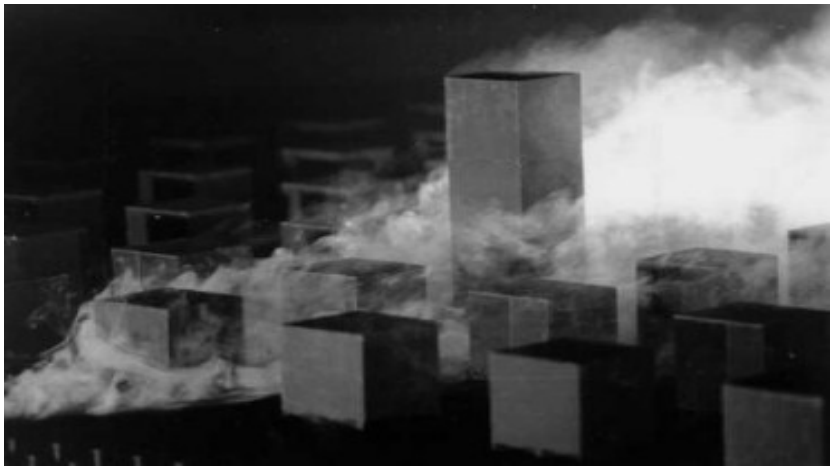

Figure 2.10 Smoke dispersing through an array with an in-line configuration and a spacing of S/H=1.5, with a taller obstacle (H=3W) located in the 3rd row of the array (from Mavroidis and Griffiths, 2001).

Additionally, the height and spacing between the obstacles also played a major role in changing the plume structure in the near field as shown in Figure 2.10.

Lazure et al., 2002 performed field studies on two of the building located at Concordia University and simulated them in the wind tunnel. Comparisons were also made with plume dilution models developed by Halitsky, 1963 and Wilson and Chui, 1985, 1987 described previously. The main focus of this research was to recommend a safe distance between sources of pollution and air intakes in an urban environment. Their results showed that the Halitsky and Wilson-Chui model gave acceptable estimates of dilution, with occasional overestimations.

Yan, 2002 studied the effects of adjacent buildings on near-field dispersion problems using wind tunnel and water channel experiments. In particular the effect of an upstream building on pollutant dispersion was studied. He found that the distance between stack and adjacent building played an important role in assessing pollutant concentrations on the upstream taller adjacent building.

Mavroidis et al., 2003 carried out pollutant dispersion studies through building arrays, using model obstacles that represented real structures at a nominal scale between 1/10 and 1/20. Their study focussed on the assessment of local characteristics of the flow and the dispersion in the vicinity of the obstacle. The results suggested that enhanced mixing and dispersion occur within the array. Their results also indicated that concentration of the pollutant was reduced within the array of obstacles compared to the isolated building case.

Stathopoulos et al., 2004 performed field studies at two of the buildings at Concordia University, Montreal. Comparisons were made between field and Wind Tunnel data. It

was observed that an upstream building's presence produced higher effluent concentrations at the rooftop of a downstream building. The top view showing the two buildings located in downtown Montreal are shown in Figure 2.11.

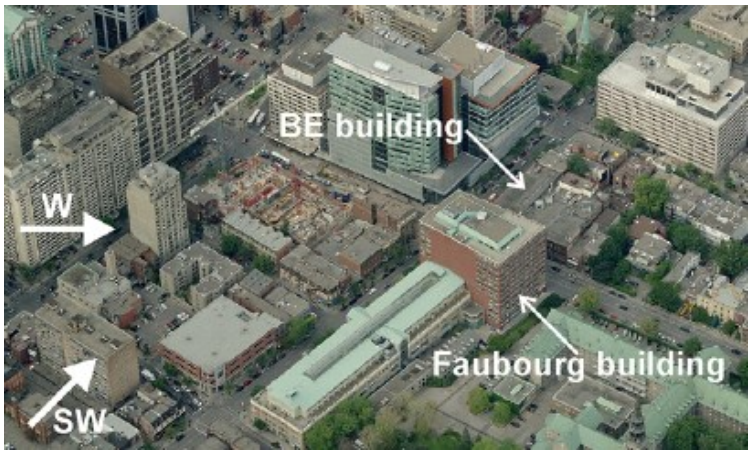


Figure 2.11 View from south of the BE building and its surroundings in downtown Montreal (from Stathopoulos et al., 2004)

The studies performed in this study were used by various researchers to validate the use of CFD in near-field pollutant dispersion which include Blocken et al., 2008 and Lateb et al., 2010, the latter used realisable k-ε model to simulate the dispersion of the plume in the urban environment. Figure 2.12 shows comparisons between CFD and wind tunnel values of normalised concentrations on the roof of both buildings.

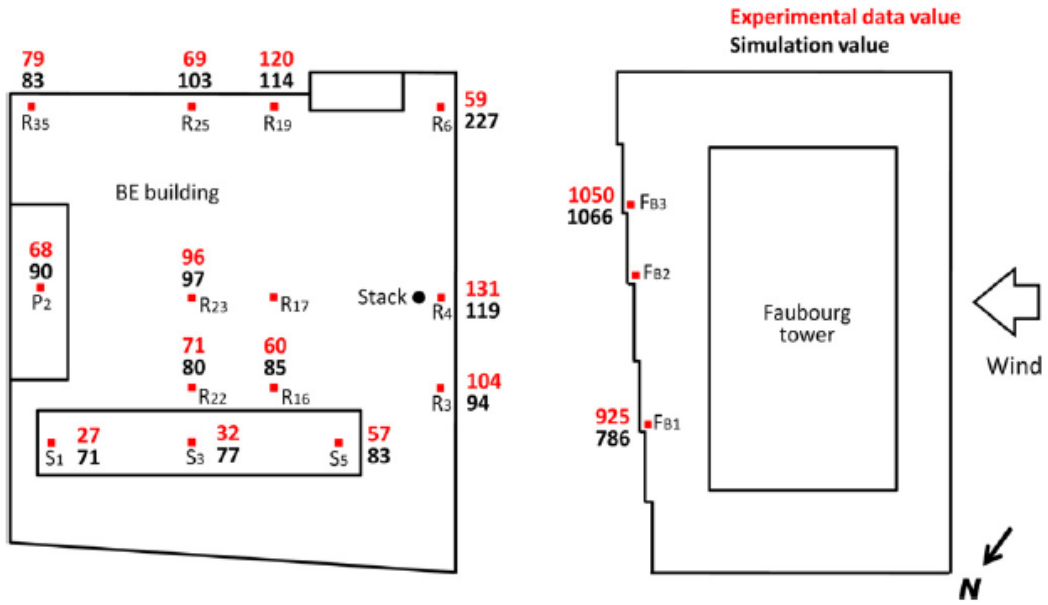


Figure 2.12 Simulation (1:200 scale) and wind tunnel values for Normalised concentrations (K) for M = 5 and $h_s$ = 1 m from Lateb et al., 2010.

The study concluded that at both scales, CFD simulations were not able to simulate the wake zone observed in the experiments. However, the lower region between the two buildings seems to be correctly reproduced, resulting in the same trends of pollutant concentrations. However, the vertical elevations of the plume were not simulated correctly as compared to the experiment observations

Yee et al., 2006 performed near-field dispersion of contaminant plumes in a large array of building-like obstacles at 1:205 scale in a water-channel simulation. These were also simulated in the field and wind tunnel. An investigation of the plume structure in the two physical modelling techniques was studied. The study reported that the plume structure by the obstacles were qualitatively similar to those observed in the field experiments. However, with the appropriate scaling, the water-channel simulations were

able to reproduce quantitatively the results of the full-scale field experiments better than the wind-tunnel simulations.

Pinto et al., 2007 performed an experimental investigation of turbulent dispersion processes in a typical three-dimensional urban geometry, in reduced scale, in neutrally stable conditions. Wind tunnel experiments were carried out for characterising the flow and the dispersion of a pollutant around a scaled model (1:400) of a group of eight 10-floor buildings surrounding a square. After the sudden interruption of the source generation, the particles persisted in the recirculation cavity between the buildings, with the concentration decaying exponentially with time. The measurements of the variation in the concentration of the fine particles were performed by means of a photo-detection technique based on the attenuation of light

Recently, Hajra et al., 2011 performed detailed wind tunnel studies on the effects of upstream building on plumes released from rooftop of a low building. The study showed that the plume geometry was greatly influenced by the height and width of the upstream building, spacing between buildings besides the height and location of the stack. They found that as the stack was gradually moved towards the downwind edge of the low building, the effect of the upstream building gradually reduced. The study also highlighted some of the deficiencies in the ASHRAE 2007 model and suggested improvements. Additionally, design guidelines for locating stack and intake on the roof of each building were proposed. CFD simulations of pollutant dispersion in the presence of adjacent buildings are discussed further.

### 2.5.2 CFD simulations of pollutant dispersion in built-up areas

Flowe et al., 2000 showed that a three-dimensional turbulent kinetic energy computational model, FLUENT, can be used to facilitate modelling of fluid flow fields with stack geometry generated by a variety of building shapes, and to use the data sets to develop parameterizations useful to air quality modelling needs. Although comparisons with a few experimental data sets revealed that FLUENT was not capable of accurately predicting dispersion characteristics in certain cases, the authors claimed that these limitations in the model could be overcome in future.

Quinn et al., 2001 have modelled the dispersion of aerial pollutants from agricultural buildings by using Computational Fluid Dynamics (CFD). The dispersion of a point source of ammonia gas in the wake of a low-rise building was predicted using a simple scalar (diffusion) model. These models were used in conjunction with flow field data from a CFD model using the standard and a modified k-ε turbulence model. The study concluded that turbulence modelling has a significant effect on the predicted concentration field in the wake of buildings and until improvements in this modelling are made the dispersion model used is of less significance.

Carruthers et al., 2004 carried out a comparative study between FLUENT and ADMS software. It was observed that when FLUENT was set up to simulate the neutrally stable atmospheric boundary layer, the mean velocity profiles were well predicted and were maintained with downwind distance. The results showed that although CFD simulations were more satisfactory compared to ADMS, the former required additional computational time apart from the complexity involved in setting up model runs compared to the latter.

Holmes et al., 2006 performed a review of the application of atmospheric models for particle dispersion which included different types of dispersion models available, from simple box type models to complex fluid dynamics models. The study concluded that the applicability of the models to particle dispersion modelling depends heavily on the nature of the concentration desired. The review also showed that considerable differences exist between the available model packages and due to the limitations of the models in terms of mathematical treatment of dispersion dynamics and treatment of the aerosol processes.

Di Sabatino et al., 2007 considered the effect of street canyons of different aspect ratios and various obstacle array configurations consisting of cubical buildings by applying the standard k-ε turbulence model and the advection-diffusion (AD) method (in contrast to the Lagrangian particle tracking method) for the CFD simulations. Results from the two approaches were compared and it was found that CFD simulations with the appropriate choice of coefficients produce similar concentration fields to those predicted by the integral approach.

Olvera et al., 2007 performed dispersion simulations of buoyant and neutral plume released within the recirculation cavity behind a cubical building using a commercially available CFD code and the RNG k–ε turbulence model. Plume buoyancy was observed to affect the size and shape of the cavity region and the flow structure and concentration profiles within. Results showed that by including the effects of plume buoyancy in the downwash algorithm better concentration predictions could be made. They concluded that this study would be extremely useful for accident assessments which require higher precision in estimating plume concentrations.

Blocken et al., 2008 performed steady-state RANS Computational Fluid Dynamics simulations of pollutant dispersion in the neutrally stable atmospheric boundary layer using the commercial code Fluent 6.1 for three case studies: plume dispersion from an isolated stack, low-momentum exhaust from a rooftop vent on an isolated cubic building model and high-momentum exhaust from a rooftop stack on a low-rise rectangular building with several rooftop structures. The results were compared with the Gaussian model, the semi-empirical ASHRAE model and wind tunnel and full-scale measurements. It was shown that in all three cases and with all turbulence models tested, the lateral plume spread is significantly underestimated.

Recently, Chavez et al., 2011 performed CFD simulations using Realisable k-ε model and compared them to ASHRAE 2007 and wind tunnel data for rooftop of a low building in the presence of adjacent buildings. In this paper they showed that the plume behaviour was affected significantly by the surroundings. In particular, it was very difficult to define a general value of $Sc_t$. The authors concluded that the flow field had to be considered before deciding on the value of $Sc_t$. ASHRAE formulations were found to be unsuitable for the given problem as they were not only overly conservative for the isolated case but also were unable to simulate the conditions of adjacent buildings.

## 2.6 Summary

The various sections of this chapter underlined the research activities that have been carried out in the past concerning pollutant dispersion from rooftop stack by experimental and numerical methods. Some papers also described the use of Gaussian-based dispersion models such as ASHRAE and ADMS. However, no significant research has been

performed on the effects of buildings that lie in close proximity to the source of pollutants. Although experimental modelling of plume dispersion through field studies was generally more accurate, due to time and financial constraints the focus has gradually shifted towards dispersion models. The advantage of wind tunnel and water channel studies over field studies is that many parameters such as wind speed and wind direction can be controlled, which is impossible to achieve in the field. Some of the simulation criteria of Snyder, 1981 (described later) are easier to achieve in water channels than in wind tunnel owing to the higher density of water over air. However, wind tunnel allows the assessment of plume concentrations through the use of a Gas Chromatograph, which is generally more convenient than water channel measurements (Hajra et al., 2011).

A major limitation of available Gaussian models is their inability to simulate the dispersion dynamics and treatment of the aerosol processes, particularly within the near vicinity of the pollutant source, where building and stack generated turbulence is dominant. Although, ADMS and PRIME do incorporate building downwash effects, their usefulness in the presence of adjacent buildings needs to be assessed. The formulations of ASHRAE need to be re-visited to enable its usage in the presence of adjacent buildings since the current model only applies to isolated buildings.

In general, dispersion models are widely used over physical modelling, but most available dispersion models are suited for far-field dispersion problems and efforts have to be made to eliminate this deficiency in current models.

Since a majority of research has been focussed primarily on far-field dispersion problems, it becomes necessary to investigate pollutant dispersion issues especially when

the receptors lie close to the stack, in the presence of neighbouring buildings. Chapter 3 describes the experimental methodology (wind tunnel tests) used for the present study.

# Chapter 3

# Experimental methodology

## 3.1 Introduction

This chapter describes the experimental technique employed in performing tracer experiments in the wind tunnel. The Boundary Layer Wind Tunnel laboratory of Concordia University was used for this study. Tracer gas was released from rooftop stack and measurements were carried out at various locations on the building surfaces.

A brief description of the atmospheric boundary layer and its simulation in the wind tunnel is first described. This is followed by a discussion on the various dispersion modelling criteria, instruments used in the present study and some preliminary results.

## 3.2 Atmospheric boundary layer

The atmospheric boundary layer also termed as planetary boundary layer is defined by Holmes, 2001 as a portion of the atmosphere that extends approximately to a few hundred metres above the earth's surface. In this part of the atmosphere, the wind interacts with buildings and structures to generate a quasi-parabolic wind profile. Based on extensive studies on the atmospheric boundary layer, Davenport, 1963 described wind velocity profiles for three different terrain exposures, as shown in Figure 3.1. Wind velocity gradually increases along the height to reach a stable value called gradient wind speed at a certain height (also called gradient height or boundary layer depth). He was able to show that the gradient height varied according to the terrain exposure. For

instance as wind flows through a rougher terrain (urban exposure) greater friction was generated causing higher gradient heights.

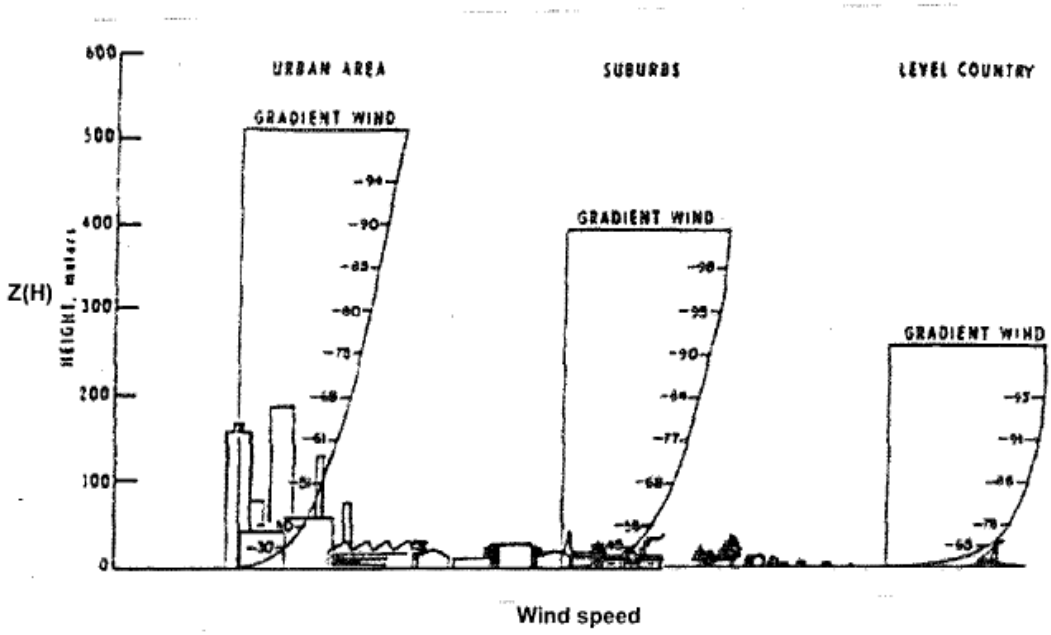


Figure 3.1 Boundary layer formations for different exposure categories (from Davenport, 1963).

The wind velocity at a height z is expressed as:

$$V(z) = \frac{u_*}{k} \ln \frac{Z}{Z_o} \qquad (3.1)$$

where

k = 0.4 (Von Karman's constant),

$u_*$ is the friction velocity (m/s),

$Z_o$ is the surface roughness (m)

However, the power law is widely used to plot the velocity profile:

$$\frac{V(z)}{V_g} = \left(\frac{Z}{Z_g}\right)^{\alpha} \qquad (3.2)$$

where

V (z) is the wind velocity (m/s) at height z (m),

$V_g$ is the gradient wind speed (m/s),

$Z_g$ is the gradient height (m)

α is the power law exponent dependent on the roughness of terrain

The other important parameter used for wind engineering applications is the turbulence intensity $I_u$ (z) defined as:

$$I_u(z) = \sigma_u(z)/V(z) \qquad (3.3)$$

where $\sigma_u(z)$ is the standard deviation of the longitudinal component of wind speed.

There are also other techniques available in literature which can be used to assess the velocity profile and turbulence intensity. For instance Engineering Science Data Unit (ESDU, 1974) concluded that the variation of the turbulent intensity with height up to 100 m is:

$$I_u(z) = \frac{(0.867 + 0.556\log_{10} z - 0.246\log^2{}_{10} z)B}{\ln(Z/Z_o)} \qquad (3.4)$$

where B = 1 for $z_0 \leq 0.02$ m,

B = 0.76 $z_o^{-0.07}$ for $0.02 < z_o < 1$ m

B = 0.76 for $z_o \geq 1$m

### 3.3 Wind tunnel modelling criteria

In general, to model non buoyant plume dispersion in a wind tunnel, the criteria suggested by Snyder, 1981, need to be satisfied. These include:

- Geometric similarity

This means that the buildings in a full scale model (prototype) should bear the same shape as the model tested in the wind tunnel, at a reduced scale.

- Building Reynolds Number > 11000
- Stack Reynolds Number > 2000

It is generally necessary to match the Reynolds number measured in the wind tunnel and full scale. However, due to smaller sized models used in the wind tunnel this is generally not possible. For near-field pollutant dispersion studies, Saathoff et al., 1995 suggested that "*it is generally not possible to satisfy the stack Reynolds number for small diameter stacks and it is also difficult to trip the flow for such stacks"*.

- Similarity of wind tunnel flow with atmospheric surface layer

This refers to similar velocity and turbulence intensity profiles obtained in full scale and wind tunnel measurements.

- Equivalent exhaust momentum ratio.

In general, exhaust momentum ratio (M) is defined as:

$$M = (\rho_e / \rho_a)^{0.5} (V_e / U_H) \qquad (3.5)$$

where

$\rho_e$ and $\rho_a$ are the densities of exhaust and air respectively (kg/m$^3$),

$V_e$ is the exhaust velocity (m/s),

$U_H$ is the wind velocity at building height (m/s)

Equation 3.5 reduces to a ratio of velocities since the densities of exhaust and air are nearly equal for non-buoyant tracer studies in the wind tunnel (Stathopoulos et al., 2008), i.e.

$$M = V_e/U_H \qquad (3.6)$$

This is an important criterion because the full scale and wind tunnel wind speeds may not be equal even if the exhaust speeds are the same. Therefore, it is necessary to

compare the ratios. A detailed review of Snyder's criteria and its applicability to micro-scale dispersion problems is discussed in Hajra et al., 2011.

Cermak, 1976 has also shown that for pollutant dispersion studies for neutral stability conditions, matching of Froude's number and Richardson number is not necessary.

Apart from dispersion modelling criteria, ASCE 1999 states that blockage ratio which is defined as $A_m/A_o$, should not exceed 5%

where

$A_m$ is Area of the model ($m^2$),

$A_o$ is the cross sectional area of the wind tunnel ($m^2$)

### 3.4 Experimental facilities

Tracer experiments were carried out on various building configurations in the wind tunnel. In this section, first a brief introduction of the wind tunnel and instrumentation used in performing the experiments are described.

#### 3.4.1 Boundary layer wind tunnel simulation

The Boundary layer wind tunnel is located in the Building Aerodynamics Laboratory at Concordia University. It is an open circuit wind tunnel of 1.8 m square in section and 12.2 m in length (Stathopoulos, 1984). In order to generate a thick boundary layer, Spires, which act as vorticity generators and coarse roughness elements, were used. This resulted in simulation of an urban terrain with a power law exponent (α) of 0.31, according to ASHRAE 2005. The roughness elements were simulated by using 5 cm cubes that were arranged staggered and spaced about 6 cm from each other. The velocity

and turbulence intensity profiles are shown in Figure 3.2. The present study also showed good comparisons of velocity and turbulence intensity profiles with ESDU, 1974.

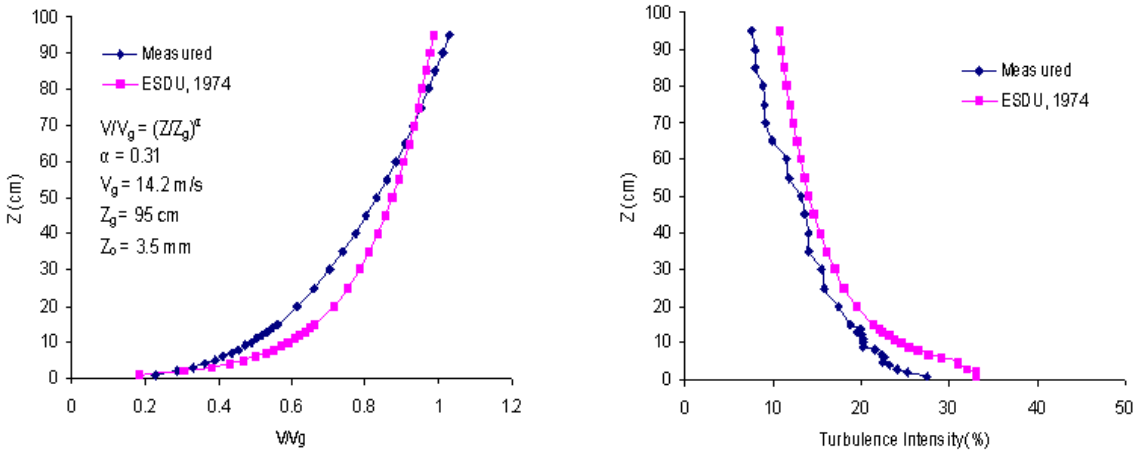


Figure 3.2 Mean velocity and turbulence intensity profiles measured at the Boundary Layer Wind tunnel of Concordia University (Hajra et al., 2011).

The flow in the wind tunnel was turbulent with stable time-averaged flow conditions throughout the tests. In order to ensure that the longitudinal static pressure gradient was negligible, the roof of the tunnel was suitably adjusted. The model value of the longitudinal integral scale was 0.4 m, which corresponds to a full-scale value of 80 m. The model roughness length of the upstream exposure was 3.5 mm, which corresponds to a full-scale roughness length of 0.7 m. The gradient height (boundary layer thickness) was 95 cm. The wind speed at building height ($U_H$) was measured to be 6.2 m/s in the wind tunnel. The front view section of the wind tunnel is shown in Figure 3.3.

Figure 3.3 Front view section of the Boundary Layer Wind tunnel at Concordia University (from Stathopoulos et al., 2008).

A mixture of sulphur hexafluoride ($SF_6$) and nitrogen was released at M ranging from 1 to 3 and $h_s$ from 1 m through 5 m from a stack whose diameter was 3 mm representing a full scale value of 0.6 m. The measurements were generally made once the wind tunnel was stable after about 4 minutes of operation. The height of the wind tunnel is sufficient for the horizontal and vertical development of the plume. The $SF_6$ samples were collected from each receptor using tubes connected to a syringe sampler, which could collect the samples during a period of one minute. The efficient ventilation facility of the laboratory was able to remove any background concentrations of $SF_6$. In fact, detailed previous experiments involving wind tunnel measurements of $SF_6$ on surface of model cubes found that subtracting background concentrations made negligible difference to the results (Saathoff et al., 1995).

A Gas Chromatograph (GC) was used to assess the concentration of the syringe samplers. It was found that the measured concentrations on the rooftop were repeatable

within ± 15 % of previously recorded data, which is generally considered to be accurate for near-field dispersion studies (Saathoff et al., 1996; Stathopoulos et al., 2008; Gupta, 2009).

In order to simulate accurate pollutant dispersion studies in the wind tunnel it is very important to maintain turbulent flow around the building and stack. In the present study, the building and stack Reynolds number were measured to be 20000 and 1800 respectively. Although, the stack Reynolds number is somewhat less than 2000, this may have had minimal effect on the measurement results, as discussed in Saathoff et al., 1995.

The effect of averaging time is not expected to affect the measurements particularly when the stack and receptor are in close proximity to each other, as in the present study. In fact, the plume spreads described in ASHRAE 2007 are based on field studies by McElroy and Pooler, 1968 which states that *"The urban ISCST equations are adjusted here from the 60 min measured averaging time to 2 min averages… Then, the vertical spread over a building roof is assumed to remain constant at the 2 min averaging time value for longer averaging times"*. ISCST stands for Industrial Source Complex Short Term model which was developed by Schulman et al., 1997.

It is known that a wind tunnel plume spreads at a rate equivalent to half hour averages in the field (Hajra et al., 2011). In the present study however, the averaging time for collecting samples was only one minute because the instrument used for collecting the samples is only capable of measuring samples at a maximum averaging time of one minute. Table 3.1 summarises the experimental parameters used for the present study.

Table 3.1 Experimental parameters used in the present study

| Experimental parameters | Present study (wind tunnel values) |
|---|---|
| Model scale | 1:200 |
| Boundary layer depth | 95 cm |
| Wind speed at building height ($U_H$) | 6.2 m/s |
| Power law exponent (α) | 0.31 |
| Upstream terrain | Urban |
| Velocity at gradient height ($V_g$) | 14.2 m/s |
| Roughness length of upstream exposure | 3.5 mm |
| Longitudinal integral scale | 0.4 m |
| Stack diameter | 0.3 cm |
| Averaging time | 1 minute |
| Upstream turbulence at building height (%) | 23[a], 17[b] |

[a] low rise building of 15 m
[b] intermediate building of 30 m

### 3.4.2 Instruments used in the study

This section describes the instruments that were used in the present study.

a) Cobra probe

The cobra probe as shown in Figure 3.4 is an instrument that is used to measure velocity and turbulence intensity profiles in the wind tunnel. The probe can be used for various wind speeds ranging from 2 m/s to 100 m/s (Turbulent Flow instrumentation, 2008).

Figure 3.4 Series 100 cobra probe

The instrument is generally mounted on a stand and placed in the wind tunnel. The various heights along which the measurements of velocity and turbulence intensity are to be made are specified on the device control software. For different heights, the velocity and turbulence intensity profiles are stored in an excel based file. Detailed information about the product is also available at: http://www.turbulentflow.com.au. The instrument was used to measure the velocity and turbulence intensity profile already shown in Figure 3.2.

b) Flow visualisation equipment

The flow visualisations were performed using the Safex NS2 probe manufactured by Dantec (http://shop.dantecdynamics.com/) as shown in Figure 3.5. The instrument consists of generating fog by heating a water-based fluid.

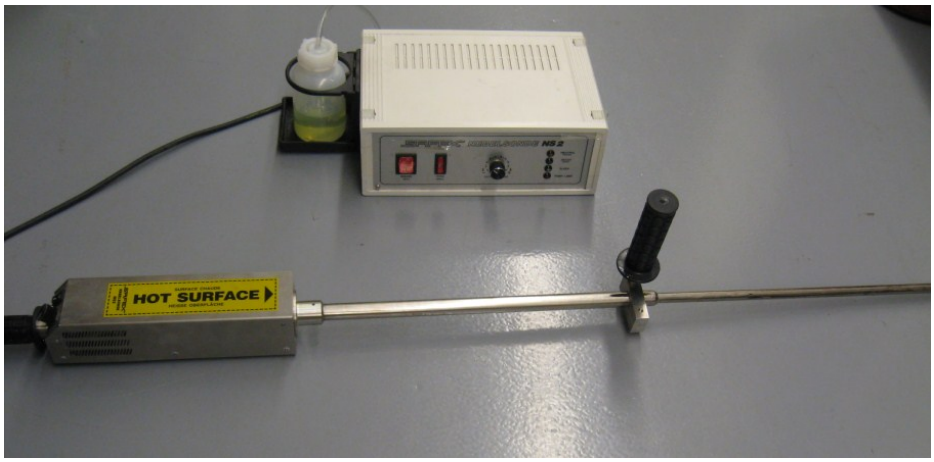


Figure 3.5 Dantec fog generator with Safex NS2 probe

The instrument was connected to the rooftop stack and in the presence of adjacent buildings the plume behaviour was studied. The pictures were taken using a digital camera of 7.1 mega-pixels. It may be noted that the visualisations are only a qualitative

approach to assess plume behaviour. More accurate means of measuring plume dilution can be done using gas chromatography – see subsection e).

c) Mass flow transducer and controller

Mass flow transducer and flow controller shown in Figure 3.6, were used to control the flow of tracer being emitted from the stack. Both instruments are manufactured by Matheson (www.mathesontrigas.com). The flow controller has a capability of releasing 10 standard litres per minute of tracer gas.


a) b)

Figure 3.6 Instruments for controlling flow: a) flow transducer; b) flow controller

The $SF_6$ gas released from a cylinder was connected to both instruments to regulate the flow. By changing the knob of the flow controller the rate of exhaust release was controlled. Additional information may be found in the instrument manual available online: http://www.mathesongas.com/pdfs/products/Model-8270-Mass-Flow-Controller-System.pdf.

d) Syringe sampler

The syringe sampler, shown in Figure 3.7, was used to collect samples of $SF_6$ from various receptors located on the building surfaces. The instrument can hold 10 syringes at a time. The instrument is manufactured by KD Scientific (model: 230).

Figure 3.7 Syringe sampler from KD Scientific (model no. 230)

The syringes are connected to each receptor via tubings underneath the wind tunnel. This was done so that there was minimum interference between the wind flow and tubings that could affect tracer measurements. Additional details about the instrument can be found from the online manual available at: http://www.kdscientific.com/technical-resources/manuals.asp. Although, the instrument is capable of measuring samples at a maximum averaging time of one minute, this had minimal effect on the measurements as discussed previously.

e) Gas chromatograph

The gas samples collected in syringes was injected in the Gas Chromatograph (GC) shown in Figure 3.8, to measure concentration of the measured samples. The GC is manufactured by Varian (model: 3400). The instrument is also connected to a nitrogen cylinder which helps in keeping the system free from traces of $SF_6$ that accumulates during the tests. Additionally nitrogen gas also acts as a coolant to keep the GC within a safe working temperature range. The GC delivers output in terms of voltages which are later converted to equivalent concentrations using calibration charts (Varian, 1988).

Figure 3.8 Gas chromatograph used for measuring concentration of tracer

The calibration equations were derived from known concentrations of $SF_6$ (see Appendix A). A summary of the entire tracer experiment process is presented in Figure 3.9. The gas released from the cylinder is controlled by the flow control meter which in turn is released through the rooftop stack placed in the wind tunnel. Samples collected from

various receptors are then injected in the GC. This is followed by the evaluation of data for a better understanding of the problem.

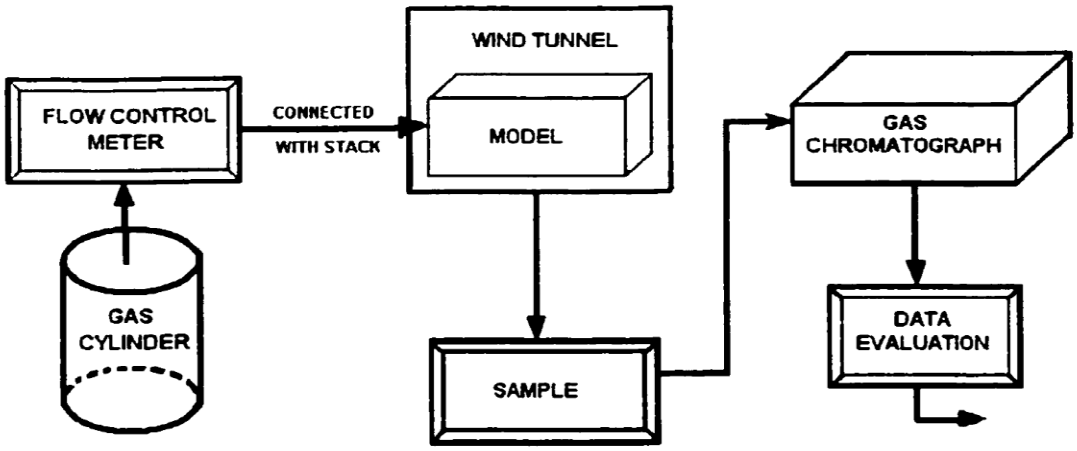


Figure 3.9 Tracer gas experiment system (Yan, 2002)

The subsequent section describes some of the preliminary studies that were carried out using flow visualisations based on which various configurations were tested in the wind tunnel.

### 3.5 Preliminary studies

There are very few studies pertaining to the near-field pollutant dispersion caused by plumes released from rooftop stacks in the presence of adjacent buildings. For instance, the Environmental Protection Agency (EPA) performed a preliminary investigation with a tall building placed upstream of a low building as shown in Figure 3.10. Pollutants were emitted from a low building in the presence of a taller upstream building. However, the plume gets engulfed within the recirculation length formed downwind of the taller upstream building thereby affecting the leeward wall of the upstream building and the rooftop of the low building.


Figure 3.10 Recirculation zone in the wake of a building (from:http://www.epa.gov)

Although this was an important finding, quantitative estimates were made only for a few cases. The present study tried to investigate this matter in greater detail by performing flow visualisations for plumes released from a low building in the presence of a taller downstream building as shown in Figure 3.11.

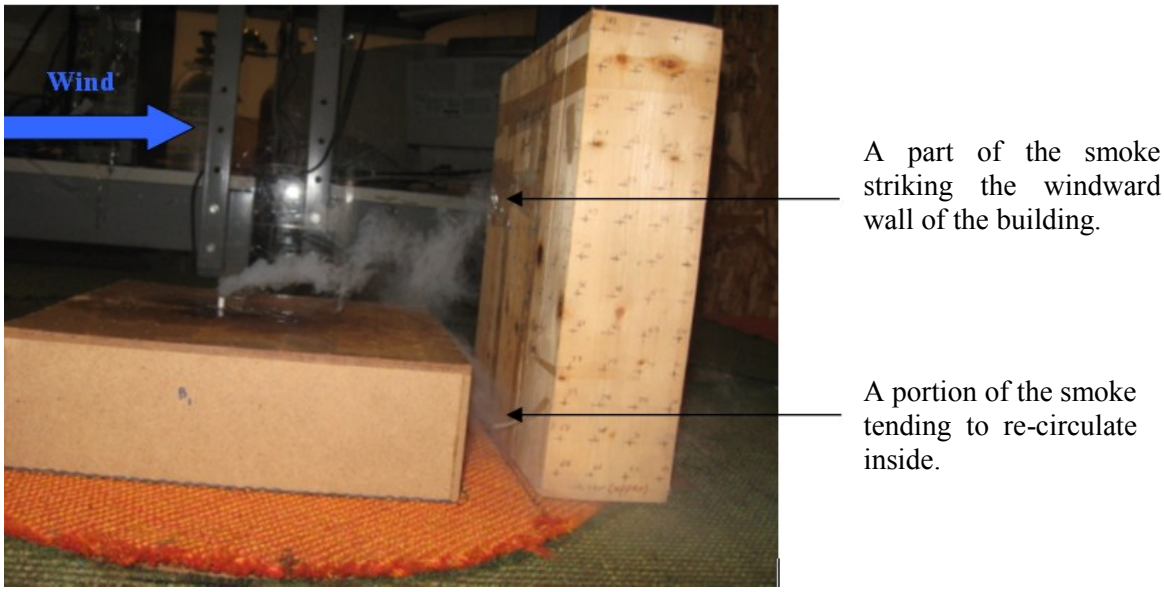


Figure 3.11 A tall building placed downstream of a low building ($\theta = 0^0$)

Pollutants were released at low exhaust speeds ($M \approx 1$) from a low building placed about 5 cm (10 m full-scale) upwind of a tall downstream building. It was observed that the roof of the low building and windward wall of the downstream building were affected. The smoke that accumulated between the buildings also had a tendency to re-enter the emitting building through the leeward wall. For further investigation, a tall building was placed upstream and downstream of the low building, which was observed to change the plume geometry markedly as shown in Figure 3.12. However, the building placed upstream of the source was narrow and hence it had a smaller recirculation length downwind of it. Hence, the plume had a tendency to move more towards the downstream building than the upstream building.

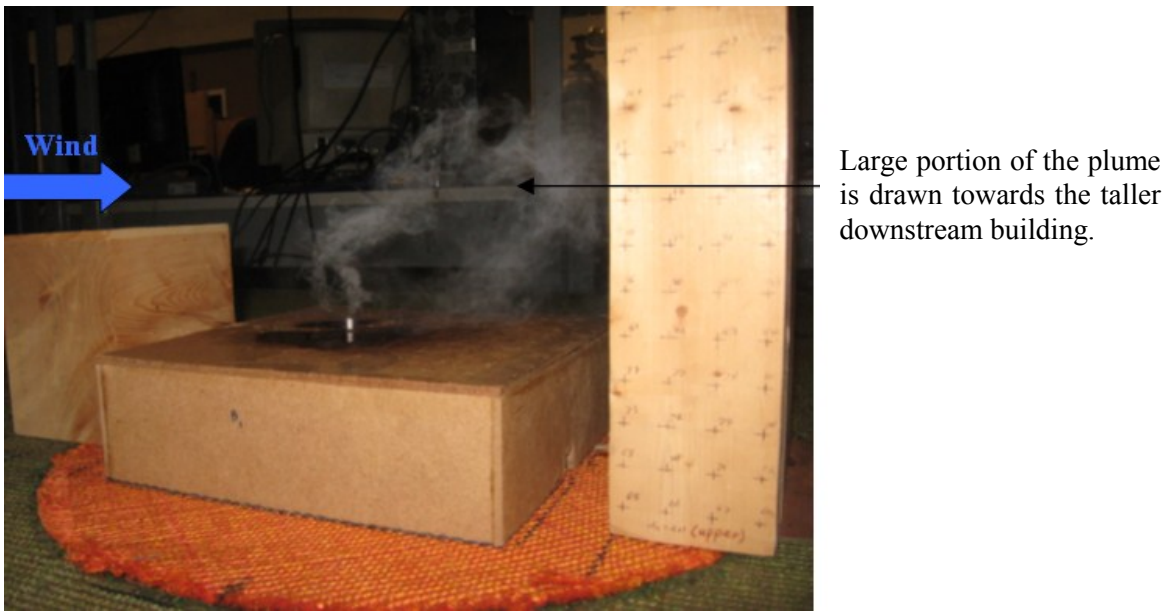


Figure 3.12 A tall building placed upstream and downstream of a low building ($\theta = 0^0$)

It was also observed that when all three buildings were of equal width, the plume had a greater back and forth motion (meandering) affecting all the three buildings. When the tall building shown in Figure 3.12 was placed upstream of a tall building with a centrally

placed stack, the plume was less affected by the upstream building as shown in Figure 3.13.

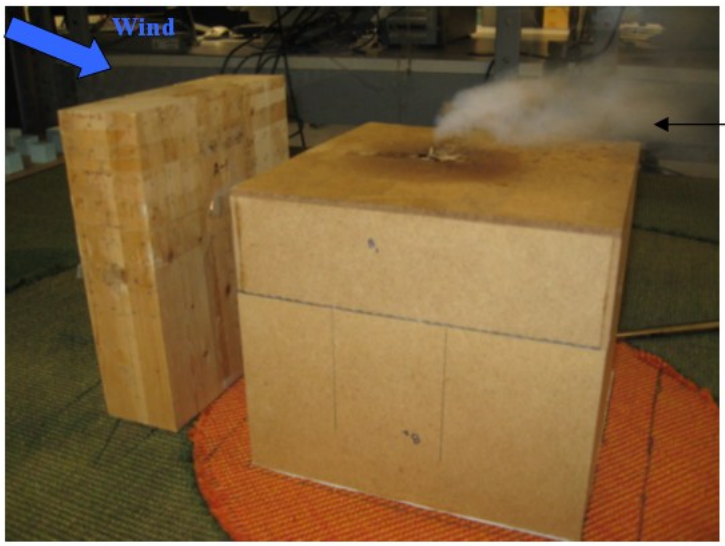


Figure 3.13 Tall building placed upstream of a tall emitting building ($\theta = 0^0$)

### 3.6 Observations from the preliminary study

The flow visualisations were able to show the following:

a) The height and width of the adjacent buildings (upstream/downstream) played a major role in altering the plume dispersion.

b) The height of the emitting building, stack location and height, exhaust speed and spacing between buildings were also critical factors that needed further investigations.

Table 3.2 lists the various parameters that were considered for the wind tunnel study. Currently, ASHRAE 2007 and 2011 are the only codes of practice available to designers which applies to isolated buildings. Most other studies were restricted to only a particular case (such as the one described in Figure 3.10 previously). Hence, a comprehensive study involving the changes in various parameters of the adjacent and emitting buildings was found to be necessary.

Table 3.2 Variable involved in the study and their respective values

| Variable | Range of Values | Reasons for adopting such values |
|---|---|---|
| M | $1 < M < 3$ | Previous studies for isolated building have used the following range of 'M' (Stathopoulos et al., 2004), which could be used for comparison with the present case. |
| Building height | 15- 50m | Results from field study for a taller upstream building were available. |
| Spacing | 5- 50 m | Previous studies were conducted on two buildings at Concordia University which were on either side of the street (Stathopoulos et al., 2004). However, additional tests to assess the effects of spacing were necessary. |
| Width | 30 – 50 m | Flow visualisations showed a narrow upstream building affected the plume less compared to a wider building. |
| Length | 15 – 30 m | Change in length was never considered by any of the previous studies including ASHRAE. |
| $X_s$ | $0 < X_s < 25m$ | Previous results for upwind and centrally placed stacks are available (Saathoff et al., 2009) |
| $h_s$ | $1 < h_s < 5m$ | Concentrations for an isolated building for stack heights ranging from 1m to 5m are available from past studies (Stathopoulos et al, 2008). |
| $\theta$ | $0 < \theta \leq 45^0$ | Most studies focussed on $\theta = 0^o$ with very few studies at $\theta = 45^o$. |

Additionally, the flow visualisations showed the nature of the plume for rooftop emissions in the presence of adjacent buildings as opposed to isolated buildings. A better understanding of the problem could be made only through concentration measurements using a gas chromatograph. Table 3.3 presents the dimensions of each building used for wind tunnel experiments.

Table 3.3 Dimensions of building models used for wind tunnel experiments

| Building | Height (m) | Width (m) | Length (m) |
|---|---|---|---|
| $B_1$ | 15 | 50 | 50 |
| $B_2$ | 30 | 50 | 30 |
| $B_3$ | 30 | 50 | 15 |
| $B_4$ | 30 | 30 | 30 |
| $B_5$ | 54 | 50 | 15 |
| $B_6$ | 30 | 50 | 50 |

Based on the flow visualisations, six building models made of wood were constructed using which eleven different configurations were examined to assess near-field plume characteristics in the presence of adjacent buildings. The various configurations tested in the wind tunnel are presented in Table 3.4.

Table 3.4 Configurations tested in the wind tunnel

| No. | Configuration | Remarks |
|---|---|---|
| 1 | $B_1$ | Isolated |
| 2 | $B_2$ upstream of $B_1$ | Taller upstream building |
| 3 | $B_3$ upstream of $B_1$ | Taller upstream building |
| 4 | $B_4$ upstream of $B_1$ | Taller upstream building |
| 5 | $B_5$ upstream of $B_1$ | Taller upstream building |
| 6 | $B_6$ | Isolated |
| 7 | $B_2$ upstream of $B_6$ | Buildings of similar height |
| 8 | $B_3$ upstream of $B_6$ | Buildings of similar height |
| 9 | $B_4$ upstream of $B_6$ | Buildings of similar height |
| 2a | $B_2$ downstream of $B_1$ | Taller downstream building |
| 3a | $B_3$ downstream of $B_1$ | Taller downstream building |
| 4a | $B_4$ downstream of $B_1$ | Taller downstream building |
| 5a | $B_5$ downstream of $B_1$ | Taller downstream building |
| 7a | $B_2$ downstream of $B_6$ | Buildings of similar height |
| 8a | $B_3$ downstream of $B_6$ | Buildings of similar height |
| 9a | $B_4$ downstream of $B_6$ | Buildings of similar height |
| 10 | $B_2$ upstream and $B_5$ downstream of $B_1$ | Buildings on either side of emitting building |
| 11 | $B_2$ upstream and $B_5$ downstream of $B_6$ | Buildings on either side of emitting building |

NB: The buildings $B_1$ (15 m) and $B_6$ (30 m) were used as emitting buildings

A pictorial representation of each configuration along with stack and receptor location is provided in Chapter 5.

### 3.7 Summary

This chapter summarised the various instruments and wind tunnel facility used for the experiments. The configurations selected were based on some preliminary investigations and past results obtained from field and wind tunnel tests. Prior to discussing the results

obtained for each configuration, a description of the ASHRAE dispersion model is presented in the following chapter.

# Chapter 4

# ASHRAE dispersion model

## 4.1 General

This chapter describes the ASHRAE 2003, 2007 and the recently published 2011 models. As mentioned previously, ASHRAE has been used by designers to model plume dispersion from rooftop stacks of isolated buildings. Hence, a detailed description of the various versions of ASHRAE model is necessary to understand the working of the model. A short note regarding the application of other Gaussian based models is also presented. In general the description of the ASHRAE 2007 model also serves as a background for understanding the development of the rectified ASHRAE approach described later in Chapter 6.

## 4.2 ASHRAE model

The ASHRAE (American Society of Heating, Refrigeration and Air conditioning Engineers) model has been in use for several decades and has undergone several modifications. The equations of Halitsky, 1963 were initially used in ASHRAE 1999. However, studies by Stathopoulos et al., 1999 showed that the results obtained by ASHRAE 1999 were overly conservative. Later the equations of Wilson, 1979 were used in ASHRAE 2003 and its subsequent versions in 2007 and 2011. Recent studies by Hajra et al., 2010 have also shown the overly conservative nature of ASHRAE 2003 model. Additionally, ASHRAE cannot model the effect of adjacent buildings and can only be

used to estimate rooftop dilution of isolated buildings. ASHRAE has devised two techniques:

a) The Geometric design method

b) Gaussian plume equations.

The former is used for assessing minimum stack height to avoid plume material entering the recirculation region, whereas the latter is used to estimate plume dilution at a given rooftop receptor.

The geometric design method has remained unchanged in the 2003, 2007 and 2011 versions of ASHRAE, as discussed further.

### 4.2.1 Geometric design method

The geometric design method is based on the geometry of the plume as shown in Figure 4.1.

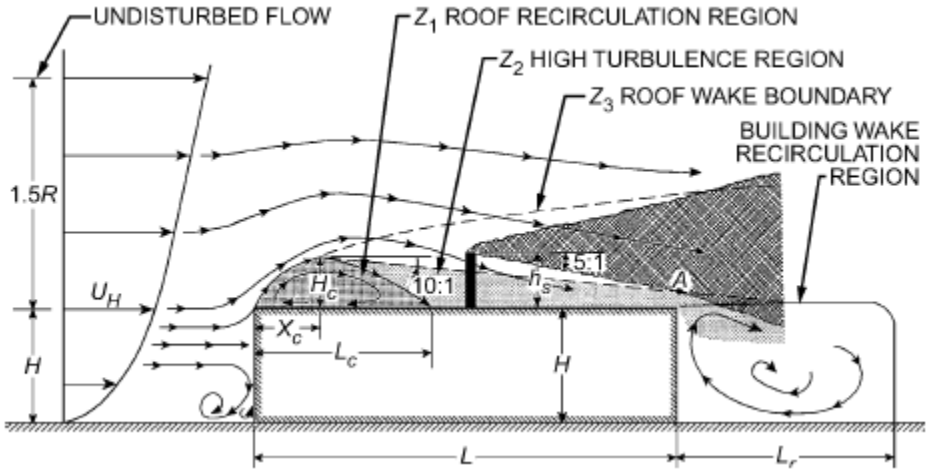


Figure 4.1. Design procedure for required stack height to avoid contamination (from Wilson, 1979)

The dimensions of flow re-circulation zones that form on the building and Roof-Top Structure (RTS) are:

$$L_r = B_s^{0.67} B_L^{0.33} \quad (4.1)$$

$$H_c = 0.22 L_r \quad (4.2)$$

$$X_c = 0.5 L_r \quad (4.3)$$

$$L_c = 0.9 L_r \quad (4.4)$$

where: $B_s$ and $B_L$ are the smallest and largest dimensions of the building face perpendicular to wind direction,

$H_c$ is the maximum height of the roof recirculation zone (m),

$X_c$ is the distance from the leading edge to $H_c$ (m),

$L_c$ is the length of the roof recirculation zone (m)

The geometric design method assumes the boundary of the high turbulence region to be a line with a slope of 10:1 extending downward from the top of the leading edge separation bubble. The location of the plume relative to the recirculation zones is determined by taking into account plume rise due to exhaust momentum and assuming a conical plume with a slope of 5:1. However, this method can only be used to assess the approximate height of the stack that would prevent pollutants from getting engulfed within $L_r$. In order to assess plume dilution, Gaussian equations are used, as discussed in the subsequent section.

### 4.2.2 Gaussian plume equations

This section explains the Gaussian plume equations described in ASHRAE 2003 and the changes made in the subsequent versions published in 2007 and 2011 respectively.

#### 4.2.2.1 ASHRAE 2003

To assess plume dilution on a rooftop receptor, ASHRAE 2003 suggests the use of Gaussian equations. Some of the parameters required for assessing dilution include the effective height of the plume (h) above the roof:

$$h = h_s + h_r - h_d \tag{4.5}$$

where:

$h_s$ is stack height (m),

$h_r$ is plume rise (m) and

$h_d$ is the reduction in plume height due to entrainment into the stack wake during periods of strong winds (m).

Plume rise, calculated using the formula of Briggs, 1984, which is assumed to occur instantaneously, only due to momentum:

$$h_r = 3\beta d_e (V_e / U_H) \tag{4.6}$$

where:

$d_e$ is the stack diameter (m),

$V_e$ is the exhaust velocity (m/s),

$U_H$ is the wind speed at building height (m/s); and

β is the stack capping whose value is 1 for uncapped and 0 for capped stacks.

The effect of plume buoyancy is not taken into account.

Wilson et al., 1998 recommended a stack wake downwash adjustment $h_d$, which is defined as:

$$h_d = d_e (3 - \beta V_e / U_H) \tag{4.7}$$

The dilution $D_r$ is defined as:

$D_r = C_e/C_r$

$C_e$ = contaminant mass concentration in exhaust, kg/m$^3$

$C_r$ = contaminant mass concentration in receptor, kg/m$^3$

The spread parameters (standard deviations of the plume) are described as follows:

$$\sigma_y / d_e = 0.071\left(t_{avg}/2\right)^{0.2}(X/d_e) + \sigma_o / d_e \quad (4.8)$$

$$\sigma_z / d_e = 0.071(X/d_e) + \sigma_o / d_e \quad (4.9)$$

The dependence of initial spread $\sigma_o$ on exit velocity to wind speed ratio $V_e / U_H$ is

$$\sigma_o / d_e = \left[0.125\beta(V_e/U_H) + 0.911\beta(V_e/U_H)^2 + 0.25\right]^{0.5} \quad (4.10)$$

where:

$t_{avg}$ is the concentration averaging time in minutes,

X is the distance downwind from the stack (m),

$\sigma_y$ and $\sigma_z$ are standard deviations of the plume (m).

$\sigma_o$ is the initial source size that accounts for stack diameter and for dilution jet entrainment during plume rise (m). A plume which is represented in three dimensions by Gaussian equations will have standard deviations $\sigma_y$ and $\sigma_z$ along 'y' and 'z' axes respectively, at a given longitudinal distance 'x', as shown in Figure 1.1. The values of $\sigma_y$ and $\sigma_z$ are calculated from equations 4.8 and 4.9 respectively at a given receptor distance, exhaust momentum ratio, stack diameter and averaging time.

As per ASHRAE 2003, dilution at roof level in a Gaussian plume emitted at the final rise plume height of h is:

$$D_r = 4(U_H/V_e)(\sigma_y/d_e)(\sigma_z/d_e)\exp(h^2/2\sigma_z^{\,2}) \quad (4.11)$$

ASHRAE 2003 uses the concept of $h_{small}$, which is calculated by drawing a triangle with edges at 5:1 from the centre (similar to the one shown in Figure 4.1) such that the side of the triangle just crosses the building wake recirculation region (shown as '$L_r$' in Figure 4.1). According to ASHRAE 2003 if $h < h_{small}$, the dilution should be estimated by considering a flush vent (exponential term of equation 4.11 becomes zero); however, if $h > h_{small}$, dilution may be estimated by equation 4.11. The value of 'h' is always calculated from equation 4.6. Physically this means that when the value of 'h', which includes stack height, plume rise and downwash, is less than the smallest possible plume height, pollutant dispersion is reduced resulting in lower dilution. In 2007 ASHRAE underwent a few changes in estimating the exponential term of equation 4.11 as described further.

#### 4.2.2.2 ASHRAE 2007

The equations for estimating the spread parameters and plume height described previously in ASHRAE 2003 remain unchanged in ASHRAE 2007. However, the formulation for estimating rooftop dilution has been modified to:

$$D_r = 4(U_H / V_e)(\sigma_y / d_e)(\sigma_z / d_e)\exp(\zeta^2 / 2\sigma_z^{\,2}) \qquad (4.12)$$

where: $\zeta = h - H_c$

$= 0$ if $h < H_c$

$\zeta$ is the vertical separation between 'h' and $H_c$.

It is worth noting that although, $D_r$ is expressed as ratio of exhaust to receptor concentration, the latter is proportional to the pollutant emission rate, Q, and not the pollutant concentration at emission. Indeed, by addition of air it is possible to change the concentrations at emission without altering receptor concentrations for a particular case.

It is generally convenient to express results in terms of dilution so that irrespective of the molecular weights of the gases, the concentrations may be expressed in non-dimensional form (Hajra et al., 2011).

Although, both the 2003 and 2007 versions follow nearly a similar approach, in ASHRAE 2007 the concept of smallest plume height has been replaced by $H_c$ as defined in equation 4.2. However, if $h < H_c$, calculations must be done assuming a flush vent, in which case the exponential term of equation 4.12 becomes zero.

For all cases the dilution calculated from Equation 4.11 and 4.12 has been converted to a normalised form according to Wilson et al., 1998 for ease of comparison with previous studies:

$$D_{normalised} = (D_r\ Q) / (U_H\ H^2) \tag{4.13}$$

The subsequent section describes ASHRAE 2011.

#### 4.2.2.3 ASHRAE 2011

ASHRAE 2011 has recently been introduced due to discrepancies with experimental data reported in previous studies for isolated building cases (e.g. Stathopoulos et al., 2008; Saathoff et al., 2009; Hajra et al., 2010). As mentioned previously, the geometric design method remains unchanged for ASHRAE 2011. However, new formulations for estimating plume rise ($h_r$), plume spread parameters ($\sigma_y$ and $\sigma_z$) and dilution for shorter time periods have been suggested. Plume rise ($h_r$) is estimated as

$$h_r = \min\{\beta h_x, \beta h_f\} \tag{4.14}$$

where

$\beta$ is the stack capping factor: 1 without cap, 0 with cap,

$h_x$ and $h_f$ are estimated as

$$h_x = \left(\frac{3V_e^{\,2} d_e^{\,2} X}{4\beta_j^{\,2} U_H^{\,2}}\right)^{1/3} \tag{4.15}$$

$$h_f = \frac{0.9[(V_e^{\,2} d_e^{\,2}/4)(U_H/U_*)]^{0.5}}{\beta_j U_H} \tag{4.16}$$

where

$U_*$ is the friction velocity (m/s),

$\beta_j$ is termed as the jet entrainment coefficient and is calculated as

$$\beta_j = \frac{1}{3} + \frac{U_H}{V_e} \tag{4.17}$$

The logarithmic wind profile equation is

$$U_H/U_* = 2.5Ln(H/Z_o) \tag{4.18}$$

where

$Z_o$ is the surface roughness length (m)

It may be noted that the plume rise as per ASHRAE 2007 (equation 4.6) were functions of the exhaust momentum ratio and stack diameter whilst the 2011 version also incorporates the effects of wind profile and stack-receptor distance (X).

The plume spread parameters ($\sigma_y$ and $\sigma_z$) are calculated using the formulations of Cimoreli et al., 2005

$$\sigma_y = (i_y^{\,2} X^2 + \sigma_0^{\,2})^{0.5} \tag{4.19}$$

$$\sigma_z = (i_z^{\,2} X^2 + \sigma_0^{\,2})^{0.5} \tag{4.20}$$

$$i_y = 0.75 i_x \tag{4.21}$$

$$i_z = 0.5 i_x \tag{4.22}$$

$$i_x = [0.24 + 0.096\log_{10}(Z_o) + 0.016(\log_{10} Z_o)^2][\ln(30/Z_o)/\ln(Z/Z_o)] \qquad (4.23)$$

where

$i_x$, $i_y$ *and* $i_z$ are the turbulence intensities in x, y and z directions,

$\sigma_o$ is the initial source size and is set equal to $0.35d_e$ (m),

*Z* is the height of the building (m)

As discussed previously, ASHRAE 2007 estimated the source size ($\sigma_o$) based on M and $d_e$ whilst ASHRAE 2011 calculates it as a function of $d_e$. The dilution is calculated using equation 4.12 which according to ASHRAE 2011 is equivalent to 10-15 minutes averaging time. Hence, dilution estimates for shorter averaging times are estimated by using the following formula:

$$(D_r)_s = D_r(t_s/15)^{0.2} \qquad (4.24)$$

where

$(D_r)_s$ is the dilution estimated for a shorter averaging time $t_s$,

$t_s$ is the averaging time in minutes,

$D_r$ is the dilution calculated as per equation 4.12.

The introduction of averaging time is a significant contribution of ASHRAE 2011 since this was not a part of previous versions of ASHRAE. Averaging time greatly influences the dispersion process especially at the micro-scale level as discussed in Hajra et al., 2011.

Besides ASHRAE, there are other Gaussian based models which are also widely used. However, these models have not been used for the present study due to various deficiencies in them, as discussed further.

### 4.3 Other dispersion models

There are many dispersion models available in literature that have been used for modelling urban plume dispersion but most of these studies focused on measuring pollutant concentrations at distances several kilometres away from the source. In fact, the flow-structure of the plume is greatly influenced by a building in the near vicinity, as opposed to far-field problems where atmospheric turbulence is more important (Murakami et al., 1990).

Some of these Gaussian based models include AERMOD, ADMS, CALPUFF etc. ADMS-BUILD is a widely used model first described in the EUROMECH conference held in Lisbon in 1982 (Hunt and Robins, 1982) and its current version, ADMS 4, incorporates the features of ADMS-BUILD. An extensive study on the suitability of these models to simulate dispersion of pollutants for the case of isolated buildings was carried out by Stathopoulos et al., 2008 which concluded that most of these models were incapable of assessing plume concentrations within the recirculation length of the building where the flow structure is complex (Hajra et al., 2010). The main deficiency of most EPA models including ADMS and AERMOD is that they assume uniform concentrations within the recirculation region making them less reliable for such cases (EPA, 1995). On the basis of micro-scale dispersion studies Riddle et al., 2004 stated "*such atmospheric dispersion packages are not able to assess the local effects of a complex of buildings on the flow field and turbulence, and whether gas will be drawn down amongst the buildings."* ASHRAE is the only Gaussian-based model, which takes into account the recirculation region formed in the wake of a building to estimate plume

dilution on the roof. ADMS and AERMOD adopt the formulations of Fackrell and Pearce, 1981 to assess recirculation lengths of a building:

$$L_r = \frac{1.8W}{[(L/H)^{0.3}(1+0.24W/H)]} \qquad (0.3 \leq \text{L/H} \leq 3.0) \qquad (4.25)$$

where

W is the width of the building (m),

H is the height of the building (m)

However, recent studies by Hajra et al., 2011 have shown that dilution predictions by equation 4.25 produce overly conservative results. Hence, these models were not used for the present study.

**4.4 Summary**

This chapter described the ASHRAE dispersion models. It was observed that the geometric design principle to estimate minimum stack height has remained unchanged. However, changes have been suggested for the calculation of dilution using Gaussian plume equations for various ASHRAE models. In particular, ASHRAE 2011 has incorporated the effects of velocity profile and roughness length in assessing plume rise besides considering the effects of averaging time which was not a part of previous versions. It was also found that most other Gaussian models like ADMS and AERMOD are unsuitable for micro-scale dispersion modelling since they assume a uniform concentration distribution within the recirculation zone of a building. The subsequent chapter is devoted to the application of ASHRAE models to various building configurations that were investigated in the wind tunnel.

# Chapter 5

# Results and discussion

## 5.1 General

This chapter presents wind tunnel results for various building configurations and compares them to ASHRAE 2007 and ASHRAE 2011 models. At the outset, the different configurations tested in the wind tunnel showing the stack and receptor locations are presented. Three different cases were considered namely: a building placed upstream of an emitting building (source), a building placed downstream of the source and another case in which a building was placed upstream and downstream of the source. Each case is presented separately along with comparisons with ASHRAE models.

## 5.2 Configurations examined

Based on the flow visualisation tests described in Chapter 3, six building models made of wood were used for the study. A total of 18 different building configurations were examined to assess near-field plume characteristics in the presence of adjacent buildings. The dimensions of each building model are presented in Table 5.1.

Table 5.1 Dimensions of building models used for wind tunnel experiments

| Building | Height (m) | Width (m) | Breadth (m) | Recirculation Length | |
|---|---|---|---|---|---|
| | | | | ASHRAE (Eq. 4.1) | ADMS (Eq. 4.26) |
| $B_1$ | 15 | 50 | 50 | 22.3 | 35.9 |
| $B_2$ | 30 | 50 | 30 | 35.5 | 50.0 |
| $B_3$ | 30 | 50 | 15 | 35.5 | 79.1 |
| $B_4$ | 30 | 30 | 30 | 30.0 | 43.5 |
| $B_5$ | 54 | 50 | 15 | 51.2 | 105.6 |
| $B_6$ | 30 | 50 | 50 | 35.5 | 55.1 |

The recirculation lengths are calculated using ASHRAE and ADMS formulations described in Chapter 4. Table 5.1 shows that based on ASHRAE calculations, the lowest value of recirculation length is 22.3 m and the highest is 51.2 m. Since the study involves the examination of plume dispersion characteristics within building recirculation lengths, spacing between buildings were varied from 10 m to 50 m. ADMS predictions based on Fackrell and Pearce, 1981 (equation 4.25) show $L_r$ values higher than ASHRAE 2007. As discussed previously, ASHRAE 2007 estimates $\zeta$ as the difference between h and $H_c$, which is the maximum height of the roof recirculation zone and is calculated from Equation 4.1 as a function of $L_r$. However, if ASHRAE 2007 predictions of $L_r$ were higher (such as those in ADMS), values of $\zeta$ would eventually lead to lower dilution (higher rooftop concentrations) making the results even more conservative (Hajra et al., 2011).

Figures 5.1 through 5.5 present the different configurations along with stack and receptor locations on the building. The receptors are located only along the building centerline and not laterally over the various surfaces. For upstream configurations involving the low building, receptors were located 10 m apart on the windward wall and 5 m apart on the leeward wall of the upstream building with very few receptors located on the roof of the upstream building (Figure 5.1). For upstream building configurations involving the intermediate building, receptors were located about 10 m apart on the windward and leeward walls of the upstream building with very few receptors on the roof of the upstream building (Figure 5.2). Receptors were also located about 5 m apart on the roof of the emitting building, with few receptors on the windward and leeward walls for all upstream configurations.

Similarly for downstream configurations receptors were located about 5 m apart on the roof and windward wall of the downstream building and on the roof and leeward walls of the low and intermediate emitting buildings.

For configurations involving a building placed upstream and downstream of the source, receptors were located 5 m apart on all building surfaces except the windward wall of the upstream building and leeward wall of the downstream building, since these surfaces were unaffected by the plume based on flow visualisation studies. The stack location ($X_s$) was varied from 0 to 20 m and the stack height ($h_s$) varied from 1 m through 5 m. Exhaust momentum ratios (M) were varied from 1 to 3. This was done so that dilution characteristics for various building surfaces could be thoroughly assessed for different building configurations. Table 5.2 presents the various experimental parameters and their range of values.

Table 5.2 Experimental parameters and their respective range

| Parameter | Range |
|---|---|
| Stack height ($h_s$) | $1 \leq h_s \leq 5$ m |
| Exhaust momentum ratio (M) | $1 \leq M \leq 3$ |
| Stack location ($X_s$) | $0 \leq X_s \leq 20$ m |
| Spacing between upstream building and emitting building ($S_1$) | $10 \leq S_1 \leq 50$ m |
| Spacing between downstream building and emitting building ($S_2$) | $10 \leq S_2 \leq 50$ m |
| Wind azimuth ($\theta$) | 0°, 22.5°, 45° |

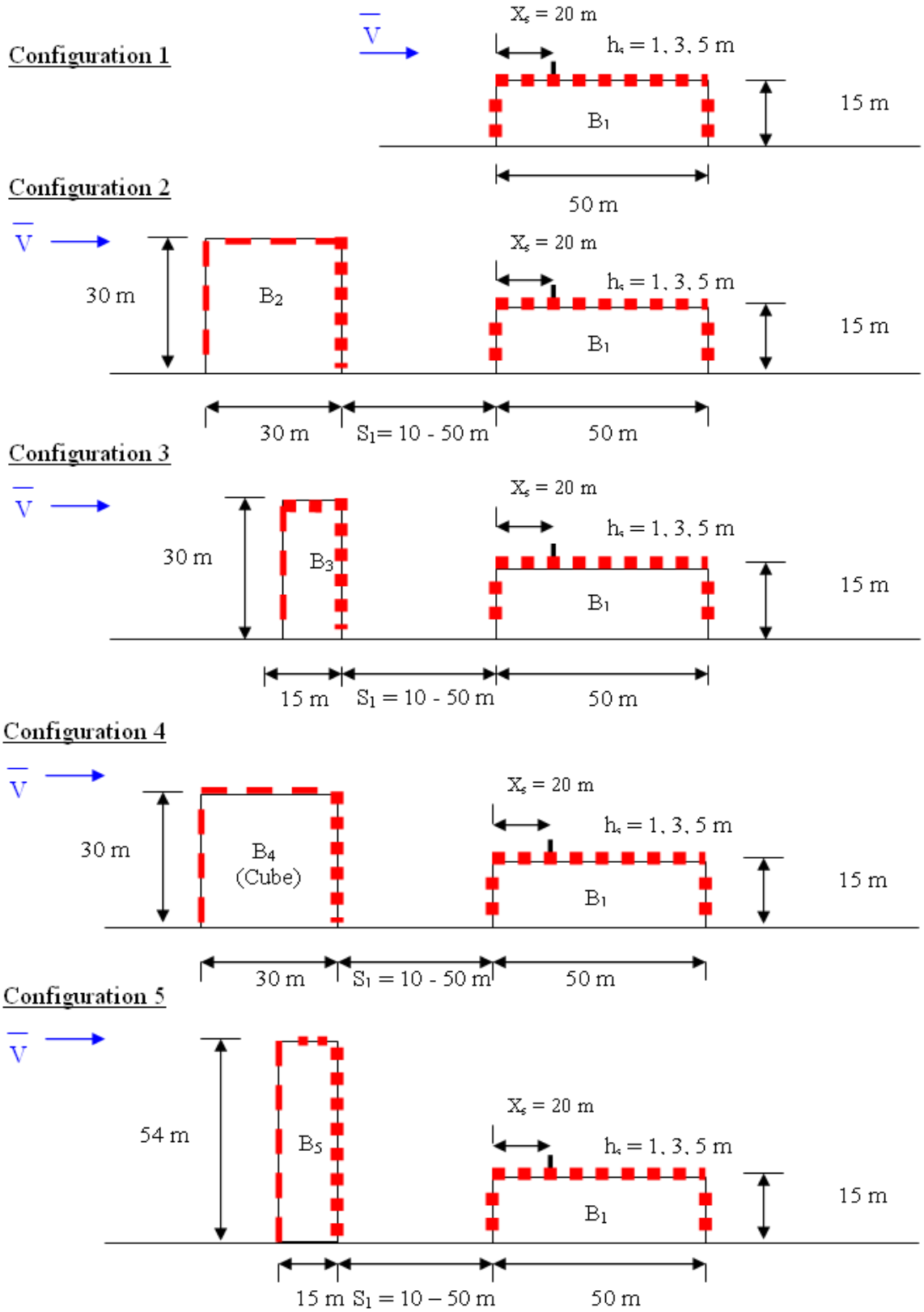


Figure 5.1: Configurations 1 to 5: Buildings of various geometries upstream of a low building

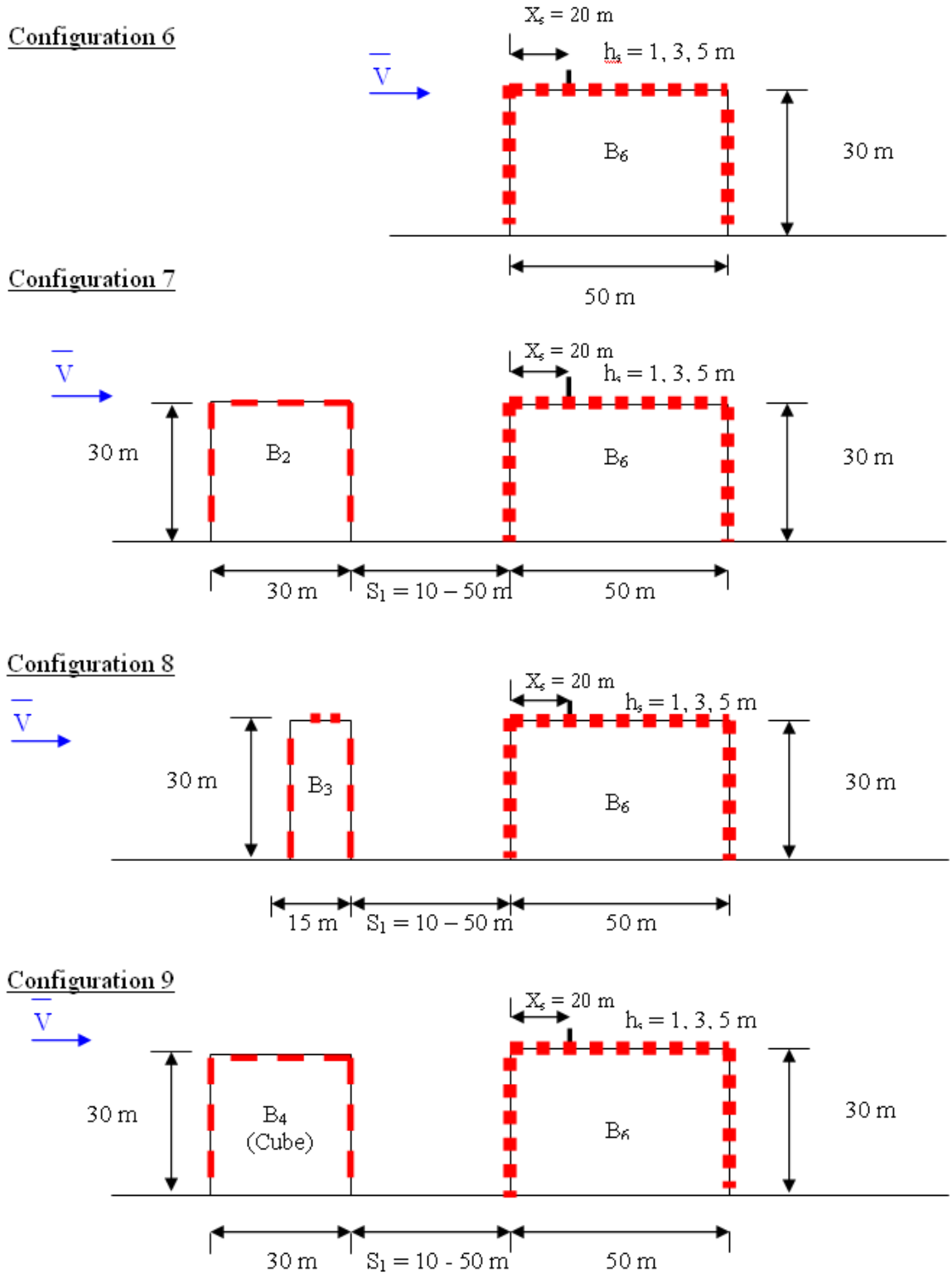


Figure 5.2: Configurations 6 to 9: Buildings of various geometries upstream of an intermediate emitting building

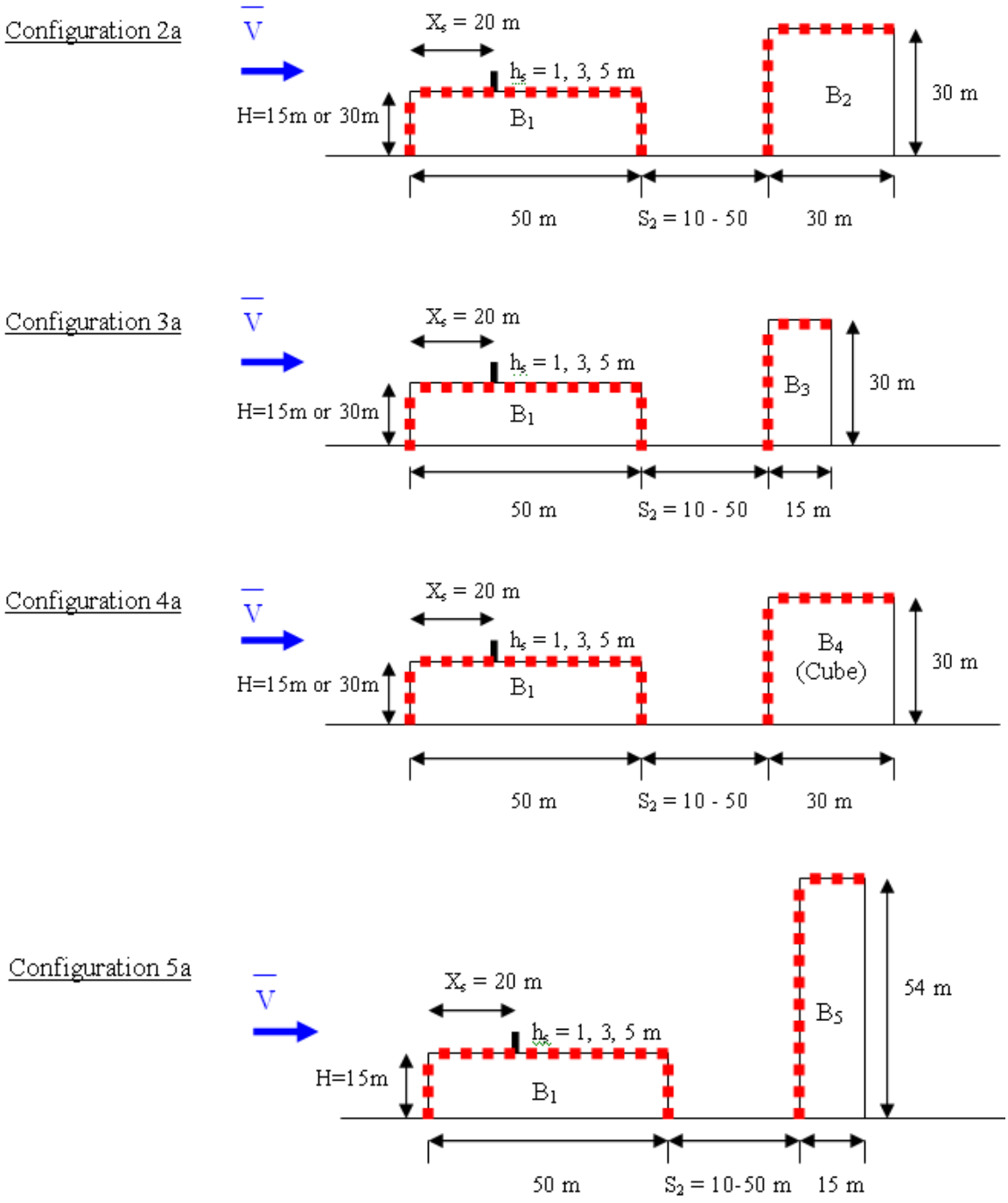


Figure 5.3: Buildings of various geometries downstream of a low building

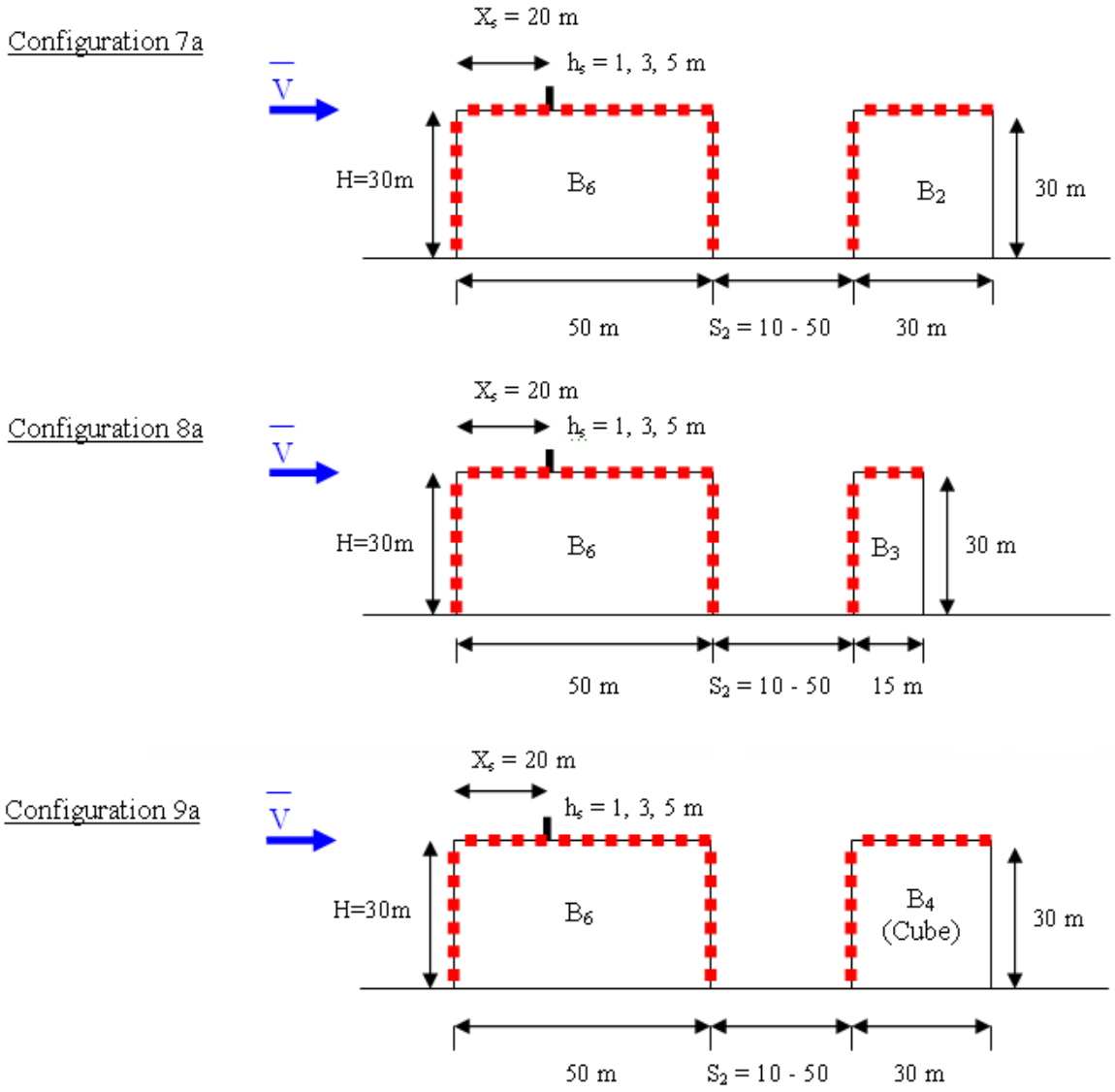


Figure 5.4: Buildings of various geometries downstream of an intermediate emitting building

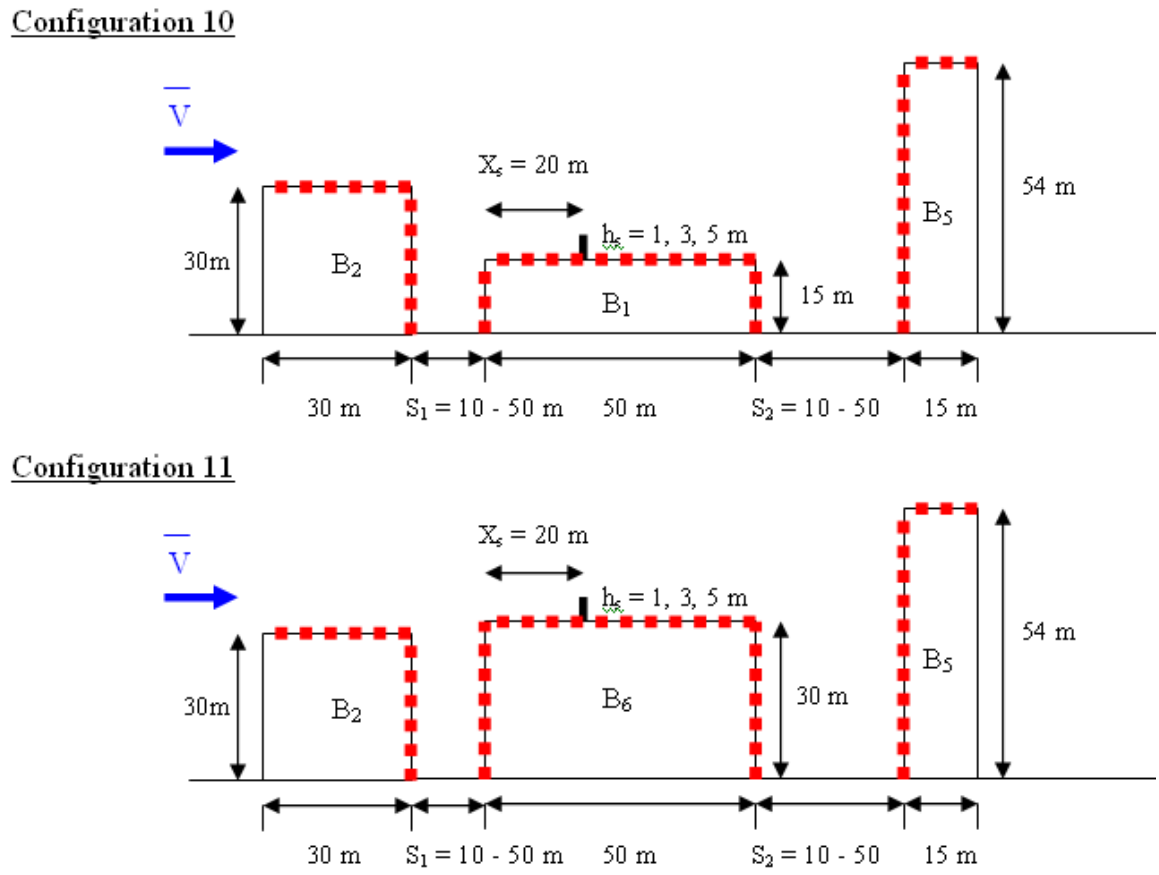


Figure 5.5: Configurations 10 and 11: Building placed upstream and downstream of a low and intermediate emitting building

Although, the tests were carried out for wind azimuth (θ) of $0^o$, $22.5^o$ and $45^o$, $\theta = 0^o$ was found to be the most critical; hence results in this chapter are only restricted to $\theta = 0^o$ (see Appendix B, Figures B8 and B9).

### 5.3 Reliability of wind tunnel data

Prior to presenting and discussing the results of this study, an attempt was made to compare the wind tunnel data with some previous results carried out by other researchers. This is necessary in order to check the reliability of wind tunnel data from the present study. In this context, Figure 5.6 shows comparisons between data from present study and

wind tunnel data from Schulman and Scire, 1991 and Lowery and Jacko, 1996 in terms of normalised dilution for an isolated building case.

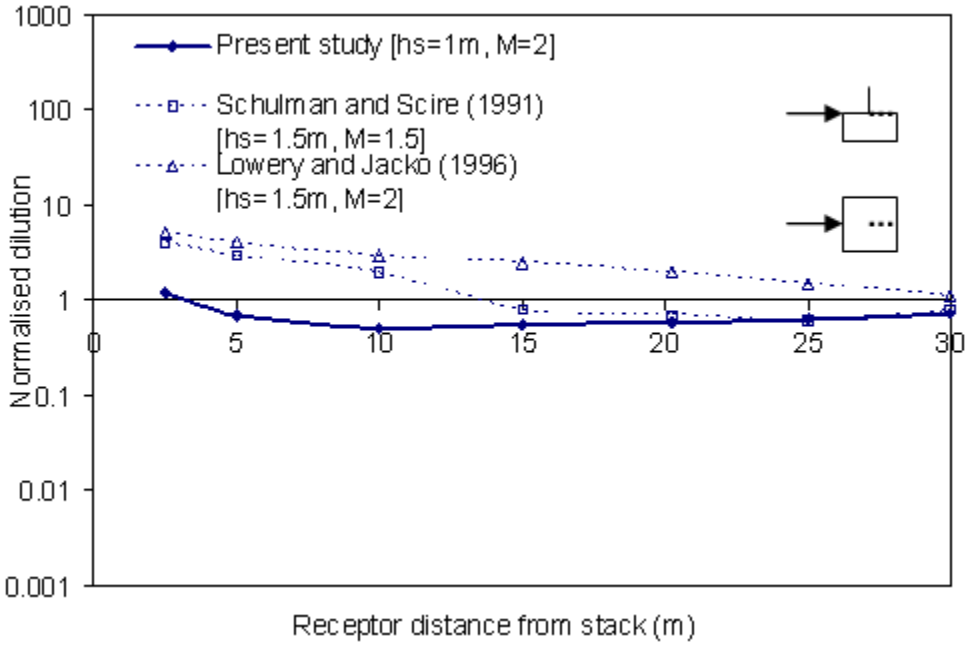


Figure 5.6 Comparison of wind tunnel measured dilution and those from previous studies

Despite different experimental conditions, as described in Table 5.3, the agreement between results obtained from the present study and Lowery and Jacko, 1996 is good, especially at points closer to the downwind edge of the emitting building. However, close to the upwind edge of the building, results from the present study are about a factor of 5 lower than the dilutions obtained from Lowery and Jacko, 1996. This discrepancy is attributed to the urban exposure used in the present study as opposed to a suburban terrain in Lowery and Jacko's study. Wind tunnel data obtained from Schulman and Scire, 1991 are higher than the present study especially at points closer to the stack, because the building is much larger and its height is about half compared to the present

study. Additionally, a suburban terrain was used as opposed to an urban terrain in the present study.

Table 5.3 Experimental parameters used for the present and previous studies.

| Experimental parameters | Present study | Schulman and Scire, 1991 | Lowery and Jacko, 1996 |
|---|---|---|---|
| Model scale | 1:200 | 1:100 | 1:120 |
| Wind speed at building height (m/s) | 6.2 | 1.37 | 3.4 |
| Upstream terrain | Urban | Suburban | Suburban |
| Power law exponent | 0.31 | 0.20 | 0.23 |
| Stack diameter (m) | 0.6 | 0.75 | 0.75 |
| Building height (m) | 15 | 15 | 7 |
| Building width (m) | 50 | 75 | 90 |
| Building breadth (m) | 50 | 75 | 90 |

NB: Width refers to building dimension perpendicular to wind direction at $0^{o}$.

Despite these differences, the overall comparisons and trends of data are encouraging. The subsequent sections of this chapter focus on the various configurations that were tested in the wind tunnel and comparisons with ASHRAE models. First the upstream building configurations are presented.

## 5.4 Upstream configurations tested in the wind tunnel

This section focuses on the various upstream configurations that were tested in the wind tunnel and is sub-divided into three parts, namely: The effects of a taller upstream building, buildings of equal height and effect of spacing between buildings on near-field pollutant dispersion. From the six building models described in Chapter 3 (Table 3.3),

nine configurations were tested in the wind tunnel (7-upstream and 2-isolated cases) as shown in Figures 5.1 and 5.2. It may be noted that results in this section are presented for the roof and leeward wall of the emitting building and leeward wall of the taller upstream building for all upstream configurations since tracer gas was only found at these locations.

### *5.4.1 Effect of a taller upstream building*

A taller building placed upstream of low building causes the plume to travel towards the leeward wall of the upstream building as discussed in Chapter 3 (Figure 3.10). This affects the roof and leeward wall of the emitting building and leeward wall of the upstream building. Results expressed as normalised dilution on the rooftop of the emitting building, are discussed further.

#### *5.4.1.1 Dilution on rooftop of emitting building ($B_1$) for $X_s = 0$*

Figure 5.7 shows comparisons of dilution between Configurations 1 through 5, ASHRAE 2007 and ASHRAE 2011 at rooftop receptors on the 15 m high building ($B_1$) for a stack placed at the upwind edge of the emitting building$_1$ ($X_s = 0$) for $S_1 = 20$ m. Figure 5.7 (a) shows comparable dilution obtained at all receptors for Configurations 1 through 4 indicating that a change in along wind and across wind dimension of the upstream building did not affect the rooftop dilution at M = 1. Configuration 5 produced measurable dilution at only the first two points from the edge. This is attributed to the recirculation length of the upstream building ($B_5$), which is quite large (51.2 m) for

Configuration 5 and possibly forces a major part of the plume to affect the leeward wall of the upstream building with a portion of it getting trapped between the buildings.

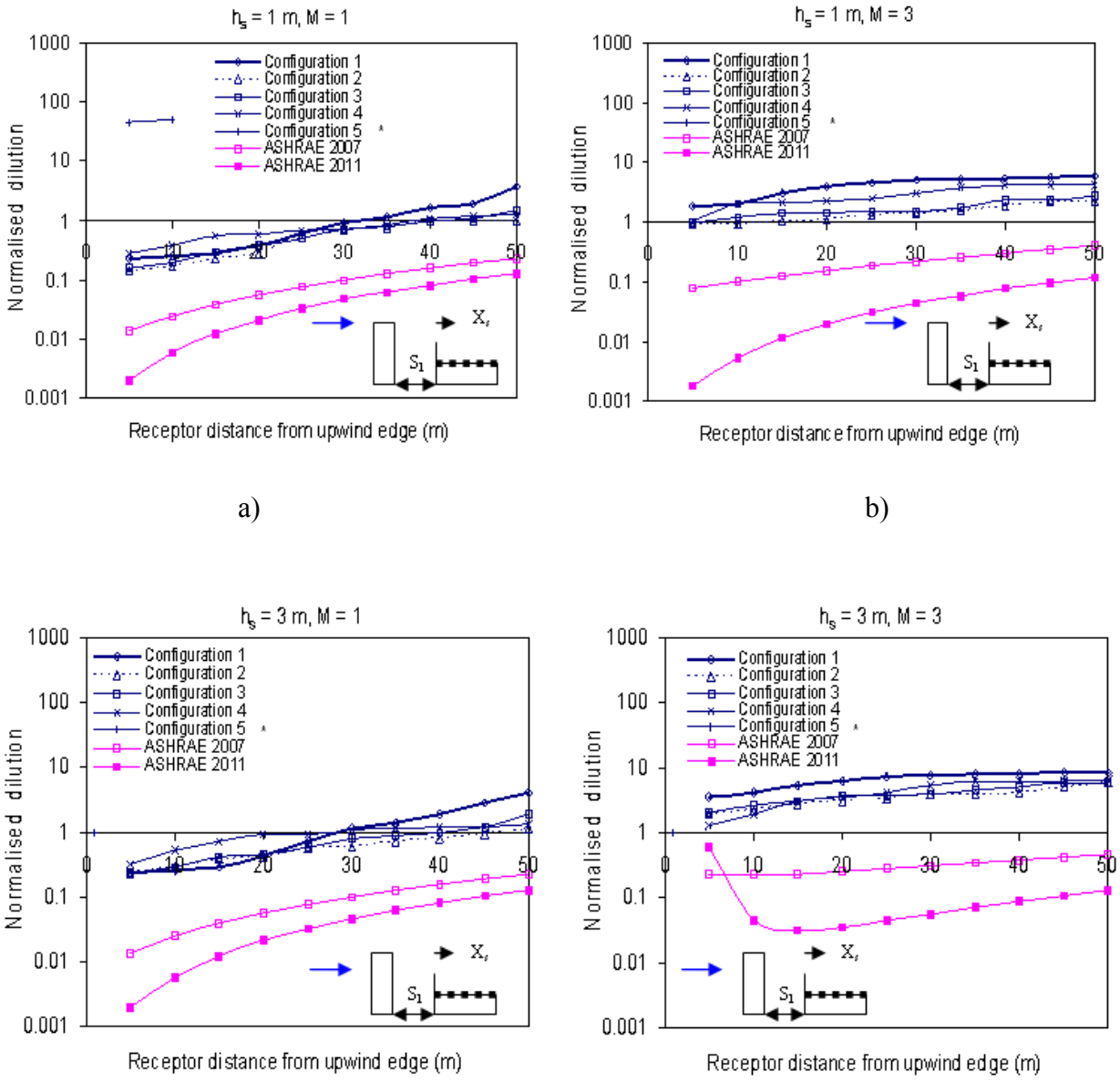


Figure 5.7. Normalised dilution on rooftop of $B_1$ for $X_s = 0$ and $S_1 = 20$ m: a) $h_s = 1$ m, M = 1; b) $h_s = 1$ m, M = 3; c) $h_s = 3$ m, M = 1; d) $h_s = 3$ m, M = 3 (* Pollutant concentrations were zero at all receptors except the first two receptors in Figure 5.7 (a))

Furthermore, due to the turbulence created in the wake of the upstream building, the plume may not traverse a path in line with the stack but may actually travel along the sides of the emitting building. However, at $h_s$ = 1 m and M = 3, although comparable dilution was found for Configurations 2 and 3, Configuration 4 produced somewhat higher dilution than Configuration 2. This is because a smaller zone of recirculation exists in the wake of the narrow upstream building in Configuration 4 (30 m); this effect is more predominant at M = 3 because downwash effects are reduced and the plume has a greater scope to escape the recirculation cavity of the upstream building. The dilution for Configurations 2, 3 and 4 were generally lower than the isolated case. When $h_s$ > 1 m the dilution for Configurations 2, 3 and 4 become comparable to the isolated case as shown in Figure 5.7 (c) due to increased plume height. A similar trend is also observed for $h_s$ = 3 m and M = 3, as shown in Figure 5.7 (d). As the stack height is increased further, the plume gets a greater scope to escape the zone of recirculation of the upstream building. This results in comparable dilution for all upstream configurations with the isolated case. ASHRAE 2007 predicts lower dilution for all configurations, clearly because it does not consider the effect of turbulence generated by the upstream building or stack and local topography. ASHRAE 2011 generally predicts lower dilution at all receptors than the isolated case for any given $h_s$ and M value due to the plume spread parameters which are functions of $Z_o$ and building height, as described in Chapter 3. Additionally the plume rise estimates (equation 4.14, Chapter 4) predict lower values than ASHRAE 2007 resulting in overly conservative estimates. Only at $h_s$ = 3 m and M = 3, very close to the stack, ASHRAE 2011 predicts about 5 times higher dilution than ASHRAE 2007 because the plume rise estimates are somewhat higher at this particular receptor due to equation

4.16. In general, ASHRAE 2011 states that "*Only jet momentum rise is used; buoyancy rise is neglected as a safety factor."* The additional safety factor in plume rise estimation limits the plume rise and predicts lower dilution than wind tunnel data at all points.

### *5.4.1.2 Dilution on leeward wall of the upstream building ($B_2$, $B_3$ and $B_4$)*

Figure 5.8 (a) presents normalised dilution on leeward walls of $B_2$ (Configuration 2), $B_3$ (Configuration 3) and $B_4$ (Configuration 4) for $h_s$ = 1 m and M = 1. ASHRAE formulations can only be used to predict rooftop dilution on an emitting building and does not predict dilution on the leeward walls of a building.

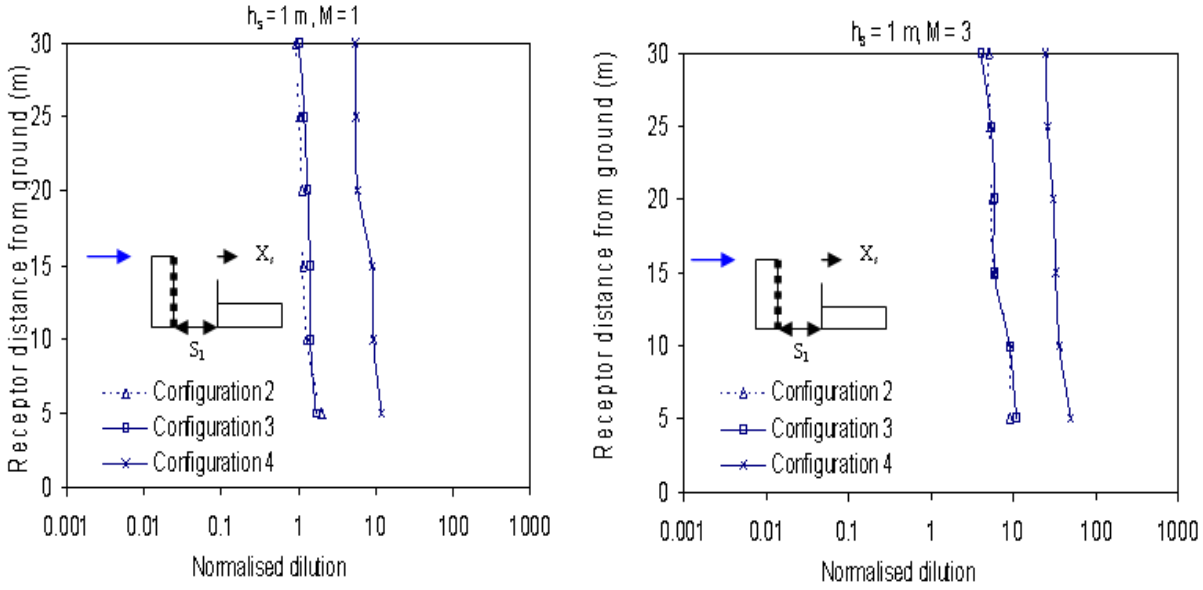


a) b)

Figure 5.8. Normalised dilution on leeward wall of upstream building for $X_s$ = 0 and $S_1$ = 20 m: a) M = 1; b) M = 3

It may be noted that the upstream building in these configurations is twice the height of the emitting building. Comparable dilution for Configurations 2 and 3 were found at

all points on the leeward wall of the upstream building whilst Configuration 4 resulted in almost 10 times higher dilution than Configurations 2 and 3. This is due to a reduced across wind dimension of the narrow upstream building in Configuration 4 that creates a smaller recirculation length downwind of the building. A similar trend is also observed for M = 3 as shown in Figure 5.8 (b). For greater stack heights ($h_s$ > 1 m) no pollutant concentration was found on the leeward wall of the upstream building due to a plume height more than 3 m above the building surface resulting in greater dispersion of the plume. In such case, the plume mostly affects the rooftop of the emitting building thereby leaving the upstream building unaffected. When the stack was placed at 20 m away from the upwind edge of the building, the plume was sufficiently away from the upstream buildings recirculation zone making the tracer concentrations so greatly diluted that they were undetectable on the leeward wall of the upstream building.

However, a taller upstream building (Configuration 5) of 54 m generated a larger recirculation zone (51.2 m as per ASHRAE) resulting in pollutant concentrations at $h_s$ < 3 m even for a centrally placed stack; although the trends were similar to Configurations 2 and 3 (see Appendix B).

#### *5.4.1.3 Dilution on leeward wall of the emitting building*

Small quantities of tracer concentrations were also found on the leeward wall of the emitting building especially for low stack heights as discussed in this section. Comparable dilution for Configurations 2, 3 and 4 were found on the leeward wall of the low building ($B_1$) as shown in Figure 5.9 (a) for $h_s$ = 1 m and M = 1. This is because most of the pollutants affected the leeward wall of the upstream building and the rooftop of the

emitting building with a very small potion of the pollutant accumulating close to the leeward wall of the emitting building.

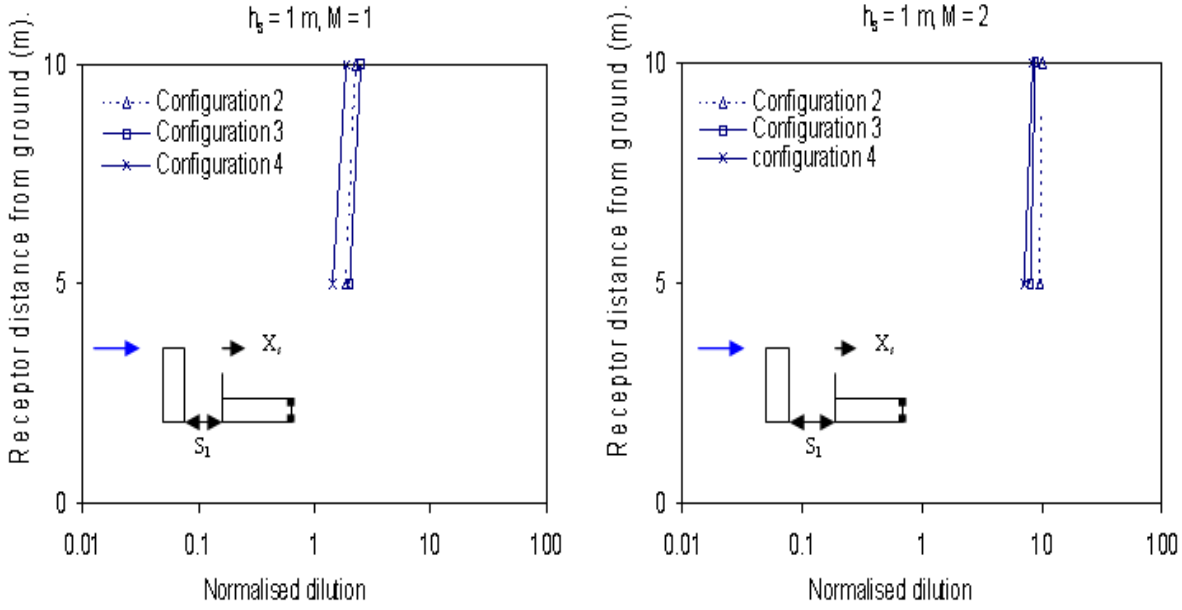


a) b)

Figure 5.9 Normalised dilution on leeward wall of emitting building for $X_s = 0$ and $S_1 = 20$ m: a) M = 1; b) M = 2

A similar trend was observed at $h_s$ = 1 m and M = 2 as shown in Figure 5.9 (b). However, at greater stack heights ($h_s$ > 1 m) concentration of the gas reduced considerably resulting in a smaller portion of effluents being engulfed within the recirculation length downwind of $B_1$. For centrally placed stacks the plume spreads even further to escape the zone of recirculation leaving the leeward wall of $B_1$ unaffected. The subsequent section describes the plume behaviour for a taller upstream building with a centrally placed stack. ASHRAE does not provide formulations to estimate wall dilutions.

#### *5.4.1.4 Dilution on rooftop of the emitting building ($B_1$) at $X_s$ = 20 m*

Figure 5.10 (a) shows rooftop dilution comparisons for Configurations 1 through 5, ASHRAE 2007 and ASHRAE 2011 for $h_s$ = 1 m, M = 1 at $X_s$ = 20 m. It may be mentioned that Configurations 3 and 5 have $B_3$ and $B_5$ upstream of $B_1$ respectively, also the height of $B_5$ is nearly twice as much as that of $B_3$ (see Figure 5.1). A larger recirculation zone is formed in the wake of the upstream building in Configuration 5 than in configuration 3 causing greater pollutant concentration on the roof of the emitting building in the former compared to the latter case. However, the dilutions become comparable beyond 20 m since the effect of upstream building height gradually reduces downwind of the stack. For upstream buildings of equal height and width, a greater along wind dimension does not affect the recirculation zone formed downwind of it. Hence, comparable dilutions for Configurations 2 and 3 are obtained at all points. If the upstream building is longer, flow reattachment is likely to occur but since the heights of the two upstream buildings are equal, the turbulence generated in the wake of the upstream buildings is likely to be of the same magnitude thereby leaving the emitting building very little affected. It is not surprising that no effluent concentrations were found on the rooftop of the emitting building for Configuration 4 within the first 20 m. This is because the upstream building ($B_4$) has a smaller recirculation length (30 m) and since the stack is placed sufficiently away from the upwind edge, the plume easily overcomes the recirculation zone of the upstream building, thereby affecting only receptors downwind of stack. ASHRAE 2007 and ASHRAE 2011 predict lower dilution than all configurations and do not report dilution at receptors upwind of stack.

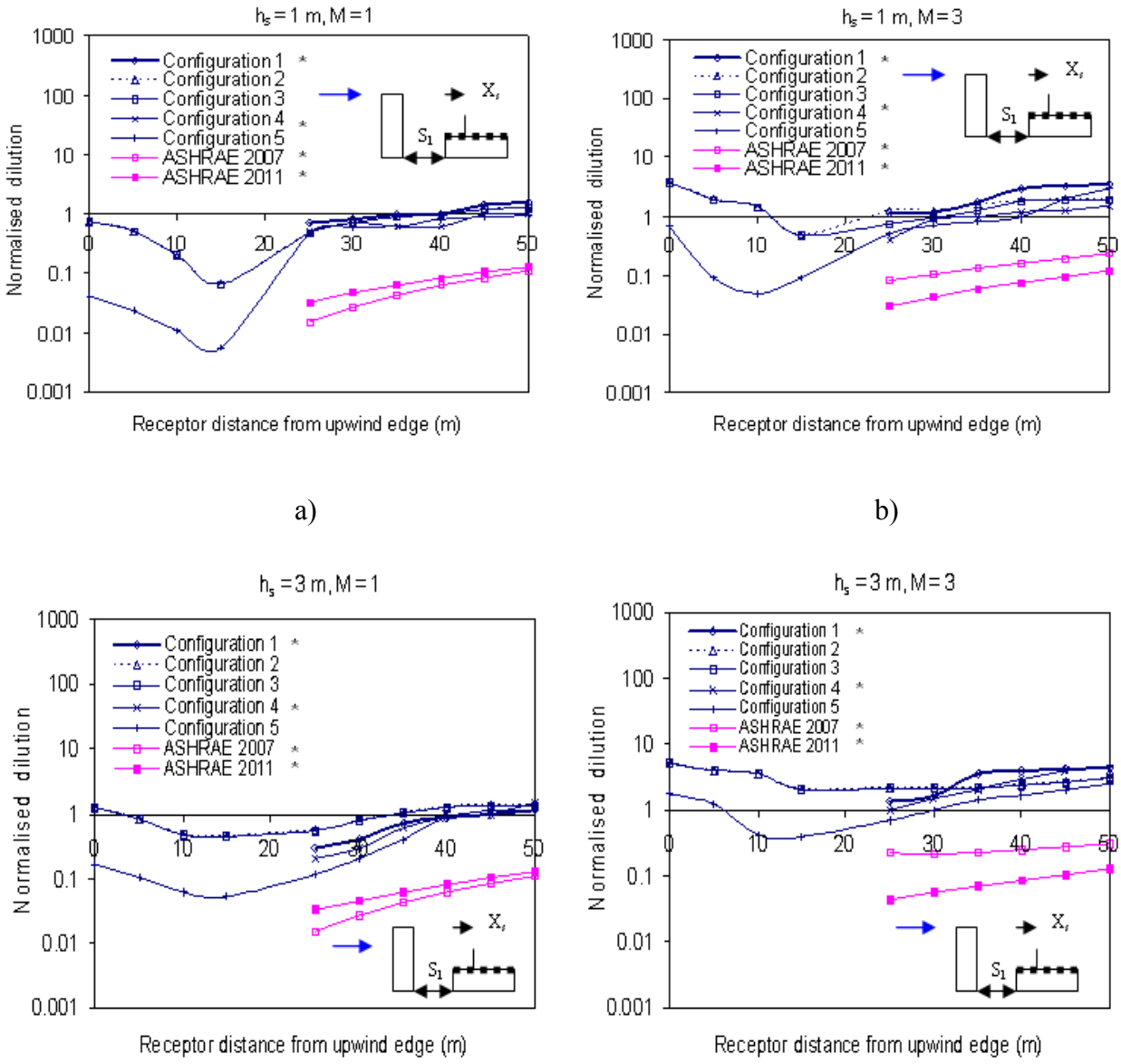


Figure 5.10 Normalised dilution on rooftop of emitting building ($B_1$) for $X_s$ = 20 m and $S_1$ = 20 m: a) $h_s$ = 1 m, M = 1; b) $h_s$ = 1 m, M = 3; c) $h_s$ = 3 m, M = 1; d) $h_s$ = 3 m, M = 3

A similar trend is also observed at $h_s$ = 1 m and M = 3 as shown in Figure 5.10 (b). At $h_s$ > 1 m, Configurations 2, 3 and 5 produce rooftop concentrations at all receptors although the dilution values increase with higher M values (Figure 5.10 (c) and (d)). In

general, the dilution obtained from all configurations become comparable at receptors downwind of stack. ASHRAE 2011 predictions become comparable to ASHRAE 2007 at some receptors at low M values due to similar plume spread parameter estimates although dilution estimates by the former are lower than the latter at M > 1, as shown in Figure 5.10 (d).

The effect of placing an upstream building of equal or similar height as the emitting building is discussed further.

### *5.4.2 Effect of an upstream building of similar height*

Figure 5.11 (a) presents rooftop dilution comparisons for Configurations 6 through 9 ASHRAE 2007 and ASHRAE 2011 for $h_s$ = 1 m, M = 1 and $X_s$ = 0. It was observed that within the first 20 m from the stack, comparable dilution was obtained for all configurations with the isolated case, following which the dilution obtained from the upstream configurations is lower than the isolated case. This is because the recirculation cavity in the wake of the upstream building is not sufficiently large to bring the plume towards itself but generates sufficient turbulence to keep the plume closer to the roof of $B_6$. It may also be noted that Configuration 9 predicts higher dilution than Configuration 7 beyond 30 m from the stack because the former has a narrow upstream building compared to the latter. This suggests that at low exhaust speeds and stack height a reduced across wind dimension of the upstream building increases rooftop dilution on the emitting building which is similar to the findings of a taller upstream building discussed previously. Comparable dilution between Configurations 7 and 8 also suggests that a change in along wind dimension of the upstream building did not affect the plume

geometry. Dilution produced by all configurations gradually become comparable to the isolated case for higher $h_s$ and M values as shown in Figures 5.11 (c) and (d).

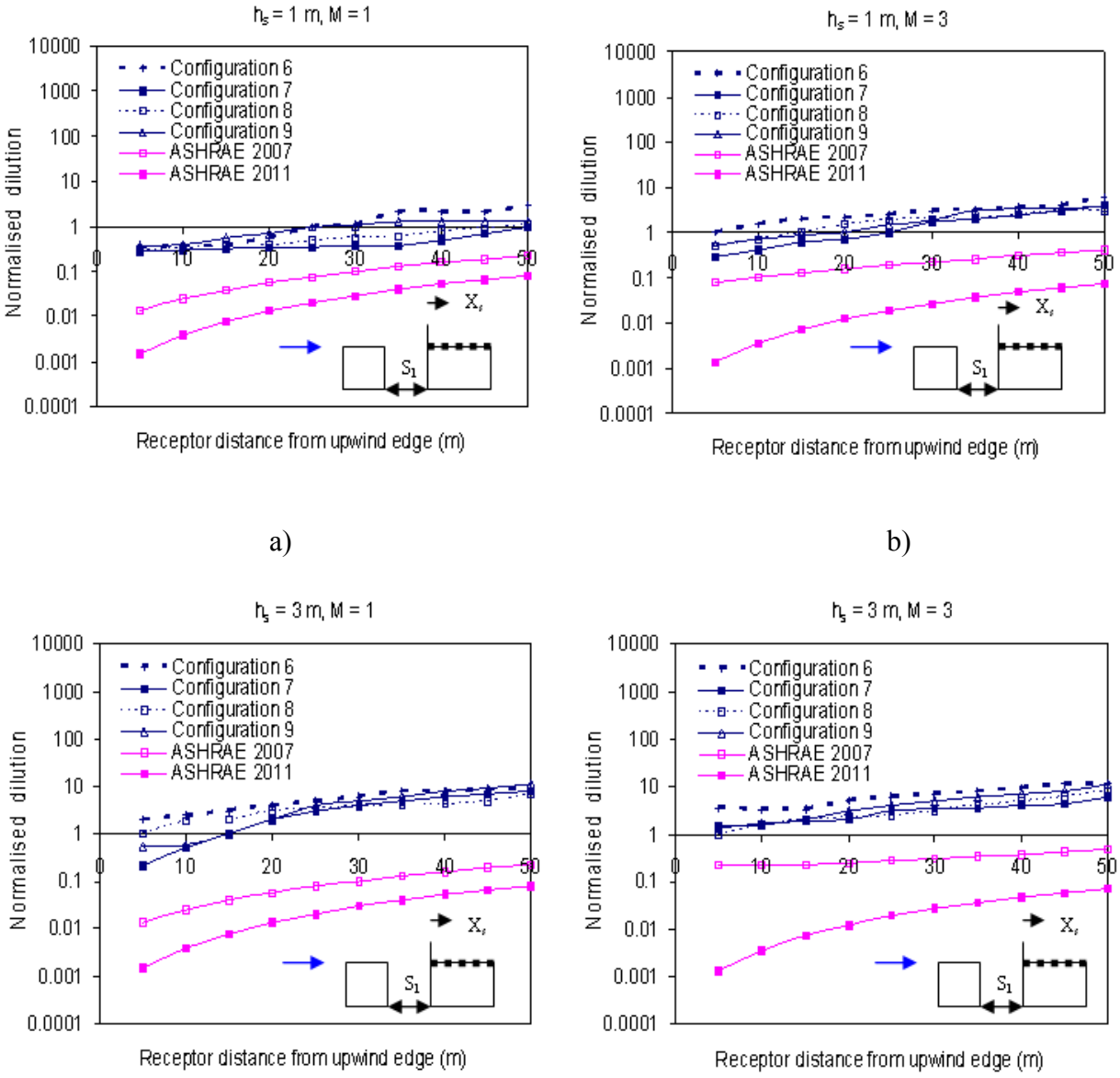


Figure 5.11 Normalised dilution on rooftop of emitting building ($B_6$) for $X_s$ = 0 and $S_1$ = 20 m: a) $h_s$ = 1 m, M = 1; b) $h_s$ = 1 m, M = 3; c) $h_s$ = 3 m, M = 1; d) $h_s$ = 3 m, M = 3

ASHRAE 2007 and ASHRAE 2011 continue to predict lower dilution than all configurations at all receptors, as discussed previously. ASHRAE 2011 predicts lower dilution than the isolated case since the plume rise estimation is quite low and the spread parameters decrease with increased building height, making it necessary to re-visit its formulations.

The results and discussion in the preceding sections were devoted to buildings spaced 20 m apart. In fact, for most cases it was found that the dilution remained unchanged for spacing between 20 m and 30 m. This is because within this range the plume geometry does not change significantly. However, as the spacing between buildings exceeds this range, the effect of the upstream building gradually reduces as discussed further.

### *5.4.3 Effect of spacing between buildings*

Figure 5.12 (a) presents normalised dilution on the leeward wall of the upstream building for Configuration 3 for $h_s$ = 1 m, M = 1 and $X_s$ = 0. Comparable dilution was obtained for $S_1$ = 20 m and $S_1$ = 30 m at all receptors on the wall since both these distances are within the recirculation length of the upstream building $B_3$ (35.5 m). However, at $S_1$ = 40 m the dilution was found to be more than about 10 times higher than that found at $S_1$ = 20 m since at distances beyond the recirculation length of $B_3$ the plume does not affect the upstream building greatly. It is not surprising, that at $S_1$ > 40 m dilutions were so high that concentrations were undetectable.

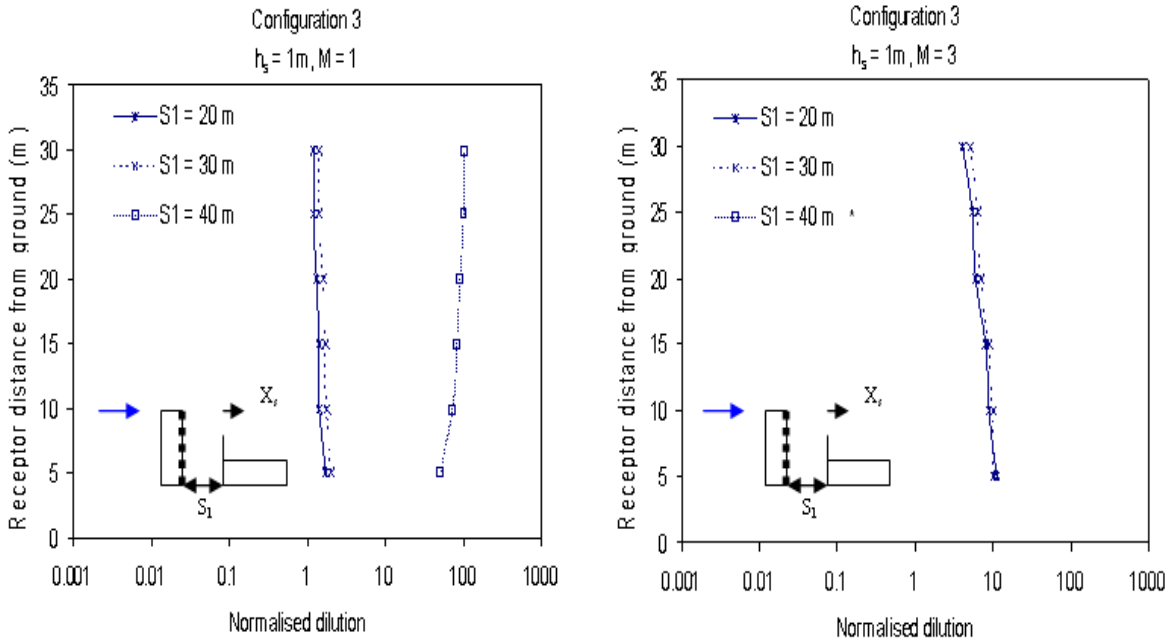


a) b)

Figure 5.12 Normalised dilution on leeward wall of $B_3$ for $X_s = 0$: a) M = 1; b) M = 3 (* Concentration of pollutants was found to be zero)

Similar findings were reported for $h_s$ = 1 m, M = 3, as shown in Figure 5.12 (b) where although dilution at $S_1$ = 20 m and $S_1$ = 30 m were comparable, no concentrations were found at $S_1$ = 40 m because at higher exhaust speeds the effluents escape the recirculation region of the upstream building.

The effect of spacing on rooftop dilution of emitting building was also studied as shown in Figure 5.13. Comparable dilution was found at $S_1$ = 20 m, 30 m and 40 m on rooftop of $B_1$ (emitting building) for Configuration 3 at $h_s$ = 1 m, M = 1 and $X_s = 0$, as shown in Figure 5.13 (a). Similar observations were made at $h_s$ = 1 m and M = 3 as shown in Figure 5.13 (b). Although dilutions at $S_1$ = 20 m and 30 m are somewhat lower

than those found at $S_1$ = 40 m and the isolated case (Configuration 1), trends are almost identical.

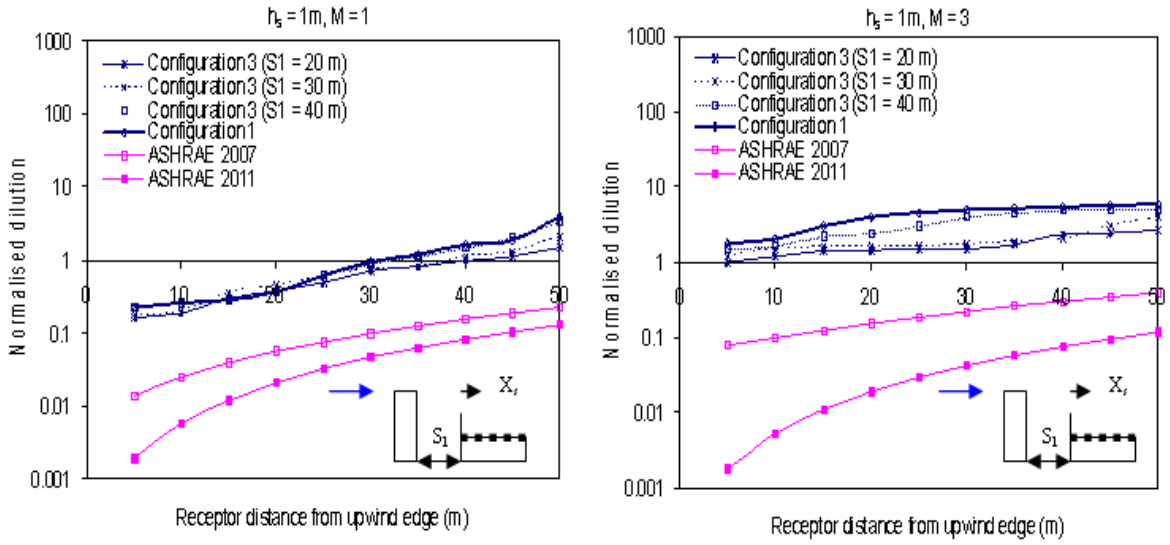


a) b)

Figure 5.13. Normalised dilution on rooftop of $B_1$ for $X_s$ = 0: a) M = 1; b) M = 3

This is because an increase in spacing reduces the upstream building's effect and allows the plume to disperse through the air, thereby affecting the roof of the emitting building. As explained previously, ASHRAE 2007 and 2011 predictions are overly conservative and are only valid for the isolated case.

A taller upstream building (such as in configuration 5) generates lower dilution on the roof of the low building ($B_1$) than Configuration 3 for similar spacing between buildings, although the trends remain unchanged - see Appendix B for additional results. The subsequent section describes the various downstream building configurations that were tested in the wind tunnel and compares them to ASHRAE models.

## 5.5 Downstream building configurations tested in the wind tunnel

This section discusses the effect of different building geometries placed downstream of the emitting building. Shorter downstream buildings do not affect the rooftop dilution on an emitting building since the plume structure remains unaffected. Similar observations were also made by Wilson et al., 1998 through water channel studies for some limited cases. Hence, the present study discusses taller downstream buildings and buildings of similar height as the emitting building, since these cases were found to be more critical. Pollutant concentrations were found on the roof and leeward wall of the emitting building as well as on windward wall and roof of the downstream building. First the effect of a taller or similar downstream building within the recirculation zone of the emitting building is discussed, followed by the effects of spacing between the buildings.

### *5.5.1 Effect of a taller or similar downstream building*

The effects of a downstream building taller or of similar height with the emitting building are presented and discussed in this section.

#### *5.5.1.1 Rooftop dilution on the emitting building*

Figure 5.14 (a) shows comparisons of Configurations 1, 2a through 5a, ASHRAE 2007 and ASHRAE 2011 for $h_s$ = 1 m, M = 1, $S_2$ = 20 m and $X_s$ = 0. It may be noted that although, $B_2$, $B_3$ and $B_4$ are twice as tall as $B_1$, the along wind dimension of $B_3$ is half of $B_2$ and across wind dimension of $B_4$ is 60% of $B_2$ (see Figure 5.3). Comparable dilution was found at all points for Configurations 2a and 3a. This is because a change in along

wind dimension of the downstream building does not affect the plume geometry significantly.

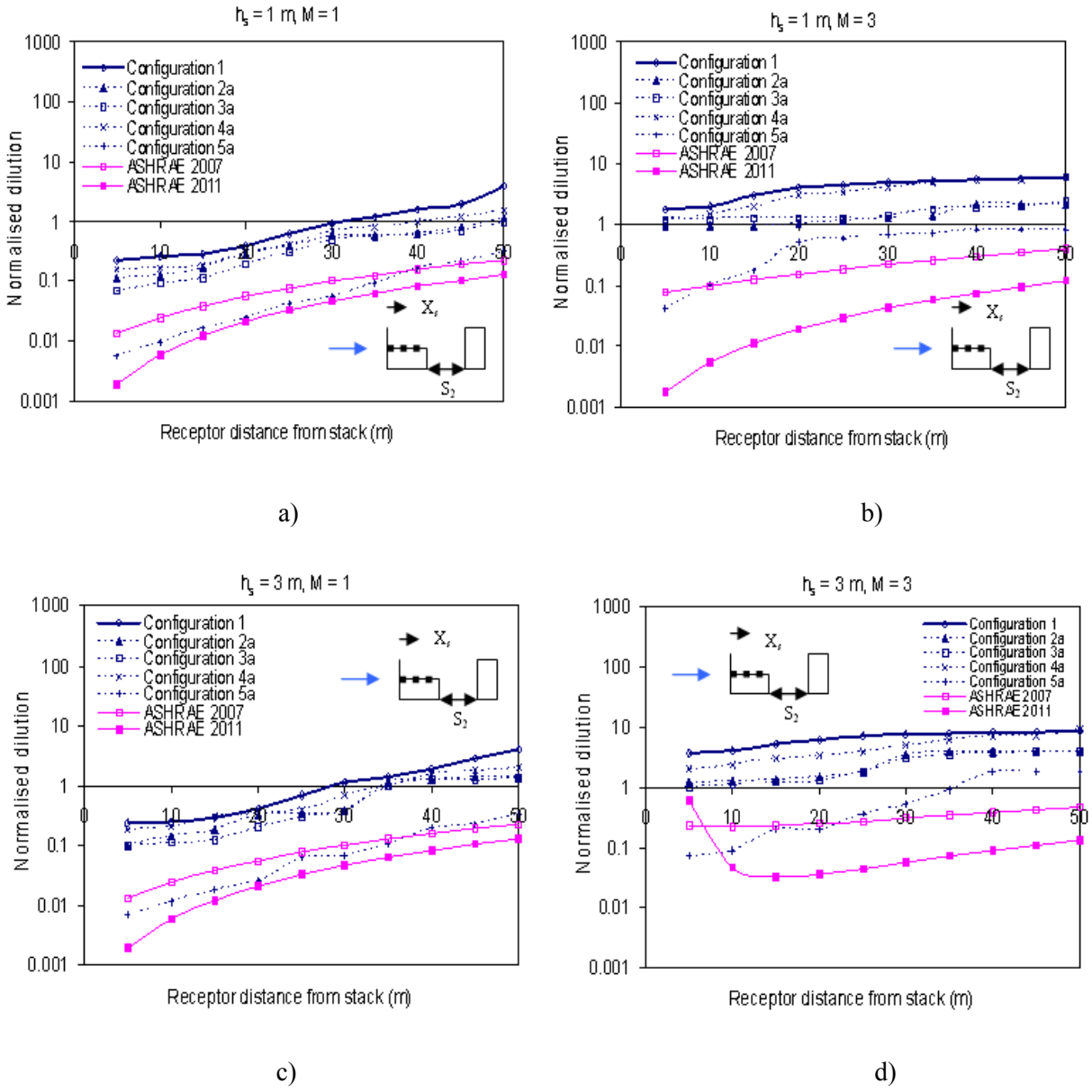


Figure 5.14. Normalised dilution on rooftop of $B_1$ for $X_s$ = 0 and $S_2$ = 20 m: a) $h_s$ = 1 m, M = 1; b) $h_s$ = 1 m, M = 3; c) $h_s$ = 3 m, M = 1; d) $h_s$ = 3 m, M = 3

However, Configuration 4a predicts higher dilution than Configurations 2a and 3a because a narrow building allows a greater portion of the plume to escape through side-

leakage leading to higher rooftop dilutions on the emitting building, although dilutions are somewhat lower than the isolated case. Configuration 5a predicts about 10 times lower dilution than Configurations 2a and 3a due to the height of the downstream building ($B_5$), which restricts the plume from dispersing through the air. ASHRAE 2007 and 2011 predict very low dilution compared to experimental data leading to overly conservative design. A similar trend is observed at $h_s$ = 1 m and M = 3, as shown in Figure 5.14 (b) although the dilution for Configurations 4a and 1 become comparable, especially at receptors close to the downwind edge of $B_1$ because higher exhaust speeds and smaller across wind dimension of the downstream building enhances greater plume spread to reduce the effect of the downstream building. At greater $h_s$ and M values the dilution predicted by Configurations 2a, 3a and 4a become comparable to the isolated case, particularly closer to the downwind edge, as shown in Figures 5.14 (c) and 5.14 (d). As explained previously, the spread parameters in ASHRAE 2011 are functions of building height and roughness length unlike the 2007 version which is based on exhaust momentum ratio. Therefore, the spread parameters in ASHRAE 2011 do not change irrespective of $h_s$ and M and are generally lower than ASHRAE 2007, making it necessary to re-visit these formulations. Additional results on downstream configurations can be found in Appendix C.

For buildings of similar height, Figure 5.15 (a) shows comparisons for Configurations 6, 7a through 9a, ASHRAE 2007 and ASHRAE 2011 in terms of normalised dilution on rooftop of $B_6$ for $h_s$ = 1 m, M = 1 and $X_s$ = 0. It must be noted that Configurations 7a and 8a have $B_2$ and $B_3$ downstream of $B_6$ respectively with the along wind dimension of the former twice as much as the latter.

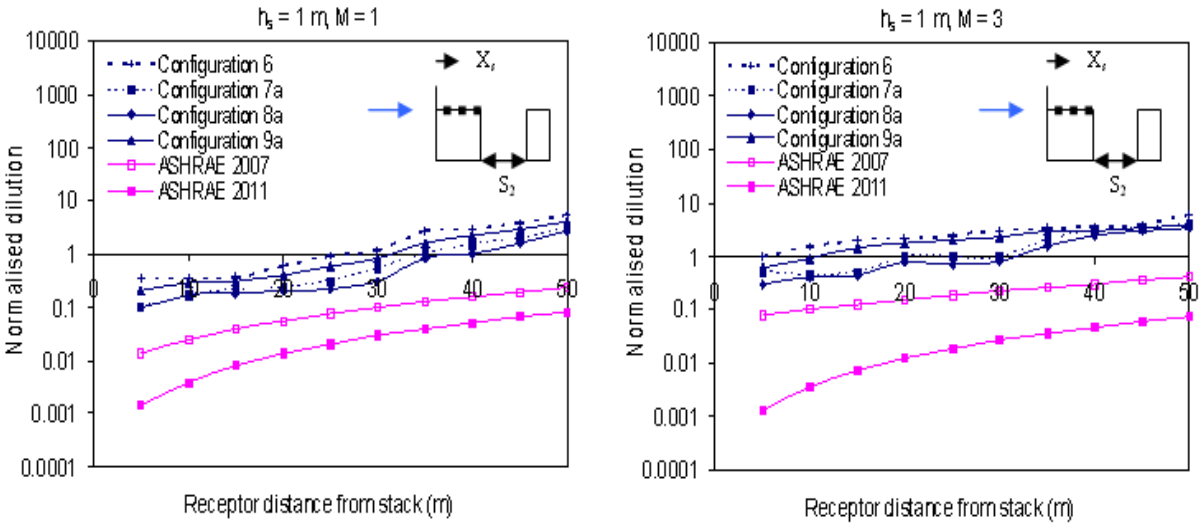


a) b)

Figure 5.15. Normalised dilution on rooftop of $B_6$ for $X_s = 0$ and $S_2 = 20$ m: a) M = 1; b) M = 3

Comparable dilution was found at all receptors on the rooftop of $B_6$ for Configurations 7a and 8a because a longer downstream building would only make the plume travel a marginal distance without affecting the plume geometry significantly. However, Configuration 9a predicts higher dilution than Configurations 7a and 8a due to increased side-leakage. In general, the dilution predicted by all the configurations is lower than the isolated case. This trend remains almost unchanged for $h_s = 1$ m and M = 3, as shown in Figure 5.15 (b) although the dilution is somewhat higher than that found for M = 1. Also at some points closer to the downwind edge of the emitting building, dilution predicted by all configurations are comparable to the isolated case. ASHRAE 2007 and ASHRAE 2011 predict lower dilution than all configurations due to the formulations discussed previously.

For higher $h_s$ and M the dilution generated by all configurations were found to be comparable to the isolated case indicating the reduced effects of the downstream building. When the stack is placed at $X_s$ = 20 m the possibility of plume meandering reduces since the downstream building is of equal height as the source. Hence, comparable dilution for all Configurations was obtained for a given M at $h_s$ > 1 m (see Appendix C). The subsequent section discusses the dilution estimated on the leeward wall of the emitting building.

### *5.5.1.2 Dilution on the leeward wall of the emitting building*

Figure 5.16 (a) shows comparisons for Configurations 2a through 5a for $h_s$ = 1 m and M = 1.

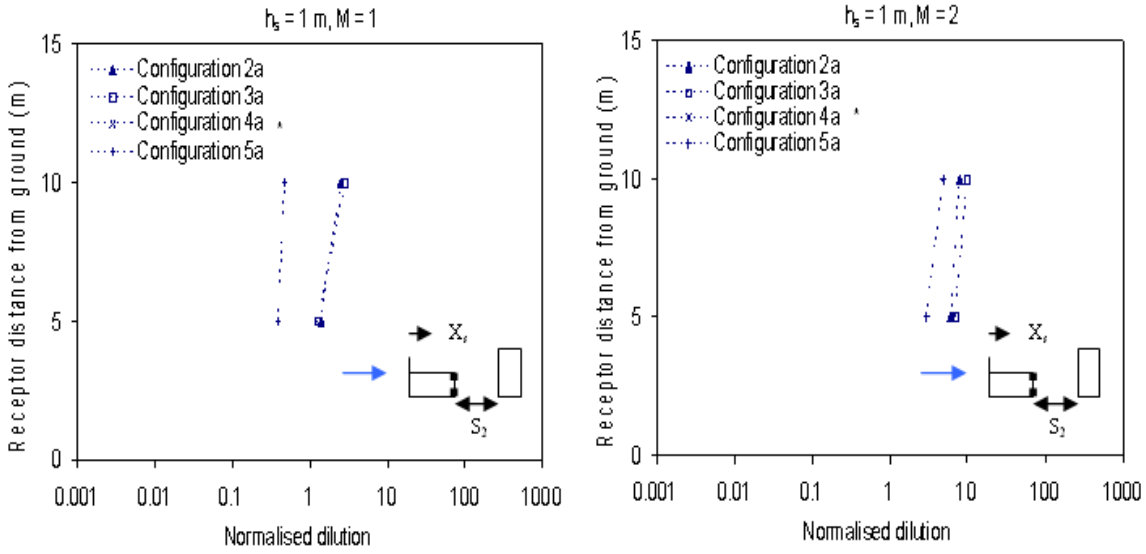


a) b)

Figure 5.16. Normalised dilution on rooftop of $B_1$ for $X_s$ = 0 and $S_2$ = 20 m: a) M = 1; b) M = 3 (* Concentration of pollutants was found to be zero)

It is understandable that the plume travels a smaller distance downwind for a longer downstream building, which does not affect the plume trajectory. Hence, Configurations 2a and 3a are comparable. Due to side leakage along the sides of a narrow downstream building in Configuration 4a, no plume concentrations were found on the wall receptors. Lower dilution was observed for Configuration 5a compared to Configurations 2a and 3a since the plume was trapped within the recirculation length of $B_1$ partly due to low exhaust speed and partly due to the back-and-forth movement (meandering) of the plume owing to the greater height of the downstream building ($B_5$). Similar observations were found at M = 2, as shown in Figure 5.16 (b) although the dilution was higher than at M = 1 by about a factor of 8 due to greater exhaust speed. For $h_s > 1$ m no plume concentrations were found since the plume rise is sufficiently high to allow it to escape the zone of recirculation in the wake of the emitting building. Additionally, when the stack was moved to $X_s = 20$ m, no plume concentrations were found on the leeward wall of the emitting building as most of the pollutants would affect the roof of the emitting building. For buildings of similar height, pollutants mostly affected the roof of both buildings and hence no effluent concentration on the leeward wall of the emitting building was found. ASHRAE 2007 and 2011 do not provide dilution values for building walls. Pollutant concentrations were also found on the windward wall of the taller downstream building, as discussed further.

#### *5.5.1.3 Dilution on the windward wall of the downstream building*

Figure 5.17 (a) presents comparisons of dilution for Configurations 2a, 3a and 4a for $h_s = 1$ m, M = 1 and $X_s = 0$.

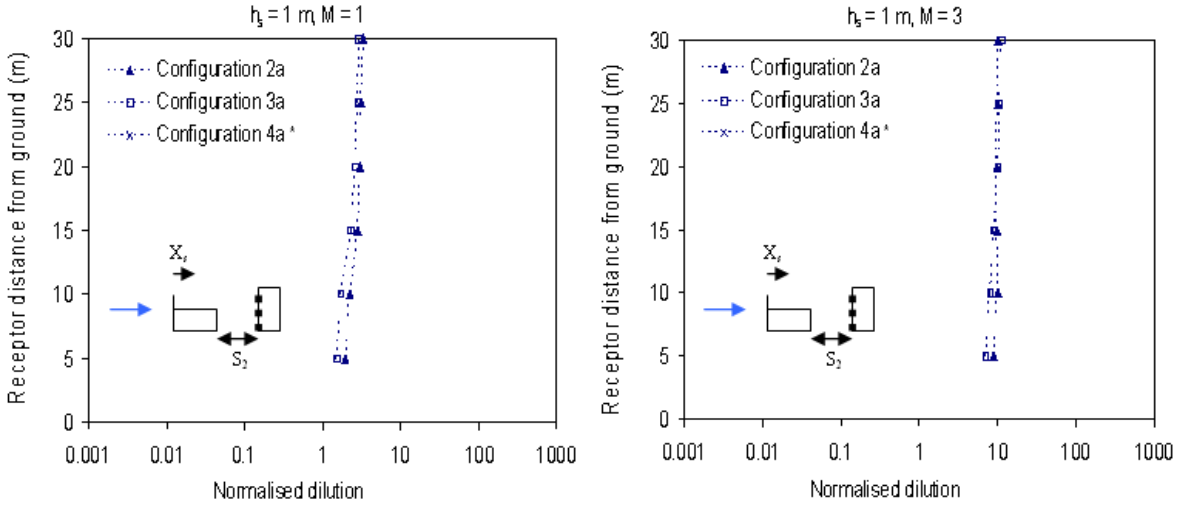


a) b)

Figure 5.17. Normalised dilution on windward wall of downstream building for $X_s$ = 0 and $S_2$ = 20 m: a) M = 1; b) M = 3 (* Concentration of pollutant was measured zero at all receptors)

Comparable dilution for Configurations 2a and 3a was obtained because a change in along wind dimension makes the tracer travel a marginal distance thereby leaving the plume geometry unaffected. It is also worth noting that the dilution is somewhat lower closer to the ground than near the upper wall, possibly due to the deposition of effluents on the ground after striking the wall. Side leakage results in no deposition of pollutants on the windward wall of the downstream building for Configuration 4a. A similar trend is observed at $h_s$ = 1 m and M = 3 as shown in Figure 5.17 (b), although the dilution is about 10 times higher than that obtained at M = 1 due to greater exhaust speeds. It is not surprising that at $h_s$ > 1 m no concentrations were found on the windward wall due to higher plume rise allowing greater dispersion of the pollutant. For centrally placed stacks ($X_s$ = 20 m) the trends remain unchanged although the dilution is somewhat higher than

at $X_s = 0$ due to greater plume spread. In fact Configuration 5a, which consisted of a downstream building ($B_5$) almost four times as tall as the emitting building also showed similar trends as Configurations 2a and 3a although the dilution was somewhat lower for corresponding values of $h_s$ and M due to the greater height of $B_5$.

Buildings of similar height also displayed similar trends on the windward wall of the downstream building, although the dilution was somewhat higher than that obtained for downstream buildings twice as high as the emitting building for corresponding values of $h_s$ and M.

The plume geometry also affects the rooftop of the downstream building as discussed in the subsequent section.

#### *5.5.1.4 Dilution on rooftop of downstream building*

Figure 5.18 (a) shows normalised dilution on the roof of $B_3$ for $h_s = 1$ m, M = 1 and $X_s = 0$ for Configuration 3a.

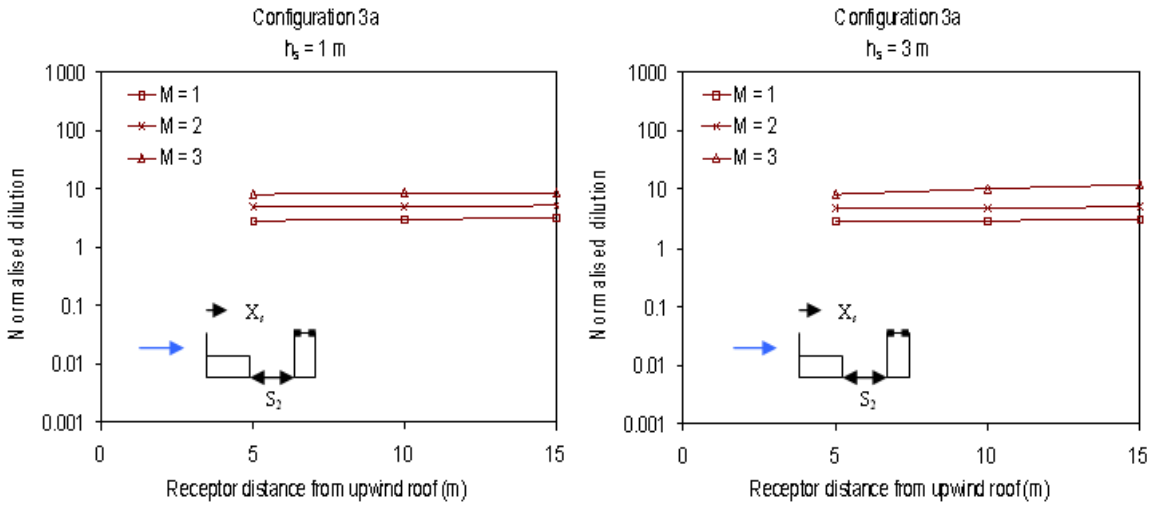


a) b)

Figure 5.18. Normalised dilution on rooftop of $B_3$ for $S_2 = 20$ m: a) $h_s = 1$ m; b) $h_s = 3$ m

Configuration 3a was chosen because the dilution trends were found to be similar to Configuration 2a; indeed a slightly longer downstream building would not change the overall plume structure. Data show that although the dilution was somewhat low for M = 1, a marginal increase was observed for M = 2 and M = 3 respectively. Since the downstream building is twice as high as the emitting building, plume rise is not sufficient for the pollutants to affect the roof of the downstream building. Also, a smaller portion of the pollutant accumulates on the roof of the downstream building because most part of the plume affects the roof of the emitting building and escapes through side leakage. A similar observation was made for $h_s$ = 3 m as shown in Figure 5.18 (b). In fact an increase in $h_s$ produced negligible change in dilution on $B_3$ possibly because the amount of pollutants deposited on the roof of $B_3$ was negligible. At $h_s$ > 3 m no effluent concentrations were found due to greater plume spread. A similar trend was also observed for a stack placed at $X_s$ = 20 m although the dilution was somewhat higher than that observed at $X_s$ = 0 for the respective $h_s$ and M values. No pollutant concentrations were found on the roof of the taller downstream building ($B_5$) for Configuration 5a because the plume rise was not sufficient to affect the roof as most of the pollutants affected the emitting building and windward wall of the downstream building.

Building of similar height generated comparable dilution for Configurations 7a, 8a and 9a on the rooftop of the downstream building for low stacks ($h_s$ = 1 m) at a given stack location, although they increased marginally for higher M values, a trend similar to the taller downstream cases. ASHRAE formulations cannot be used to estimate pollutant concentrations on rooftop of downstream building.

The subsequent section discusses plume concentration on the roof of the emitting building for centrally placed stacks.

### *5.5.1.5 Dilution on rooftop of emitting building for centrally-placed stacks*

Figure 5.19 (a) shows normalised dilution on rooftop of the emitting building ($B_1$) for $h_s$ = 1 m, M = 1 and $X_s$ = 20 m.

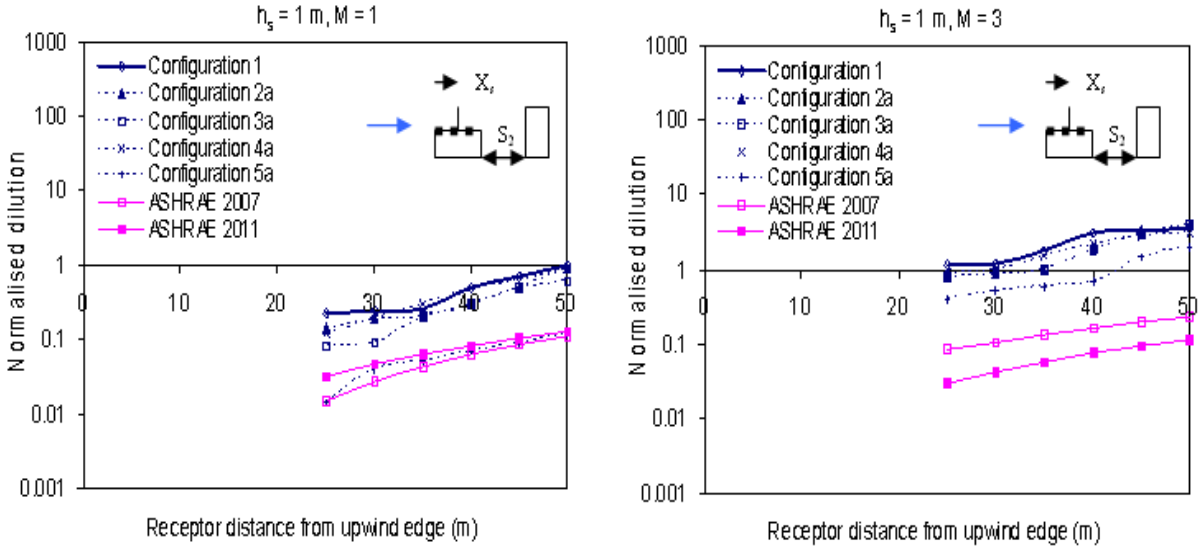


a) b)

Figure 5.19. Normalised dilution on rooftop of $B_1$ for $X_s$ = 20 m and $S_2$ = 20 m: a) M = 1; b) M = 3 (Concentration of pollutant was measured zero at receptors upwind of the stack)

It was observed that Configurations 2a through 4a predict comparable dilution with the isolated case (Configuration 1) at all downwind receptors. This is because the plume gets enough scope to escape through side leakage thereby reducing the effect of the downstream building. However, Configuration 5a continued to predict lower dilution than the isolated case. A similar trend is observed at $h_s$ = 1 m and M = 3 as shown in

Figure 5.19 (b), although the dilution was somewhat higher for all cases due to increased exhaust speed. This also suggests that with increased stack height and M the effect of the downstream building gradually diminishes. It is obvious that the dilution produced by all configurations were comparable to the isolated case at $h_s$ > 1 m. ASHRAE 2007 and ASHRAE 2011 continue to predict lower dilution for all configurations at all receptors irrespective of $h_s$ and M.

The trends remained unchanged for buildings of similar height with centrally placed stacks which allows the plume to escape through the sides of the downstream building resulting in comparable dilution for all configurations with the isolated case.

The preceding sections were focussed on the effect of downstream buildings within the zone of recirculation of the low building (20 m - 25 m). However, as the distance between the buildings increases the plume dilution also increases on the various building surfaces as discussed further.

### *5.5.2 Effect of spacing between buildings*

Figure 5.20 (a) shows the effect of spacing between the buildings for Configuration 2a at $h_s$ = 1 m and M = 1. Comparable dilution was obtained for $S_2$ = 20 m and $S_2$ = 25 m on the windward wall of the downstream building ($B_2$) as most part of the plume remains trapped within the wake of the emitting building. Hence, an additional spacing of 5 m makes the plume travel a very small distance downwind resulting in comparable dilution for $S_2$ = 20 m and $S_2$ = 25 m.

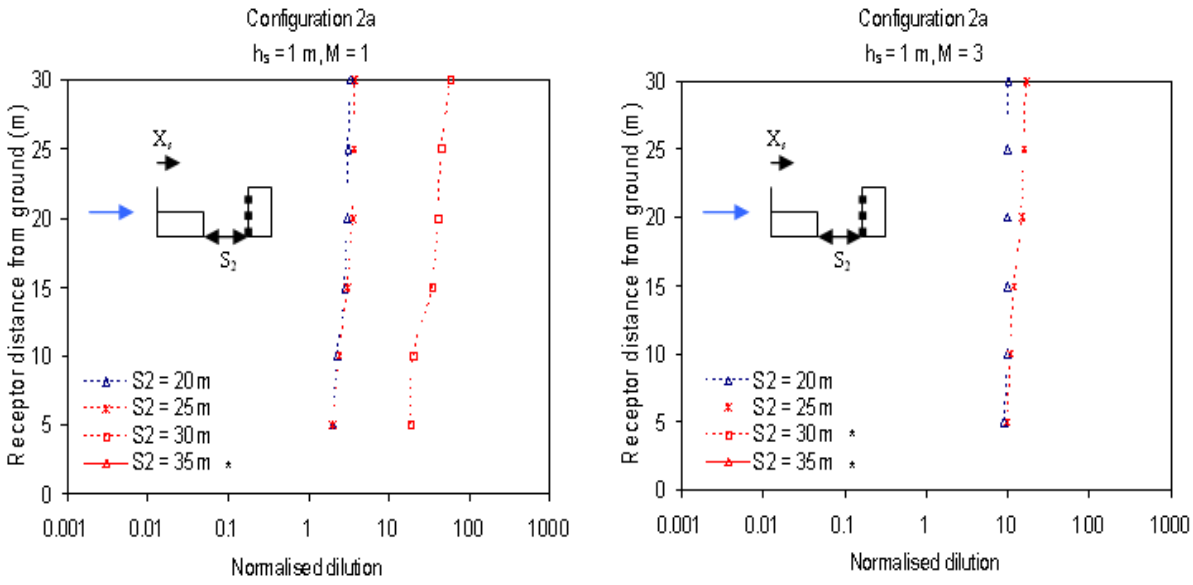


a) b)

Figure 5.20. Normalised dilution on windward wall of $B_2$ for different building distances ($S_2$) and $X_s = 0$: a) M = 1; b) M = 3 (* Concentration of pollutants was found to be zero)

However, as the buildings are moved further apart at $S_2$ = 30 m, there is increased side leakage resulting in higher dilution (almost 10 times higher) than at $S_2$ = 20 m. It is not surprising that at $S_2$ > 30 m no concentrations were found on the windward wall of $B_2$ suggesting that the effect of downstream building was greatly reduced. It is worth noting that the recirculation length of the emitting building ($B_1$) is 22.3 m as per ASHRAE 2007 and dilution on windward wall of $B_2$ were found to be comparable when the buildings were placed within this region. This trend remains almost the same at $h_s$ = 1 m and M = 3 as shown in Figure 5.20 (b), although the dilution was found to be somewhat higher than at M = 1. Beyond 25 m no tracer concentrations were found due to greater plume spread at higher exhaust speeds.

Comparable dilution at $S_2$ = 20 m and $S_2$ = 25 m were also found on rooftop of $B_1$ for Configuration 2a at $h_s$ = 1 m, M = 1 and $X_s$ = 0, as shown in Figure 5.21 (a) although the dilution was somewhat lower than the isolated case.

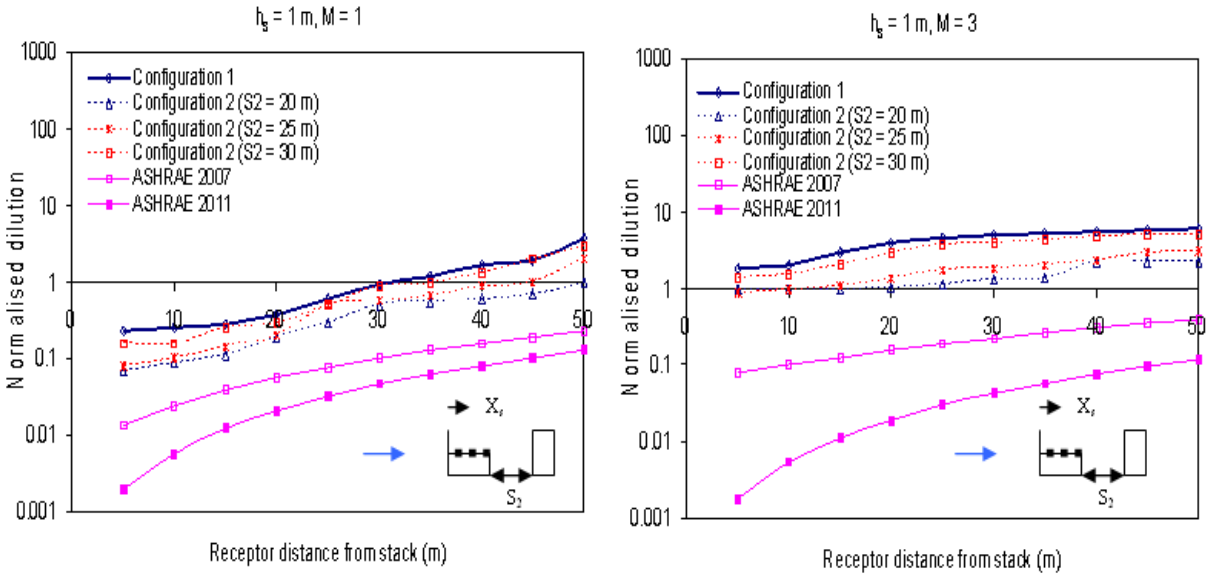


a) b)

Figure 5.21. Normalised dilution on rooftop of $B_1$ for different building distances ($S_2$) and $X_s$ = 0: a) M = 1; b) M = 3

However, at $S_2$ = 30 m comparable dilution was obtained with the isolated case. Similar trends were also observed at $h_s$ = 1 m and M = 3, as shown in Figure 5.21 (b) although the dilution was somewhat higher than the respective values at M = 1. ASHRAE 2007 and ASHRAE 2011 predictions are always for isolated building cases, so these values are used here only for reference.

Spacing does not play a major role for buildings of similar height, where irrespective of stack height, stack location and M, as spacing exceeds the recirculation length of the

emitting building, rooftop dilution on the emitting building becomes comparable to the isolated case, whilst the plume does not affect the downstream building surface since the pollutants get enough scope to disperse through the air. Additional results for higher $h_s$ and M are presented in Appendix C.

The subsequent section presents the case a building placed upstream and downstream of the emitting building.

## 5.6 Building placed upstream and downstream of the emitting building

This section presents the results of a building placed upstream and downstream of an emitting building. The dimensions of the buildings along with stack and receptor locations are shown in Figure 5.5. First the results of a taller building placed upstream and downstream of an emitting building (Configuration 10) is presented. This is followed by the results for Configuration 11 and the effects of spacing between buildings.

### *5.6.1 Results for building placed upstream and downstream of $B_1$ (Configuration 10)*

In this section the results obtained on the leeward wall of the upstream building and the rooftop of the emitting building are discussed since these building surfaces were more affected by the plume geometry.

#### *5.6.1.1 Dilution on the leeward wall of the upstream building ($B_2$)*

Figure 5.22 (a) shows normalised dilution on the leeward wall of the taller upstream building for $X_s = 0$ and $h_s = 1$ m. Due to the recirculation zone created in the wake of the upstream building, the plume is drawn towards the wall of $B_2$. The dilution increases by a factor of about 4 for every increase in M value. This is because an increase in exhaust

speed leads to greater dispersion of pollutants, a part of which remains engulfed within the wake of the upstream building while a part of it escapes along the roof of the emitting building.

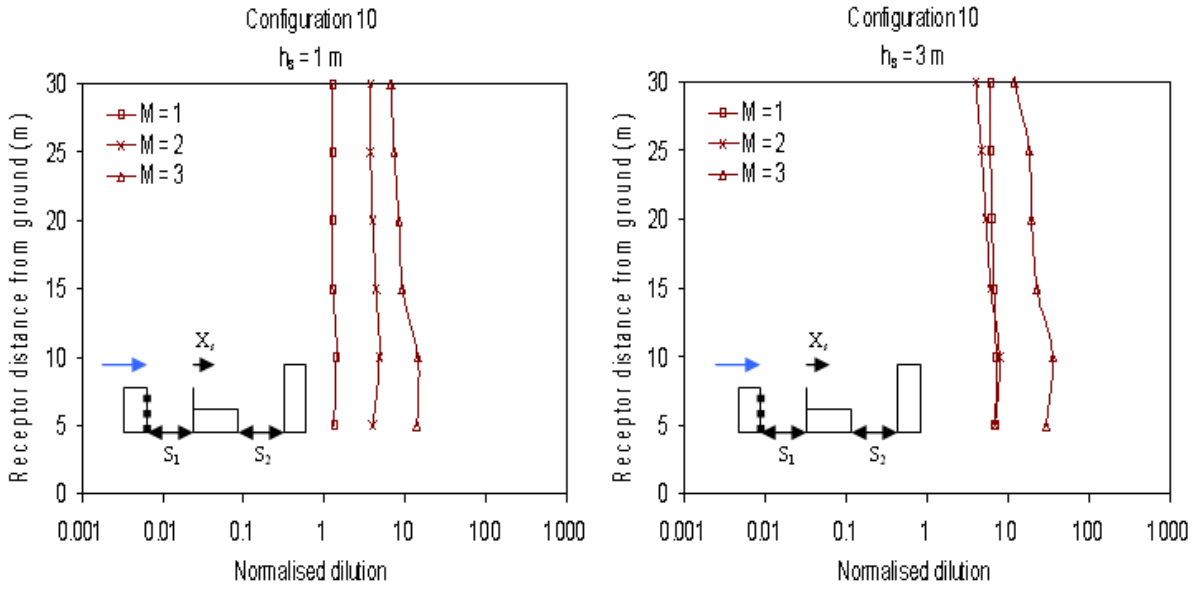


Figure 5.22 Normalised dilution on leeward wall of $B_2$ for $X_s = 0$ and $S_1 = S_2 = 20$ m: a) $h_s = 1$ m; b) $h_s = 3$ m

At $h_s = 3$ m the plume rise increases further causing greater dilution of the tracer gas; in fact comparable dilution was obtained at M = 1 and M = 2 as shown in Figure 5.22 (b). However, as the exhaust speed increases further the pollutants escape the recirculation zone causing higher dilution at M = 3 than at M = 2. At $h_s > 3$ m no concentrations were found on the wall possibly because the plume rise was high enough to overcome the wake recirculation of $B_2$ and affect only the emitting and downwind building. A similar trend was also observed for $X_s = 20$ m although the dilution was somewhat higher than

their respective values at $X_s$ = 0. The plume also affects the rooftop of the emitting building as discussed further.

### *5.6.1.2 Dilution on the rooftop of emitting building ($B_1$) for $X_s$ = 0*

Figure 5.23 (a) shows normalised dilution on the rooftop of $B_1$ for $h_s$ = 1 m, M = 1 and $X_s$ = 0 for Configurations 1, 10, ASHRAE 2007 and ASHRAE 2011.

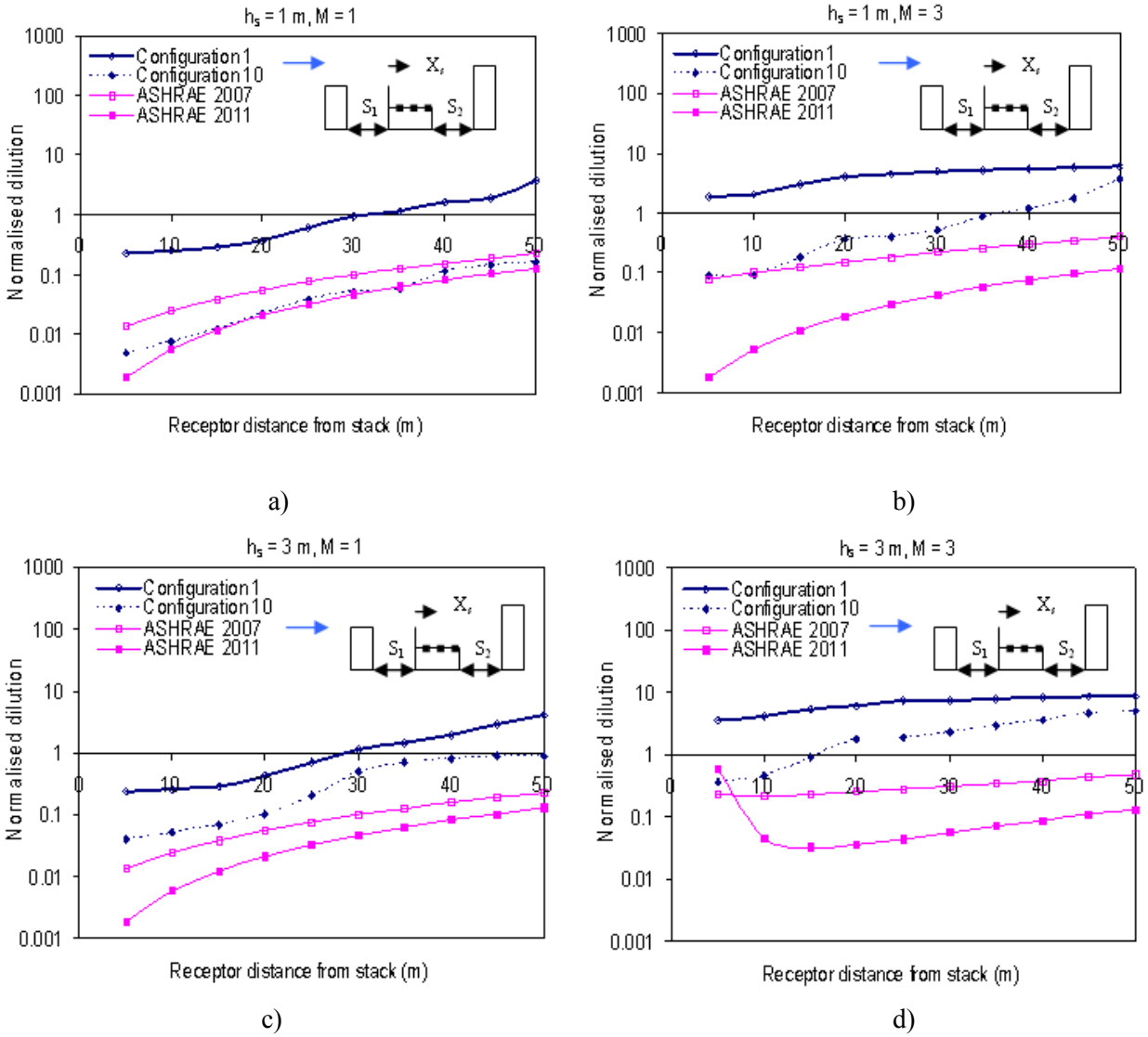


Figure 5.23 Normalised dilution on rooftop of $B_1$ for $X_s$ = 0 and $S_1$ = $S_2$ = 20 m: a) $h_s$ = 1 m, M = 1; b) $h_s$ = 1 m, M = 3; c) $h_s$ = 3 m, M = 1; d) $h_s$ = 3 m, M = 3

Results show that the dilution predicted by Configuration 10 is almost 20 times lower than that predicted by Configuration 1 (isolated case). This is because the plume gets trapped in between two buildings. Also, the recirculation zone of the taller upstream building brings the plume closer to the leeward wall of the upstream building and the rooftop of emitting building. A similar trend is observed at $h_s$ = 1 m and M = 3 as shown in Figure 5.23 (b) although the dilution is somewhat higher than those produced at M = 1 due to higher exhaust speeds. This trend remains unchanged for higher $h_s$ and M as shown in Figures 5.23 (c) and 5.23 (d). At higher $h_s$ and M values (say $h_s$ = 5 m and M = 3) the dilution obtained from Configuration 10 and the isolated case become comparable possibly because the plume rise is sufficient to overcome the effect of adjacent buildings. ASHRAE 2007 and 2011 are incapable of simulating adjacent building effects and predict very low dilution for all cases leading to overly conservative design. Centrally placed stacks generate a different plume trajectory as discussed further.

#### *5.6.1.3 Dilution on the rooftop of emitting building ($B_1$) for $X_s$ = 20 m*

For a stack placed at 20 m from the upwind edge, the plume trajectory assumes a similar shape as that of a taller upstream building discussed previously (Figure 2.8). Figure 5.24 (a) shows comparisons for Configurations 1 and 10, ASHRAE 2007 and ASHRAE 2011 for $h_s$ = 1 m, M = 1 and $X_s$ = 20 m. Configuration 10 predicts lower dilution than Configuration 1 at all receptors. Additionally, Configuration 10 generates dilution upwind of stack due to the plume geometry in the presence of an upstream building.

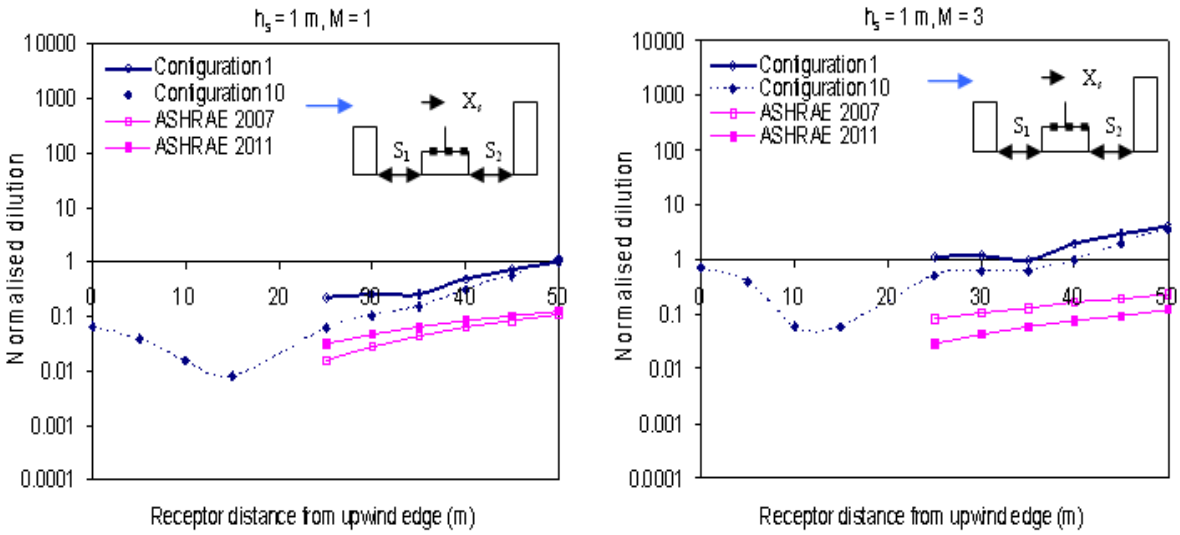


a) b)

Figure 5.24 Normalised dilution on rooftop of $B_1$ for $X_s$ = 20 m and $S_1 = S_2$ = 20 m: a) M = 1; b) M = 3

The dilution is particularly low closer to the stack because the plume strikes the leeward wall of the upstream building and travels back towards the roof of the emitting building increasing effluent concentrations at receptors upwind of the stack. Thereafter the dilution increases and at receptors closer to the edge of $B_1$ the dilution become comparable to the isolated case because the effect of the upstream building reduces and some of the pollutants escape through side leakage. A similar trend is observed at $h_s$ = 1 m and M = 3 as shown in Figure 5.24 (b) although the dilution is somewhat higher due to higher exhaust speeds. This trend remains unchanged for $h_s$ = 3 m at any given M value.

At $h_s$ = 5 m the dilution obtained by Configuration 10 become comparable to the isolated case at all receptors downwind of stack, although rooftop concentrations were

obtained upwind of stack even at this stack height. ASHRAE predictions are overly conservative and the formulations only apply to the isolated building case.

#### *5.6.1.4 Dilution on the windward wall of the downstream building ($B_5$)*

Since most of the pollutants were either engulfed within the recirculation length of the upstream building whilst a part of it affected the roof of the emitting building as well as some parts escaping through side leakage, a small portion of the plume also affects the windward wall of the downstream building at low stack heights ($h_s$ = 1 m) for $X_s$ = 0 (see Appendix D). At $h_s$ > 1 m the plume gathers enough height to disperse through the air, thereby leaving the downstream building unaffected. Centrally placed stacks allow greater plume spread making it less likely to affect the downstream building.

The subsequent section describes Configuration 11 in which an upstream building of similar height as the emitting building lies along with a taller downstream building. The plume geometry mostly affects the emitting and downstream building surfaces leaving the upstream building unaffected.

### *5.6.2 Results for a building placed upstream and downstream of $B_6$ (Configuration 11)*

Configuration 11 consists of an upstream building ($B_2$) of equal height as the emitting building ($B_6$) and a taller downstream building ($B_5$). In this section results for the rooftop of the emitting and downstream building are presented, since these building surfaces are greatly affected by the plume, although a small portion of the plume also affects the windward wall of the downstream building especially at low stack heights ($h_s$ = 1 m).

### *5.6.2.1 Dilution on rooftop of emitting building ($B_6$)*

Figure 5.25 (a) shows comparisons between Configurations 6 and 11, ASHRAE 2007 and ASHRAE 2011 in terms of normalised dilution on rooftop of the intermediate emitting building ($B_6$) for $h_s$ = 1 m, M = 1 and $X_s$ = 0.

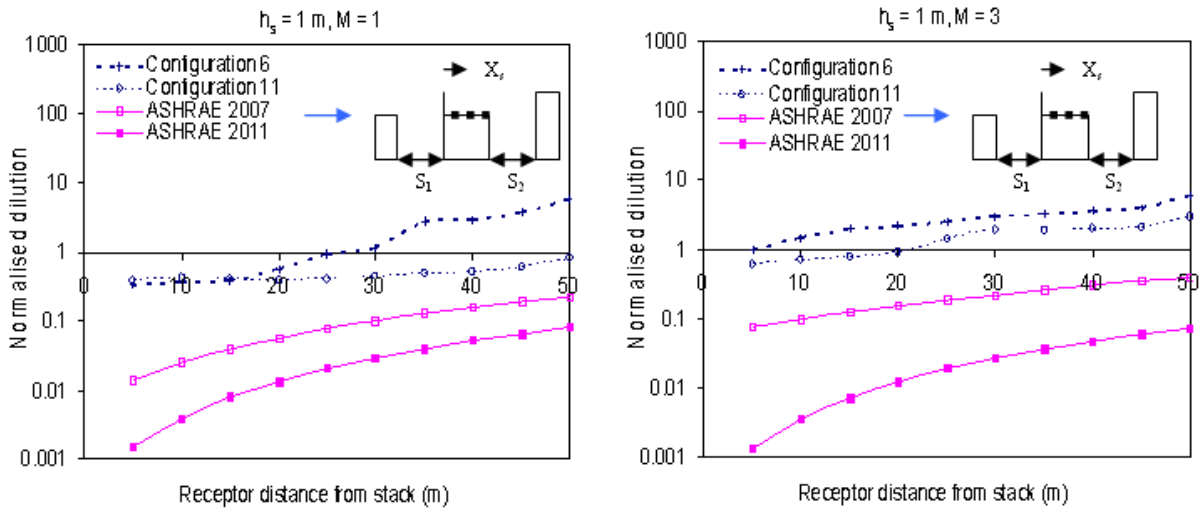


a) b)

Figure 5.25 Normalised dilution on rooftop of $B_6$ for $X_s$ = 0 and $S_1$ = $S_2$ = 20 m: a) M = 1; b) M = 3

It was observed that Configurations 6 and 11 predict comparable dilution up to receptors located 15 m downwind of stack. Thereafter, Configuration 11 predicts lower dilution than the isolated case. This is because the turbulence generated by the upstream building tries to keep the plume closer to the roof at low M value. This trend changes at $h_s$ = 1 m and M = 3 as shown in Figure 5.25 (b) where the dilution predicted by Configuration 11 are lower than the isolated case by a factor of about 2. At $h_s$ > 1 m comparable dilution are obtained at all downwind receptors for both configurations.

Additionally, for centrally placed stacks the effect of adjacent buildings diminishes completely as dilution at all downwind receptors are comparable to the isolated case. Also, unlike Configuration 10 discussed previously, no rooftop concentrations were found upwind of stack due to equal heights of upstream and emitting buildings. ASHRAE predictions are overly conservative for all cases examined. The subsequent section describes the dilution produced on the rooftop of the downstream building.

#### *5.6.2.2 Dilution on rooftop of downstream building ($B_5$)*

Figure 5.26 (a) show normalised dilution on the roof of the downstream building ($B_5$) for Configurations 11 at $h_s$ = 1 m, M = 1 and $X_s$ = 0.

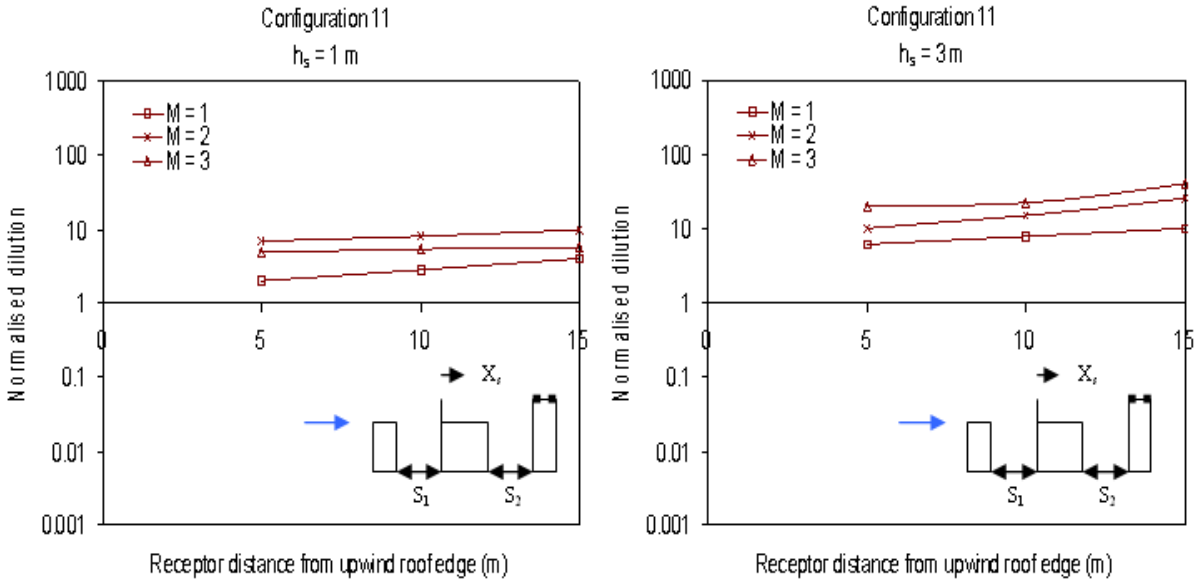


a) b)

Figure 5.26 Normalised dilutions on rooftop of $B_5$ for $X_s$ = 0 and $S_1$ = $S_2$ = 20 m: a) $h_s$ = 1 m; b) $h_s$ = 3 m

It was observed that although the dilution was somewhat low for M = 1, they reduce marginally for M = 3 than at M = 2. This is because an increased exhaust speed deposits more pollutants on the roof of the downstream building due to upwash. Additionally the height of the emitting building is about half of the downstream building thereby allowing pollutant accumulation on the roof of the downstream building. This trend changes at $h_s$ = 3 m where the dilution increases with an increase in M value. At $h_s$ > 3 m no rooftop concentrations were found on the roof of $B_5$ since a major part of the plume affects the emitting building with a portion of it escaping through side leakage. Similar observations were also made for stack placed at $X_s$ = 20 m although the dilution was somewhat higher than those measured at $X_s$ = 0.

The subsequent section describes the dilution obtained on the windward wall of the downstream building of Configuration 11.

#### *5.6.2.3 Dilution on windward wall of downstream building ($B_5$)*

Since most of the pollutants affect the roof of the emitting building, a very small portion of the plume affects the windward wall of the downstream building. When a low stack is placed at the edge of the emitting building ($X_s$ = 0, $h_s$ = 1 m) the plume affects the wall of the downstream building. At $h_s$ > 1 m the plume mostly affects the emitting building leaving the windward wall of $B_5$ unaffected. It is not surprising that centrally placed stacks allow the plume to disperse further leaving the windward wall of $B_5$ unaffected (see - Appendix D for additional results).

In the preceding sections, the results were focussed on spacing between buildings ($S_1$ = $S_2$) to only 20 m. The next section presents a few results for different spacing between buildings.

## 5.7 Effect of spacing between buildings

In this section the effect of spacing between buildings on the plume dilution on leeward wall of the upstream building and roof of the emitting building for Configuration 10 is discussed, since the effect of spacing was found to be more critical for this case.

### *5.7.1 Dilution on leeward wall of the upstream building ($B_2$) for Configuration 10*

Figure 5.27 (a) shows the effect of spacing between the buildings for Configuration 10 on the leeward wall of the upstream building ($B_2$) at $h_s$ = 1 m, M = 1 and $X_s$ = 0.

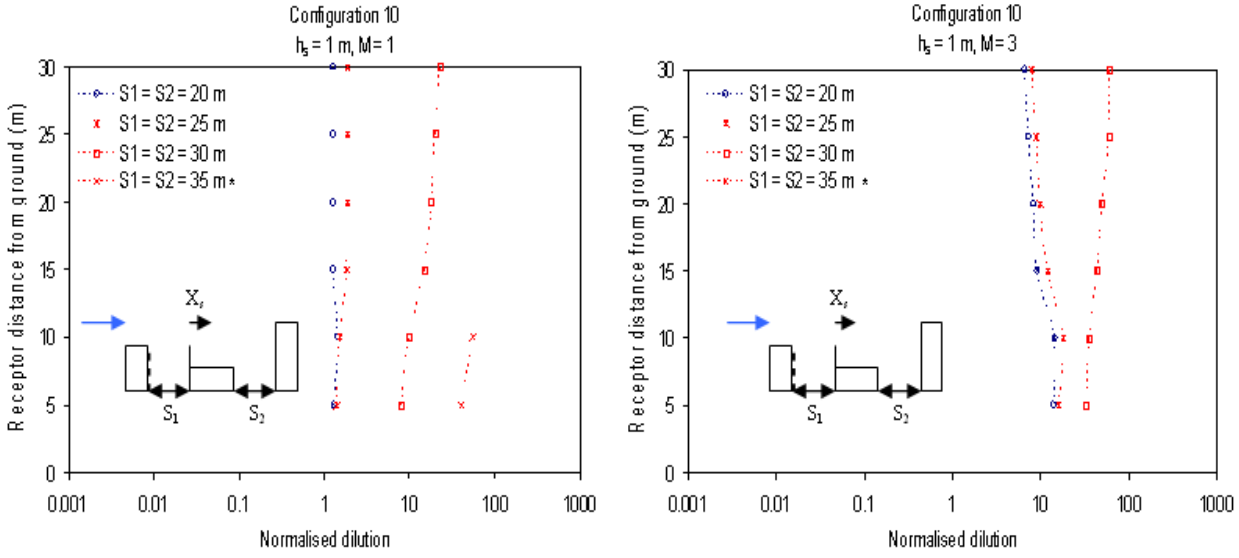


a) b)

Figure 5.27 Normalised dilution on leeward wall of $B_2$ for $X_s$ = 0: a) M = 1; b) M = 3 (* Concentration of pollutant was found to be zero at the receptor)

Spacing between buildings was uniformly varied such that $S_1$ was always equal to $S_2$. It was observed that at $S_1$ = 20 m and $S_1$ = 25 m comparable dilution was obtained on the leeward wall of the upstream building. This is because due to the recirculation length in the wake of the upstream building a large portion of the plume remains trapped and despite a change in spacing (increase in 5 m) the dilutions remain unchanged. However, this trend changes at $S_1$ = 30 m where dilutions are almost 10 times higher than those obtained at $S_1$ = 20 m. This is because the buildings are sufficiently away from the wake recirculation of the upstream building resulting in less plume material being engulfed. At $S_1$ = 35 m the dilution is even greater resulting in plume concentrations only on the first two receptors closer to the ground. A similar trend is observed at $h_s$ = 1 m and M = 3 as shown in Figure 5.27 (b) where although dilution at $S_1$ = 20 m and $S_1$ = 25 m are comparable, they are higher at $S_1$ = 30 m. In fact, at $S_1$ > 30 m no plume concentrations were found on the leeward wall as most of the plume affects only the emitting and downstream building. The following section describes the effect of spacing on the low emitting building.

### *5.7.2 Dilution on rooftop of low building ($B_1$) for Configuration 10*

Comparable rooftop dilution on emitting building ($B_1$) at $S_1$ = 20 m and $S_1$ = 25 m was found at $h_s$ = 1 m, M = 1 and $X_s$ = 0 for Configuration 10 although the dilution was about 10 times lower than the isolated case as shown in Figure 5.28 (a). At $S_1$ = 30 m the dilution increases by a factor of about 10, although at points closer to the leeward edge the dilution was lower than that of the isolated case. This is because at distance between 20 m and 25 m the plume geometry does not change markedly.

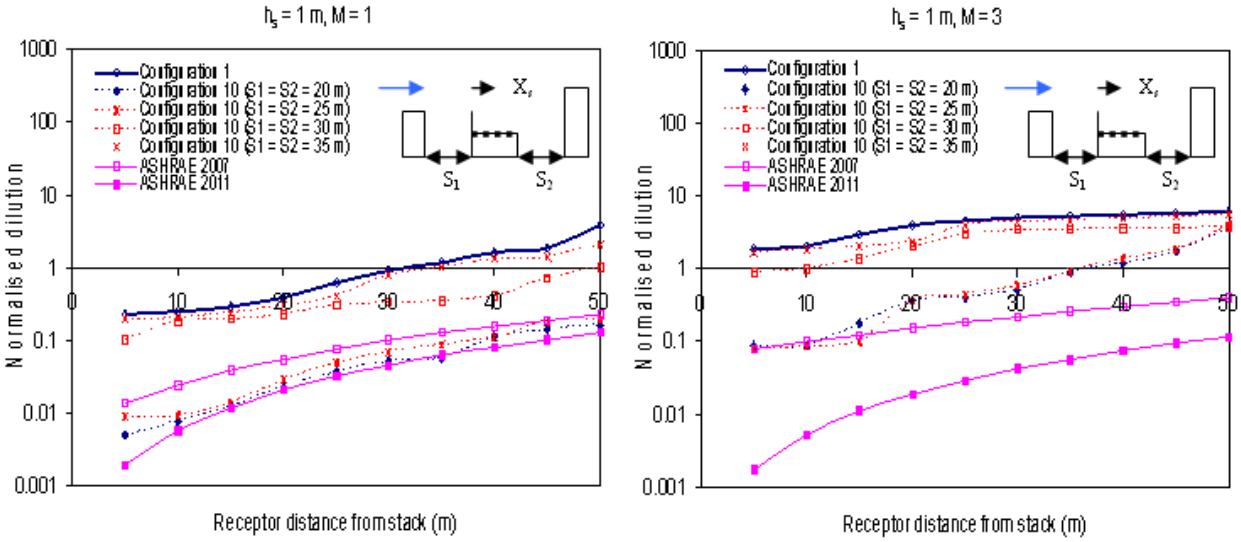


a) b)

Figure 5.28 Normalised dilution on rooftop of $B_1$ for $X_s$ = 0: a) M = 1; b) M = 3

At spacing greater than 30 m the dilutions gradually become closer to the isolated case because the shape of the plume tends to be more conical, similar to that of an isolated building. Similar trends were observed for $h_s$ = 1 m, M = 3 as shown in Figure 5.28 (b), although the dilution was somewhat higher than those obtained at M = 1. As already mentioned ASHRAE 2007 and ASHRAE 2011 are not capable of incorporating the effect of spacing between buildings and generate dilution only for the isolated case.

ASHRAE 2007 and 2011 were also applied to experimental results from previous studies, as described in the following section.

### 5.8 Application of ASHRAE 2007 and 2011 models to previous studies

This section presents comparisons for AHRAE 2007, ASHRAE 2011 and experimental results obtained from previous studies on isolated buildings. In this context,

studies from Schulman and Scire, 1991, Wilson et al., 1998 and Petersen et al., 1999 have been used. The experimental parameters used in each of these studies are described in Table 5.4.

Table 5.4. Experimental parameters used for previous studies

| Schulman and Scire, 1991 | Wilson et al., 1998 | Petersen et al., 1999 |
|---|---|---|
| H = 15 m | H = 12.2 m | H = 15 m |
| W = 75 m | W = 31 m | W = 15 m |
| L = 75 m | L = 31 m | L = 30 m |
| $U_H$ = 1.37 m/s | $U_H$ = 0.179 m/s | $U_H$ = 4 m/s |
| $d_e$ = 0.75 m | $d_e$ = 0.60 m | $d_e$ = 0.40 m |
| $\alpha$ = 0.2 | $\alpha$ = 0.26 | $\alpha$ = 0.19 |
| Suburban terrain | Suburban terrain | Suburban terrain |
| $Z_o$ = 0.3m | $Z_o$ = 0.38m | $Z_o$ = 0.28m |

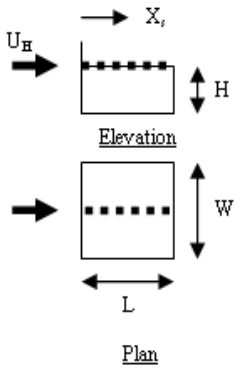


Schulman and Scire, 1991 performed wind tunnel tracer studies on a 15 m low building for a suburban terrain by varying the stack heights from 1 m to 7.5 m. Wilson et al., 1998 performed water channel studies on a 12.2 m low building. A coloured dye was released from the rooftop stack and images were taken using a camera. Petersen et al., 1999 also performed similar tracer studies in a boundary layer wind tunnel for a suburban terrain. Additional details of each study are mentioned in Chapter 2.

Figure 5.29 shows comparisons for ASHRAE 2007, ASHRAE 2011 and wind tunnel data from Schulman and Scire, 1991 for $h_s$ = 1.5, M = 1 and $X_s$ = 45 m. Results show that ASHRAE 2007 predicts almost 10 times lower dilution than experimental data at all receptors. This is because of the conservative nature of the ASHRAE formulations described in Chapter 4. The low plume rise value reduces the effective height of the plume thereby predicting lower dilution values.

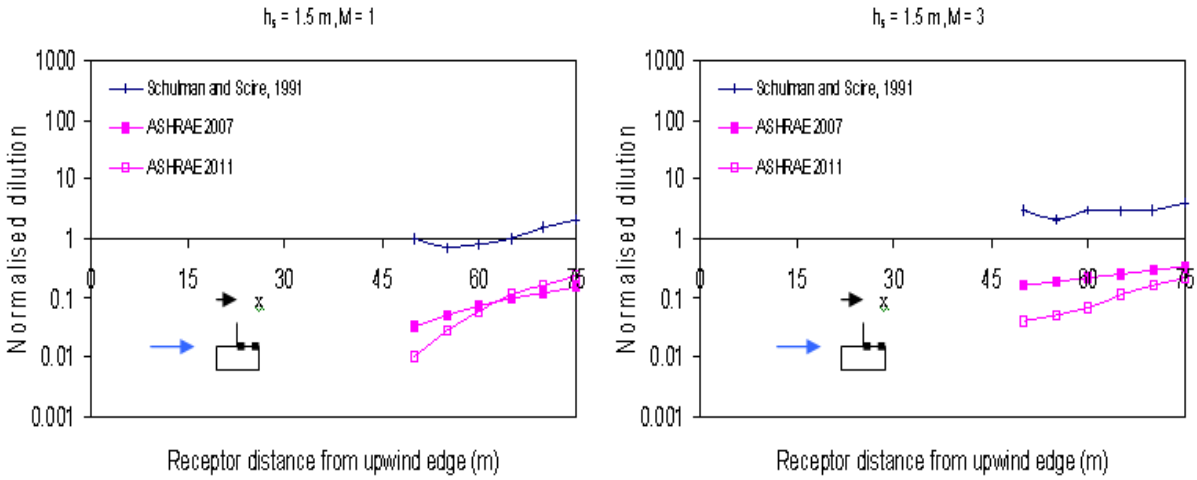


a) b)

Figure 5.29 Normalised dilution on rooftop of isolated building: a) M = 1; b) M = 3

ASHRAE 2011 also generates lower dilution than wind tunnel data because the plume rise predictions are even lower than the 2007 model. Additionally, the plume spread parameters used in ASHRAE 2011 (equation 4.19 and 4.20) restrict the spread of the plume. This causes the dilution obtained by 2011 version to be lower than the 2007 values very close to the stack. A similar trend is also observed for $h_s$ = 1.5 m and M = 3 as shown in Figure 5.29 (b) although the dilution values are somewhat higher than their respective values at M = 1.

Figure 5.30 (a) presents comparisons for ASHRAE 2007, 2011 and water channel data from Wilson et al., 1998 for $h_s$ = 2 m, M = 1 and $X_s$ = 0. Results show that ASHRAE 2007 predicts almost 10 times lower dilution than experimental data at all receptors downwind of stack due to reasons previously explained. ASHRAE 2011 also predicts lower dilution than experimental data; the predictions are even lower than 2007 values.

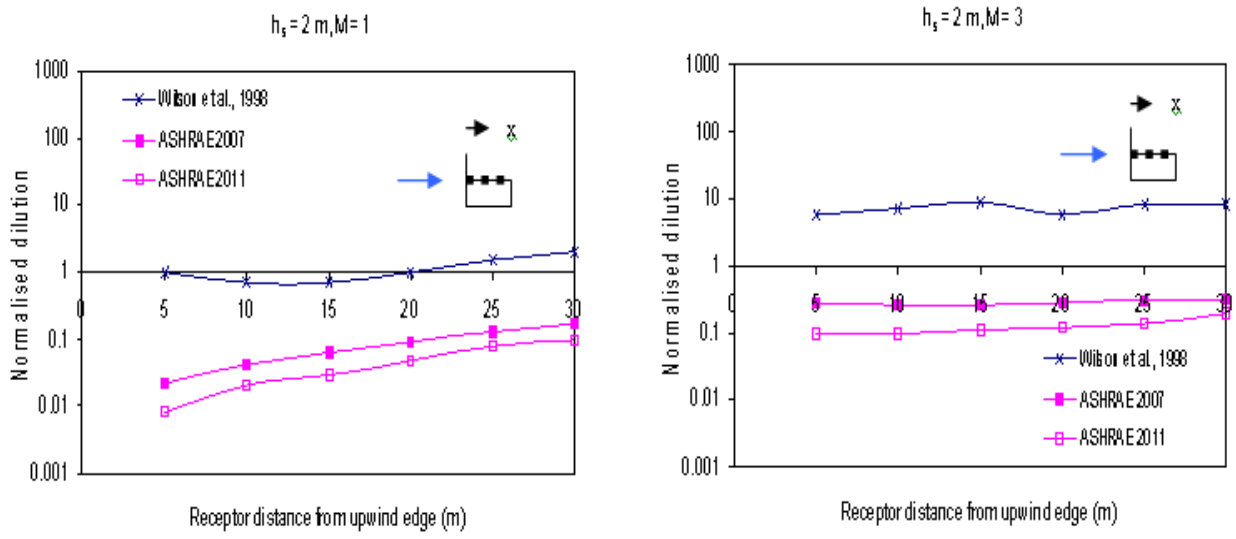


a) b)

Figure 5.30 Normalised dilution on rooftop of isolated building: a) M = 1; b) M = 3

A similar trend is observed for $h_s$ = 2 m and M = 3 as shown in Figure 5.30 (b). It may be noted that Wilson's data were obtained for a suburban terrain. A major deficiency of the ASHRAE formulations is that they do not incorporate the effects of terrain and local topography.

Comparisons for ASHRAE 2007, 2011 and wind tunnel data from Petersen et al., 1999 are shown in Figure 5.31 (a) for $h_s$ = 2 m, M = 1 and $X_s$ = 15 m. It may be mentioned that the building is about 15 m high, 15 m wide and 30 m long, located in a suburban terrain. Results show that the ASHRAE 2007 and 2011 values are almost 10 times lower than the experimental data at all receptors. In fact, ASHRAE 2011 predictions are about two times lower than the 2007 model very close to the stack.

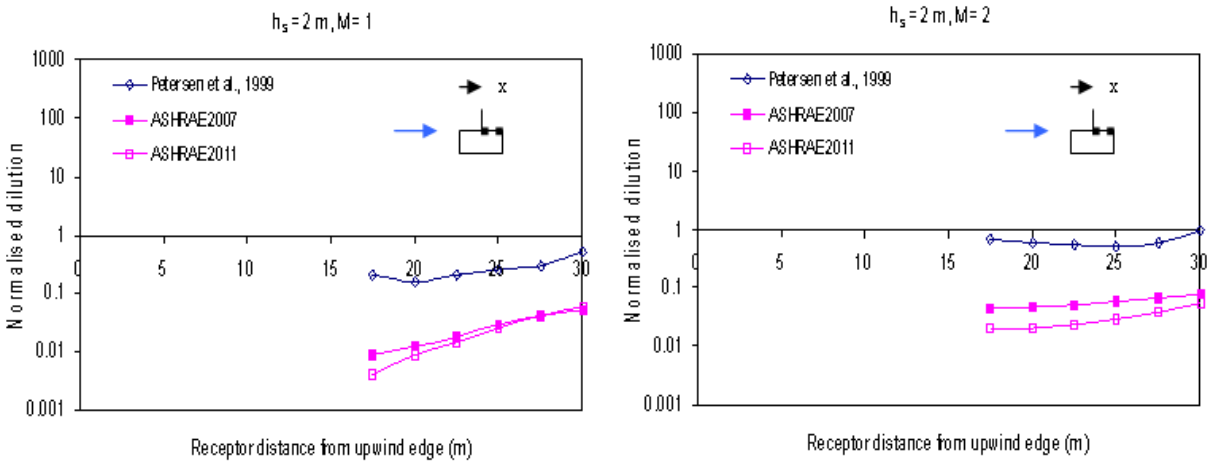


a) b)

Figure 5.31 Normalised dilution on rooftop of isolated building: a) M = 1; b) M = 2

A similar trend is observed for $h_s$ = 2 m and M = 2 as shown in Figure 5.31 (b). In general ASHRAE predictions are overly conservative for any $h_s$ and M value.

The subsequent section describes the results in non-dimensional form.

### 5.9 Results in non-dimensional form

In this section some of the results discussed previously have been converted to non-dimensional form using the geometry of the building. This is necessary because the results in the previous section are presented in the form of actual receptor distances for various building surfaces. However, in reality buildings can be of any size and geometry. Therefore, by expressing the receptor distances in non dimensional form it is possible to generalise the results. According to Streeter et al., 1998 "*By grouping significant quantities into dimensionless parameters it is possible to reduce the number of variables and to make this compact result (equations or data plots) applicable to all similar situations.*" To achieve this, the receptor distances on the roof of the emitting and

adjacent buildings have been divided by their respective along wind dimensions (length). Similarly, the receptor distances on the wall of the emitting and adjacent buildings have been converted to non dimensional form using the height of the building; the non-dimensionalised form of the receptor distance range from 0 to 1. The spacing between buildings and stack location from the upwind edge have also been expressed in terms of the length of the emitting building. Results for upstream building configurations are presented in the subsequent section.

### 5.9.1 Upstream building configurations

Figure 5.32 presents wind tunnel data for Configurations 1, 3, 4 and 5 in terms of normalised dilution. The receptor distance from the upwind edge of the emitting building (x) has been expressed as x / L and the stack location from the upwind edge ($X_s$) has also been expressed in terms of the along wind dimension of the emitting building (L). Results are shown for stack located at the upwind edge ($X_s = 0$) and centrally placed stacks ($X_s = 0.4L$). It may be mentioned that since similar results were obtained for Configurations 2 and 3, hence only dilution obtained for Configuration 3 has been shown. At $h_s = 1$ m, M = 1 and $X_s = 0$, Configurations 3 and 4 predict comparable dilution with Configuration 1 at all receptors except at points closer to the downwind edge of the building. This is because Configuration 4 consists of a narrow upstream building which has a smaller recirculation length in its wake that disallows the plume from getting engulfed within it. Similarly, Configuration 3 has an upstream building which has an across wind dimension equal to the emitting building and is twice as tall as the emitting building.

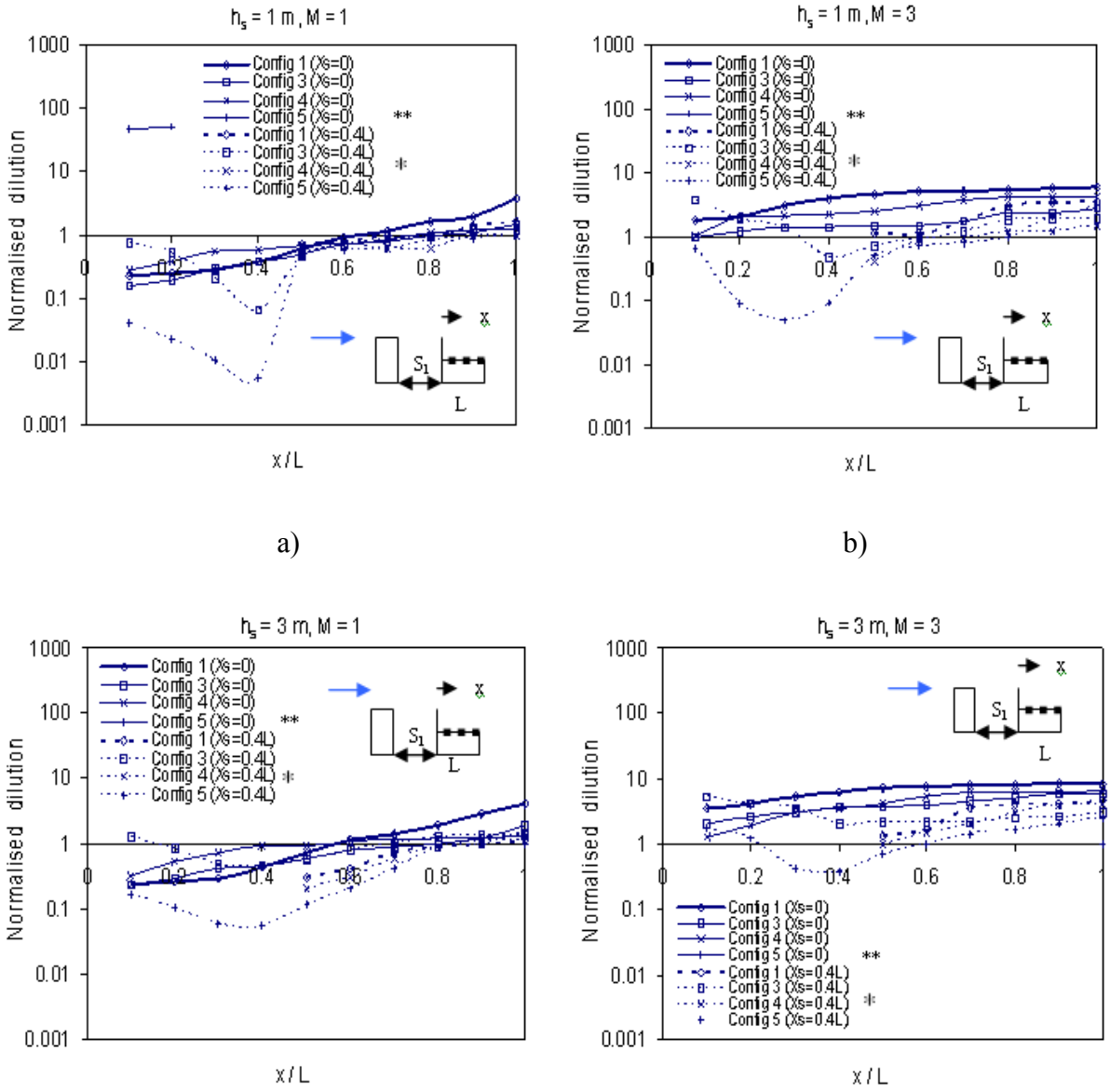


Figure 5.32 Normalised dilution on rooftop of $B_1$ for $S_1$ = 0.4L: a) $h_s$ = 1 m, M = 1; b) $h_s$ = 1 m, M = 3; c) $h_s$ = 3 m, M = 1; d) $h_s$ = 3 m, M = 3 (* Concentration of the pollutant was only found downwind of stack, ** No concentration of the pollutant was detected except for the first two receptors close to the upwind edge)

The low exhaust speed causes some part of the plume to be retained very close to the downwind edge of the emitting building. For centrally placed stacks ($X_s$ = 0.4L) a taller

upstream building of equal across wind dimension as the emitting building, causes the plume to travel towards the upstream building thereby increasing plume concentrations close to the stack. Hence Configurations 3 and 5 produce plume dilution upwind of stack; the latter predicts about 10 times lower dilution than the former case due to a taller upstream building in Configuration 5 than Configuration 3. However, gradually away from the stack the dilution for Configurations 3 and 5 become comparable due to reasons explained in previous sections. Configuration 4 predicts lower dilution than the isolated case and generates dilution only downwind of stack. This trend remains unchanged for higher stacks and M values as shown in Figure 5.32 (b), (c) and (d). At $h_s > 3$ m the dilution obtained from all configurations become comparable to the isolated cases.

Figure 5.33 (a) presents normalised dilution for Configuration 5 on the leeward wall of the tall upstream building for $h_s = 1$ m and $S_1 = 0.4L$.

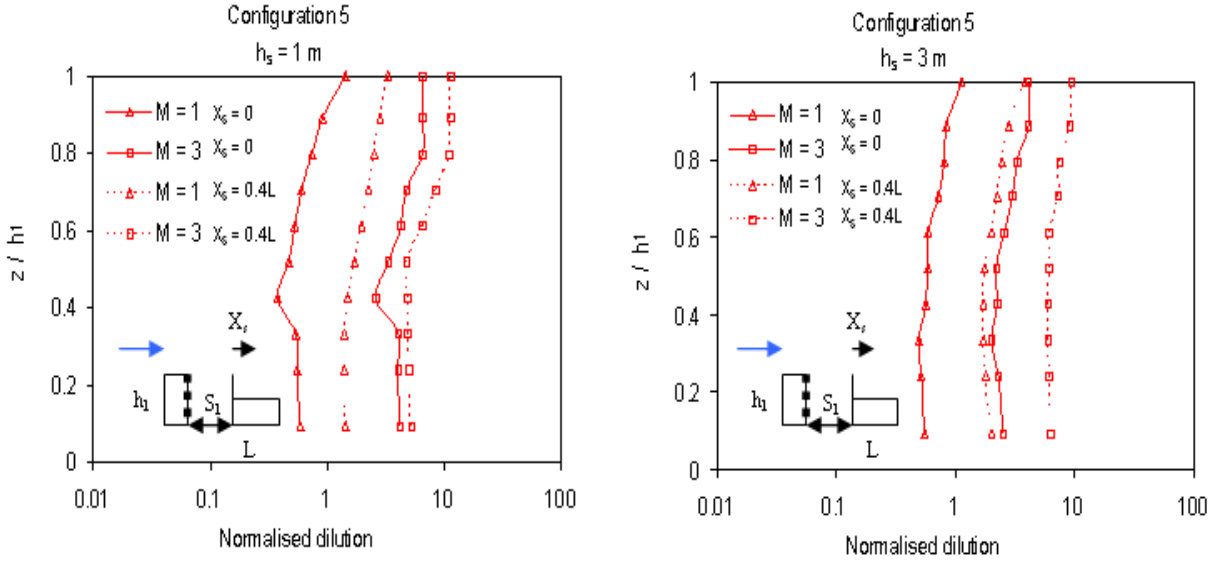


a) b)

Figure 5.33 Normalised dilution on leeward wall of $B_5$ for $S_1 = 0.4L$: a) $h_s = 1$ m; b) $h_s = 3$ m

The receptor distance from the ground (z) has been divided by the height of the upstream building ($h_1$) to make it non dimensional. It is observed that centrally located stack produces about 10 times higher dilution as compared to the stack located at the upwind edge at M = 1. The dilutions at M = 3 continue to be higher by about a factor of 4 for a centrally placed stack as compared to stack located on the upwind edge. This trend remains unchanged for $h_s$ = 3 m as shown in Figure 5.33 (b).

The effect of spacing between buildings is presented in Figure 5.34 for Configuration 3. The spacing between buildings ($S_1$) is expressed in terms of the along wind dimension (L) of the emitting building. Figure 5.34 (a) shows comparable dilution obtained for Configuration 3 at spacing of 0.4L, 0.6L and 0.8L and Configuration 1 for $h_s$ = 1 m and M = 1.

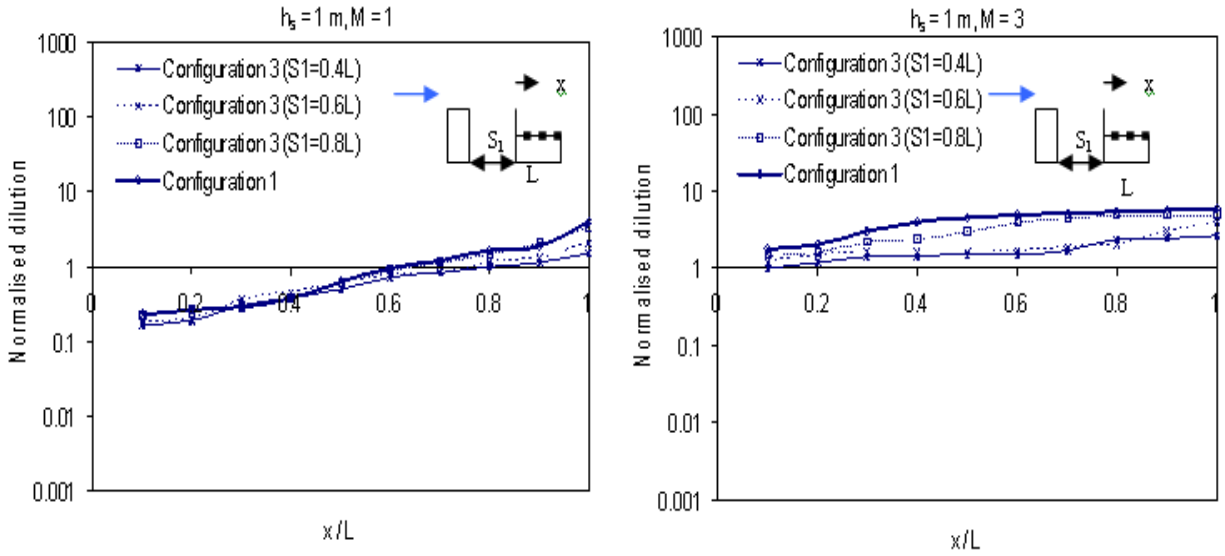


a) b)

Figure 5.34 Normalised dilution on rooftop of emitting building ($B_1$) for: a) $h_s$ = 1 m; b) $h_s$ = 3 m

However, very close to the downwind edge of the building, the dilution obtained at $S_1$ = 0.4L and 0.6L are somewhat lower than the isolated case suggesting that the upstream buildings influence exists at this particular spacing. As the spacing increases further, the dilution at $S_1$ = 0.8L and the isolated case compare well at all receptors. A similar trend is observed at M = 3 as shown in Figure 5.34 (b) although the dilution values are somewhat higher than those at M = 1.

Results in non-dimensional form are also presented for a few downstream building configurations in the subsequent section.

### 5.9.2 Downstream building configurations

Figure 5.35 (a) presents comparisons for Configurations 1, 3a, 4a and 5a for $X_s$ = 0.

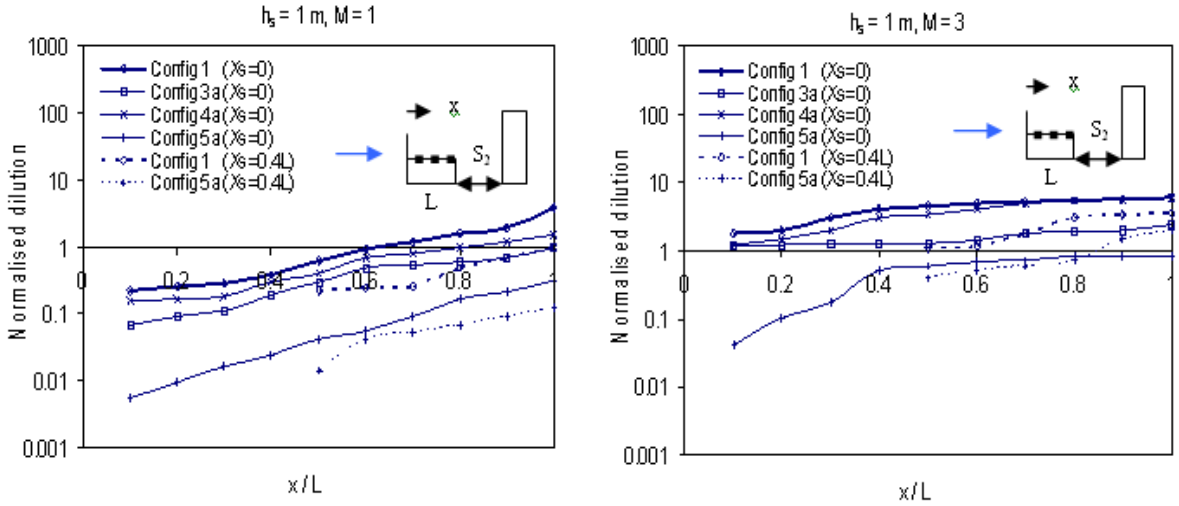


a) b)

Figure 5.35 Normalised dilution on rooftop of emitting building ($B_1$) for: a) M = 1; b) M = 3

Results obtained for Configuration 1 and 5a for centrally placed stack ($X_s$ = 0.4L) are also shown for $h_s$ = 1 and M = 1. Results show that at $X_s$ = 0, Configuration 3a predicts

about 5 times lower dilution than the isolated case because of a downstream building which is twice as tall as the emitting building. Configuration 5a predicts about 12 times lower dilution than the isolated case since it has a downstream building about 4 times as tall as the emitting building which disallows the plume to escape freely. A narrow downstream building produces dilution about a factor of 1.5 less than the isolated case due to increased side leakage. For centrally placed stacks, only Configurations 1 and 5a have been shown. This is because a downstream building about twice as high as the emitting building would produce comparable dilution with the isolated case as explained in previous sections. However, when the downstream building is more than twice the height of the emitting building (as in Configuration 5a), the rooftop dilution decreases by a factor of about 10 compared to the isolated case. Similar trends are also observed at M = 3 as shown in Figure 5.35 (b). At greater $h_s$ and M values the rooftop dilution becomes closer to the isolated case.

A small portion of the pollutant also accumulates close to the leeward wall of the emitting building as shown in Figure 5.36 (a) at $h_s$ = 1 m and M = 1. It may be mentioned that the receptor distance from the ground (z) has been expressed in non-dimensional form by dividing it with the height of the emitting building (h). Also Configurations 2a and 3a predicted comparable dilution, hence only the results for Configuration 3a have been shown. Configuration 5a consists of a downstream building which is about 4 times taller than the emitting building, which causes lower dilution than Configuration 3a (a factor of about 6).

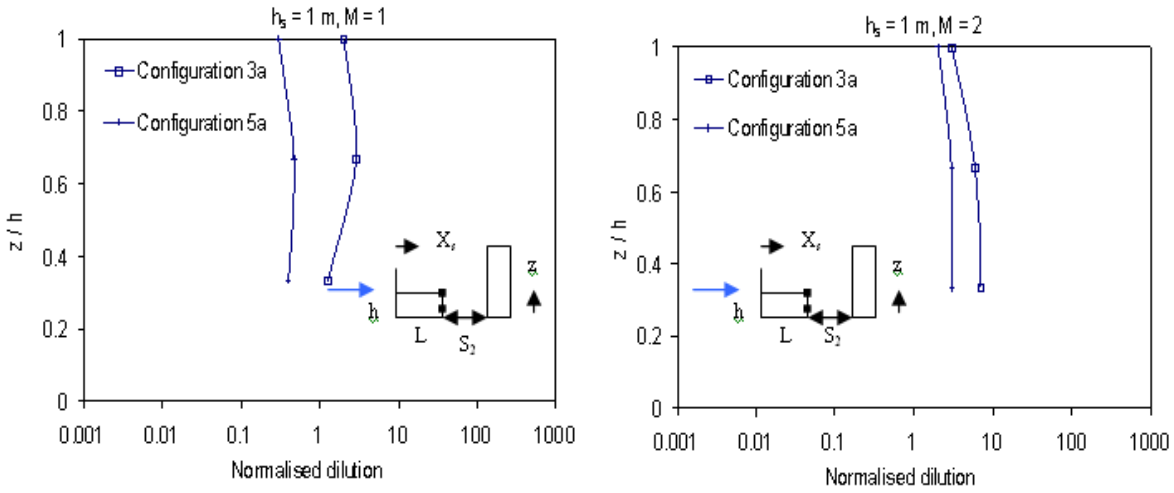


a) b)

Figure 5.36 Normalised dilution on leeward wall of the emitting building ($B_1$) for: a) M = 1; b) M = 2

At M = 2, Configuration 5a generates about a factor of 3 lower dilution than Configuration 3a, as shown in Figure 5.36 (b). At greater $h_s$, pollutant concentrations on the wall were undetectable because the plume has a greater scope to disperse and hence escapes the recirculation zone of the emitting building.

Figure 5.37 presents normalised dilution for different spacing between buildings for Configuration 3a and compares them to Configuration 1 (isolated case). The spacing between buildings ($S_2$) and the receptor distance from the upwind edge (x) are expressed in terms of the along wind dimension of the emitting building (L). At $h_s$ = 1 m and M = 1 comparable dilution was obtained at $S_2$ = 0.4L and 0.5L since this subtle change in spacing between buildings does not change the plume geometry significantly. However, at $S_2$ = 0.6L, the effect of the downstream building reduces further and the dilution becomes comparable to the isolated case.

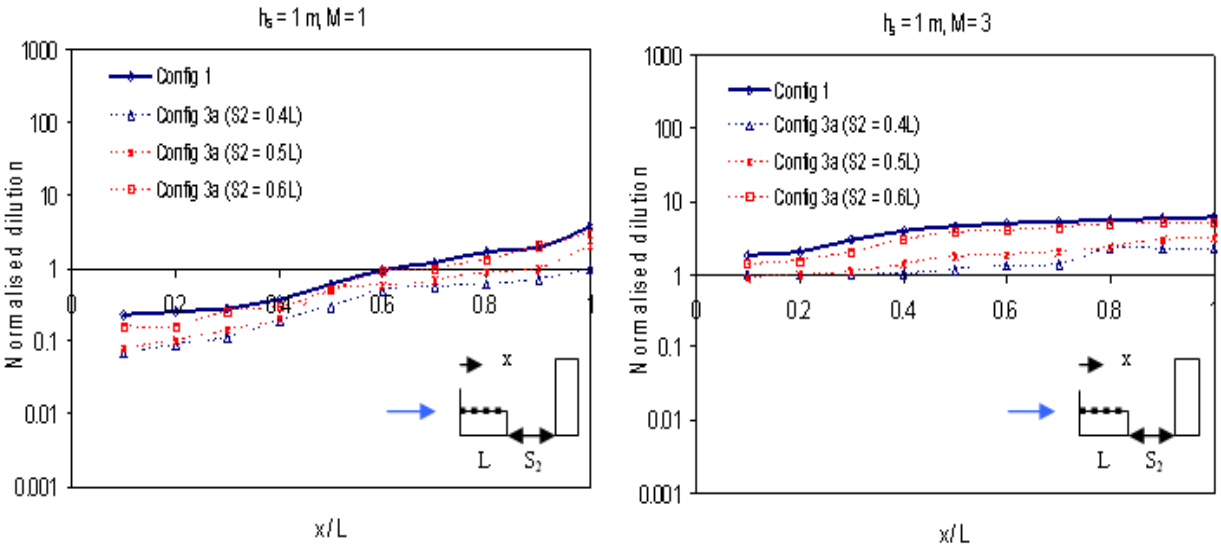


a) b)

Figure 5.37 Normalised dilution on rooftop of emitting building for: a) M = 1; b) M = 3

A similar trend is also observed for $h_s$ = 1 m and M = 3 as shown in Figure 5.37 (b).

Additional results are presented in Appendix E; a summary of this chapter is discussed further.

## 5.10 Summary

This chapter primarily focussed on four cases namely:

a) Isolated building (source).

b) Buildings of different geometries placed upstream of the source.

c) Buildings of different geometries placed downstream of the source.

d) A building placed upstream and downstream of the source.

Wind tunnel data obtained from the tracer gas study for different building configurations were compared to the isolated building. It was found that a taller upstream building caused the plume to travel towards the leeward wall of the upstream building thereby increasing plume concentrations on the leeward wall of the upstream building and rooftop of the emitting building. A taller downstream building disallows the plume from escaping and increases rooftop concentrations on the emitting building. A building placed upstream and downstream of the emitting building reduced plume dilution on rooftop of the emitting building due to increased plume meandering. As the spacing between buildings increases, the plume geometry gradually shifts towards the isolated building.

ASHRAE models can only be used to estimate plume dilution on the rooftop of isolated building. Additionally, it cannot be used for assessing dilution on the walls of a building (Hajra and Stathopoulos, 2012). The model does not incorporate the effects of turbulence due to adjacent buildings and local topography. In general ASHRAE predictions were found to be overly conservative.

In order to generalise the findings of this study, the results were also expressed in non-dimensional form since buildings in the urban environment can be of any size. For instance, the receptor distance from the stack on an emitting building was expressed in terms of the along wind dimension of the emitting building.

The subsequent chapter utilises the results of this study to rectify the ASHRAE 2007 and 2011 models to get reasonable dilution estimates on building surfaces.

# Chapter 6

# Implementation of research results

## 6.1 Introduction

This chapter uses the results obtained from this study to assess plume dilution on building surfaces from rooftop emissions. In this context, the pollutant dilution on adjacent building surfaces is expressed in terms of the roof dilution on the isolated building, followed by rectifying the ASHRAE model. Section 6.2 describes the grouping of different building configurations, based on the dilution results discussed in Chapter 5. Comparison of dilution for different adjacent building configurations and the isolated case are presented in section 6.3, followed by the proposed rectification of the ASHRAE models in section 6.4. Application of the rectified ASHRAE models is presented in section 6.5 followed by a summary of this chapter in section 6.6.

## 6.2 Grouping of different building configurations

In Chapter 5 it was shown that a total of 18 different building configurations were tested in the wind tunnel; these included: 2 – isolated cases (source), 7 – upstream building configurations, 7 – downstream configurations and 2 – adjacent building configurations involving a building placed upstream and downstream of the source. Figure 6.1 shows a schematic (elevation) of various configurations tested in the wind tunnel for a wind direction perpendicular to building face. The numbers shown in the figure are the "configuration numbers". The black dots indicate receptor locations on the building surfaces. Although receptors were placed at various locations (as shown in

Figures 5.1 through 5.5), only locations where plume concentrations were detected have been shown here.

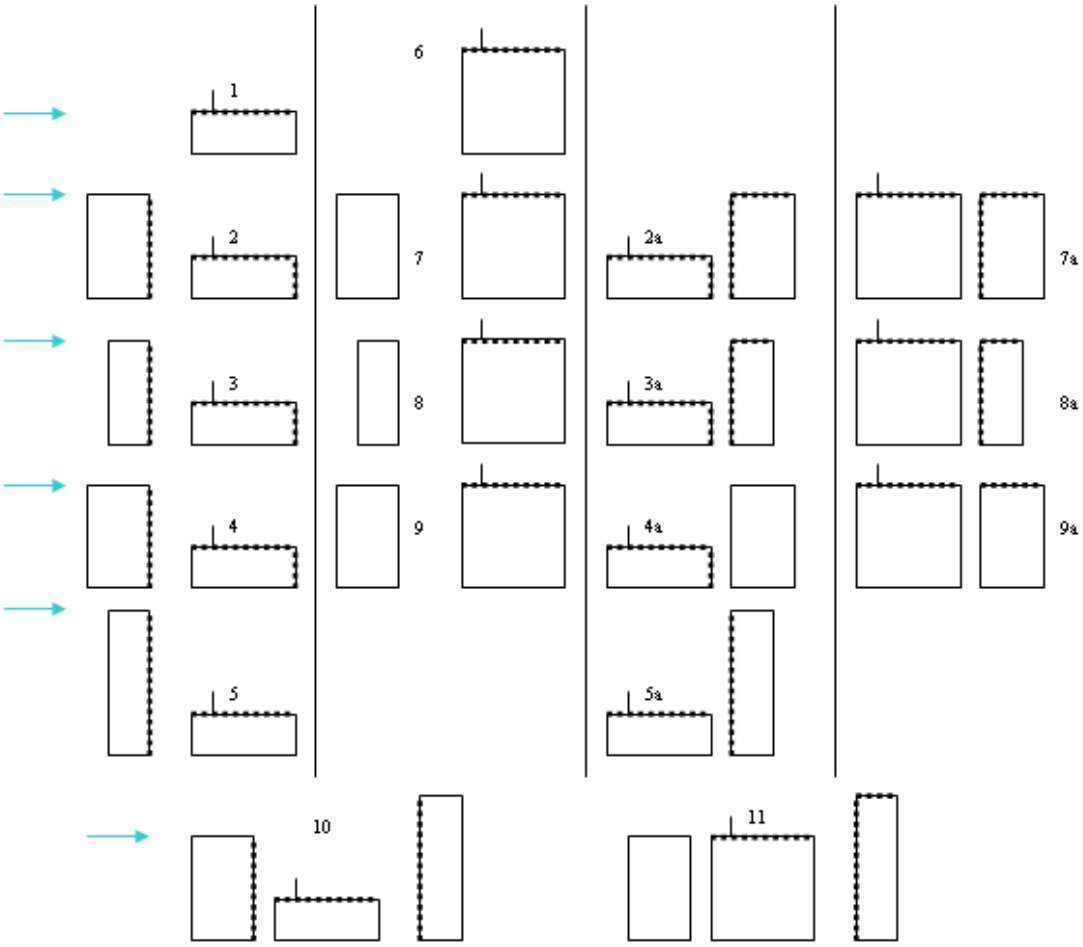


Figure 6.1 Schematic representation of various configurations tested in the wind tunnel

Considering the plume structure of the isolated case and comparing it to adjacent building configurations it is generally observed that:

a) Upstream Configurations 2 and 3 (Figure 6.1) generate comparable dilution on all building surfaces (see Figures 5.7 and 5.8). A similar trend is also observed for downstream Configurations 2a and 3a as shown in Figures 5.14, 5.16 and 5.17.

b) Configuration 4 (Figure 6.1) generates comparable roof dilution on emitting building with the isolated case (eg. Figure 5.7). Similarly, Configurations 1 and 4a produce comparable dilution on rooftop of emitting building.

c) A building of lower than or equal height with the emitting building, placed upstream (or downstream) of the emitting building does not influence the plume geometry significantly. For instance, the rooftop dilutions obtained on the emitting building from Configurations 7, 8 and 9 are comparable to Configuration 6 (eg. Figure 5.11).

d) Configuration 10 which consists of a tall building on either side of the emitting building can be expressed as a combination of Configurations 2 and 5a based on the results presented in Chapter 5 (section 5.6). Similarly, Configuration 11 may be expressed as a combination of Configuration 6 and Configuration 5a.

This allows one to reduce and simplify the 18 configurations described in Figure 6.1 to 6, as shown in Figure 6.2.

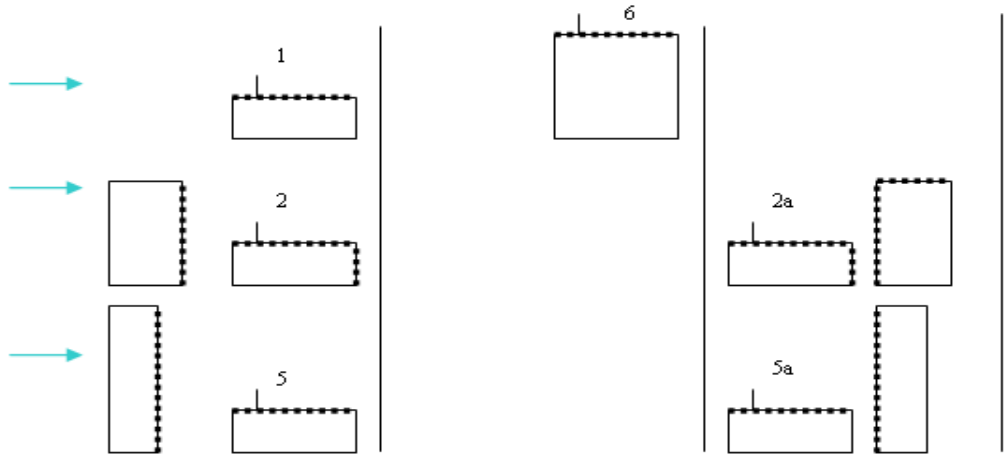


Figure 6.2 Reduced set of building configurations based on the plume characteristics for various proximity cases

## 6.3 Comparisons for adjacent building configurations with the isolated case

This section compares wind tunnel dilution estimates obtained for different adjacent building configurations and the isolated case. The building surfaces include the roof of the emitting and downstream buildings as well as the wall of the adjacent buildings. Estimation of factors for each building surface has been discussed separately in the following sub-sections.

### 6.3.1 Roof dilution on emitting building

The factors have been estimated separately for roof dilution on emitting building for "a taller upstream building" and "a taller downstream building". Configurations 2, 3 and 5 have been considered to assess plume dilution on roof of emitting building with respect to the isolated case (Configuration 1). In order to assess and compare the dilution between various configurations, the ratio of the dilution on roof of isolated building to dilution on roof of emitting building for adjacent building configurations is introduced:

$$f1 = \frac{D_i}{D_a} \tag{6.1}$$

where

$D_i$ is the dilution on roof of isolated building,

$D_a$ is the dilution on roof of emitting building for adjacent building configurations

For stack located at the upwind edge ($X_s$ = 0) comparisons between the average dilution of Configurations 2 and 3 and the isolated case (Configuration 1) are presented in Figure 6.3. The receptor distance from the upwind edge (x) has been expressed in terms of the along wind dimension (L) of the emitting building as explained in Chapter 5. An

average dilution for Configurations 2 and 3 was estimated since the rooftop dilutions from both these configurations were comparable (see Figure 5.7, Chapter 5). An average factor (f1) was estimated by dividing the dilution obtained for the isolated case by the average dilution of Configurations 2 and 3 at each receptor as explained in equation 6.1.

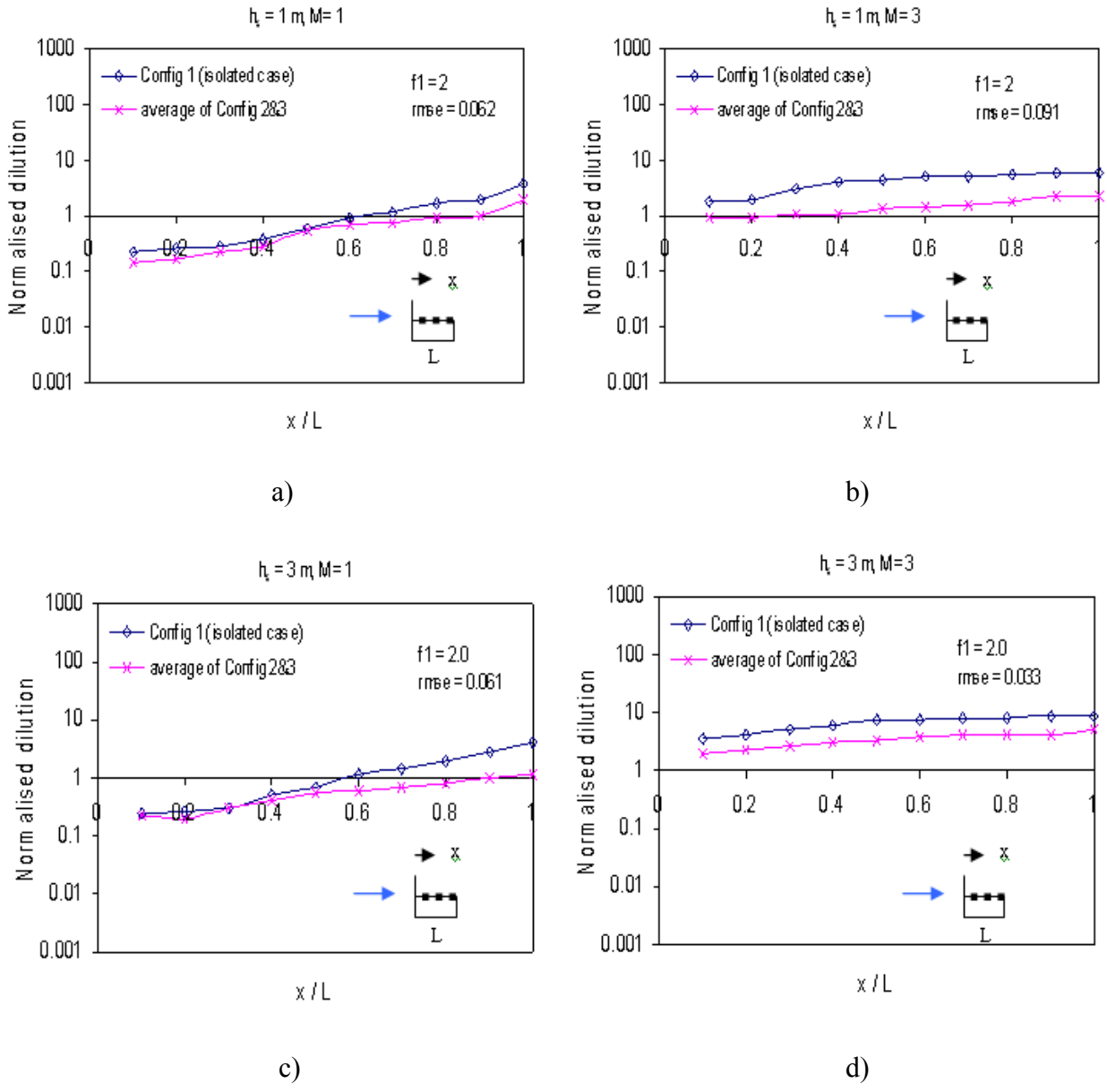


Figure 6.3 Normalised dilution on rooftop of emitting building for: a) $h_s$ = 1 m, M = 1; b) $h_s$ = 1, M = 3; c) $h_s$ = 3 m, M = 1; d) $h_s$ = 3, M = 3

This was done so that a relationship for a taller upstream building twice as high as the emitting building and an isolated building, could be established. It may be mentioned that the buildings in this case are spaced 0.4L apart. It may be recalled from Chapter 5 that for upstream configurations within 0.6L and downstream configurations within 0.5L, a change in spacing does not alter the plume geometry significantly. The factor f1 shown in Figure 6.3 was found by minimising the root mean square error (rmse) which is defined as:

$$rmse = \frac{1}{n}\sqrt{\sum (1 - \frac{p_i}{m_i})^2} \qquad (6.2)$$

where:

n represents the total number of receptor locations,

$p_i$ and $m_i$ are the predicted and measured normalised dilutions at receptor i.

In this case the measured dilution ($m_i$) is wind tunnel data of Configuration 1 and predicted dilution ($p_i$) is the factored dilution. For instance, in Figure 6.3 (a) f1 = 2 was determined by dividing the dilution estimated on the roof of the isolated building (Configuration 1) by the average dilutions of Configurations 2 and 3 at each receptor and by minimising the rmse which was found to be 0.062.

Taller upstream building configurations with centrally placed stacks change the plume geometry significantly, thereby affecting the building roof upwind and downwind of the stack. Figure 6.4 presents comparisons for Configuration 1 and the average of Configurations 2, 3, 4 and 5 for $X_s$ = 0.4L.

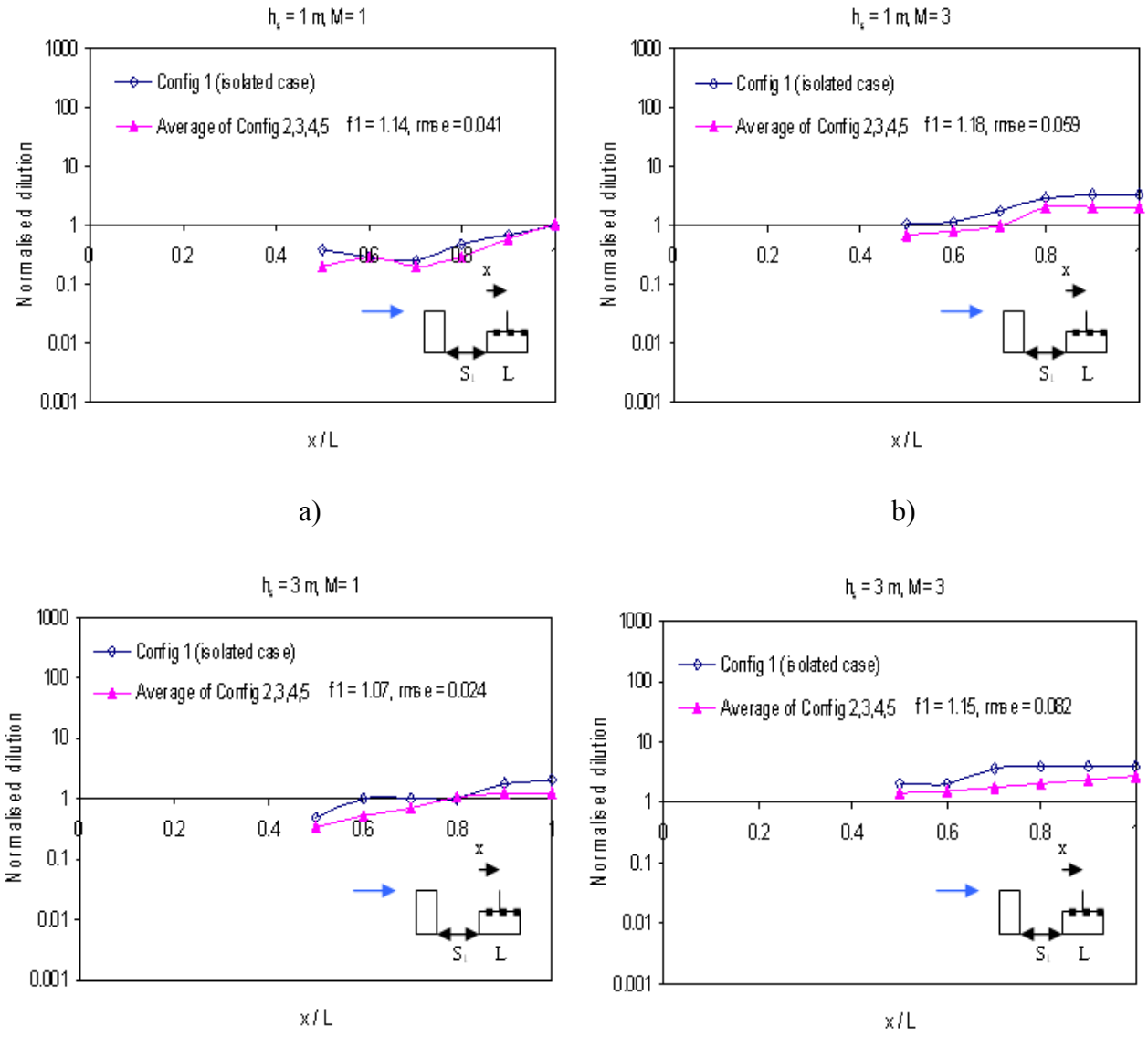


Figure 6.4 Normalised dilution on rooftop of low building ($B_1$): a) $h_s$ = 1 m, M = 1; b) $h_s$ = 1, M = 3; c) $h_s$ = 3 m, M = 1; d) $h_s$ = 3, M = 3

It may be mentioned that downwind of stack, the dilution obtained from all taller upstream configurations were found to be nearly comparable because the effect of the upstream building diminishes. Hence, the average dilutions from Configurations 2, 3, 4 and 5 have been plotted and compared with results from Configuration 1. For an isolated

building with a centrally placed stack, dilution is obtained only downwind of the stack. It is observed that at different $h_s$ and M values f1 is nearly 1, with rmse generally below 0.1. Taller downstream building configurations with centrally located stacks produce comparable dilution with the isolated case. However, this trend changes when the stack is located at the upwind edge as shown in Figure 6.5.

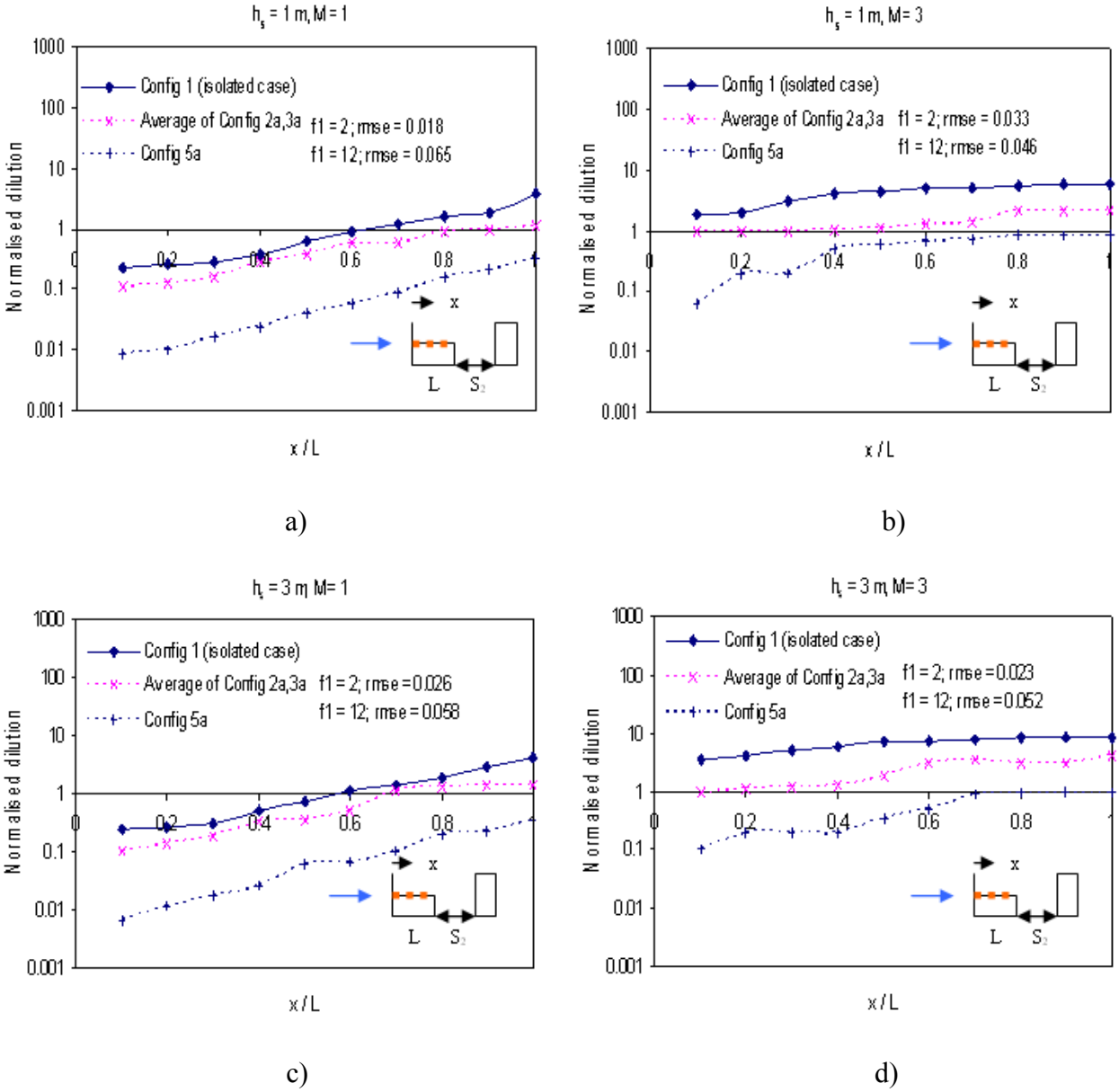


Figure 6.5 Normalised dilution on rooftop of low building ($B_1$): a) $h_s$ = 1 m, M = 1; b) $h_s$ = 1, M = 3; c) $h_s$ = 3 m, M = 1; d) $h_s$ = 3, M = 3

It may be recalled that Configurations 2a and 3a consist of a building twice as tall as the emitting building and Configuration 5a consists of a building 3.6 times higher than the emitting building. As discussed in Chapter 5, the dilution obtained from Configurations 2a and 3a are comparable and, hence their average dilution has been considered. From Figure 6.5 it is clear that the average dilution values of Configurations 2a and 3a are within a factor of 2 lower than the isolated case. Similarly, Configuration 5a predicts dilution within a factor of about 12 lower than the isolated case. The rmse values were found to be below 0.07. Factor (f1) was evaluated using a similar approach for different cases, as summarised at the end of the section in Table 6.1.

The following sub-section describes the estimation of factors for the roof of the downstream building using the dilution value on the downwind edge of the emitting building.

### 6.3.2 Roof dilution on downstream building

In the previous section an attempt was made to relate the dilution on the rooftop of the emitting building for adjacent building configurations as a function of the isolated building. In this section the relationship between the roof dilution on the downstream building and the roof dilution on the downwind edge of the emitting building is examined. The ratio of the dilution on roof of downstream building to dilution on downwind edge of emitting building is introduced and defined as:

$$f2 = \frac{D_d}{D_{de}} \tag{6.3}$$

where

$D_d$ is the dilution on the roof of the downstream building,

$D_{de}$ is the dilution on downwind edge of emitting building

It may be recalled from the results of Chapter 5 that dilution on the roof of the downstream building was found only when the downstream building is of equal height or about twice as tall as the emitting building. Buildings more than twice the height of the emitting building disallow the plume to accumulate on the roof of the downstream building due to their greater height. It is understandable that the dilution on the downwind edge of the emitting building may be closely related to the roof dilution of the downstream building since this is the closest surface of the emitting building from the downstream building. This can be explained further from Figure 6.6 where the dilution value obtained on the downwind edge of the emitting building for Configuration 2a for $h_s$ = 1 m and M = 1 is plotted along with the dilution obtained on the roof of the downstream building ($B_2$).

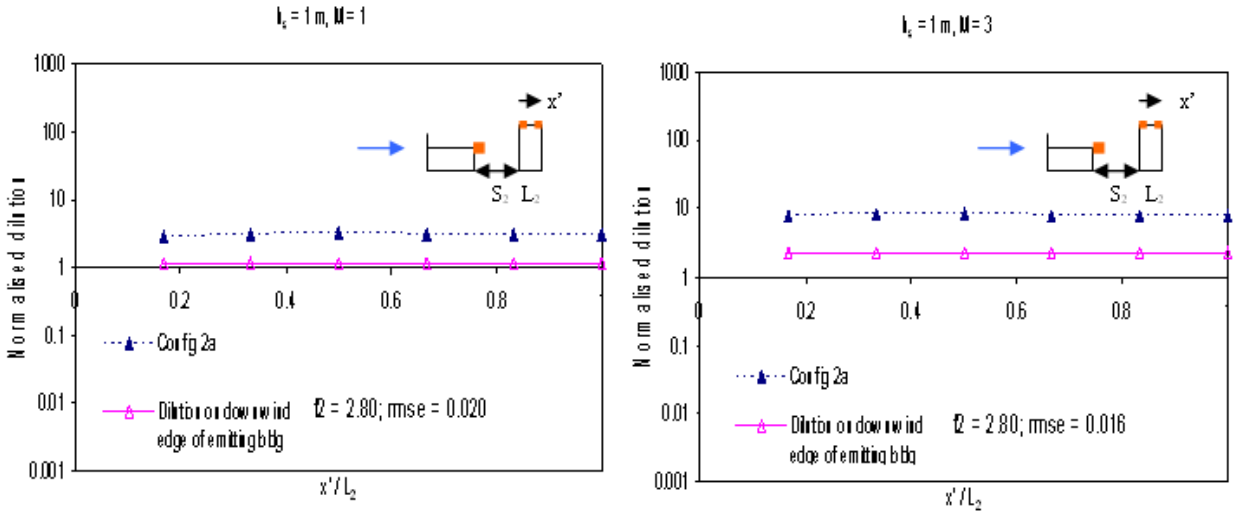


a) b)

Figure 6.6 Normalised dilution on rooftop of downstream building ($B_2$): a) M = 1; b) M = 3

The normalised dilutions are plotted in terms of the receptor distance from the upwind edge of the downstream building (x') and the along wind dimension of the

downstream building ($L_2$).It is observed that the dilution on the roof of the downstream building is about 2.8 times higher than the dilution on the downwind edge of the emitting building with rmse within about 0.02. The value of the factor f2 (equation 6.3) was found to be within about 3 for $h_s$ = 3 m (see Table 6.1).

### 6.3.3 Wall dilution on various building surfaces

Wall dilution consists of dilution on leeward wall of the upstream building and windward wall of the downstream building as well as dilution on the leeward wall of the low building. It is reasonable to relate the dilution downwind of the stack and the dilution obtained on the leeward wall of the upstream building since these building surfaces are close to each other. Therefore, a factor f3 may be defined as:

$$f3 = \frac{D_s}{D_{lu}} \tag{6.4}$$

where

$D_s$ is the dilution downwind of stack

$D_{lu}$ is the dilution on leeward wall of the upstream building

Since dilutions were found on the leeward wall of the emitting building for both upstream and downstream building configurations, the ratio of the dilution on downwind edge of emitting building to the dilution on leeward wall of emitting building is defined as:

$$f4 = \frac{D_{de}}{D_{le}} \tag{6.5}$$

where

$D_{de}$ is the dilution on the downwind edge of the emitting building,

$D_{le}$ is the dilution on the leeward wall of the emitting building

Similarly, the dilution on the windward wall of the downstream building may be found by relating it to the dilution on the downwind edge of the emitting building since these building surfaces are close to each other. Hence, a factor f5 can be defined:

$$f5 = \frac{D_{de}}{D_{wd}} \tag{6.6}$$

where

$D_{de}$ is the dilution on downwind edge of emitting building,

$D_{wd}$ is the dilution on windward wall of downstream building

From Chapter 5 it was understood that for taller upstream configurations the leeward wall of the upstream building was affected especially for buildings of equal across wind dimension. Figure 6.7 shows comparisons for the average normalised dilution for Configurations 2 and 3 and the dilution at the upwind edge of the emitting building. It may be recalled that the upstream buildings in Configurations 2 and 3 are twice as tall as the emitting building. The factors (f3) shown in Figure 6.7 are average factors and are summarised later in Table 6.2. In general, for the wall of a building, the dilution has been assumed constant (straight line) for simplicity due to the results obtained.

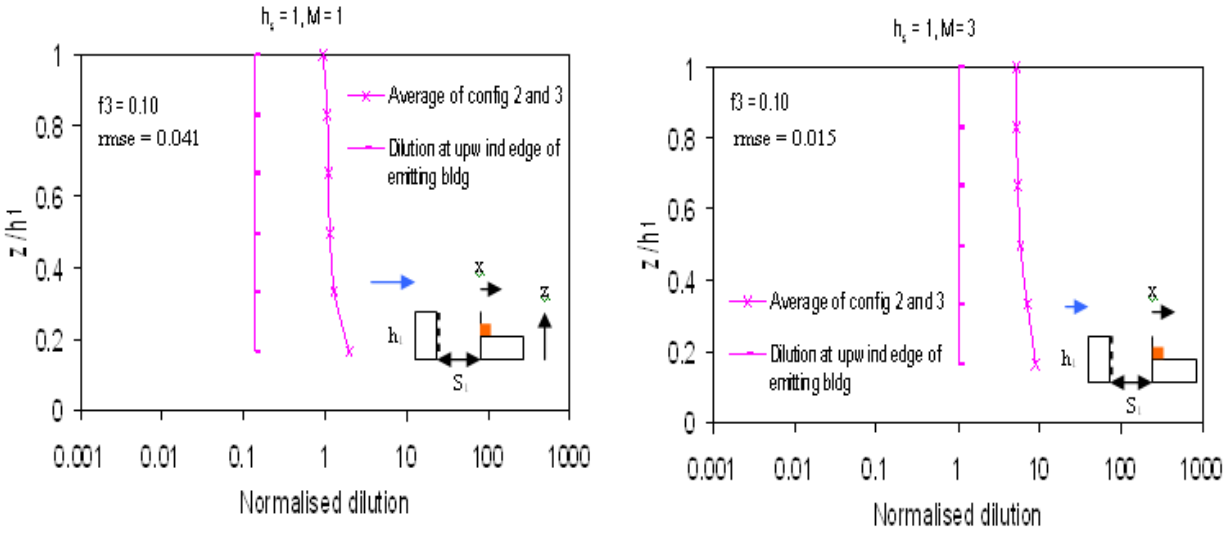


a) b)

Figure 6.7 Normalised dilution on leeward wall of upstream building: a) M = 1; b) M = 3

This method was also extended to downstream building configurations. For instance, the average dilution obtained from Configurations 2a and 3a are compared to the dilution on the downwind edge of the emitting building, as shown in Figure 6.8.

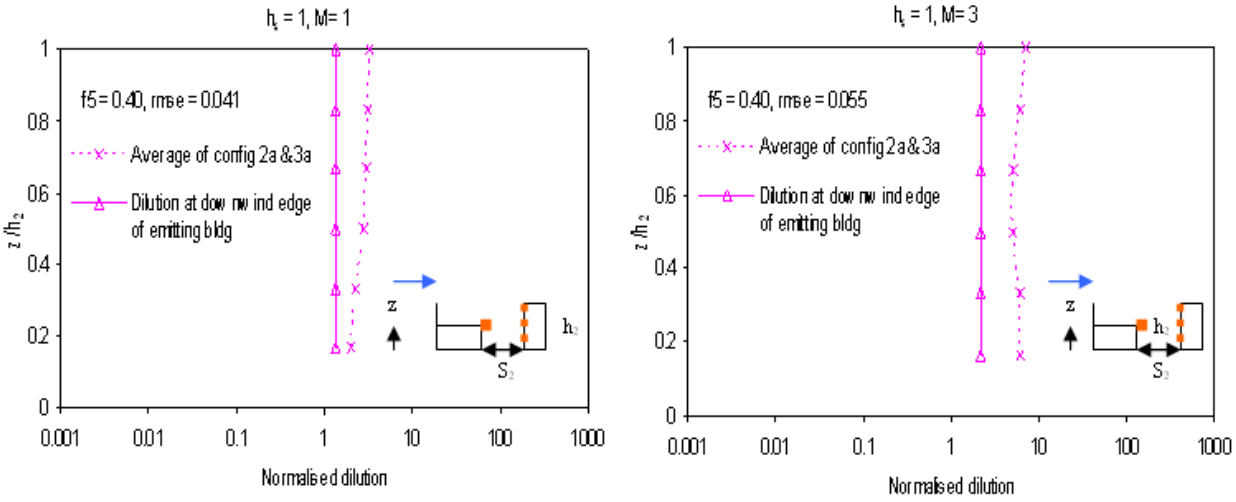


a) b)

Figure 6.8 Normalised dilution on windward wall of the downstream building: a) M = 1; b) M = 3

The value of f5 was found to be 0.4 for M = 1 and M = 3 with rmse values below 0.06.

Dilution was also obtained on the leeward wall of the emitting building at $h_s$ = 1 m and at M < 2 for taller upstream/downstream configurations (Configurations 2 and 2a). It was noted that for a given $h_s$ and M value the dilution on the leeward wall of the emitting building is nearly equal to the dilution obtained on the downwind edge of the emitting building roof. Therefore, one may safely assume f4 = 1 from equation 6.5. Tables 6.1 and 6.2 summarise the findings of this section.

Table 6.1 Roof dilution as a function of the isolated building

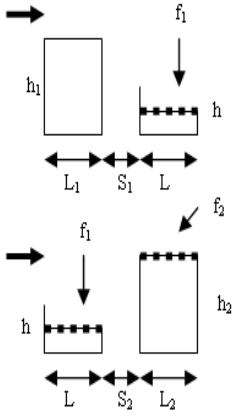


| Configuration | $X_s$ | $h_s$ | M | value of factor (rmse) |
|---|---|---|---|---|
| $h_1/h = 2$ | 0 | 1,2,3 | 1,2,3 | f1 = 2 (0.033-0.091) |
| $h_1/h = 2$ or 4 | 0.4L | 1,3 | 1,3 | f1 = 1.0 (0.024-0.082)* |
| $h_2/h = 2$ | 0 | 1,2,3 | 1,2,3 | f1 = 2.0 (0.018-0.033) |
| $h_2/h = 4$ | 0 | 1,2,3, | 1,2,3 | f1 = 12 (0.046-0.065) |
| $h_2/h = 2$ | 0 or 0.4L | 1, 3 | 1,2,3 | f2 = 2.8 (0.016-0.020) |
| $h_2/h = 1$ | 0 or 0.4L | 1, 3 | 1,2,3 | f2 = 1.12 (0.011-0.036) |

* dilution obtained only downwind of stack
f1 = (dilution on roof of isolated building)/ (dilution on roof of emitting bldg. for adjacent bldg. config.)
f2 = (dilution on roof of downstream building)/ (dilution on downwind edge of emitting building)

Table 6.2 Wall dilution as a function of the rooftop dilution of the emitting building

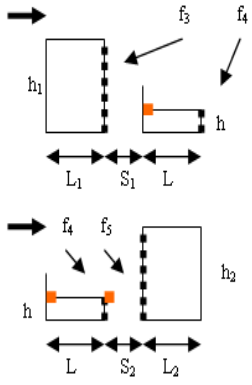


| Configuration | $X_s$ | $h_s$ | M | value of factor (rmse) |
|---|---|---|---|---|
| $h_1/h = 2$ | 0 | 1,3 | 1, 3 | f3 = 0.10 (0.041-0.055) |
| $h_1/h = 4$ | 0 | 1,3 | 1,3 | f3 = 0.3 (0.0431-0.0891) |
| $h_1/h = 4$ | 0.4L | 1 | 1,3 | f3 = 0.15 (0.0581) |
| $h_1/h = 4$ | 0.4L | 3 | 1,3 | f3 = 0.25 (0.073) |
| $h_1/h = h_2/h = 2$ | 0 | 1 | 1,2 | f4 = 1 (0.016-0.066) |
| $h_2/h = 2$ or 4 | 0,0.4L | 1,3 | 1,3 | f5 = 0.40 (0.041-0.085) |

f3 = (dilution downwind of stack)/(dilution on leeward wall of upstream bldg.)
f4 = (dilution on downwind edge of emitting bldg.)/(dilution on leeward wall of emitting building)
f5 = (dilution on downwind edge of emitting bldg.)/(dilution on windward wall of downstream bldg.)

It must be noted that for all these cases the across wind dimensions of both buildings are equal. The tables in this section were primarily prepared to relate the dilution on the roof/wall of the emitting and adjacent building surfaces in terms of the isolated case. As an example one may consider, Figure 6.5 where the average values of Configurations 2a and 3a have been compared to the isolated case (Configuration 1). It may be recalled that Configurations 2a and 3a consist of a downstream building twice as tall as the low building. From Table 6.1, $h_2/h = 2$, $h_s = 1$ m, m = 1, $X_s = 0$, f1 = 2 is obtained. This factor (f1) represents the ratio of the dilution obtained from Configuration 1 to the average dilution of Configurations 2a and 3a.

### 6.4 Rectification of the ASHRAE 2007 and 2011 models

This section presents the factors that were evaluated by comparing ASHRAE 2007 and 2011 models with experimental data for the isolated building. These factors combined with those described in Tables 6.1 and 6.2 can be used to estimate plume dilution on various building surfaces. Comparisons for ASHRAE 2007, 2011 and wind tunnel data for isolated buildings have been presented in Chapter 5 and the formulations used in each model were described in Chapter 4. For additional details one may also refer to Hajra et al., 2011. The ASHRAE models were applied to the two isolated buildings - low-rise (15 m) and intermediate (30 m) - that were tested in the wind tunnel and a factor was obtained for each model. For instance, Figure 6.9 shows comparisons for wind tunnel data, ASHRAE 2007 and 2011 and their respective rectified values for $h_s = 1$ m and $X_s = 0$. An average factor for each model was obtained by dividing the wind tunnel data by the respective ASHRAE model values and minimising the rmse. A rectified model was then

obtained by multiplying that factor by the corresponding ASHRAE value. As shown in Figure 6.9 (a), a factor of 10 and 20 were obtained for rectifying the ASHRAE 2007 and 2011 estimates respectively. Similarly, factors were obtained for M = 3 as shown in Figure 6.9 (b). The factors for rectifying the ASHRAE 2011 model were higher than the 2007 values since the dilutions of the former are more conservative than the latter.

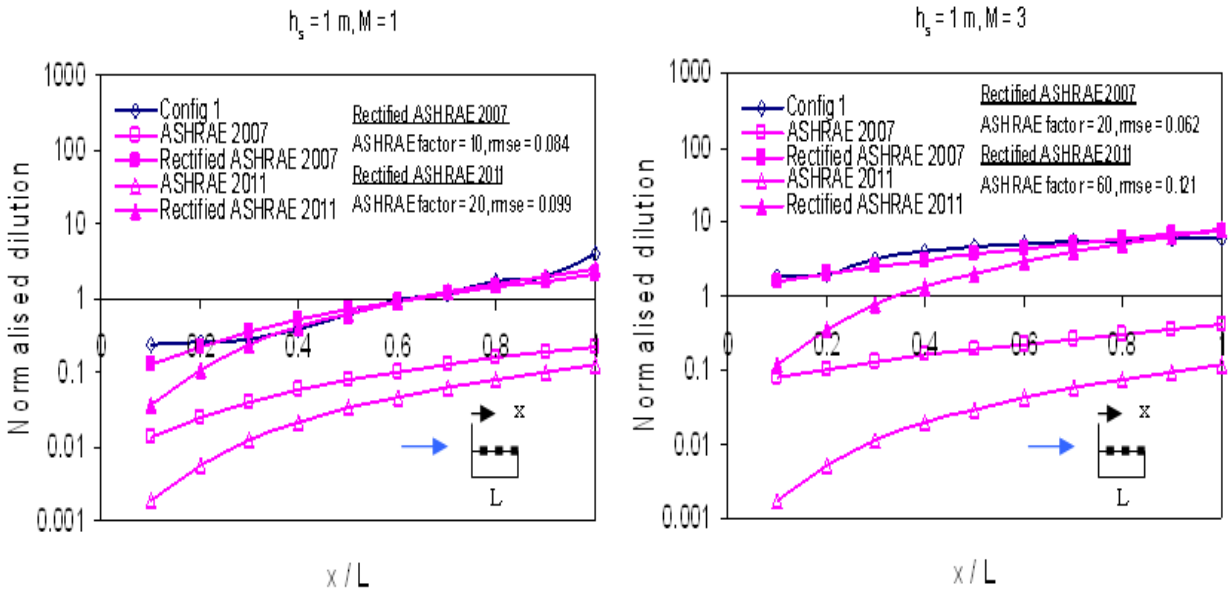


a) b)

Figure 6.9 Normalised dilution on rooftop of low rise building: a) M = 1; b) M = 3

Similarly, factors were also determined for higher $h_s$ and M values as well as for centrally placed stacks ($X_s$ = 0.4L) for the low building (15 m high). Another example is shown in Figure 6.10 for an intermediate emitting building (30 m high) for $h_s$ = 1 m. As shown in Figure 6.10 (a) a factor of about 10 and 50 were obtained to rectify ASHRAE 2007 and 2011 values.

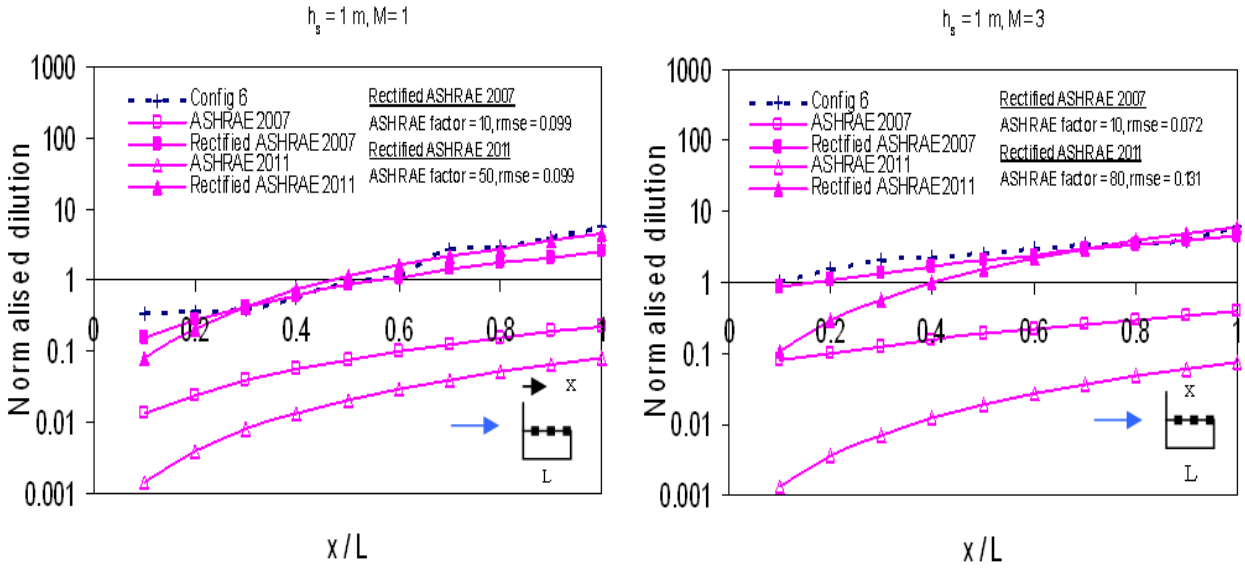


a) b)

Figure 6.10 Normalised dilution on rooftop of intermediate building: a) M = 1; b) M = 3

Similarly, by suitably minimising the root mean square errors, factors of 10 and 80 were obtained for M = 3 (Figure 6.10 (b)).

It may be noted that due to the formulations discussed in Chapter 4, ASHRAE 2011 estimates are generally lower than the 2007 values close to the stack. Hence, the rectified ASHRAE 2011 estimates also tend to be conservative close to the source. For instance, at M = 1 and 3 rectified ASHRAE 2011 predicts about 10 times lower dilution than wind tunnel data. Factors for different $h_s$, M and $X_s$ values were estimated using a similar approach for the low-rise and intermediate buildings. These factors and their respective rmse values (shown in brackets) have been tabulated in Table 6.3.

According to Stern and Yamartino, 2001 "*buildings can dramatically alter atmospheric flows to include vortices and other recirculations; urban scale models cannot adequately simulate the concentration patterns within the canopy, for instance, within a street canyon*". It is normal to expect low correlation between experimental data

and model estimates (higher root mean square errors) in such micro-scale modelling problems. For instance, Stern and Yamartino (2001) had correlations ranging from 0.637 - 0.888 and root mean square error from 0.041 – 1.341, for micro scale dispersion model within a street canyon to estimate concentrations due to traffic flow. Similarly, Ramsdell and Fosmire (1998) developed a model for predicting dilutions in the vicinity of buildings and found about *"55% of the model predictions within a factor of 4 of the measured values"*.

Table 6.3 Factors applicable for the isolated building

| $X_s$ | $h_s$ | M | ASHRAE 2007 | | ASHRAE 2011 | |
|---|---|---|---|---|---|---|
| | | | ASHRAE factor (low-rise building – 15 m) | ASHRAE factor (intermediate building – 30 m) | ASHRAE factor (low-rise building – 15 m) | ASHRAE factor (intermediate building – 30 m) |
| 0 | 1 | 1 | 10 (0.084) | 10 (0.099) | 20 (0.099) | 50 (0.099) |
| 0 | 1 | 2 | 15 (0.091) | 10 (0.081) | 50 (0.086) | 70 (0.074) |
| 0 | 1 | 3 | 20 (0.062) | 10 (0.072) | 60 (0.121) | 80 (0.131) |
| 0 | 3 | 1 | 10 (0.080) | 10 (0.099) | 20 (0.094) | 120 (0.099) |
| 0 | 3 | 2 | 15 (0.088) | 10 (0.085) | 50 (0.089) | 130 (0.066) |
| 0 | 3 | 3 | 20 (0.083) | 10 (0.094) | 60 (0.894) | 160 (0.101) |
| 0 | 5 | 1 | 10 (0.092) | 10 (0.085) | 140 (0.921) | 500 (0.113) |
| 0 | 5 | 3 | 20 (0.044) | 10 (0.089) | 60 (0.099) | 2000 (0.191) |
| 0.4L | 1 | 1 | 10 (0.098) | 10 (0.098) | 5 (0.079) | 5 (0.088) |
| 0.4L | 1 | 2 | 10 (0.088) | 10 (0.091) | 10 (0.092) | 20 (0.096) |
| 0.4L | 1 | 3 | 10 (0.081) | 10 (0.096) | 20 (0.049) | 40 (0.062) |
| 0.4L | 3 | 1 | 10 (0.094) | 20 (0.099) | 5 (0.065) | 20 (0.078) |
| 0.4L | 3 | 2 | 10 (0.098) | 20 (0.092) | 10 (0.097) | 60 (0.099) |
| 0.4L | 3 | 3 | 10 (0.099) | 20 (0.099) | 20 (0.066) | 120 (0.083) |
| 0.4L | 5 | 1 | 10 (0.051) | 10 (0.096) | 10 (0.095) | 60 (0.121) |
| 0.4L | 5 | 3 | 10 (0.093) | 20 (0.095) | 10 (0.102) | 330 (0.129) |

Therefore, the proposed factors presented in Tables 6.1 to 6.3 can be used to estimate dilution on building surfaces.

Therefore, the Rectified ASHRAE approach:

- applies to different building surfaces.
- modifies the ASHRAE 2007 and 2011 values to correctly estimate roof dilution.
- introduces separate factors for estimating plume dilution on adjacent building surfaces.
- restricts the use of the model within certain limits to avoid confusion amongst designers and inaccurate use of the model.

Based on the results obtained from ASHRAE 2011 it is understood that the rectified ASHRAE 2011 approach is difficult to apply. This is because of the low plume rise and spread parameters estimated by ASHRAE 2011 (Chapter 4). The inappropriateness of the ASHRAE 2011 model can be observed from the factors in Table 6.3 which are quite non-uniform and erratic compared to the 2007 factors which display a relatively uniform trend. For instance, from Table 6.3 at $X_s = 0.4L$, $h_s = 3$ m for an intermediate building, the factor for rectified ASHRAE 2007 model is equal to 20 for M = 1 and 3 respectively; whilst the corresponding factors are 20 and 120 for rectified ASHRAE 2011. This erratic change in factors is primarily because the dilution estimates are very low close to the stack. Since the rectified process tries to estimate the factors by minimising rmse values, a smaller value of rmse is achieved only through a larger factor for ASHRAE 2011. This problem is less in the ASHRAE 2007 model because the plume rise estimates close to the stack are not as low as the 2011 model. Due to the uniformity in the factors used to rectify the ASHRAE 2007 model, Table 6.3 can be reduced to a smaller form, as presented in Table 6.4.

Table 6.4 Factors to rectify ASHRAE 2007 for the isolated building

| $X_s$ | $h_s$ | M | ASHRAE 2007 | |
|---|---|---|---|---|
| | | | ASHRAE factor (low-rise building – 15 m) | ASHRAE factor (intermediate building – 30 m) |
| 0 | 1,3,5 | 1 | 10 (0.084-0.092) | 10 (0.085-0.099) |
| 0 | 1,3 | 2 | 15 (0.088-0.091) | 10 (0.081-0.085) |
| 0 | 1,3,5 | 3 | 20 (0.044-0.083) | 10 (0.072-0.094) |
| 0.4L | 1 | 1,2,3 | 10 (0.081-0.098) | 10 (0.091-0.098) |
| 0.4L | 3 | 1,2,3 | 10 (0.094-0.099) | 20 (0.092-0.099) |
| 0.4L | 5 | 1 | 10 (0.051) | 10 (0.096) |
| 0.4L | 5 | 3 | 10 (0.093) | 20 (0.095) |

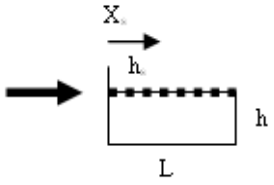


Table 6.4 presents ASHRAE factors for rectifying the ASHRAE 2007 model for the isolated building cases. Factors obtained from Tables 6.1, 6.2 and 6.4 are applied to present and previous studies to rectify ASHRAE 2007 estimates, as discussed further.

## 6.5 Application of the rectified ASHRAE 2007 model to present and previous studies

The rectified ASHRAE 2007 model was applied to experimental data obtained from present and previous studies. At the outset, few comparisons with the experimental results from the present study are presented.

### 6.5.1 Application of the rectified ASHRAE 2007 to present study

Figure 6.11 shows comparisons for wind tunnel data, ASHRAE 2007 and its rectified form for Configuration 1 (low building) for $h_s$ = 1 m and $X_s$ = 0. ASHRAE 2007 values are lower than wind tunnel data at all points due to reasons explained previously (Chapter 5). The factors were estimated from Table 6.4 and multiplied with the ASHRAE 2007

values to obtain the rectified form. Rectified ASHRAE 2007 compares well with experiment at all receptors for M = 1 and M = 3. For instance, for a low-rise building at $X_s = 0$, $h_s = 1$ and M = 1, Table 6.4 gives 10 with rmse = 0.084 (Figure 6.11 (a)).

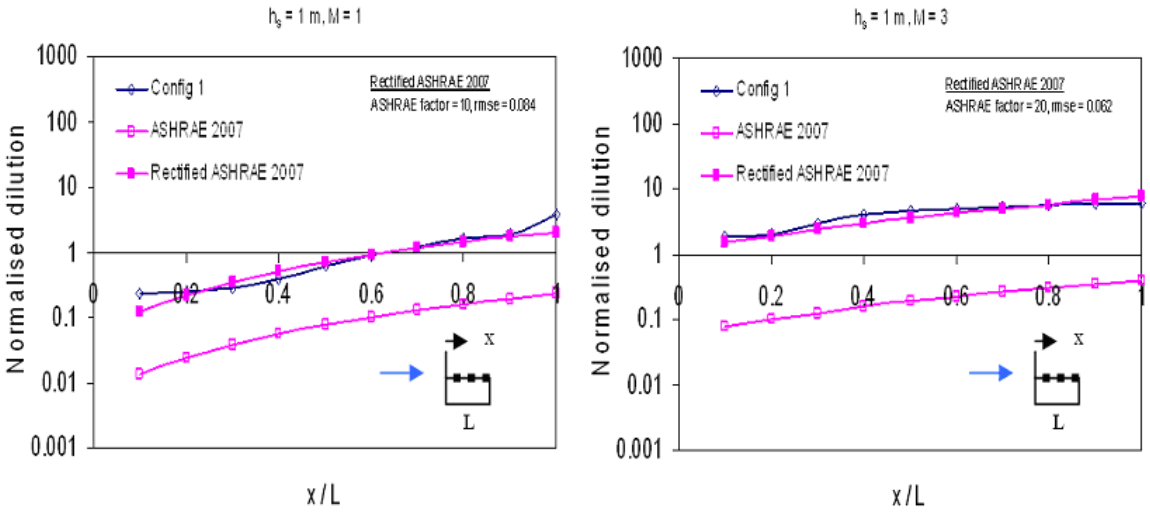


a) b)

Figure 6.11 Normalised dilution on rooftop of low building: a) M = 1; b) M = 3

This approach was also extended to a taller upstream building twice as high as the low building (Configuration 2) for $h_s = 1$ m and $X_s = 0$ as shown in Figure 6.12. In this case the ASHRAE 2007 values were obtained for the isolated case (identical values from Figure 6.11) and multiplied by the appropriate factor. The factor was determined from Tables 6.1 and 6.4. For instance, from Table 6.1 for $h_1/h = 2$, $X_s = 0$, $h_s = 1$ m and M = 1, f1 = 2 can be obtained. It may be recalled that this factor was obtained by dividing the roof dilution for the isolated case and upstream building configuration. For $X_s = 0$, $h_s = 1$ m, M = 1, Table 6.4 gives ASHRAE factor of 10, which is the ratio of wind tunnel dilution for the isolated case and ASHRAE 2007 values.

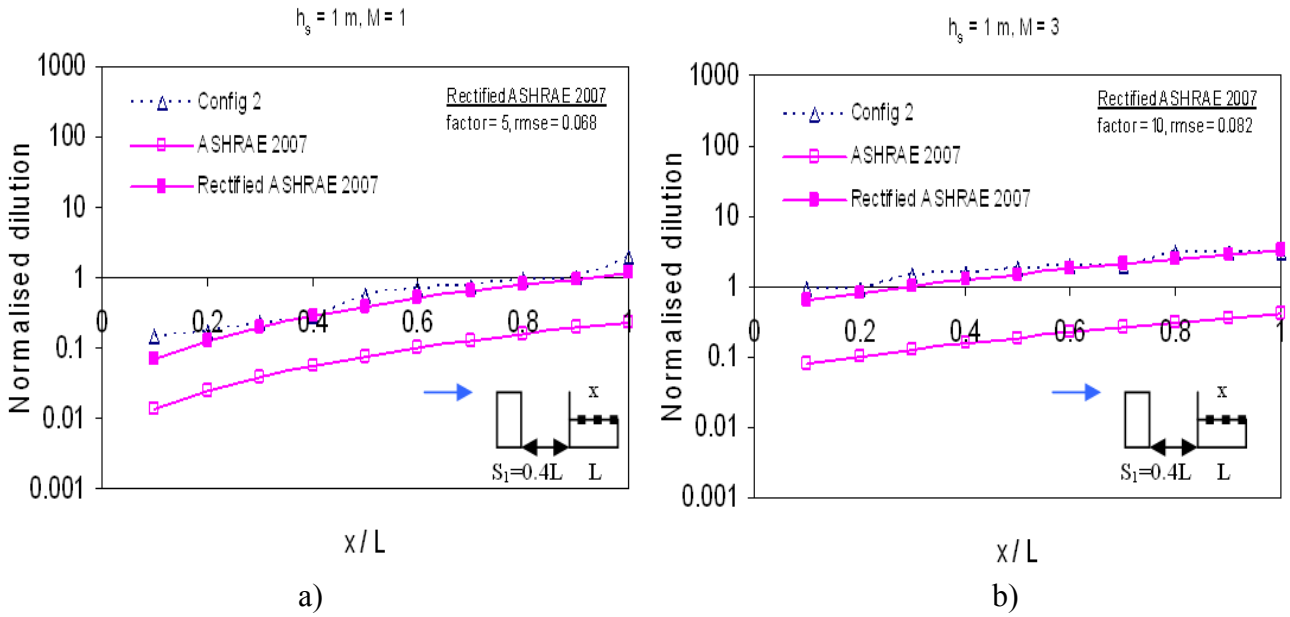


Figure 6.12 Normalised dilution on rooftop of low building: a) M = 1; b) M = 3

Therefore, in order to relate ASHRAE 2007 values to the wind tunnel dilution of Configuration 2 a factor of 5 is obtained by dividing 10 by 2, as shown in Figure 6.12 (a). The rectified ASHRAE 2007 results compare well with experiment at all receptors. Figure 6.13 explains the process of estimating factors corresponding to Figure 6.12 (a).

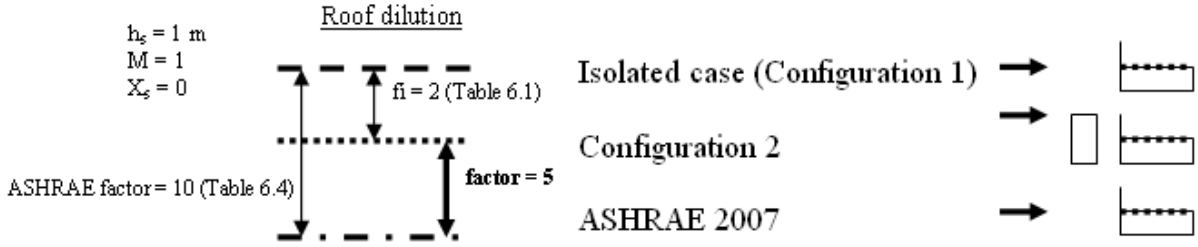


Figure 6.13 Sketch showing the calculation of factor corresponding to Figure 6.12 (a)

Figure 6.14 shows dilution on the leeward wall of the upstream building of Configuration 2 for $h_s$ = 1 m, $X_s$ = 0 and $S_1$ = 0.4L. It may be mentioned that the factors

may be applied for adjacent building configurations within spacing of 0.6L for upstream building configurations and 0.5L for downstream configurations. Beyond 0.6L the dilution on emitting building may be estimated by using the factors for the isolated case (Table 6.4).

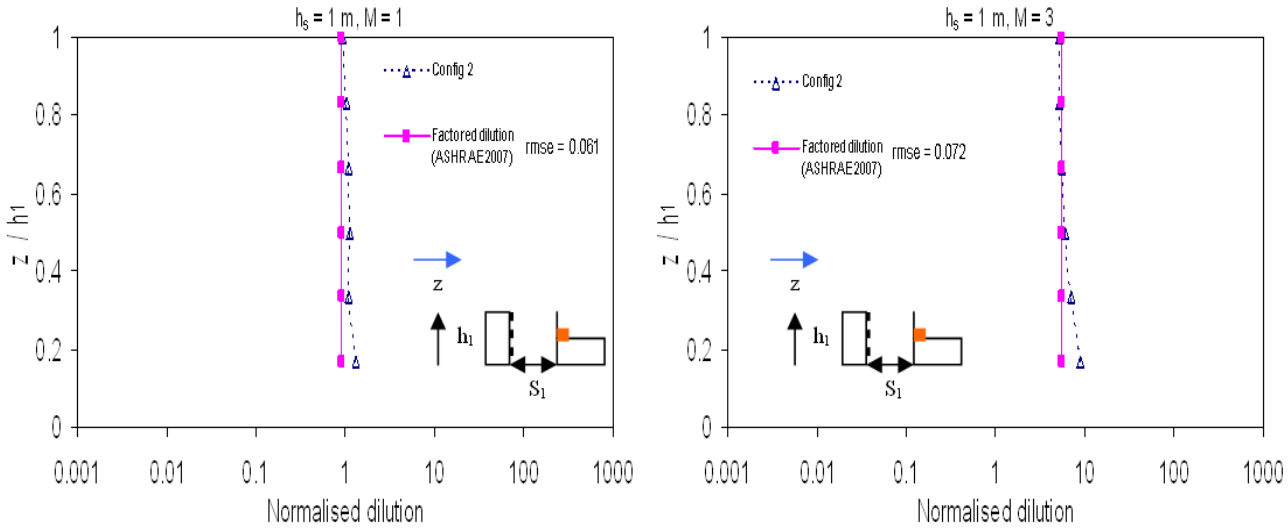


a) b)

Figure 6.14 Normalised dilution on leeward wall of upstream building: a) M = 1; b) M = 3

The dilution on the leeward wall of the upstream building is estimated from the roof dilution obtained on the receptor immediately downwind of stack. For instance, from Figure 6.12 (a) for $h_s$ = 1 m and M = 1, the rectified ASHRAE 2007 dilution at 0.1L is 0.095. From Table 6.2, f3 = 0.1 is obtained for $h_1/h$ = 2. It may be recalled that f3 represents the ratio of roof dilution downwind of stack to the dilution on leeward wall of upstream building. Therefore, 0.095 divided by 0.1 gives about 0.95 as the factored dilution from the rectified ASHRAE 2007 model (Figure 6.14 (a)). Similarly, factored dilution values were also obtained for M = 3 (Figure 6.14 (b)). In general the factored

dilution obtained from the 2007 model compared well with experimental data at all receptors.

Figure 6.15 also shows roof dilution on the emitting building for a taller downstream building twice as high as the emitting building (Configuration 2a) for $h_s$ = 1 m, $X_s$ = 0 and $S_2$ = 0.4L.

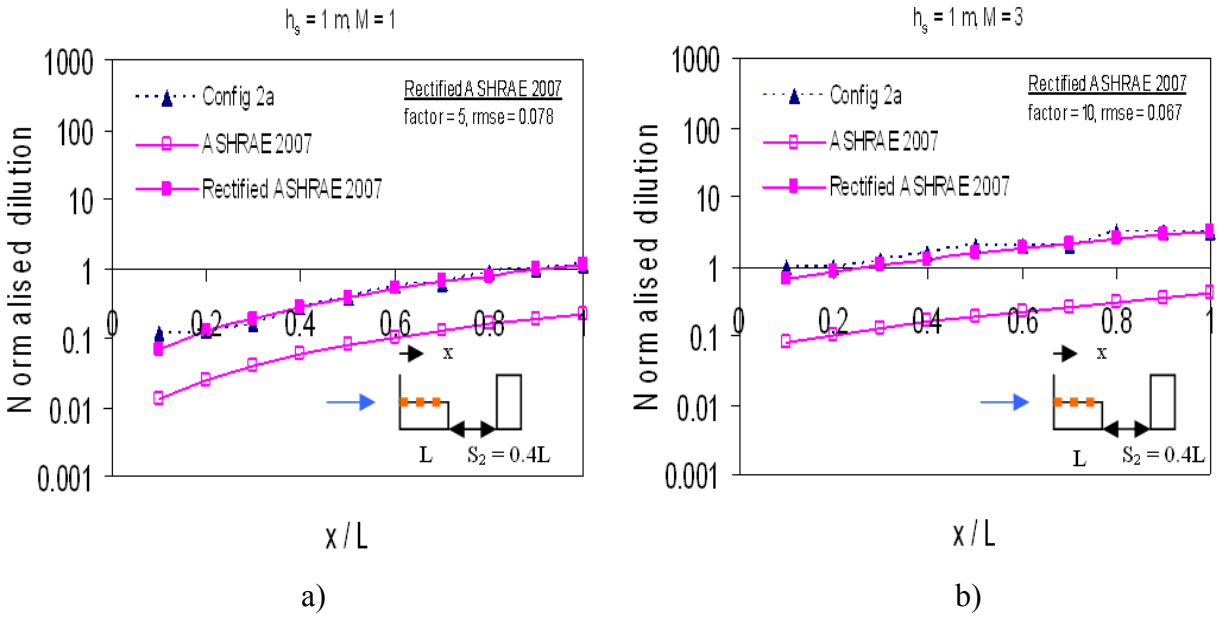


Figure 6.15 Normalised dilution on rooftop of low building: a) M = 1; b) M = 3

The factors were determined from Tables 6.1 and 6.4, as described previously. Good comparisons between rectified ASHRAE 2007 and wind tunnel data were obtained at all receptors for M = 1 and M = 3.

A comparison between factored ASHRAE 2007 dilution and wind tunnel data on the windward wall of the downstream building is presented in Figure 6.16. Good comparisons between factored dilution and wind tunnel data were found at all receptors for M = 1 and M = 3. The wall dilution is obtained in a similar way as in upstream building configurations except that the dilution on the windward wall is related to the

roof dilution on the downwind edge of the emitting building. For instance, for $h_s$ = 1 m, M = 1, $X_s$ = 0, f5 = 0.4 was obtained from Table 6.2. A dilution value of 1.1 was obtained on the downwind edge of the roof (Figure 6.15 (a)). On dividing 1.1 by 0.4 yields a factored dilution of 2.75, as shown in Figure 6.16 (a). Similarly, factored dilution was also obtained for M = 3 (Figure 6.16 (b).

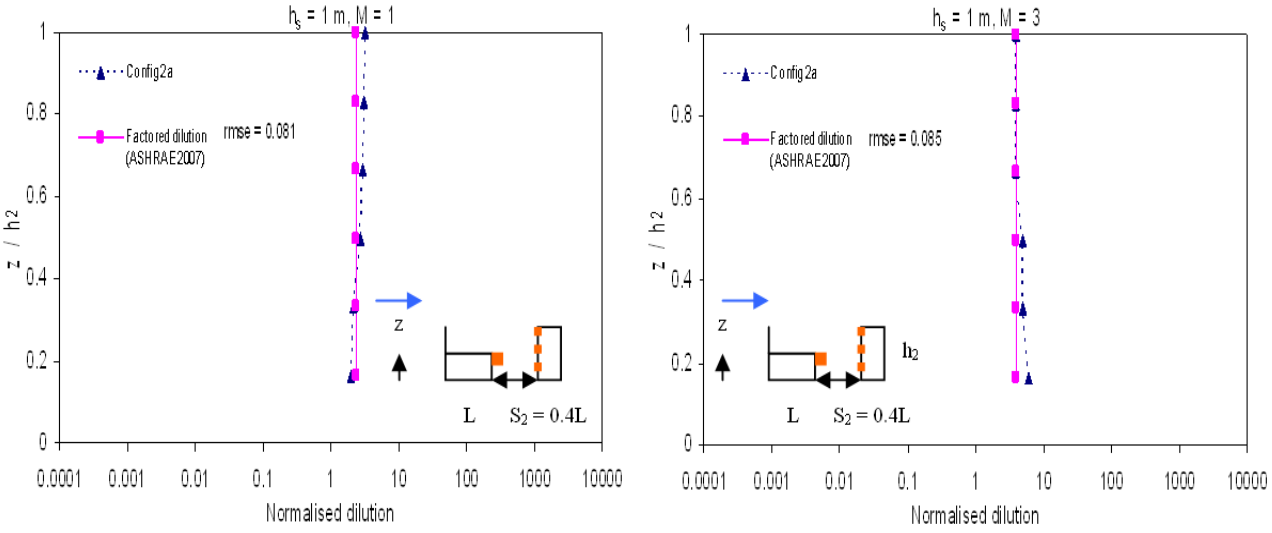


a) b)

Figure 6.16 Normalised dilution on windward wall of the downstream building: a) M = 1; b) M = 3

Figure 6.17 also shows dilution on the roof of the downstream building of Configuration 2a for $h_s$ = 1 m. From Table 6.1 the value of f2 = 2.8 for $h_2/h$ = 2, $h_s$ = 1 m, M = 1 and $X_s$ = 0. This implies that the dilution on the roof of the downstream building is about 2.8 times the dilution obtained on the downwind edge of the low building. For $h_s$ = 1 m and M = 1 the dilution on downwind edge of the roof is 1.1 for Configuration 2a (Figure 6.15 (a)).

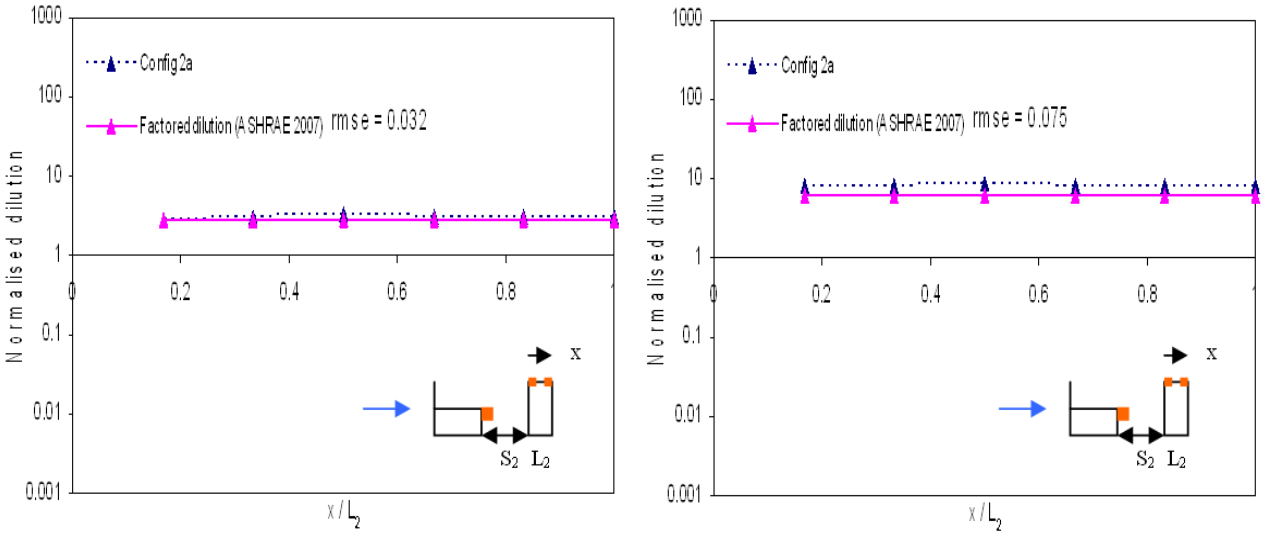


a) b)

Figure 6.17 Normalised dilution on rooftop of downstream building: a) M = 1; b) M = 3

Therefore multiplying this dilution value to 2.8 yields 3.08 (Figure 6.17(a)). In general, the factored dilution obtained from the rectified ASHRAE 2007 approach compares well with wind tunnel dilution at all receptors for any given $h_s$ and M value.

This approach can also be extended to estimate dilution on the building surfaces of Configurations 10 and 11 which consists of an emitting building placed in between two adjacent buildings. Additional results are presented in Appendix F. The subsequent section describes the application of the rectified ASHRAE approach to previous studies.

### 6.5.2 Application of the rectified ASHRAE 2007 to previous studies

In this section the rectified ASHRAE 2007 approach has been applied to previous experimental studies. This includes studies for isolated building and adjacent building

configurations. At the outset, comparisons with the rectified ASHRAE 2007 approach and results obtained from different isolated building cases are discussed.

#### 6.5.2.1 Application to isolated building

Experimental data from three studies, namely Schulman and Scire, 1991, Wilson et al., 1998 and Petersen et al., 1999 were used for the present study. The experimental parameters used in those studies are presented in Table 5.4 (Chapter 5).

Comparisons with Schulman and Scire, 1991, ASHRAE 2007 and rectified ASHRAE 2007 are presented in Figure 6.18 in terms of normalised dilution for a 15 m high isolated building for $h_s$ = 1.5 m, M = 1 and $X_s$ = 0.6L.

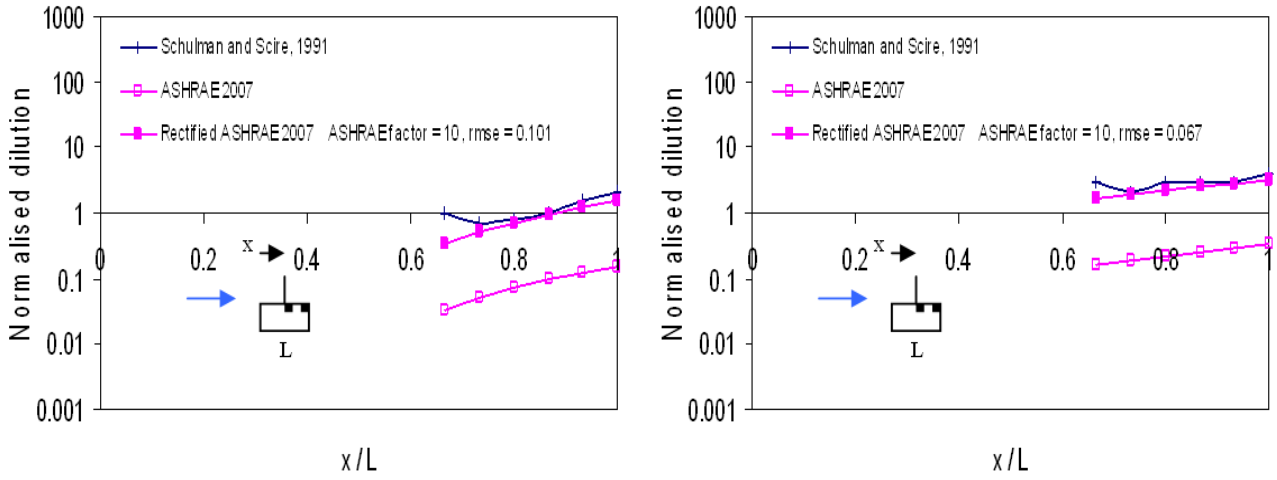


Figure 6.18 Rectified ASHRAE model applied to the wind tunnel data from Schulman and Scire, 1991 for the flat roofed low-rise building for $X_s$ = 0.6L: a) M = 1; b) M = 3

Results show that although Rectified ASHRAE 2007 predicts lower dilution than wind tunnel data close to the stack (about a factor of 5), good comparisons are obtained at points beyond 0.7 L from stack. This is because the proposed model is based on

ASHRAE 2007 which is always conservative. The factor can be estimated from Table 6.4. For instance, an ASHRAE factor of 10 is obtained for $h_s$ = 1.5 m and M = 1, which has been used to rectify ASHRAE 2007 estimates (Figure 6.18 (a)). It may be mentioned that the stack is located at 0.6L for Schulman and Scire's study whilst the present study estimates the factor for stack location of 0.4L from Table 6.4. Estimating the factor at $X_s$ = 0.6L by further extrapolation using the factors at $X_s$ = 0 and 0.4L, is not recommended as this may lead to numerical errors. A similar approach was used to estimate the factor for M = 3. In general, the rectified ASHRAE estimates compared well with experiment, except very close to the stack.

Comparisons for ASHRAE 2007, experimental data from Wilson et al., 1998 and Rectified ASHRAE for $h_s$ = 2 m are shown in Figure 6.19. Results show that at $h_s$ = 2 m and M = 1 for stack placed at the upwind edge ($X_s$ = 0) good comparisons between rectified ASHRAE 2007 and experimental data were obtained beyond 0.3L from stack. However, very close to the stack the rectified ASHRAE 2007 predicts somewhat lower dilution than wind tunnel results due to reasons explained previously (Chapter 5). The factor can be found from Table 6.4 - for instance, the ASHRAE factor corresponding to Figure 6.19 (a) is 10, which has been used to rectify ASHRAE estimates. A similar approach was adopted for $h_s$ = 2 m and M = 3 as shown in Figure 6.19 (b). Good comparisons were obtained between rectified ASHRAE and experiments with rmse values less than 0.1.

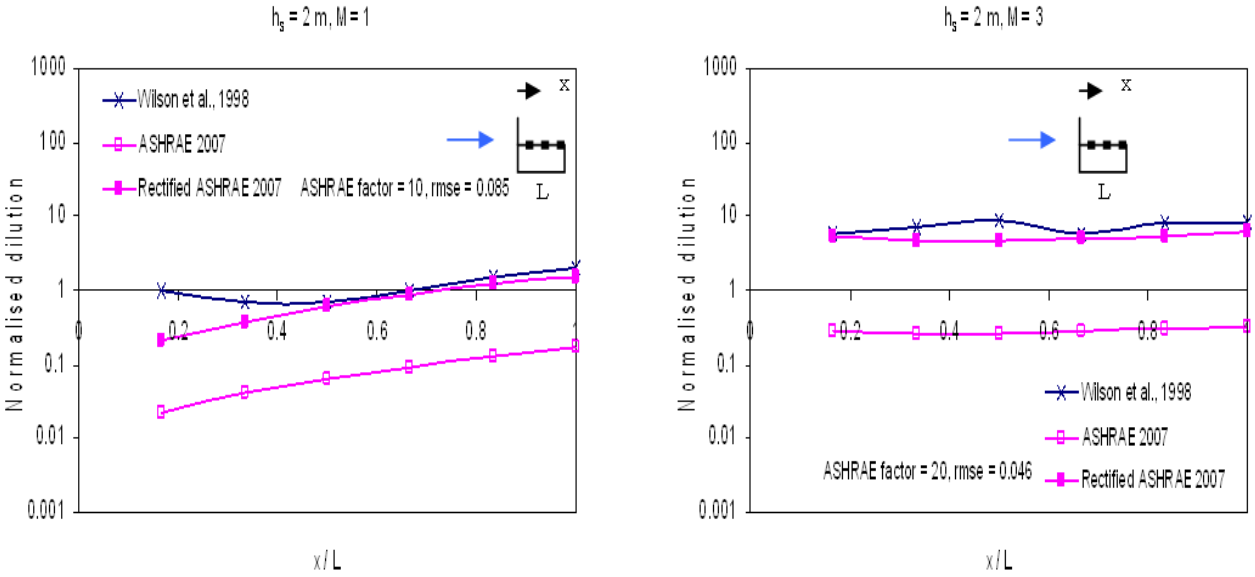


a) b)

Figure 6.19 Model validation with wind tunnel data from Wilson et al., 1998 for the flat roofed low-rise building for $X_s = 0$: a) M = 1; b) M = 3

Some discrepancies between model and experiments can be attributed to different terrain conditions; the rectified approach is based on wind tunnel data from an urban terrain as opposed to a suburban terrain used by Wilson and his co-researchers.

Comparisons were also made for wind tunnel data from Petersen et al., 1999, ASHRAE 2007 and its rectified form, as shown in Figure 6.20. It may be mentioned that in this case the stack was located at $X_s = 0.5L$. At $h_s = 2$ m and M = 1 good comparisons between Rectified ASHRAE 2007 estimates and experimental data were obtained beyond 0.7L. However, very close to the stack, the rectified ASHRAE 2007 estimates are lower than experiment by about a factor of 4. The ASHRAE factors were estimated from Table 6.4. A similar trend was observed at M = 2 as shown in Figure 6.20 (b). ASHRAE continues to predict overly conservative estimates for all cases.

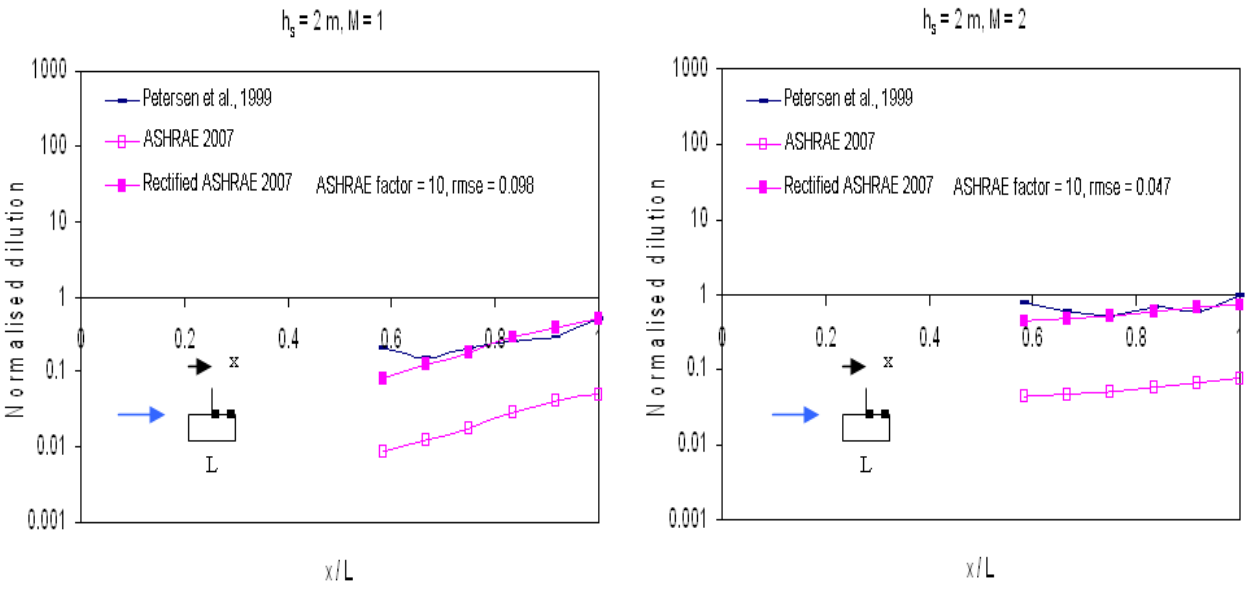


a) b)

Figure 6.20 Model validation with wind tunnel data from Petersen et al., 1999 for the flat roofed low-rise building for $X_s$ = 0.5L: a) M = 1; b) M = 2

The subsequent section presents comparisons between rectified ASHRAE 2007 approach and experimental dispersion studies on adjacent buildings.

### 6.5.2.2 Application to adjacent building configurations

Validations of the rectified ASHRAE approach were also carried out with experimental data from Wilson et al., 1998 and Stathopoulos et al., 2004 for near-field pollutant dispersion studies due to adjacent buildings. The experimental conditions and building dimensions are mentioned in Table 6.5. Wilson's study was based on water channel measurements whilst Stathopoulos et al., 2004 performed field tracer measurements on two of the buildings of Concordia University. A detailed description of both studies has been presented in Chapter 2.

Table 6.5 Experimental conditions used for previous studies

| Wilson et al., 1998 (water channel study) | Stathopoulos et al., 2004 (Field study) |
|---|---|
| $h = 12.2$ m; $h_1 = 24.2$ m | $h = 12$ m; $h_1 = 45$ m |
| $w = w_1 = 31$ m | $w = w_1 = 50$ m |
| $L = L_1 = 31$ m | $L = 50$ m; $L_1 = 32$ m |
| $U_H = 0.179$ m/s * | $U_H = 3$ m/s * |
| $d_e = 0.60$ m | $d_e = 0.60$ m |
| $\alpha = 0.26$ | $\alpha = 0.33$ |
| Suburban terrain | Urban terrain |
| $Z_o = 0.38$ m | $Z_o = 0.66$ m |

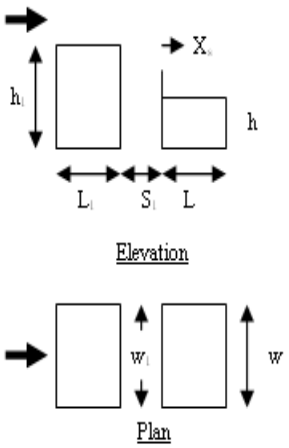


* Measured at the height of the emitting building.

Comparisons for experimental data from Wilson et al., 1998, ASHRAE 2007 and the rectified ASHRAE 2007 values are presented in Figure 6.21 for the tall building (24.2 m) upstream of the low building (12.2 m). Both buildings were 31 m square in plan spaced 12.2 m (0.4L) apart. The factor can be determined by using Tables 6.1 and 6.4. For instance, at $h_s = 2$ m, M = 1 and $X_s = 0$ (Figure 6.21 (a)), Table 6.1 gives f1 = 2 which represents a factor between roof dilution for isolated case and taller upstream case. Thereafter, an ASHRAE factor = 10 is obtained from Table 6.4 for $h_s = 2$ m, M = 1 and $X_s = 0$ which represents a factor between ASHRAE 2007 and experimental data for the isolated case. Therefore, dividing 10 by 2 yields 5 as shown in Figure 6.21 (a) (refer to Figure 6.13 for a better understanding of the process). A similar approach was also adopted to estimate the factor for $h_s = 2$ m and M = 3 as shown in Figure 6.21 (b).

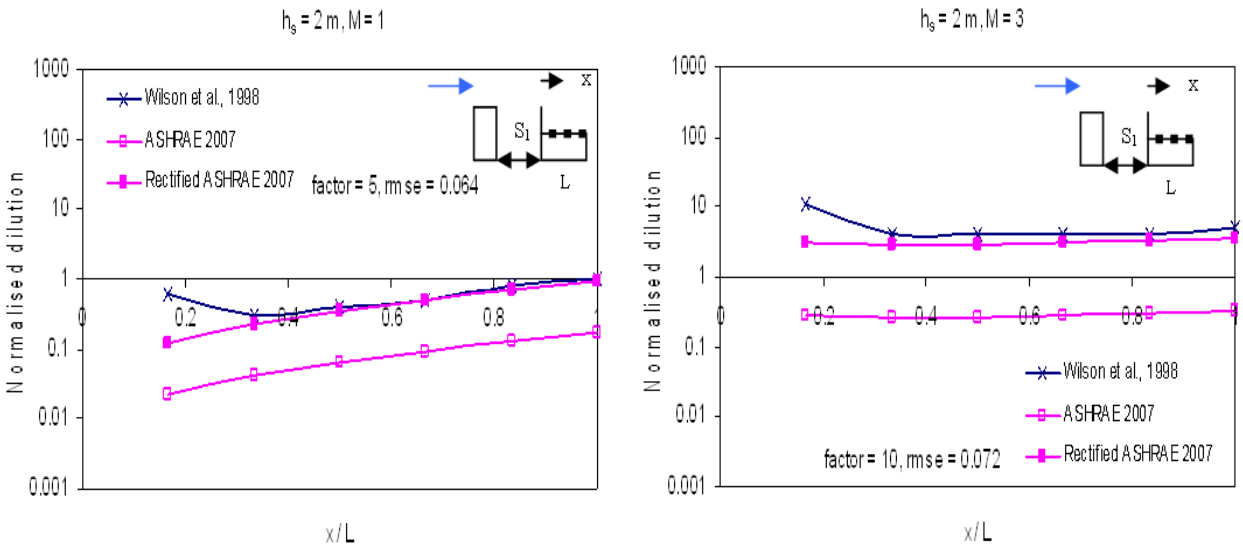


a) b)

Figure 6.21 Model validation with wind tunnel data from Wilson et al., 1998 for the roof of the emitting building for $X_s = 0$: a) M = 1; b) M = 3

In general ASHRAE 2007 estimates were lower than experiment at all receptors whilst the Rectified ASHRAE 2007 predictions compare well with experimental data with rmse values less than 0.1.

Comparisons for experimental data for roof dilution on emitting building for a taller downstream building, ASHRAE 2007 and rectified ASHRAE are presented in Figure 6.22. The emitting building was 12.2 m tall and downstream building was 24.4 m tall spaced 12.2 m apart. The factors are obtained in a similar way using Table 6.1 and 6.4 and multiplied by the ASHRAE dilution values. Good comparisons were obtained between rectified ASHRAE model and experiment for M = 1, particularly at points beyond 0.4L. However, due to the conservative nature of ASHRAE, very close to the stack the dilutions are generally lower than experiment.

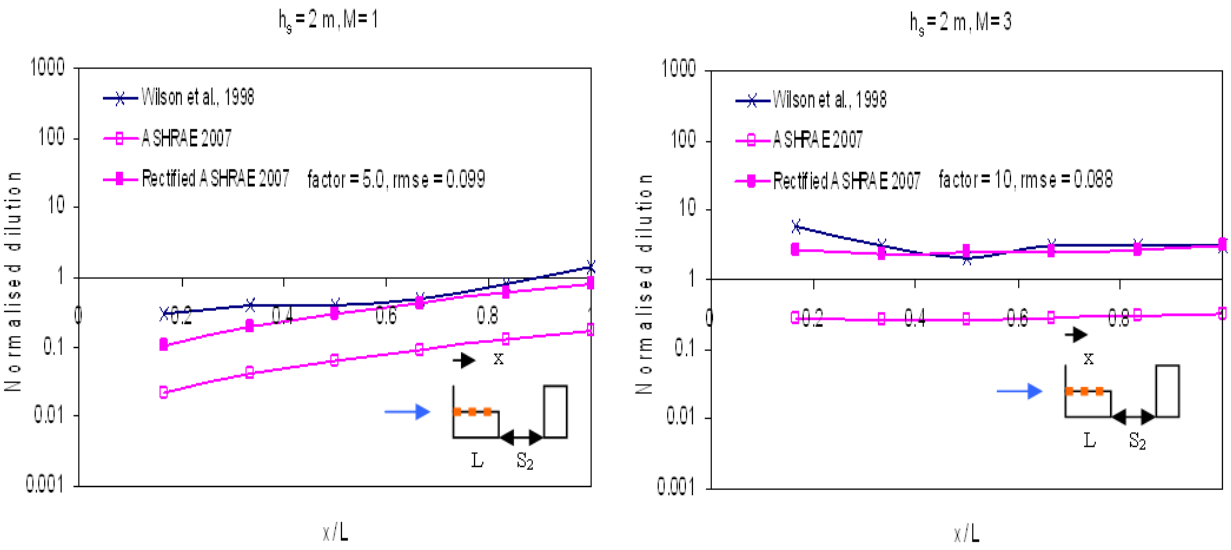


a) b)

Figure 6.22 Model validation with wind tunnel data from Wilson et al., 1998 for the roof of the emitting building for $X_s = 0$: a) M = 1; b) M = 3

A similar trend was also observed at M = 3 as shown in Figure 6.22 (b). ASHRAE 2007 predicts lower dilution than water channel data for all cases. The factor estimation corresponding to Figure 6.22 (a) can be explained as follows. From Table 6.1 for $h_2/h$ = 2, $h_s$ = 2 m, M = 1 and $X_s$ = 0, f1 = 2 is obtained. This factor is the ratio between roof dilution for isolated case and the taller downstream configuration (equation 6.1). Similarly, from Table 6.4, by interpolating between $h_s$ = 1 m and 3 m for M = 1, ASHRAE factor = 10 is obtained for $h_s$ = 2 m and M = 1. Dividing 10 by 2 yields a factor = 5, as shown in Figure 6.22 (a).

The rectified approach was also applied to estimate the dilution on the roof of the downstream building as shown in Figure 6.23. The dilution on the roof of the downstream building is based on the dilution obtained on the downwind edge of the emitting building (Figure 6.22). For instance, in Figure 6.22 (a) the dilution obtained

from rectified ASHRAE 2007 for $h_s$ = 2 m and M = 1 on the downwind edge of the emitting building is approximately 0.74.

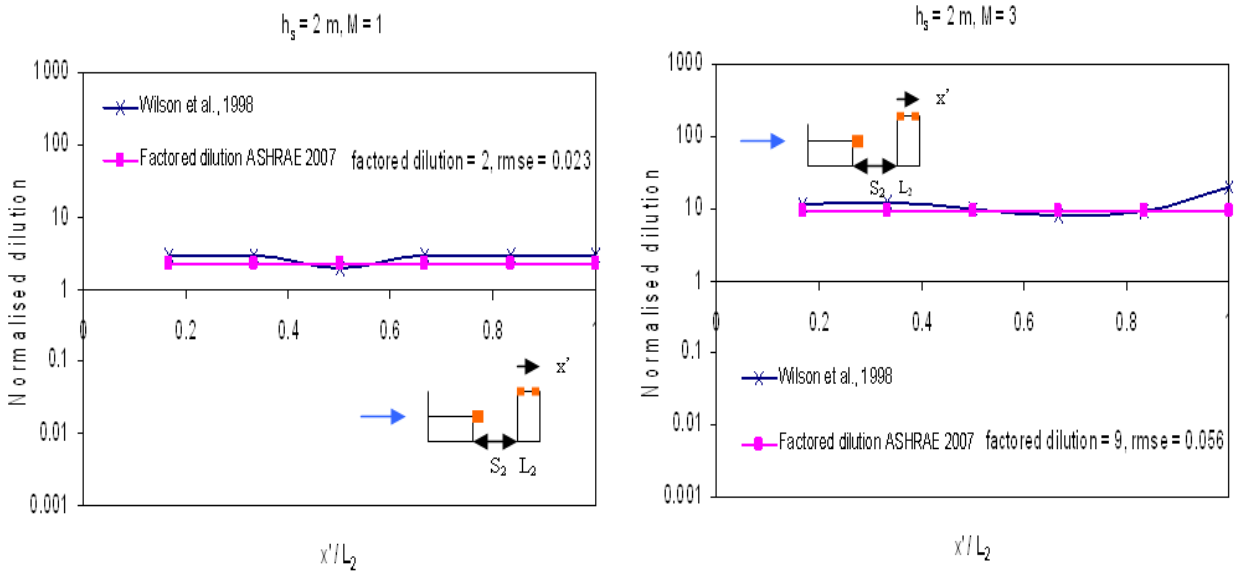


a) b)

Figure 6.23 Model validation with wind tunnel data from Wilson et al., 1998 for the roof of the downstream building for $X_s$ = 0: a) M = 1; b) M = 3

From Table 6.1 for $h_2/h$ = 2, $h_s$ = 2, M = 1, $X_s$ = 0, f2 = 2.8 is obtained, which is the ratio of the dilution on the roof of the downstream building to the dilution on downwind edge of the emitting building. Multiplying 2.8 by 0.74 gives 2.072, which has been rounded to 2.0 (Figure 6.23 (a)). A similar approach was used to determine the factored dilution for M = 3. In general, the factored dilutions which were based on rectified ASHRAE 2007 estimates, compared well with the experimental data at all receptors with rmse less than 0.06.

Comparisons for field data obtained from Stathopoulos et al., 2004, ASHRAE 2007 , and Rectified ASHRAE 2007 estimates are presented in Figure 6.24 for $h_s$ = 1. It may be

mentioned that for a centrally located stack a taller upstream building produces dilution upwind and downwind of stack.

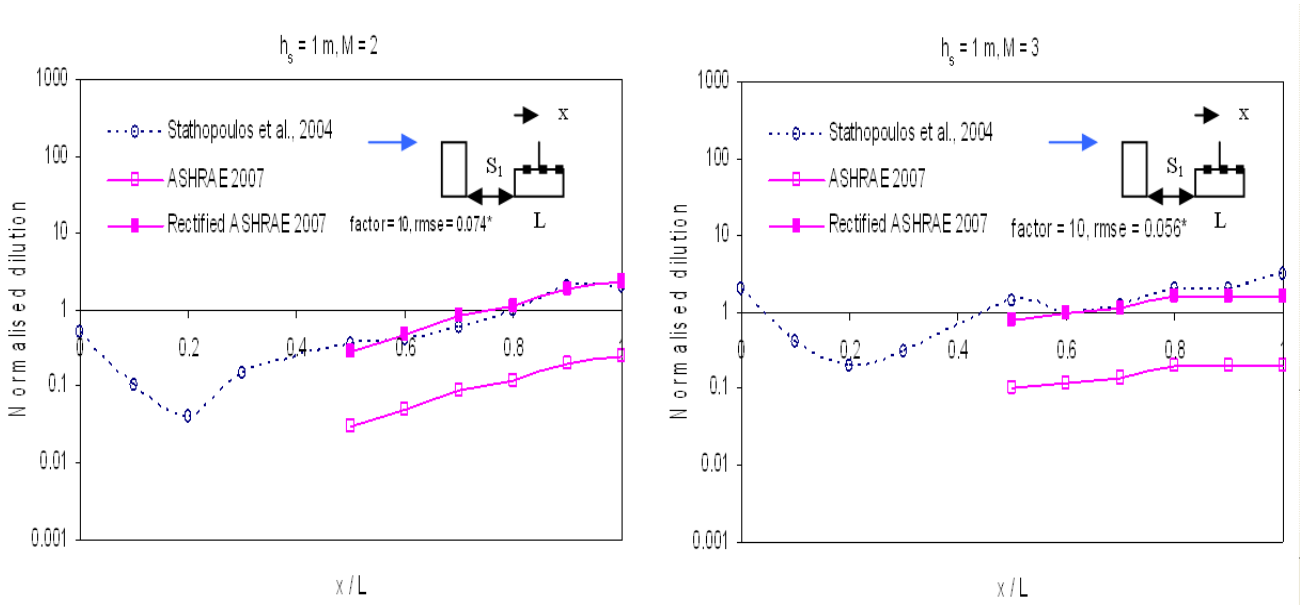


Figure 6.24 Model validation with field data from Stathopoulos et al., 2004 for the low building for $X_s = 0.4L$: a) M = 2; b) M = 3 (* rmse was evaluated using the wind tunnel and rectified ASHRAE, only for receptors downwind of stack (6 receptors))

However, since ASHRAE predicts only dilution downwind of stack, the rectified approach also provides dilution estimates downwind of the stack. The factors were estimated using Table 6.1 and 6.4 as explained previously. Good comparisons were obtained between rectified ASHRAE 2007 and field data at all receptors for M = 2 (rmse = 0.074). A similar trend was also observed at M = 3 as shown in figure 6.24 (b).

Comparisons between factored dilution, which are based on Rectified ASHRAE 2007 estimates and, field data for the leeward wall of the upstream building are shown in Figure 6.25. As explained previously, the wall dilution is estimated from the roof dilution on upwind edge of the emitting building. Good comparisons were obtained between

factored dilution of ASHRAE 2007 and field data at all points except the receptor close to the top of the building where the latter generates higher dilution.

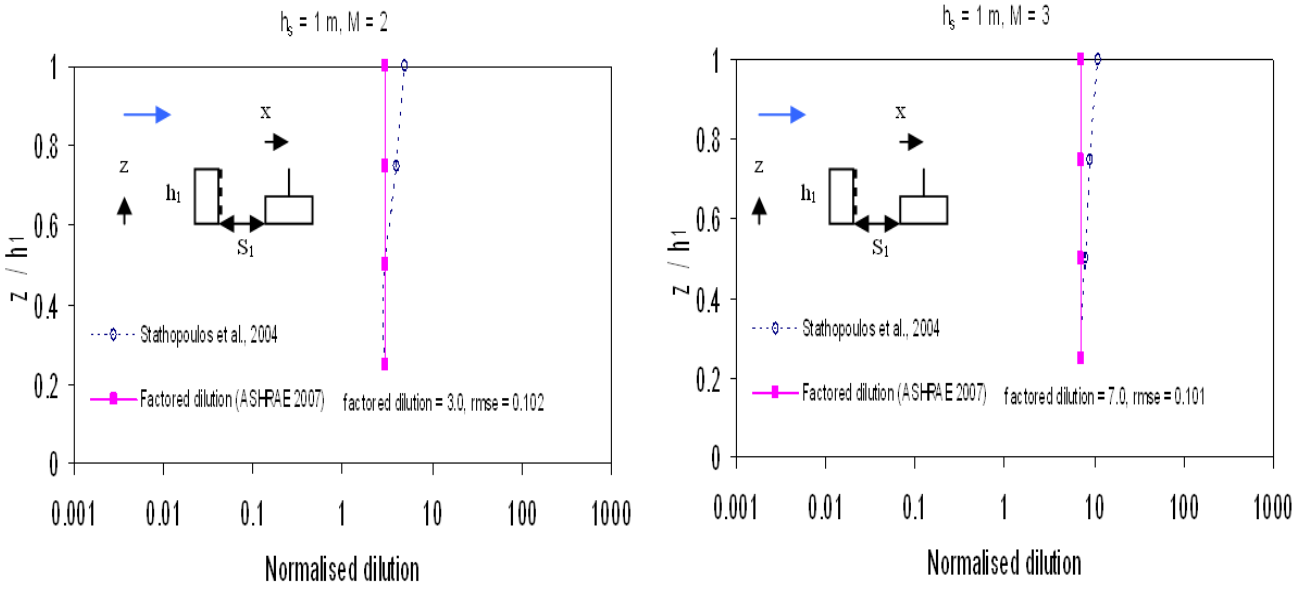


a) b)

Figure 6.25 Normalised dilution on the leeward wall of the upstream building: a) M = 2; b) M = 3

For $h_s$ = 1 m, M = 2, $X_s$ = 0.4L and $h_1/h$ = 4, f3 = 0.15 is obtained from Table 6.2, which is the ratio of dilution downwind of stack to the dilution on leeward wall of the taller upstream building. The rectified ASHRAE 2007 estimate for $h_s$ = 1 m and M = 2 is 0.4, immediately downwind of stack (Figure 6.24 (a)). Therefore, on dividing 0.4 by 0.15 a factored dilution of 2.67 is obtained, which has been rounded to 3 (Figure 6.25 (a)). A similar approach was also used for $h_s$ = 1 m and M = 3 as shown in Figure 6.25 (b).

Additional validation studies are available in Appendix F. A summary of this chapter is presented in section 6.6.

## 6.6 Summary

This chapter presented a method to determine pollutant dilution on various building surfaces through a two step process:

a) Establishing a relationship between dilution estimates from adjacent building configurations and the isolated case (Tables 6.1 and 6.2).

b) Comparing ASHRAE 2007 dilution values for isolated case and wind tunnel data from the present study (Table 6.4).

The rectified ASHRAE 2011 approach is not recommended due to the erratic values of factors obtained (Table 6.3). The rectified ASHRAE 2007 approach compared well with present and previous experimental studies and provides better dilution estimates than most available dispersion models despite being slightly conservative.

Some recent CFD validations using the wind tunnel data of the present study showed that $Sc_t$ cannot be generalised for any flow condition (Chavez et al., 2011). It is understandable that to achieve reasonable CFD dilution estimates for near-field dispersion, more accurate simulation of the turbulence caused by buildings is required.

The subsequent chapter presents design guidelines for safe placement of stack and intake on various building surfaces, based on this study.

# Chapter 7

# Design guidelines for safe placement of stack and intake on building surfaces

## 7.1 General

This study examined the near-field pollutant dispersion characteristics of rooftop emissions in the presence of adjacent buildings through tracer gas studies in the wind tunnel. Most previous studies focussed on wind tunnel experiments on dispersion of pollutants from isolated buildings and this is very rare. ASHRAE dilution estimates were found to be quite unrealistic and only apply to isolated buildings; rectifications were also proposed to correct this problem and efforts were made to extend their application to adjacent building surfaces. Based on the experimental results, design guidelines for safe placement of stack and intake on various building surfaces are described in this Chapter.

## 7.2 Design guidelines for placement of intake and stack

This section presents some guidelines for engineers regarding the safe placement of stack and intake on a building. The suitability of the location of stacks and intakes on a building surface will depend on a number of factors such as local topography, turbulence and the material being released from the stack (Hajra et al., 2011). The guidelines have been presented separately for each building configuration.

### *7.2.1 Upstream building configurations*

Building configurations tested in the wind tunnel include taller upstream building configurations and an upstream building of similar height as the emitting building.

Taller upstream building

1. When the spacing between the buildings exceeds the recirculation length of the upstream building, intakes may be placed on both the leeward wall of the upstream building and close to the downwind edge of the emitting building, for a given stack height and M value (Hajra et al., 2011).

2. When the emitting building lies within the recirculation zone of the upstream building, intakes should not be located upwind of the stack; they may be placed closer to the leeward wall of the emitting building.

Upstream building of lower or similar height with the emitting building

1. When an upstream building of lower or similar height is spaced greater than the recirculation length of the upstream building, irrespective of stack location and height, intakes may be placed on the roof of the upstream building.

2. When a building is located within the recirculation zone of the upstream building, for a given stack location, intakes may be placed on the leeward wall of the emitting building and close to the windward wall of the upstream building.

Guidelines for placement of stack and intake for downstream building configurations are presented in the following sub-section.

### *7.2.2 Downstream building configurations*

Design guidelines for the placement of intake and stack are discussed for downstream building configurations of taller or similar height as the emitting building since the plume structure does not change significantly.

Taller or similar height downstream building

1. When a downstream building is placed within the recirculation length of the emitting building, intakes should not be located close to the leeward wall of the emitting building as shown schematically in Figure 7.1 (a)

2. When spacing between buildings exceeds the recirculation length of the emitting building; intakes may be placed on either building surface as shown in Figure 7.1 (b)).

3. For any value of $h_s$, M and spacing, intakes must be avoided immediately downwind of a low stack with low exhaust speeds (say $h_s$ = 1 m and M = 1) due to increased plume downwash effects, although it is safer to place them upwind of stack.

Subsection 7.2.3 describes the guidelines for a building placed upstream and downstream of the emitting building.

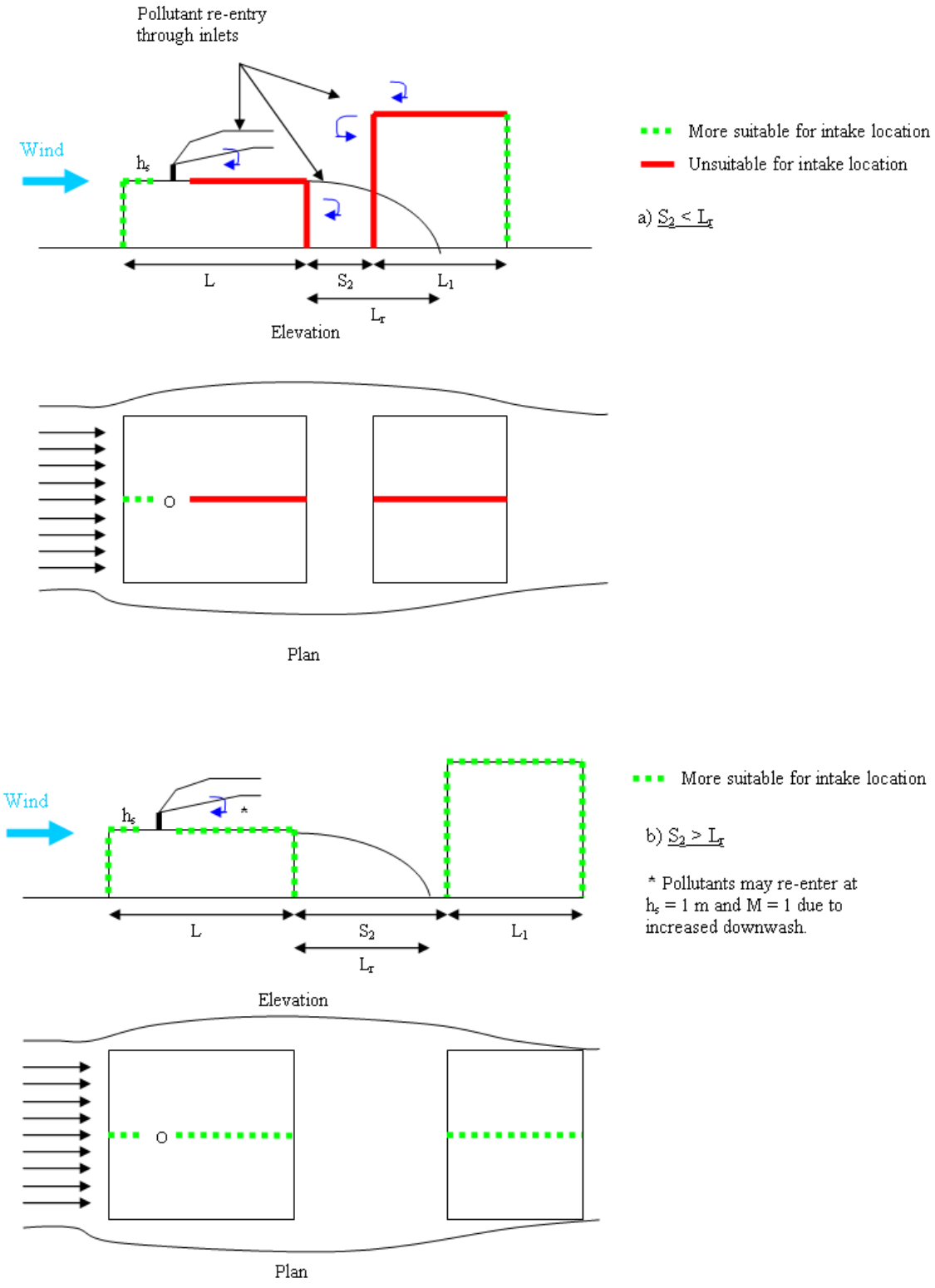


Figure 7.1. Schematic representation for suitability of intake location at various building surfaces for: a) $S_2 < L_r$; b) $S_2 > L_r$ (from Hajra and Stathopoulos, 2012)

### *7.2.3 Building placed upstream and downstream of the emitting building*

A building placed upstream and downstream of the emitting building, affects the leeward wall of the upstream building, roof of the emitting building as well as the windward wall and roof of the downstream building. As discussed in Chapter 5, Configuration 10 consisted of a low building ($B_1$) with a taller upstream building ($B_2$) and a taller downstream building ($B_5$). Configuration 11 consisted of $B_2$ upstream and $B_5$ downstream of the intermediate emitting building ($B_6$). The following guidelines may be adopted:

1) For Configuration 10, if spacing between the buildings is within the recirculation length of the taller upstream building, intakes must be avoided upwind of stack for any $h_s$ and M; it may be safer to place them closer to the leeward wall of the downstream building.

2) For Configuration 11, intakes may be placed on building surfaces upwind of stack and closer to the leeward wall of the taller downstream building for any given $h_s$, M and spacing between buildings.

3) In general, the flow characteristic suggest that the guidelines for a taller upstream building and a taller downstream building configuration described previously may be adopted for Configuration 10, whilst the latter may be sufficient for Configuration 11.

# Chapter 8

# Conclusions, contributions and recommendations for future work

## 8.1 General

This thesis focussed on a detailed wind tunnel study of near-field pollutant dispersion for different adjacent building configurations. In this context, pollutant concentrations were measured at various building surfaces and the effect of various parameters such as $h_s$, M, spacing between buildings, $X_s$ and geometries of adjacent and emitting buildings were studied. Comparisons with ASHRAE models showed that the models were overly conservative and incapable of simulating adjacent building effects. This was followed by suggestions to rectify the ASHRAE approach to obtain reasonable dilution estimates on various building surfaces. Design guidelines for the safe placement of stack and intake were also suggested based on the results of this study.

## 8.2 Conclusions

The conclusions based on this study have been divided into three subsections as follows.

### *8.2.1 Wind tunnel study*

1. The results of this study suggest that when the emitting building lies within the recirculation length of the taller upstream building a change in along wind dimension of the adjacent building has a negligible effect on the plume dilutions on various building surfaces.

2. A taller downstream building placed within the recirculation length of the emitting building ($L_r$) causes the plume to be engulfed within $L_r$, thereby affecting the leeward wall of the emitting building and the windward wall of the downstream building.

3. Irrespective of $h_s$, M and spacing between buildings, a narrow adjacent building (upstream or downstream) has minimal influence on the plume trajectory as opposed to wider adjacent buildings. In such cases the emitting building is equivalent to an isolated building.

4. Rooftop dilution on the emitting building gradually increases (towards the isolated building case) as the spacing between buildings exceeds the recirculation length of the upstream building.

5. Buildings of lower or similar height as the emitting building have minimal influence on the plume characteristics irrespective of $h_s$, M and spacing between buildings.

6. The presence of a taller upstream and a taller downstream building increases rooftop concentration on the emitting building due to the back and forth movement of the plume.

### *8.2.2 ASHRAE provisions*

1. ASHRAE 2007 and 2011 models yield higher concentration readings than the experimental findings and are therefore overly conservative.

2. When the ASHRAE provisions are applied to multiple building configurations, the dilution estimates are lower than experimental data.

3. The current ASHRAE provisions must be re-visited. In particular, the formulations must incorporate the effect of neighbouring buildings and terrain exposure.

### *8.2.3 Rectified ASHRAE approach*

1. The rectified ASHRAE approach utilises the wind tunnel results of the present study and ASHRAE estimates to propose certain factors which can be applied to obtain realistic dilution estimates.

2. The factors can be applied to estimate dilution on emitting and adjacent building surfaces.

3. In general, the rectified ASHRAE 2007 model is recommended for use as it gives better dilution estimates compared with present and previous experimental results.

## 8.3 Contributions of the present study

The contribution of this study can be summarised as follows:

1. A detailed study of adjacent building effects on micro-scale pollutant dispersion.

2. A study of various dispersion models applied to isolated emitting buildings revealed that with the exception of ASHRAE most dispersion models can only be used for far-field pollutant dispersion problems (Hajra et al., 2010).

3. Experimental findings for various adjacent building configurations were able to shed light on the plume behaviour for different building geometries (Hajra et al., 2011).

4. Based on the experimental data from the present study, a rectified ASHRAE 2007 approach was proposed to assess plume dilution on various building surfaces.

5. Design guidelines for safe placement of stack and intake on various building surfaces were suggested (Hajra and Stathopoulos, 2012).

6. Validations of CFD models have also been carried out using the experimental findings of this study by Chavez et al., 2011 and Chavez et al., 2012. It is understandable that the results of this study can be an asset to numerical scientists to validate CFD models.

The journal publications from this study are mentioned below:

- **Hajra, B**., Stathopoulos, T., Bahloul, A. 2010. Assessment of pollutant dispersion from rooftop stacks: ASHRAE, ADMS and Wind Tunnel Simulation. Building and Environment, 45, 2768-2777.
- **Hajra, B**., Stathopoulos, T., Bahloul, A. 2011. The effect of upstream buildings on near-field pollutant dispersion in the built environment. Journal of Atmospheric Environment, 45, 4930-4940.
- Chavez, M., **Hajra, B**., Stathopoulos, T., Bahloul, A. 2011. Near-field pollutant dispersion in the built environment by CFD and wind tunnel simulations. Journal of Wind Engineering and Industrial Aerodynamics, 99, 330-339.
- **Hajra, B.**, Stathopoulos, T. 2012. A wind tunnel study of the effect of downstream buildings on near-field pollutant dispersion. Building and Environment, 52, 19-31.
- Chavez, M., **Hajra, B**., Stathopoulos, T., Bahloul, A. 2012. Assessment of near-field pollutant dispersion: Effect of upstream buildings. Journal of Wind Engineering and Industrial Aerodynamics, 104–106, 509–515.

### 8.4 Recommendations for future research

The present study focuses on near-field pollutant dispersion from rooftop emissions for various adjacent building configurations. Future researchers can investigate the following issues:

a) Emitting buildings with rooftop structures may be tested in the wind tunnel in the presence of adjacent buildings, as the present study only focuses on buildings with flat roofs. Rooftop structures are known to increase rooftop concentrations for isolated buildings (Gupta, 2009).

b) Results of the present study were restricted to a near-neutral stability condition. It is known that atmospheric stability can affect the effluent dispersion phenomena for isolated buildings (Li and Meroney, 1983). Hence, studying the effect of near-field pollutant dispersion for different atmospheric stability conditions in a thermally stratified wind tunnel would be an interesting endeavour.

c) The results of this study included only a single upstream or downstream building. However, in a densely populated urban environment a cluster of buildings is more likely to exist. Therefore, future researchers could increase the number of buildings in the vicinity of the source to simulate a more realistic situation.

d) Very few wind tunnel tracer studies (such as Gromke et al., 2008) have investigated the effects of tree plantation on near-field dispersion. A detailed study in this direction could be of great interest for future experimentalists.

**REFERENCES**

ADMS User Guide. 2004. Cambridge Environmental Research consultants Limited. Cambridge, UK

ASCE. 1999. Wind Tunnel Studies of Buildings and Structures. Manual of Practice No. 67, American Society of Civil Engineers, Reston, VA, 20191-4400, USA.

ASHRAE 1993. Chapter 43. Building Air Intake and Exhaust Design. ASHRAE Applications Handbook American Society of Heating, Refrig. and Air-Cond. Eng., Inc., Atlanta, USA.

ASHRAE 1997. Chapter 43, Building Air Intake and Exhaust Design. ASHRAE Applications Handbook American Society of Heating, Refrig. and Air-Cond. Eng., Inc., Atlanta, USA.

ASHRAE 1999. Chapter 43, Building Air Intake and Exhaust Design. ASHRAE Applications Handbook American Society of Heating, Refrig. and Air-Cond. Eng., Inc., Atlanta, USA.

ASHRAE 2003. Chapter 44. Building Air Intake and Exhaust Design. ASHRAE Applications Handbook, American Society of Heating, Refrig. And Air-Cond. Eng., Inc., Atlanta, USA.

ASHRAE 2005. Airflow around buildings. ASHRAE Application Handbook, Chapter 16, Atlanta, USA

ASHRAE 2007. Chapter 44, Building Air Intake and Exhaust Design. ASHRAE Applications Handbook, American Society of Heating, Refrig. And Air-Cond. Eng., Inc., Atlanta, USA.

ASHRAE 2011. Chapter 45, Building Air Intake and Exhaust Design. ASHRAE Applications Handbook, American Society of Heating, Refrig. And Air-Cond. Eng., Inc., Atlanta, USA.

Bentham, T., Britter, R. 2003. Spatially averaged flow within obstacle arrays. Atmospheric Environment, 37, 2307- 2043.

Blocken, B., Stathopoulos, T., Saathoff, P., Wang, X. 2008. Numerical evaluation of pollutant dispersion in the built environment: comparisons between models and experiments. Journal of Wind Engineering and Industrial Aerodynamics, 96, 1817–1831.

Briggs, G.A. 1984. Plume rise and buoyancy effects in Atmospheric Science and Power Production. Randerson. Ed, U.S. Department of energy D.O.E./TIC-27601 (DE 84005177), Washington, D.C, USA.

Canepa, E. 2004. An Overview of downwash effects on dispersion of airborne pollutants. Environmental modelling and software, 19, 1077-1087.

Cheung, J.C.K., Melbourne, W.H. 1995. Building downwash of plume and plume interactions. Journal of Wind Engineering and Industrial Aerodynamics, 54, 543-548.

Carruthers, D.J., Holroyd, R.J., Hunt, J.C.R., Weng, W.S., Robins, A.G., Apsley, D.D., Thomson, D.J., Smith, F.B. 1994. UK-ADMS: A new approach to modelling dispersion in the earth's atmospheric boundary layer. Journal of Wind Engineering and Industrial Aerodynamics, 52, 139-153.

Carruthers, D.J., Mckeown, A.M., Hall, D.J., Porter, S. 1999. Validation of ADMS against wind tunnel data of dispersion from chemical warehouse fires. Atmospheric Environment. 33, 1937–1953.

Carruthers D., Riddle A., Sharpe A., McHugh C., Stocker J. 2004. Comparison between FLUENT and ADMS for atmospheric dispersion modelling. Atmospheric Environment, 38, 1029-1038.

Castro, I.P., Robins, A.G. 1977. The flow around a surface-mounted cube in uniform and turbulent streams. Journal of Fluid Mechanics, 79, 307-335.

Cermak, J.E. 1976. Nature of air flow around buildings. ASHRAE Transactions, 82, 1044- 1060.

Chavez, M., Hajra, B., Stathopoulos, T., Bahloul, A. 2011. Near-field pollutant dispersion in the built environment by CFD and wind tunnel simulations. Journal of Wind Engineering and Industrial Aerodynamics, 99, 330-339.

Chavez, M., Hajra, B., Stathopoulos, T., Bahloul, A. 2012. Assessment of near-field pollutant dispersion: Effect of upstream buildings. Journal of Wind Engineering and Industrial Aerodynamics, 104–106, 509–515.

Cimoreli, A.J., Perry, S.G., Venkatram, A., Weil, J.C., Paine, R.J., Wilson, R.B., Lee, R.F., Peters, W.D., Brode, R.W. 2005. AERMOD: A dispersion model for industrial source applications. Part I: General model formulation and boundary layer characterisation. Journal of Applied Meteorology, 44, 682-693.

Davenport, A.G. 1963. The relationship of wind structure to wind loading. Proceedings of the International Conference on The Wind Effects on Building and Structures. Teddinton, Middlesex, England: June 26-28.

Davidson, M.J., Mylne, K.R., Jones, C.D., Phillips, J.C., Perkins, R.J., Fung, J.C.H., Hunt, J.C.R. 1995. Plume dispersion through large groups of obstacles - a field investigation. Atmospheric Environment, 29, No. 22, 246 - 256.

Davidson, M.J., Snyder, W.H., Lawson, R.E and Hunt, J.C.R. 1996. Wind tunnel simulations of plume dispersion through groups of obstacles. Atmospheric Environment, 30, No. 22, 3715 – 3731.

Di Sabatino, S., Buccolieri, R., Bulvirenti, B., Britter, R. 2007. Simulations of pollutant dispersion within idealized urban-type geometries with CFD and integral models. Atmospheric Environment, 41, 8316-8329.

Dockery, D.W., Pope, C.A., Xu, X., Spengler, J.D., Ware, J.H., Fay, M.E., Ferris, B.G., Speizer, F.E. 1993. An Association between Air Pollution and Mortality in Six U.S. Cities. The New England Journal of Medicine, 329, No. 24, 1753-1759.

Dunkerley, F., Hall, D.J., Spanton, A.M., Bennett, M and Griffiths, R.F. 2000. An intercomparison of the AERMOD, ADMS and ISC Dispersion Models for Regulatory Applications. Proceedings of the Seventh International Conference on Harmonisation within Atmospheric Dispersion Modelling for Regulatory purposes, Italy.

ESDU, 1974. Characteristics of atmospheric turbulence near the ground. Engineering Science Data Unit, no. 74030 and 74031, London, UK.

EPA, 1995. A user's guide for the Industrial Source Complex (ISC3) dispersion models: Vol. 2—description of model algorithms. EPA-454/B-95-003. U.S. Environmental Protection Agency, Research Triangle Park, NC, USA.

Fackrell, J.E., Pearce, J.E. 1981. Parameters affecting dispersion in the near wake of buildings. CEGB report RD/M/1179/N81.

Fackrell, J.E. 1984. Parameters characterizing dispersion in the near wake of buildings. Journal of Wind Engineering and Industrial Aerodynamics, 16, 97—118.

Fisk, W.J., Price, P.N., Faulkner, D., Sullivan, D.P., Liu, G., Lahiff, M. 2002. Worker Performance and Ventilation: Analyses of Time-Series Data for a Group of Call Center Workers. Proceedings of Indoor Air Conference, Monterey, CA, June 30 – July 5.

Flowe, A.C., Kumar, A. 2000. Analysis of velocity fields and dispersive cavity parameters as a function of building width to building height ratio using a 3-D computer model for squat buildings. Journal of Wind Engineering and Industrial Aerodynamics, 86, 87-122.

Griffiths, R.F., Mavroidis, I. 2001. Local characteristics of atmospheric dispersion within building arrays. Atmospheric Environment, 35, 2941-2954.

Gromke, C., Buccolieri, R., Di Sabatino, S., Ruck, B. 2008. Dispersion study in a street canyon with tree planting by means of wind tunnel and numerical investigations -evaluation of CFD data with experimental data. Atmospheric Environment, 42, 8640 - 8650.

Guenther, A., Lamb, B and Peterson, R. 1989. Modelling of plume downwash and enhanced diffusion near buildings: Comparisons to wind tunnel observations for an arctic industrial site. American Meteorological Society, 28, 343-353.

Gupta, A. 2009. Physical Modelling of the Downwash Effect of Rooftop Structures on Plume Dispersion. PhD Thesis in the Dept. of BCEE, Concordia University, Canada.

Hajra, B., Stathopoulos, T., Bahloul, A. 2010. Assessment of pollutant dispersion from rooftop stacks: ASHRAE, ADMS and Wind Tunnel Simulation. Building and Environment, 45, 2768-2777.

Hajra, B., Stathopoulos, T., Bahloul, A. 2011. The effect of upstream buildings on near-field pollutant dispersion in the built environment. Journal of Atmospheric Environment, 45, 4930-4940.

Hajra, B., Chavez, M., Stathopoulos, T., Bahloul, A. 2011. Modelling of near-field pollutant dispersion in the built environment: methods and challenges. Proceedings of the – International Workshop on Physical Modelling of Flow and Dispersion Phenomena, Klima Campus, University of Hamburg, Germany, August 22-24.

Hajra, B, Stathopoulos, T. 2012. A wind tunnel study of the effect of downstream buildings on near-field pollutant dispersion. Building and Environment, 52, 19-31.

Halitsky, J. 1962. Diffusion of vented gas around buildings. Journal of The Air Pollution Control Association, 12, 74-80.

Halitsky, J. 1963. Gas Diffusion near buildings. ASHRAE Transactions, 69, 464-484.

Halitsky, J. 1990. Calculation of minimum available atmospheric dilution downwind of building exhausts. ASHRAE Transactions, 96, 46-51.

Hanna, S.R., Egan, B.A., Purdum, J., Wagler, J. 2001. Evaluation of the ADMS, AERMOD and ISC3 dispersion models with the Optex, Duke Forest, Kincaid, Indianapolis and Lovett field data sets. International Journal of Environmental Pollution. 16, 900-911.

Higson, H. L., Griffiths, R.F., Jones, C.D. and Hall, D.J. 1994. Concentration measurements around an isolated building: a comparison between wind tunnel and field data. Atmospheric Environment, 28, 1827-1836.

Higson, H.L, Griffiths, R.F, Jones, C.D., Biltoft, C. 1995. Effect of atmospheric stability on concentration fluctuations and wake retention times for dispersion in the vicinity of an isolated building. Environmetrics, 6, 571-581.

Holmes, J.D. 2001. Wind Loading of Structures. Taylor and Francis group, second edition, London, UK

Holmes, N.S., Morawska, L. 2006. A review of dispersion modelling and its application to the dispersion of particles: An overview of different dispersion models available. Atmospheric Environment, 40, 5902–5928.

Hoydysh, W. G., Dabberdt, W. F. 1988. Kinematics and dispersion characteristics of flow in asymmetric street canyons. Atmospheric Environment, 22, 2677–2689.

Hunt, J.C.R., Robins, A.G., 1982. A model for assessing dispersion of plumes from sources in the vicinity of cuboid shaped buildings. In: Proceedings of the EUROMECH Conference on Surface Mounted Bluff Bodies in Turbulent Boundary Layers, Lisbon.

Hunt, A., Castro, I.P. 1984. Scalar dispersion in model building wakes. Journal of Wind Engineering and Industrial Aerodynamics, 17, 89-115.

Khan, I.J, Simons, R.R., Grass, A.J. 2005. Upstream Turbulence Effect on Pollution Dispersion. Environmental Fluid Mechanics, 5, 393–413.

Koga, D.J., Way, J.L. 1979. Effects of Stack height and position on pollutant dispersion in building wakes. Proceedings of the fifth International Conference on Wind Engineering, Colorado state University, USA,

Lamb, B., Cronn, D. 1986. Fume Hood exhaust reentry into a chemistry building. Journal of American Industrial Hygiene Association, 47 (2), 115-123.

Law, A. W., E. C. Choi. 2004. Reentrainment around a low-rise industrial building: 2D versus 3D wind tunnel study. Atmospheric Environment, 23, 3817-3825.

Lazure, L., Saathoff, P., Stathopoulos, T. 2002. Air intake contamination by building exhausts: Tracer gas investigation of atmospheric dispersion models in the urban environment. Journal of Air and waste Management Association. 52, 160-166.

Lateb, M., Masson, C., Stathopoulos, T., Bedard, C. 2010. Numerical simulation of pollutant dispersion around a building complex, Building and Environment, 44, 166-177.

Li, W.W., Meroney, R.N. 1983. Gas dispersion near a cubical model building part II. Concentration fluctuation measurements. Journal of Wind Engineering and Industrial Aerodynamics, 12, 35-47.

Li, Y., Stathopoulos, T. 1998. Computational evaluation of pollutant dispersion around buildings: Estimation of numerical errors. Journal of Wind Engineering and Industrial Aerodynamics, 77&78, 619-630.

Lowery, K.P., Jacko, R.B. 1996. A wind tunnel study into the effects of raised intakes and parapets on fresh air intake contamination by a rooftop stack. Journal of the Air and Waste Management Association, 46, 847-852.

Macdonald, R.W., Griffiths, R.F., Cheah, S.C. 1997. Field experiments of dispersion through regular arrays of cubic structures. Atmospheric Environment, 31, No. 6, 783-795.

Martin, J.E. 1965. The correlation of wind tunnel and field measurements of gas diffusion using Krypton tracer gas. PhD Thesis, Dept. of Health Science, University of Michigan, USA.

Mavroidis, I., Griffiths, R.F., Jones, C.D., Biltoft, C.A. 1999. Experimental investigation of the residence of contaminants in the wake of an obstacle under different stability conditions. Atmospheric Environment, 33, 939-949.

Mavroidis, I., Griffiths, R.F. 2001. Local characteristics of atmospheric dispersion within building arrays. Atmospheric Environment, 35, 2941–2954.

Mavroidis, I., Griffiths, R.F., Hall, D.J. 2003. Field and wind tunnel investigations of plume dispersion around single surface obstacles. Atmospheric Environment, 37, 2903-2918.

McElroy, J.L., Pooler, F. 1968. The St. Louis dispersion study. U.S. Public Health Service, National Air Pollution Control Administration, USA.

Meroney, R.N., Yang, B.T. 1970. Gaseous plume diffusion about isolated structures of simple geometry. Proceedings of the 2nd International Air pollution conference of the International Union of air pollution prevention associations, December-6-11.

Murakami, S., Mochida, A., Hayashi, Y. 1990. Examining the $k$-$\varepsilon$ model by means of a wind tunnel test and large-eddy simulation of the turbulence structure around a cube. Journal of Wind Engineering and Industrial Aerodynamics, 35, 87 − 100.

Ogawa, Y., Oikawa, S., Uehara, K. 1983. Field and wind tunnel study of the flow and diffusion around a model cube-II. Near-field and cube surface flow patterns and concentration patterns. Atmospheric Environment, 17, 1161-1171.

Oikawa, S., Meng, Y. 1997. A field study of diffusion around a model cube in a suburban area. Boundary-Layer Meteorology, 84, 399–410.

Olvera, H.A., Choudhuri, A.R. 2006. Numerical simulation of hydrogen dispersion in the vicinity of a cubical building in stable stratified atmospheres. International Journal of Hydrogen Energy, 31, 2356 – 2369.

Olvera, H.A., Choudhuri, A.R., Li, W.W. 2007. Effects of plume buoyancy and momentum on the near-wake flow structure and dispersion behind an idealized building. Journal of Wind Engineering and Industrial Aerodynamics, 44, 221-233.

Paine, R.J., Lew, R. 1998. Project PRIME: evaluation of building downwash models using field and wind tunnel data. Preprint volume for the Tenth Joint Conference on Applications of Air Pollution Meteorology with A&WMA, American Meteorological Society, Phoenix, Arizona, USA.

Pasquill, F. 1961. The estimation of the dispersion of wind borne material. Meteorological magazine, 90, 33-39.

Petersen, R.L., Wilson, D.J. 1989. Analytical v/s wind tunnel determined concentrations due to laboratory exhaust. ASHRAE Transactions, 95, 8 pages.

Petersen, R.L., Carter, J.J., Ratcliff, M. 1999. Influence of architectural screens on rooftop concentrations due to effluent from short stacks. ASHRAE Transactions, 105 (1), 11-20.

Petersen, R.L. 2001. Wind-tunnel validation of the EPA approved ISC-PRIME model for stacks at various distances from buildings. Proceedings of PHYSMOD conference, Hamburg University, Germany.

Petersen, R.L., Le-Compte, J. 2002. Exhaust contamination of hidden versus visible air intakes – Final Report. ASHRAE Research Project 1168-TRP, American Society of Heating, Refrig. and Air-Cond. Eng., Inc., Atlanta, USA.

Pinto, J.M., Sebastiao, M., Isnard, A.A. 2007. Wind tunnel investigation on the retention of air pollutants in three-dimensional recirculation zones in urban areas. Atmospheric Environment, 41, 4949–4961.

Quinn, M., Wilson, A.M., Reynolds, S.B., Hoxey, R.P. 2001. Modelling the dispersion of aerial pollutants from agricultural buildings—an evaluation of computational fluid dynamics. Computers and Electronics in Agriculture, 30, 219–235.

Ramsdell, J.V., Fosmire, C.J. 1990. Diffusion in building wakes for ground-level releases. Atmospheric Environment, 24, 377-388.

Ramsdell, J.V., Fosmire, C.J. 1998. Estimating Concentrations in plumes released in the vicinity of buildings: Model development. Atmospheric Environment, 32, No.10, 1663-1677.

Riddle, A., Carruthers, D., Sharpe, A., Mc Hugh, C., Stocker, J. 2004. Comparisons between FLUENT and ADMS for atmospheric dispersion modeling. Atmospheric Environment, 38, 1029-1038.

Rodi, W. 1979. Influence of buoyancy and rotation on equations for the turbulent length scale. Proceedings of the second symposium on turbulent shear flows, USA.

Saathoff, P.J., Stathopoulos, T., Dobrescu, M. 1995. Effects of model scale in estimating pollutant dispersion near buildings. Journal of Wind Engineering and Industrial Aerodynamics, 54/55, 549-559.

Saathoff, P.J, Wu, H and Stathopoulos, T. 1996. Dilution of exhaust from roof top stacks-Comparison of wind tunnel data with full scale measurements. Proceedings of

the 9th joint conference on applications of Air pollution meteorology, AMS/AWMA, Atlanta 341-345.

Saathoff, P.J., Stathopoulos, T. 1997. Dispersion of exhaust gases from roof-level stacks and vents on a laboratory building: Discussion. Atmospheric Environment, 31, No. 7, 1087-1089.

Saathoff, P.J., Stathopoulos, T., Wu, H. 1998. The influence of free-stream turbulence on near-field dilution of exhaust from building vents. Journal of Wind Engineering and Industrial Aerodynamics, 77, 741-752.

Saathoff, P., Gupta, A., Stathopoulos, T., Lazure, L. 2009. Contamination of Fresh Air Intakes Due to Downwash from a Rooftop Structure. Journal of Air & Waste Management Association. 59, 343–353.

Santos, J.M., Griffiths, R.F., Roberts, I.D., Reis Jr, N.C. 2005. A field experiment on turbulent concentration fluctuations of an atmospheric tracer gas in the vicinity of a complex-shaped building. Atmospheric Environment, 39, 4999–5012.

Sada, K., Sato, A. 1999. Wind tunnel experiment of tracer gas concentration fluctuation in turbulent boundary layer: characteristics of concentration fluctuation with low concentration threshold. Journal of the Japan Society of Atmospheric Environment, 34, 337–351.

Sada, K., Sato, A. 2000. Numerical simulation of tracer gas concentration fluctuation in atmospheric boundary layer. Transactions of the Japan Society of Mechanical Engineers, 66, 2800–2806.

Sada, K., Sato, A. 2002. Numerical calculation of flow and stack-gas concentration fluctuation around a cubical building. Atmospheric Environment, 36, 5527–5534.

Schulman, L., Scire, J. 1991. The effect of stack height, exhaust speed, and wind direction on concentrations from a rooftop stack. ASHRAE Transactions, 97, 573-582.

Schulman L., Scire J.S. 1993. Building Downwash screening modelling for the downwind circulation cavity. Journal of the Air waste management association, 43, 1122-1127.

Schulman L., Strimaitis D. G., Scire J.S. 1997. Addendum to ISC3 User' s Guide, the PRIME Plume Rise and Building Downwash Model. Electric Power Research Institute, USA.

Schulman, L., Strimatis, D., Scire, J. 2000. Development and Evaluation of the PRIME Plume Rise and Building Downwash Model. Journal of Air & Waste Management Association, 50, 378-390.

Schwartz, J. 1994. Air pollution and daily mortality: A review and meta analysis. Journal of Environmental research, 64, 36-52.

Sharan, M., Gopalakrishnan, S.G. 2003. Mathematical modeling of diffusion and transport of pollutants in the atmospheric boundary layer. Pure and Applied Geophysics, 160, 357-394

Smagorinsky, J.S. 1963. General circulation experiments with the primitive equations: Part 1, Basic experiments, Monthly Weather Review, 91, 99-164.

Snyder W.H. 1981. Guidelines for fluid modelling of atmospheric diffusion. EPA office of Air quality, planning and standards, Research triangle park, NC, EPA-600/8-81-009

Stathopoulos, T. 1984. Design and fabrication of a wind tunnel for building aerodynamics. Journal of Wind Engineering and Industrial Aerodynamics, 16, 361-376.

Stathopoulos, T., Lazure, L, Saathoff, P.J. 1999. Tracer gas investigation of reingestion of building exhaust in an urban environment. IRSST research report R-213, Institut de recherche Robert-Sauvé en santé et en sécurité du travail, Montreal, Canada

Stathopoulos, T., Lazure, L., Saathoff, P.J., Gupta, A. 2004. The effect of stack height, stack location and rooftop structures on air intake contamination A laboratory and full-scale study. Research report (R-392), Institut de recherché Robert Sauvé en santé et en sécurité du travail, Montreal, Canada

Stathopoulos, T., Bahloul, A., Hajra, B. 2008. Analytical evaluation of the dispersion of polluting emissions from building stacks. Research report (R-576), Institut de recherché Robert Sauvé en santé et en sécurité du travail, Montreal, Canada

Stern, R, Yamartino, R.J. 2001. Development and first evaluation of micro-calgrid: a 3-D, urban-canopy-scale photochemical model. Atmospheric Environment, 35, 149-165.

Streeter, V.L, Wylie, E.B, Bedford, K.W. 1998. Fluid Mechanics. McGraw Hill Publishers, ninth edition.

Sykes, R.I., Henn, D.S., 1992. An improved moment conservation method for the advection-diffusion equation. Journal of Applied Meteorology, 31, 112–118

Tominaga, Y., Stathopoulos, T. 2007. Turbulent Schmidt numbers for CFD analysis with

various types of flowfield. Atmospheric Environment, 41, 8091–8099.

Tominaga, Y., Stathopoulos, T. 2011. CFD modelling of pollution dispersion in a street canyon: Comparison between LES and RANS. Journal of Wind Engineering and Industrial Aerodynamics, 99, 340-348.

Trent S. D., Eyler L. L. 1989. TEMPEST, A three dimensional time-dependent computer program for hydrothermal analysis. In Numerical Methods and Input instructions, Vol. 1, PNL-4348. Pacific Northwest Laboratory, Battelle, Washington, USA.

Turbulent Flow Instrumentation. 2008. Series 100 Cobra Probe Manual, Turbulent Flow Instrumentation, pages- 1-13.

Turner, D.B. 1970. Workbook of Atmospheric Dispersion Estimates. U.S. department of H.E.W., NTIS publication no. 191, Springfield, VA: US dept. of commerce.

Turner, D.B. 1994. Workbook of Atmospheric Dispersion Estimates, 2nd Ed., CRC Press.

Upadhay, J.K, Kobayashi, N, Venkatram, A, Klewicki, J. 2004. Study of near-field dispersion through large groups of obstacles. Journal of Asian Architecture and Building Engineering, 3, 305-309.

Varian. 1988. Gas chromatograph operators manual (model-3300/3400). vol-1, Varian associates inc, California, USA.

Versteeg, H.K., Malalasekera, W. 1995. An introduction to computational fluid dynamics—the finite volume method. New York: Longman Scientific and Technical; 1995.

Wilson, D.J. 1977. Dilution of exhaust gases from building surface vents. ASHRAE Transactions, 83, 168-176.

Wilson, D.J. 1979. Flow patterns over flat-roofed buildings and application to exhaust stack design. ASHRAE Transactions, 85, part 2, 284-295.

Wilson, D.J., Winkel, G. 1982. The effect of varying exhaust stack height on contaminant concentration at roof level. ASHRAE Transactions, 88, part 1, 515-533.

Wilson, D.J., Britter, R.E. 1982. Estimates of building surface concentrations from nearby point sources. Atmospheric Environment, 16, 2631-2646.

Wilson, D.J. 1983. A design procedure for estimating air intake contamination from nearby exhaust vents. ASHRAE Transactions, 89, part 2, 136-150.

Wilson, D.J., Chui, E. 1985. Influence of exhaust velocity and wind incidence angle on dilution from roof vents. ASHRAE Transactions, 91, 1693-1706.

Wilson, D.J., Chui, E. 1987. Effect of turbulence from upwind Buildings on Dilution of Exhaust gases. ASHRAE Transactions, 93, 2186-2197.

Wilson, D.J., Chui, E. 1994. Influence of building size on rooftop dispersion of exhaust gas. Atmospheric Environment, 28, 2325-2334.

Wilson, D.J., Lamb, B. 1994. Dispersion of exhaust gases from roof level stacks and vents on a laboratory building. Atmospheric Environment, 28, 3099-3111.

Wilson, D.J., Fabris, I., Chen, J., Ackerman, M. 1998. Adjacent building effects on laboratory fume hood exhaust stack design. ASHRAE Research Report 897, American Society of Heating and Refrigerating and Air-conditioning Engineers, Atlanta, USA.

Wilson, D.J., Fabris, I., Ackerman, M.Y. 1998. Measuring adjacent effects on laboratory exhaust stack design. ASHRAE Transactions, 88(1), 513-533.

Yan, H. 2002. Reduction of Air Intake in High rise Residential Buildings in an urban Environment. Masters Thesis in the Dept. of BCEE, Concordia University, Canada

Yee, E., Gailis, R.M., Hill, A., Hilderman, T., Kiel, D. 2006. Comparison of wind tunnel and water channel simulations of plume dispersion through a large array of obstacles with a scaled field experiment. Boundary- Layer Meteorology, 121, 389–432.

Zhang, Y.Q., Arya, S.P., Snyder, W.H. 1996. A comparison of numerical and physical modelling of stable atmospheric flow and dispersion around a cubical building. Atmospheric Environment, 30, 1327-1345.

# Appendix A

# Calibration equations to estimate concentration in ppb (y) for corresponding GC value (x)

This appendix presents the calibration equations which were used to convert the GC values (x) into concentrations in ppb (y). The GC values corresponding to known concentrations of $SF_6$ for different ranges were used. The equations were then derived using regression analysis software MINITAB 15 (www.minitab.com). The value of $R^2$ was found to be nearly one for all cases.

1) $y = -13.77 + 62x - 61x^2 + 23.73x^3$

$R^2 = 0.997$

Range: $0 \leq x \leq 2.0$

2) $y = 1522 – 2769x + 1878x^2 – 556x^3 + 61x^4$

$R^2 = 0.991$

Range: $2 < x \leq 4.0$

3) $y = 22.122x^2 - 154.3x + 221.1$

$R^2 = 0.994$

Range: $4 < x \leq 6.0$

4) $y = 1500x^2 - 19644x + 64299$

$R^2 = 0.995$

Range: $6 < x \leq 8.0$

# Appendix B

# Additional results for upstream building configurations

This appendix presents dilution results for building configurations with a taller upstream building. Dilutions were found on the rooftop of the emitting building and the leeward wall of the upstream building. Comparisons are shown for wind tunnel data, ASHRAE 2007 and ASHRAE 2011 dilution values. Figures B1 to B3 present results for buildings placed 20 m apart whilst B4 through B7 show the effect of spacing between buildings for Configuration 5. Figures B8 and B9 present results for $\theta = 0^o$, $22.5^o$ and $45^o$.

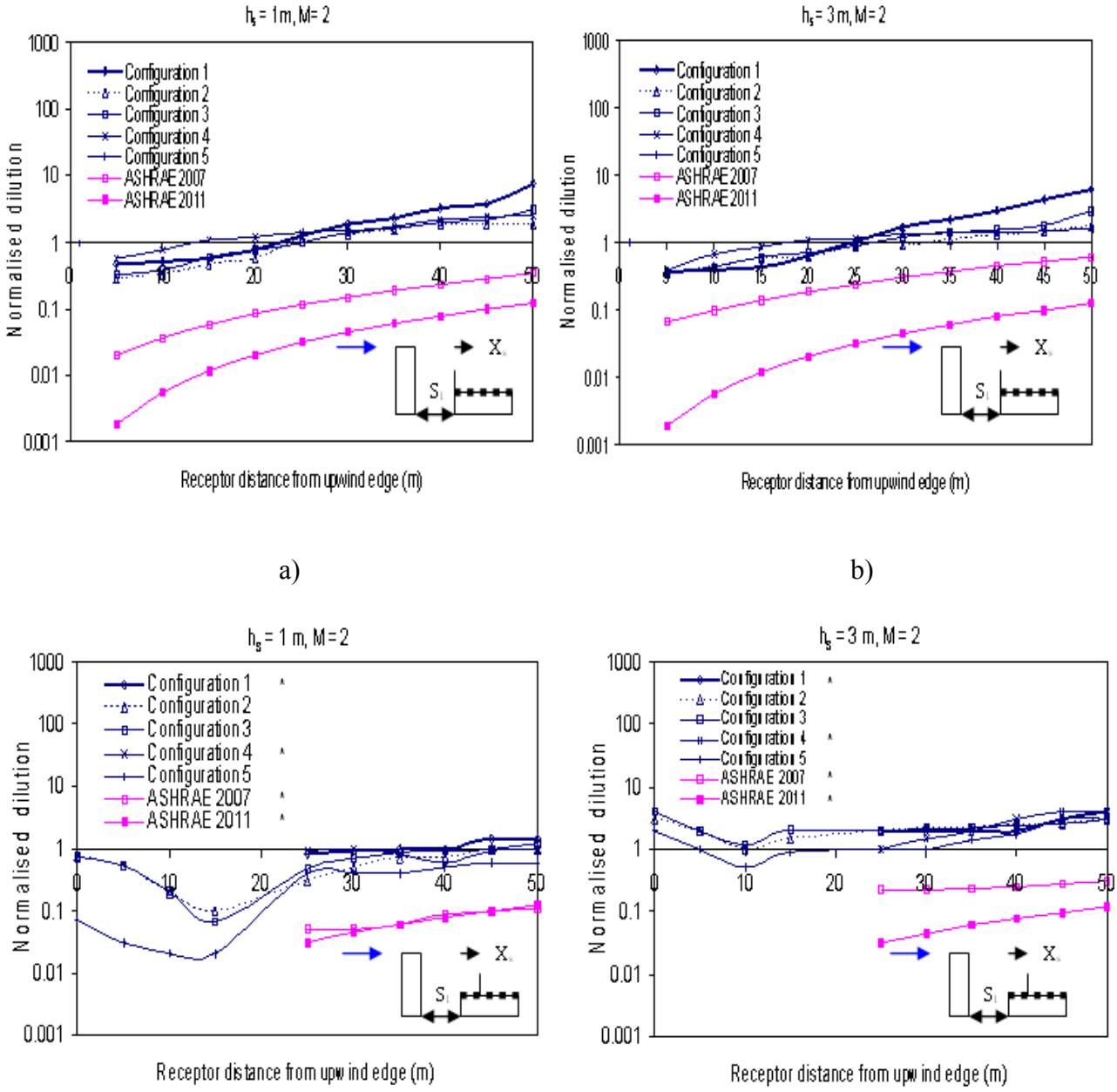


Figure B1. Normalised dilution on rooftop of $B_1$ for M = 2 and $S_1$ = 20 m: a) $h_s$ = 1 m, $X_s$ = 0; b) $h_s$ = 3 m, $X_s$ = 0; c) $h_s$ = 1 m, $X_s$ = 20 m; d) $h_s$ = 3 m, $X_s$ = 20 m (* Concentration of pollutants was found to be zero upwind of stack)

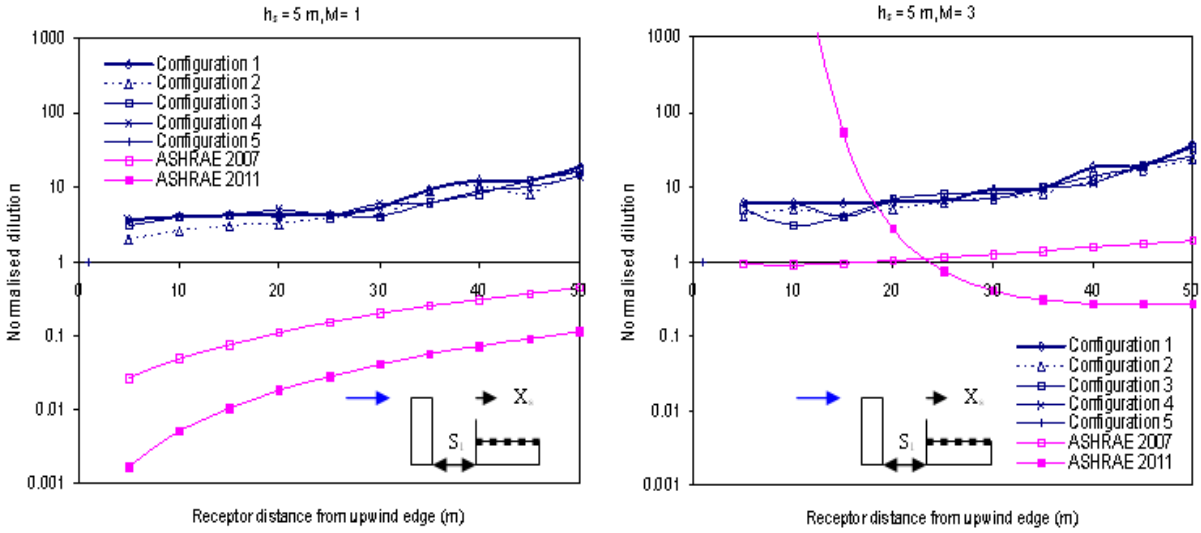


a) b)

Figure B2. Normalised dilution on rooftop of $B_1$ for $X_s = 0$ and $S_1 = 20$ m: a) M = 1; b) M = 3

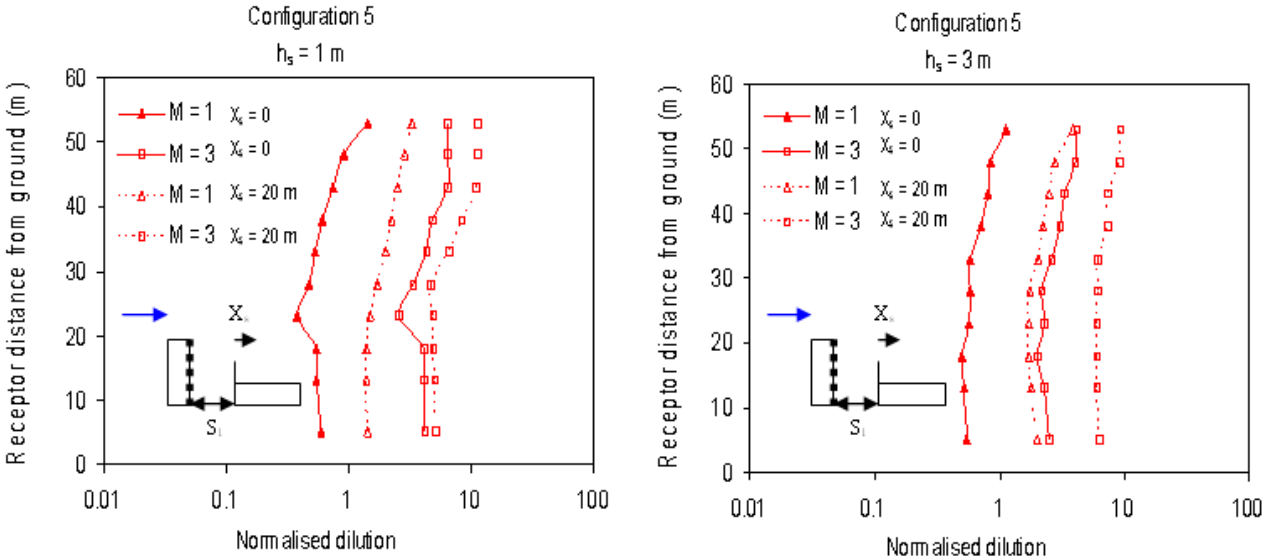


a) b)

Figure B3. Normalised dilution on leeward wall of $B_5$ of Configuration 5 for $S_1 = 20$ m: a) $h_s = 1$ m; b) $h_s = 3$ m

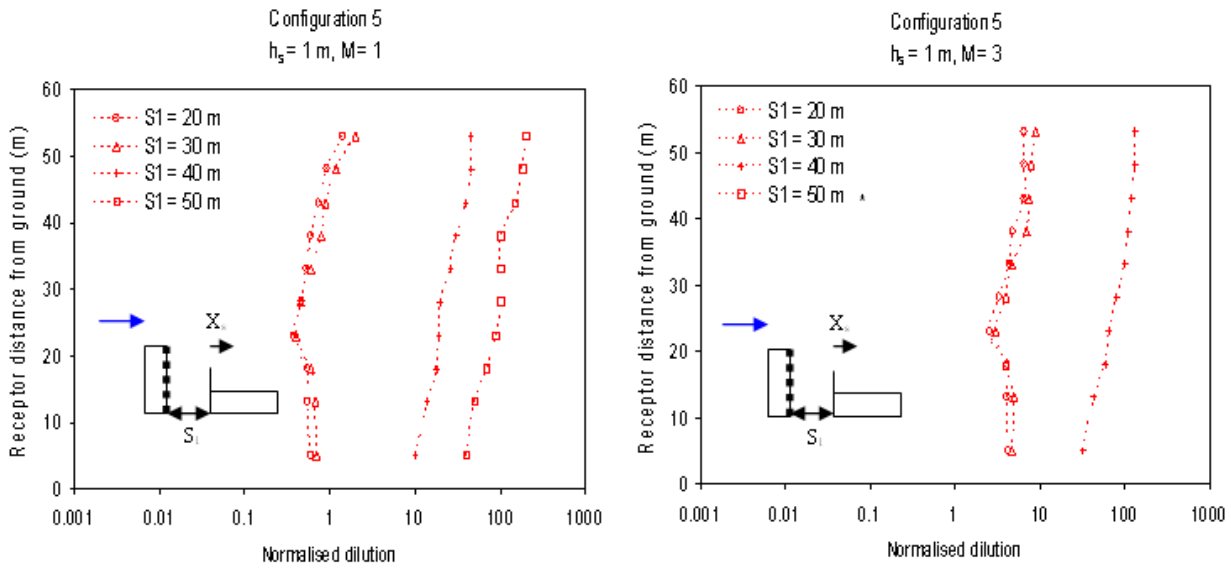


a) b)

Figure B4. Normalised dilution on leeward wall of $B_5$ for different spacing ($S_1$) at $X_s$ = 0 and $h_s$ = 1 m: a) M = 1; b) M = 3 (* Concentration of pollutants was found to be zero)

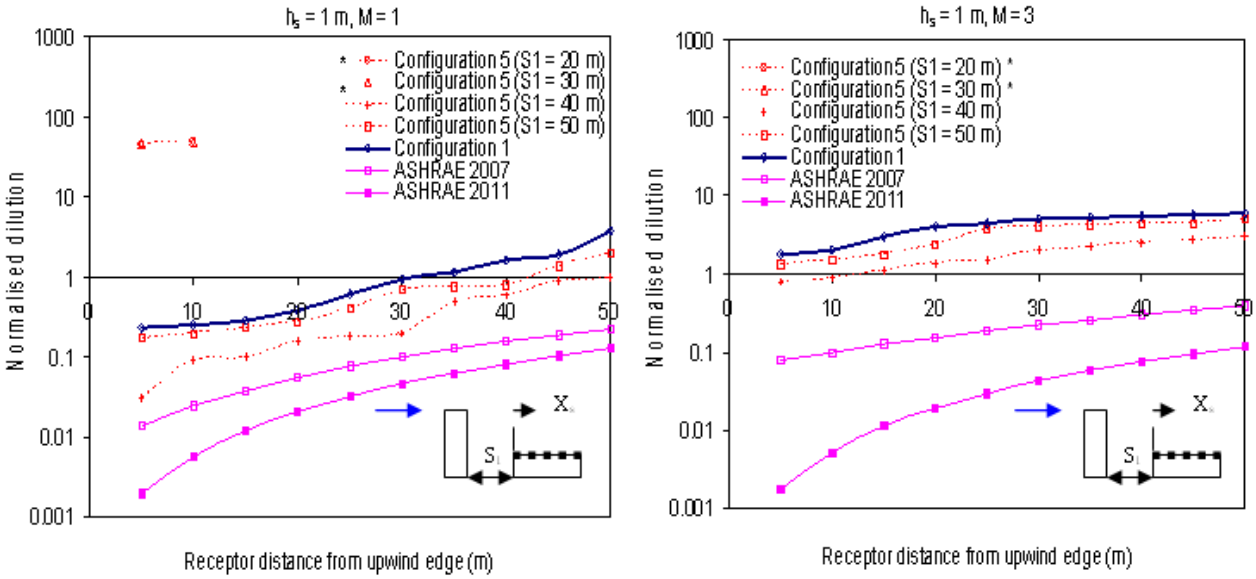


a) b)

Figure B5. Normalised dilution on rooftop of $B_1$ for different spacing ($S_1$), $X_s$ = 0 and $h_s$ = 1 m: a) M = 1; b) M = 3 (* Concentration of pollutants was found to be zero)

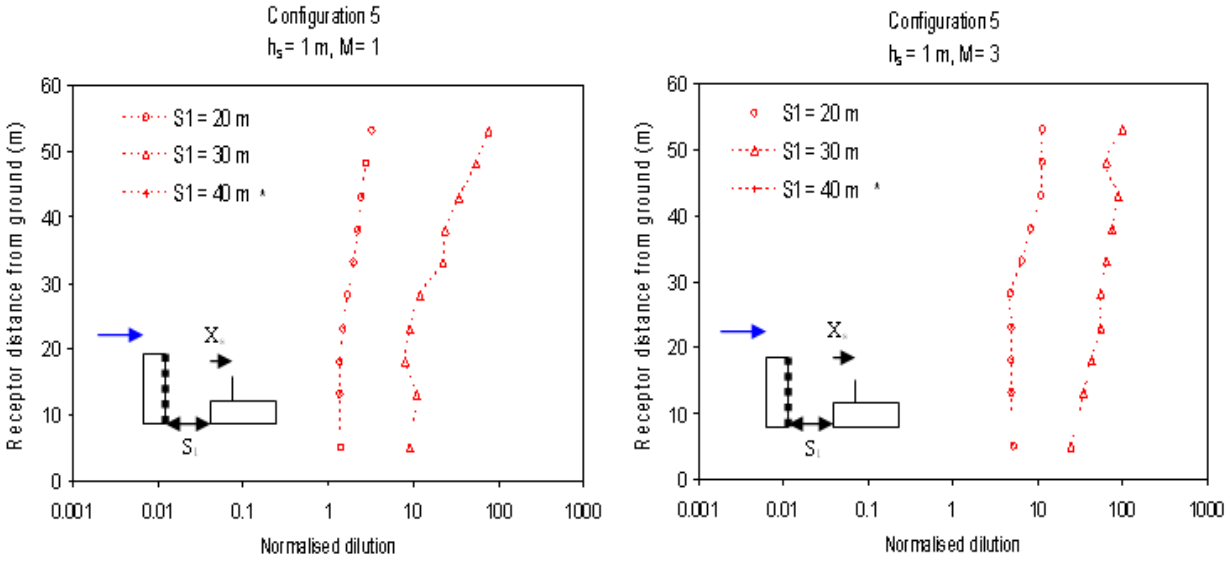


a) b)

Figure B6. Normalised dilution on leeward wall of $B_5$ for different spacing ($S_1$), $X_s$ = 20 m and $h_s$ = 1 m: a) M = 1; b) M = 3 (* Concentration of pollutants was found to be zero)

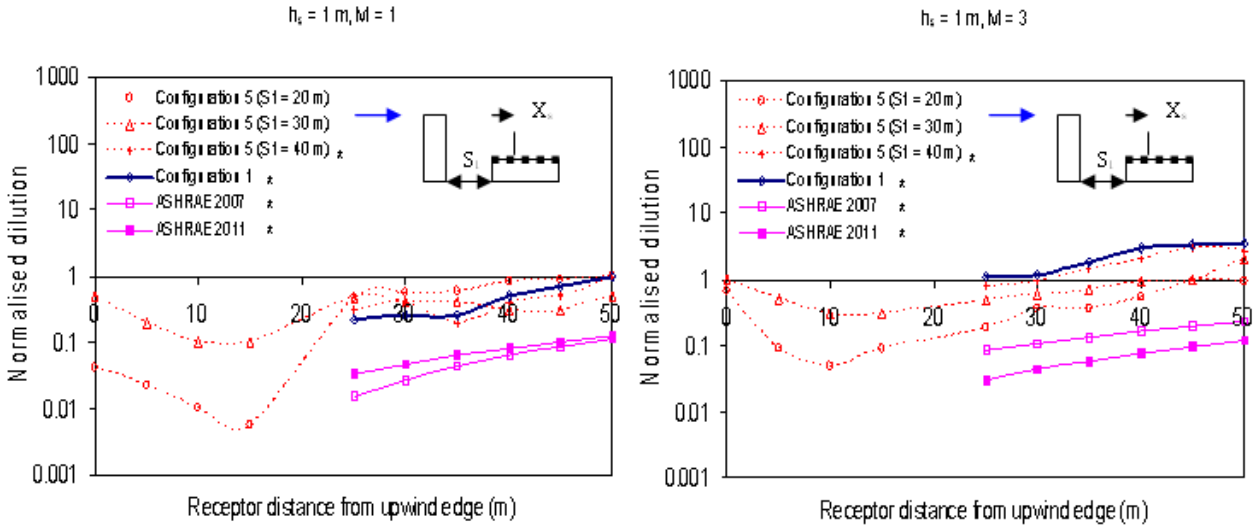


a) b)

Figure B7. Normalised dilution on rooftop of $B_1$ for different spacing ($S_1$), $X_s$ = 20 m and $h_s$ = 1 m: a) M = 1; b) M = 3 (* Concentration of pollutants was found to be zero upwind of stack)

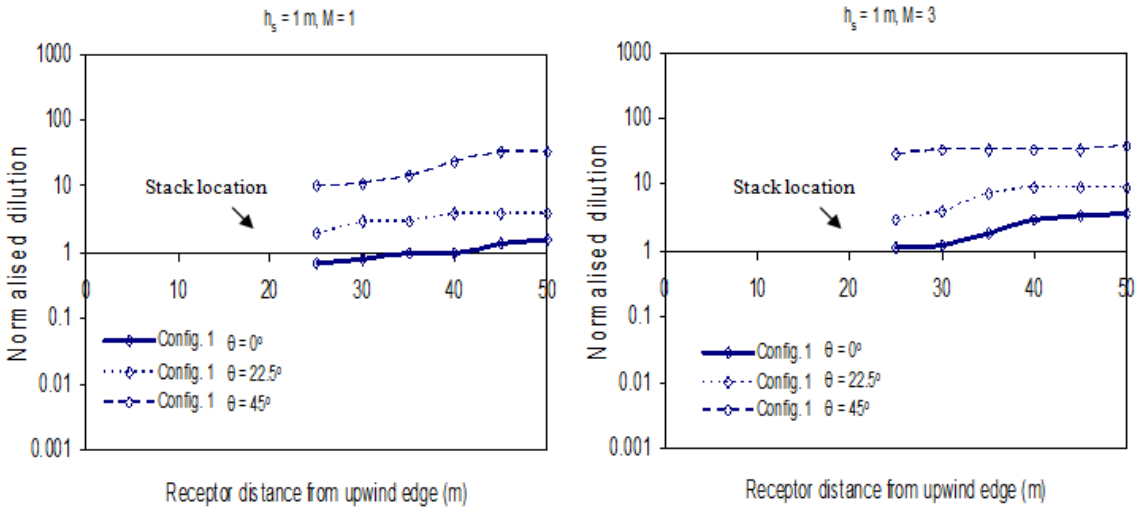


a) b)

Figure B8. Normalised dilution on rooftop of low isolated building for $X_s$ = 20 m: a) M = 1; b) M = 3

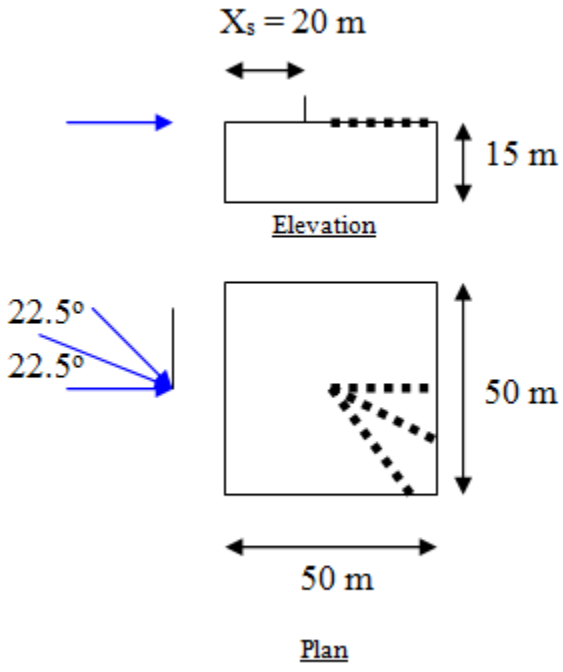

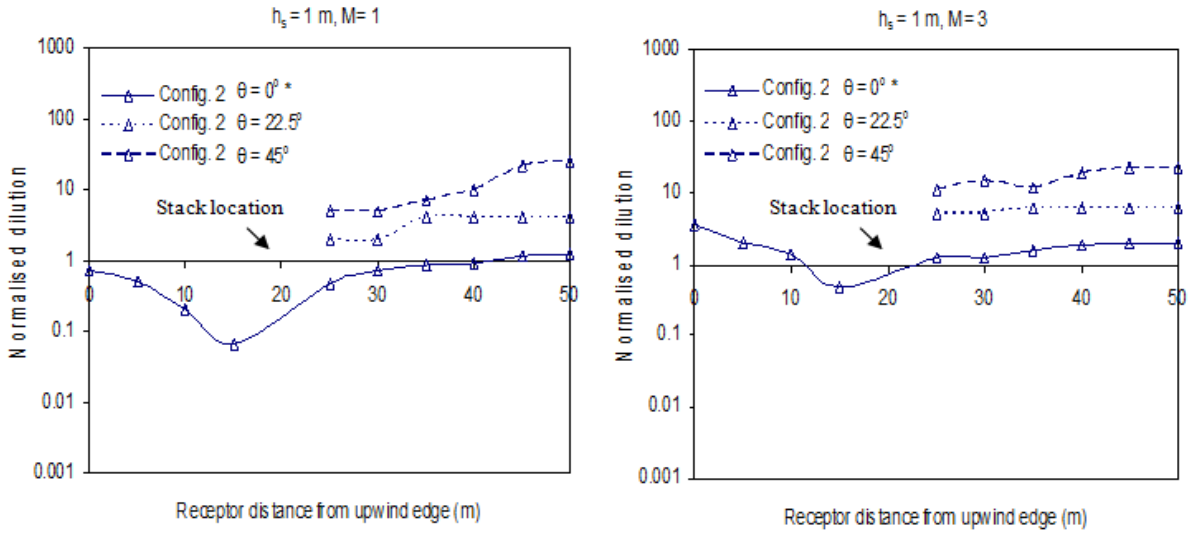


a) b)

Figure B9. Normalised dilution on rooftop of low building in the presence of a taller upstream building at $X_s$ = 20 m and $S_1$ = 20 m: a) M = 1; b) M = 3 (* concentrations were also detected upwind of stack)

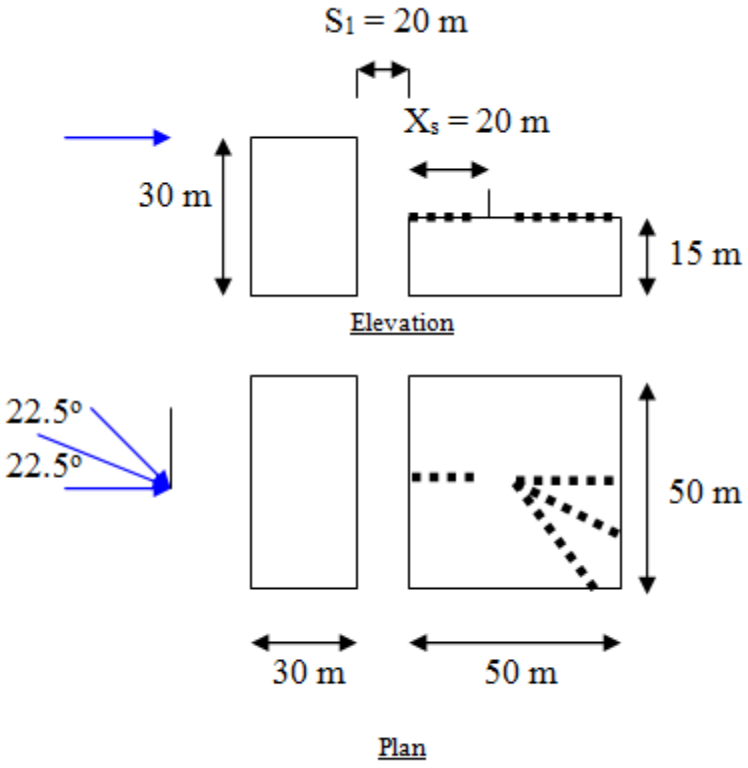

# Appendix C

# Additional results for downstream building configurations

This appendix presents results for downstream building configurations. Figure C1 presents comparisons for wind tunnel data and ASHRAE models for rooftop dilutions on emitting building for taller downstream configurations with buildings spaced 20 m apart. Figures C2 to C5 show results for downstream building of equal height as the emitting building for spacing of 20 m. Figure C6 shows the effect of spacing between buildings for Configuration 2a.

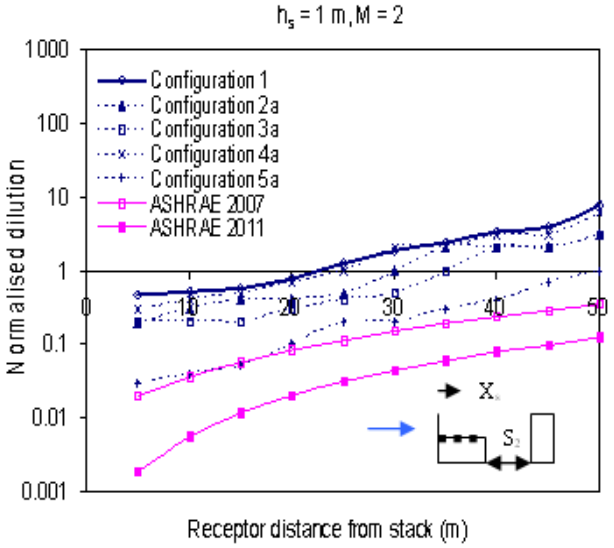


a)

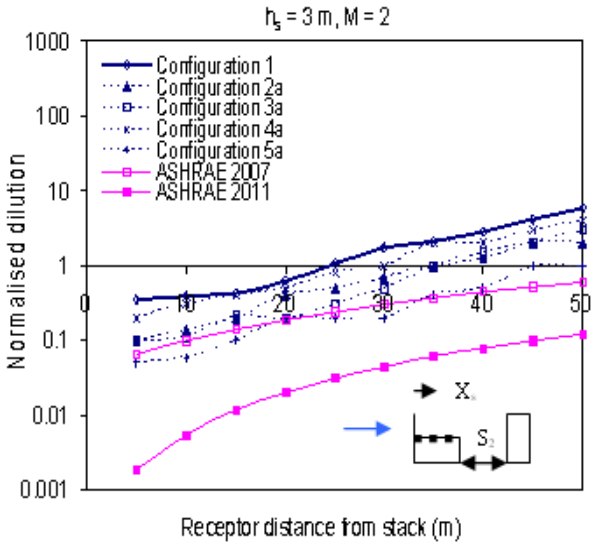


b)

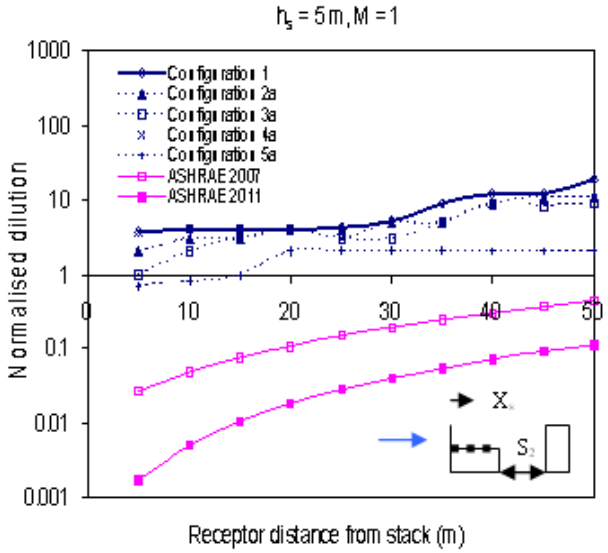


a)

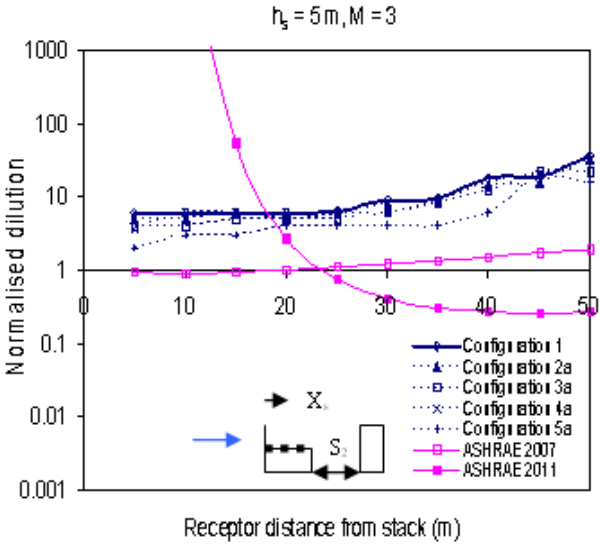


b)

Figure C1. Normalised dilution on rooftop of $B_1$ for $S_2$ = 20 m, $X_s$ = 0: a) $h_s$ = 1 m, M = 2; b) $h_s$ = 3 m, M = 2; c) $h_s$ = 5 m, M = 1; d) $h_s$ = 5 m, M = 3

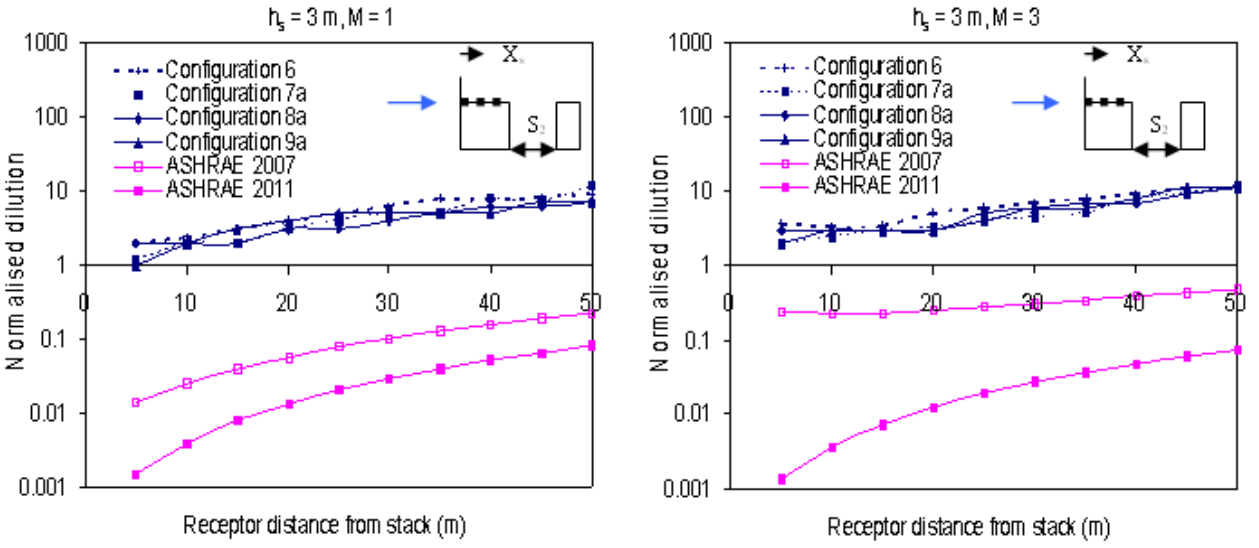


a) b)

Figure C2. Normalised dilution on rooftop of $B_6$ for $S_2$ = 20 m, $X_s$ = 0 and $h_s$ = 3 m: a) M = 1; b) M = 3

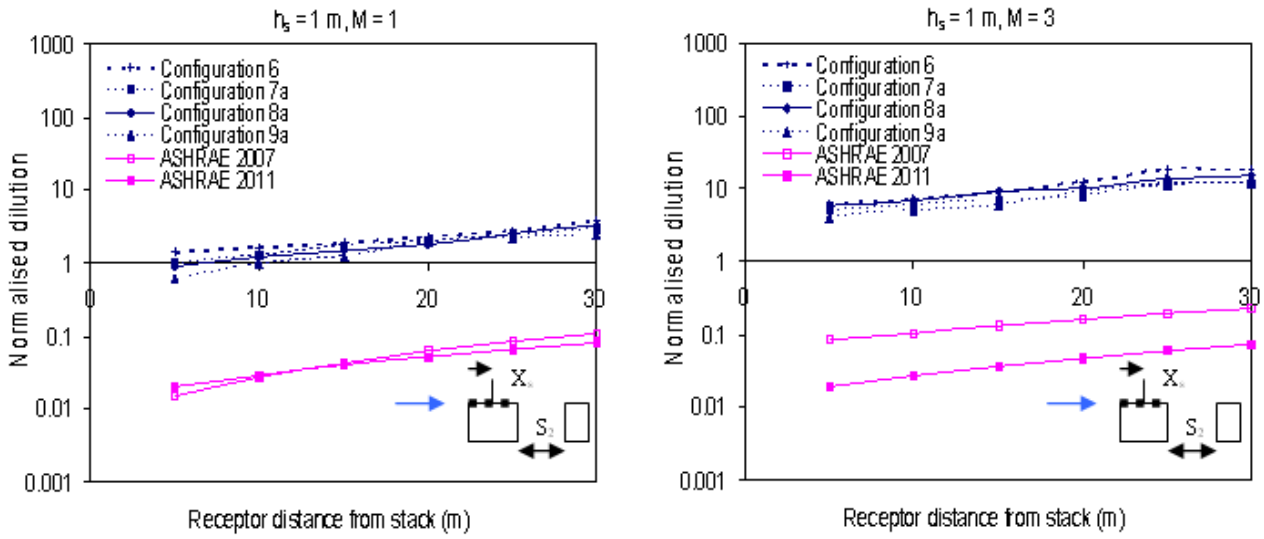


a) b)

Figure C3. Normalised dilution on rooftop of $B_6$ for $S_2$ = 20 m, $X_s$ = 20 m and $h_s$ = 1 m: a) M = 1; b) M = 3 (pollutant concentrations were found to be zero at receptors upwind of stack)

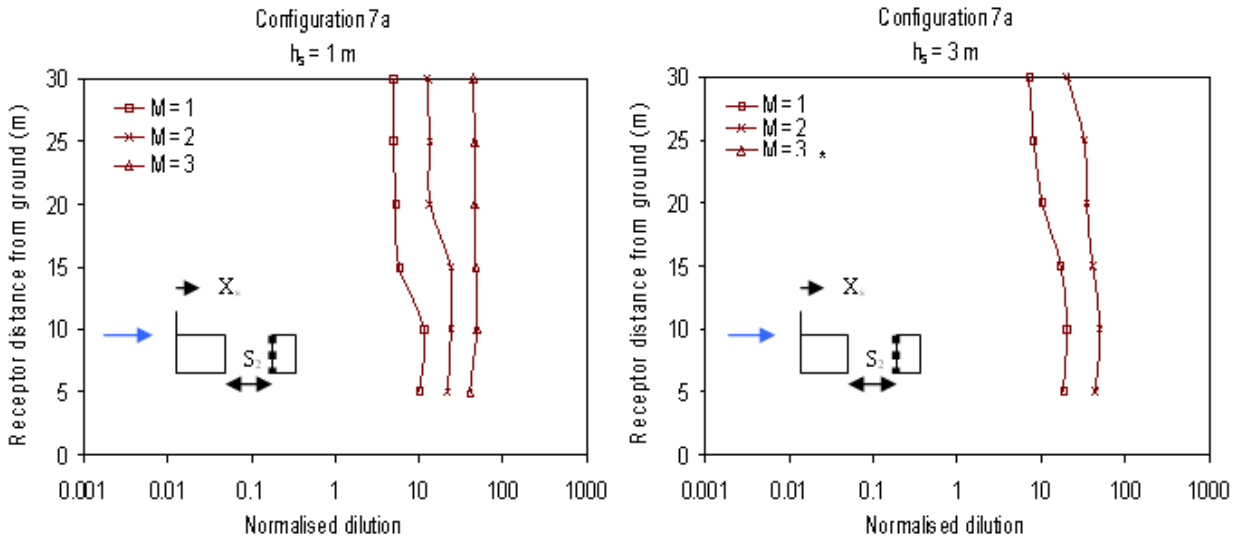


a) b)

Figure C4. Normalised dilution on windward wall of $B_2$ for $S_2$ = 20 m and $X_s$ = 0: a) $h_s$ = 1 m; b) $h_s$ = 3 m (* Pollutant concentrations were found to be zero at all receptors)

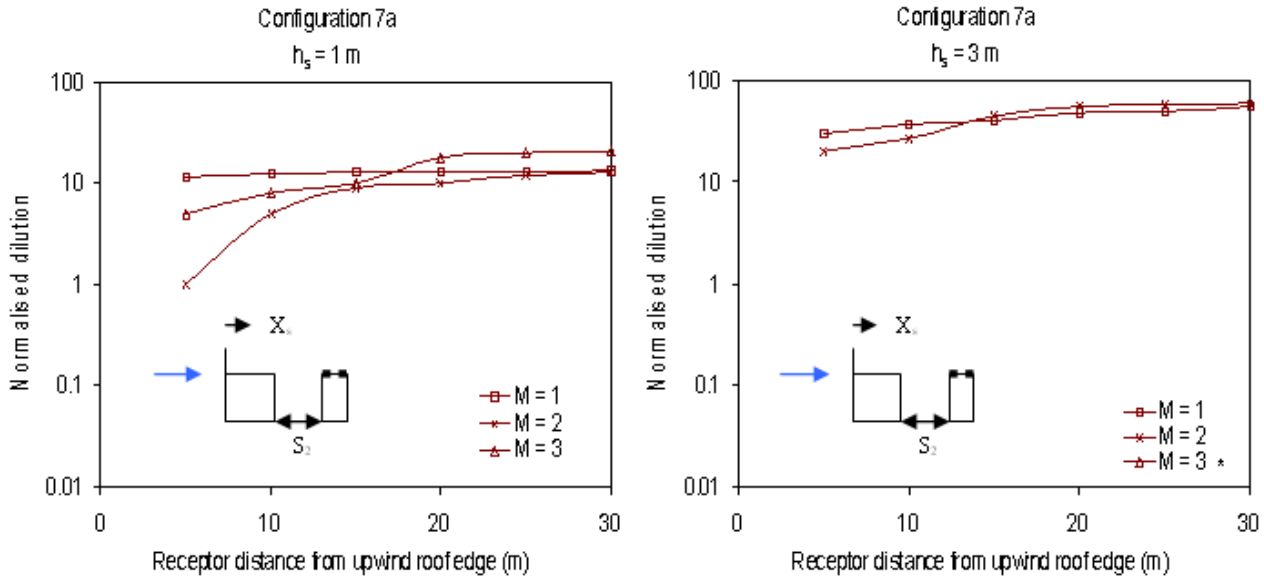


a) b)

Figure C5. Normalised dilution on rooftop of $B_2$ for $S_2$ = 20 m and $X_s$ = 0: a) $h_s$ = 1 m; b) $h_s$ = 3 m (* Pollutant concentrations were found to be zero at all receptors)

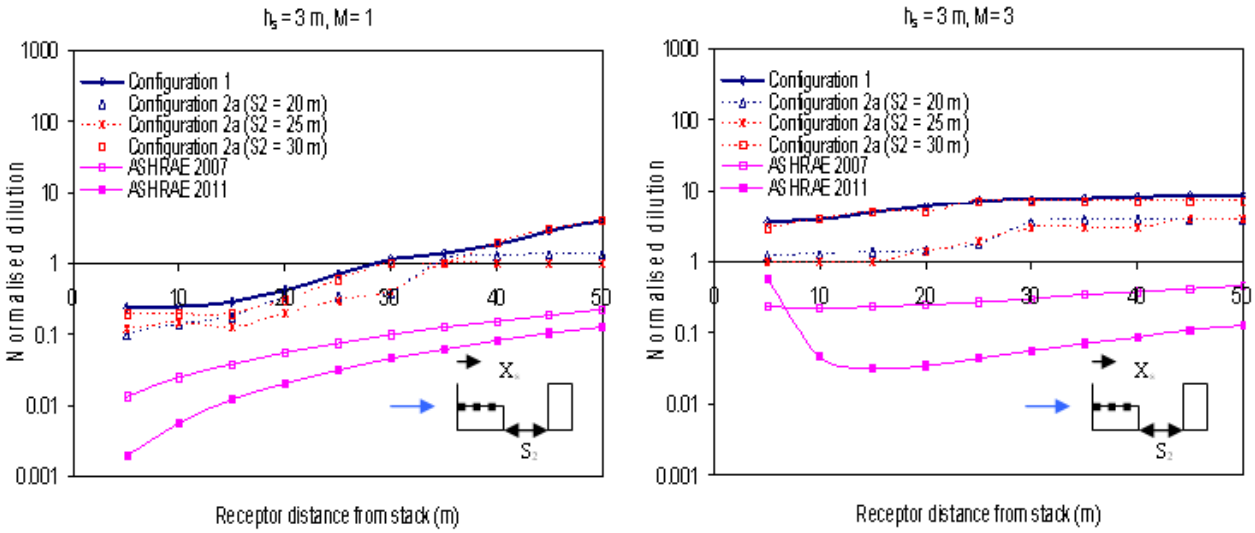


a) b)

Figure C6. Normalised dilution on rooftop of $B_1$ for $h_s$ = 3 m and $X_s$ = 0: a) M = 1; b) M = 3

# Appendix D

# Additional results for Configurations 10 and 11

This appendix presents dilution results for Configurations 10 and 11. Configuration 10 consists of a taller building placed upstream and downstream of the emitting building whilst Configuration 11 consists of a taller downstream building and an upstream building of equal height as the emitting building. Figures D1 through D6 correspond to results for buildings spaced 20 m apart. Comparisons for wind tunnel data and ASHRAE models for Configuration 10 are presented in Figures D1 to D4 whilst Figures D5 and D6 show additional results for Configuration 11. The effect of spacing between buildings on the windward wall of the downstream building of Configuration 10 is presented in Figure D7.

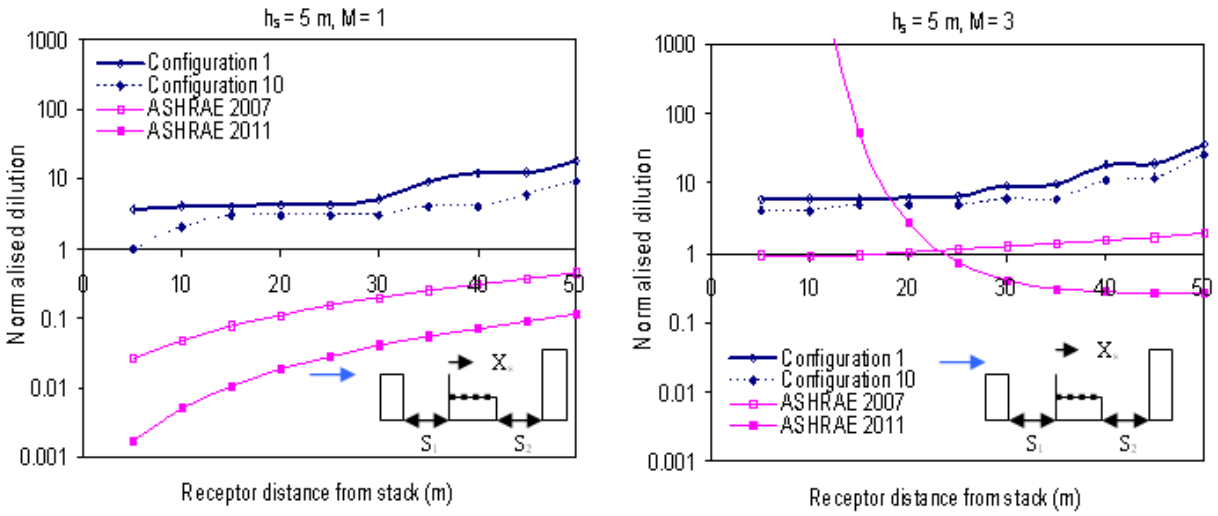


a) b)

Figure D1. Normalised dilution on rooftop of $B_1$ for $h_s$ = 5 m and $X_s$ = 0: a) M = 1; b) M = 3

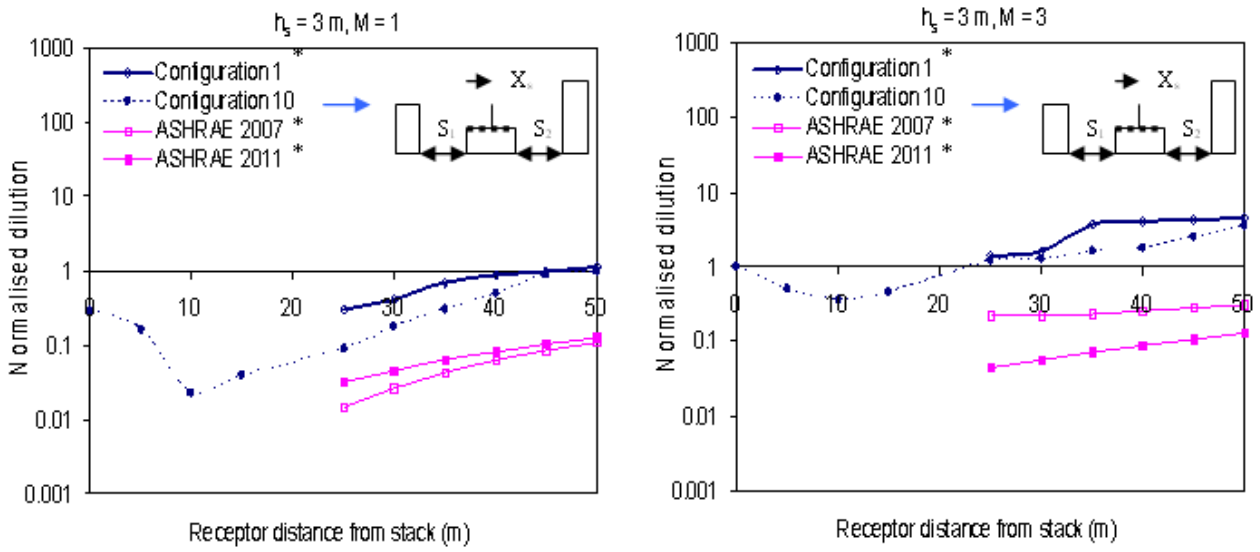


a) b)

Figure D2. Normalised dilution on rooftop of $B_1$ for $h_s$ = 3 m and $X_s$ = 20 m: a) M = 1; b) M = 3 (* pollutant concentration was zero at receptors upwind of stack)

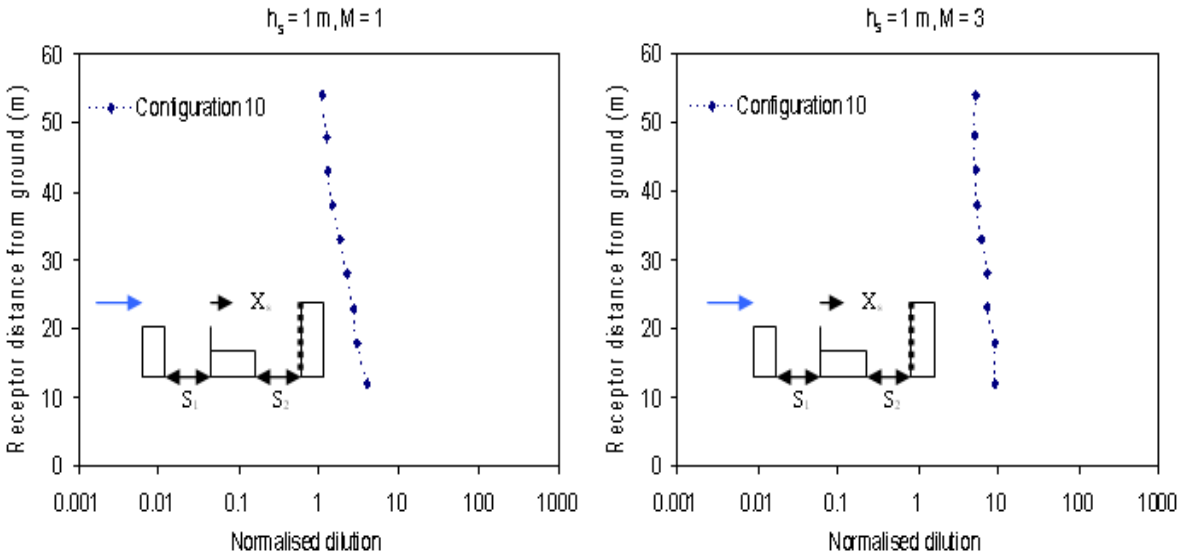


a) b)

Figure D3. Normalised dilution on windward wall of $B_5$ for $h_s$ = 1 m and $X_s$ = 0: a) M = 1; b) M = 3

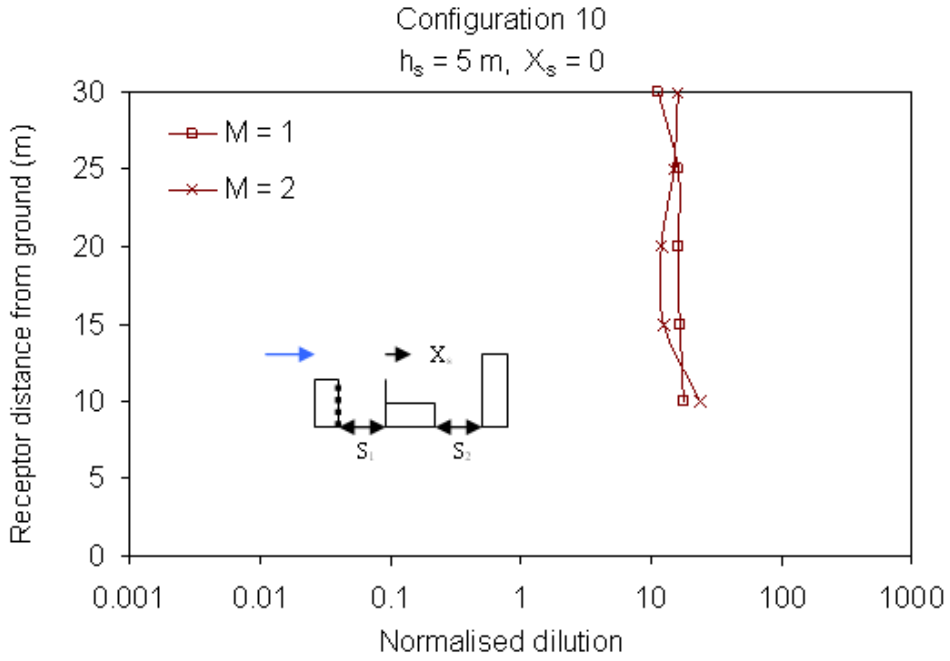


Figure D4. Normalised dilution on leeward wall of $B_2$ for Configuration 10 at $h_s$ = 5 m

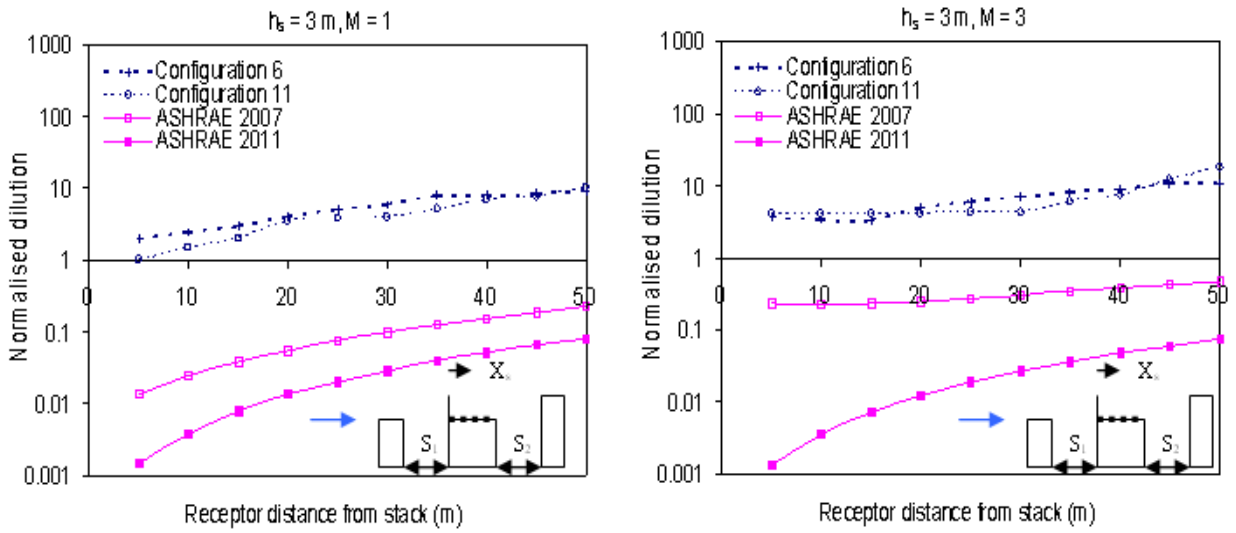


a) b)

Figure D5. Normalised dilution on rooftop of $B_6$ for $h_s$ = 3 m and $X_s$ = 0: a) M = 1; b) M = 3

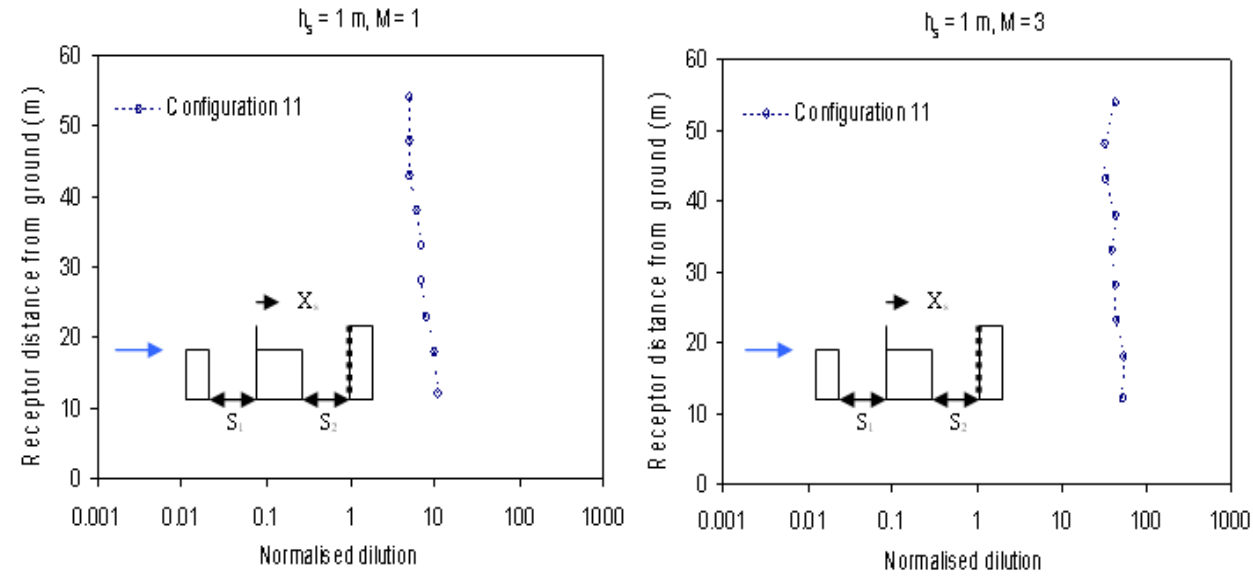


a) b)

Figure D6. Normalised dilution on windward wall of $B_5$ for $h_s$ = 1 m and $X_s$ = 0: a) M = 1; b) M = 3

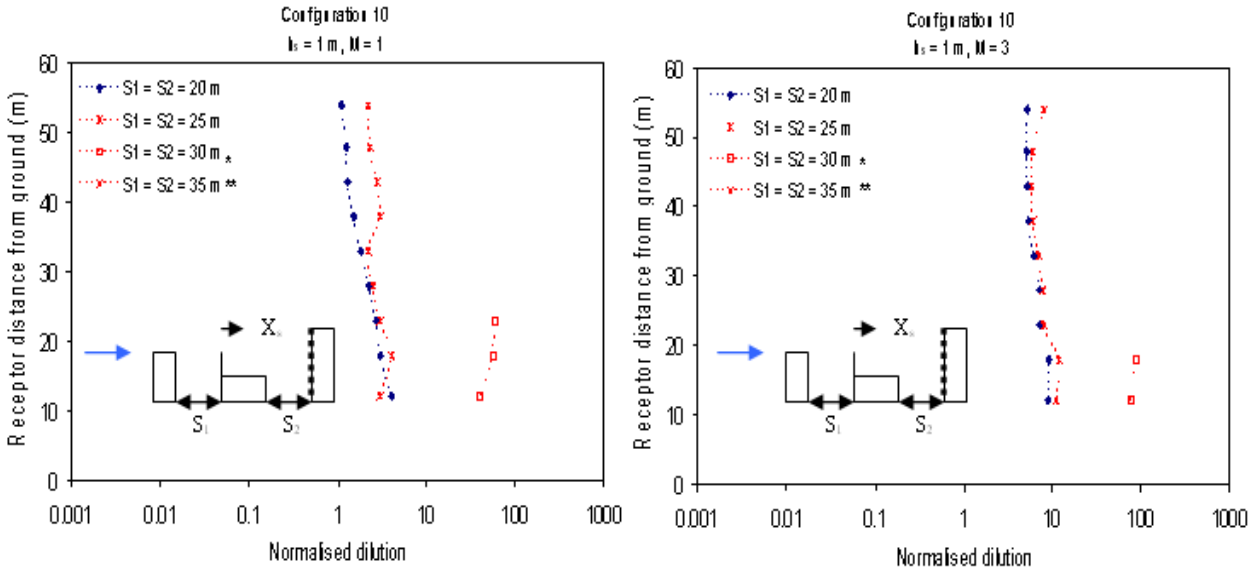


a) b)

Figure D7. Normalised dilution on windward wall of $B_5$ for $h_s$ = 1 m and $X_s$ = 0: a) M = 1; b) M = 3

* Pollutant concentration was found at few receptors closer to the ground,

** Pollutant concentration was found to be zero at all receptors on the wall

# Appendix E

# Additional results in non-dimensional form

This appendix presents dilution results in non-dimensional form. Section 5.9 of Chapter 5 explains the method of converting the results to non dimensional form. Figures E1 through E4 present results for upstream building configurations whilst Figures E5 to E8 correspond to non dimensional results for downstream building configurations. Additional results for Configurations 10 are presented in Figures E9 to E13.

Upstream building configurations

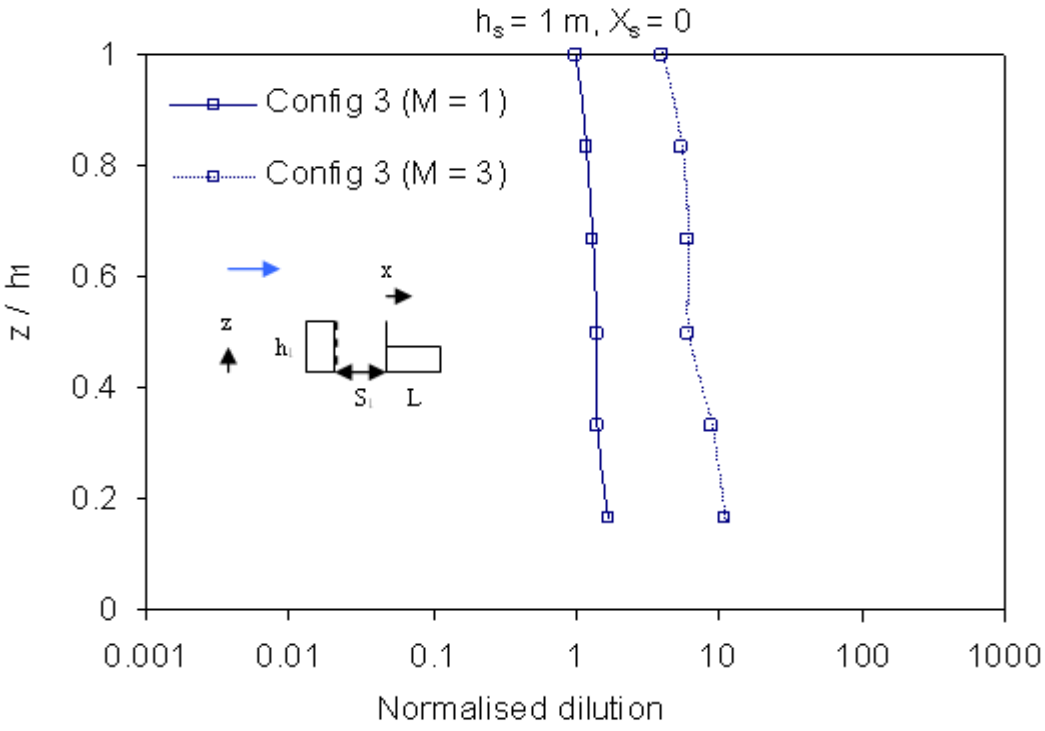


Figure E1. Normalised dilution on leeward wall of $B_3$ for $S_1$ = 0.4L and $X_s$ = 0

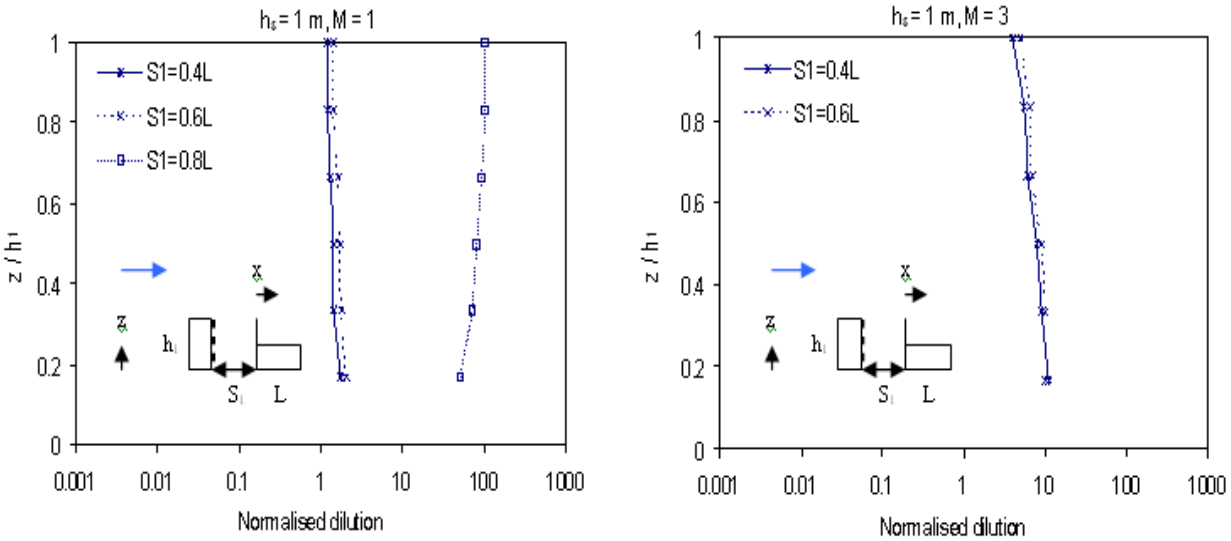


a) b)

Figure E2. Normalised dilution on leeward wall of $B_3$ for Configuration 3 at $X_s$ = 0: a) M = 1; b) M = 3

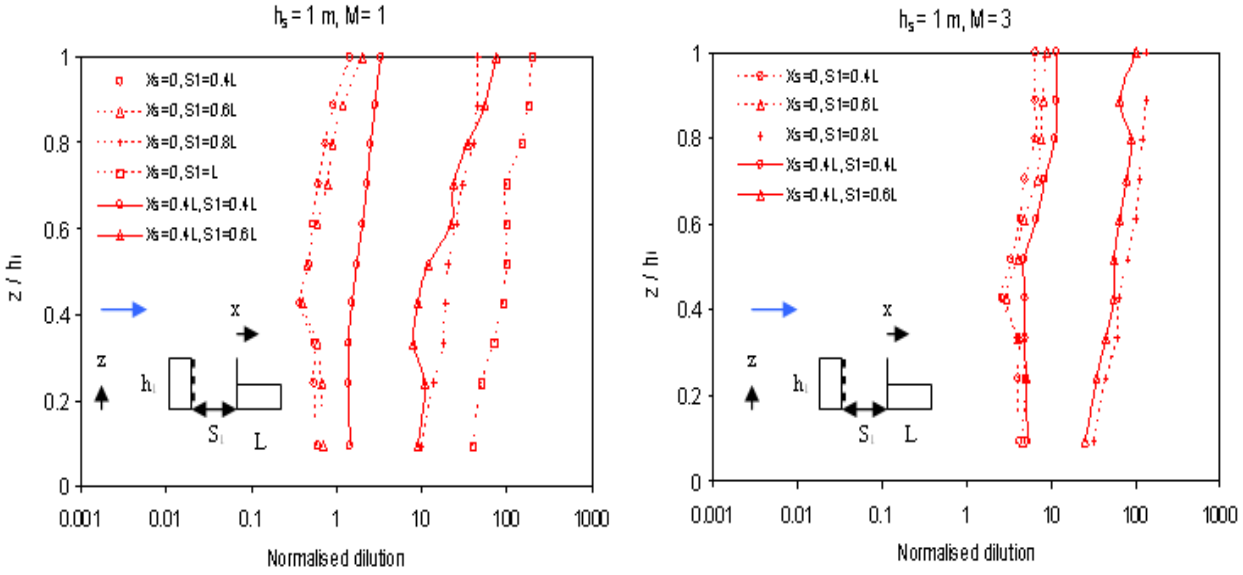


a) b)

Figure E3. Normalised dilution on leeward wall of $B_5$ for Configuration 5: a) M = 1; b) M = 3

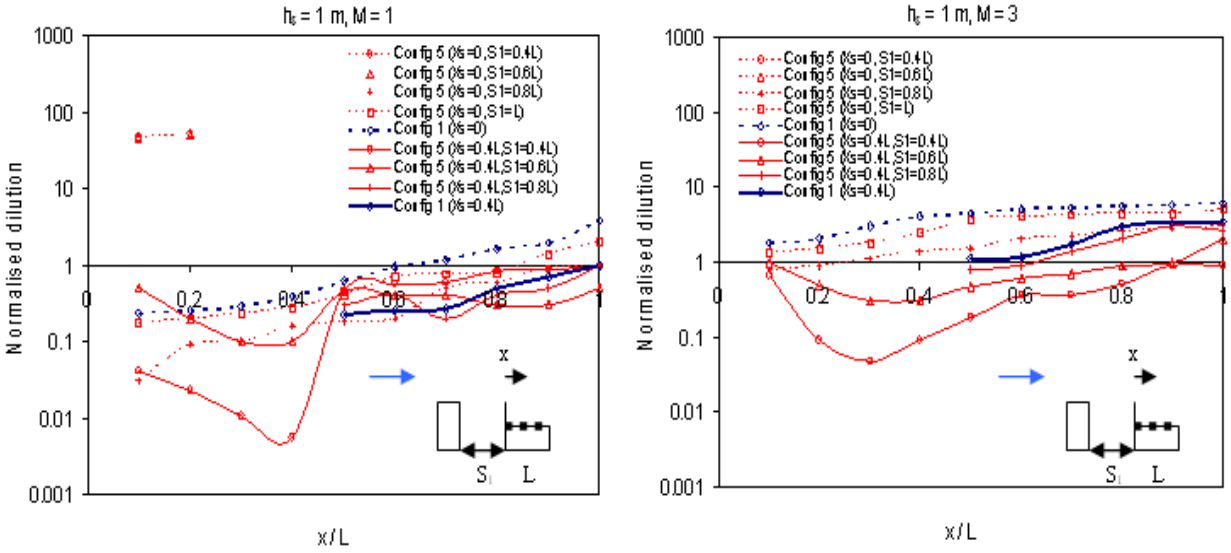


a) b)

Figure E4. Normalised dilution on rooftop of $B_1$: a) M = 1; b) M = 3

Downstream building configurations

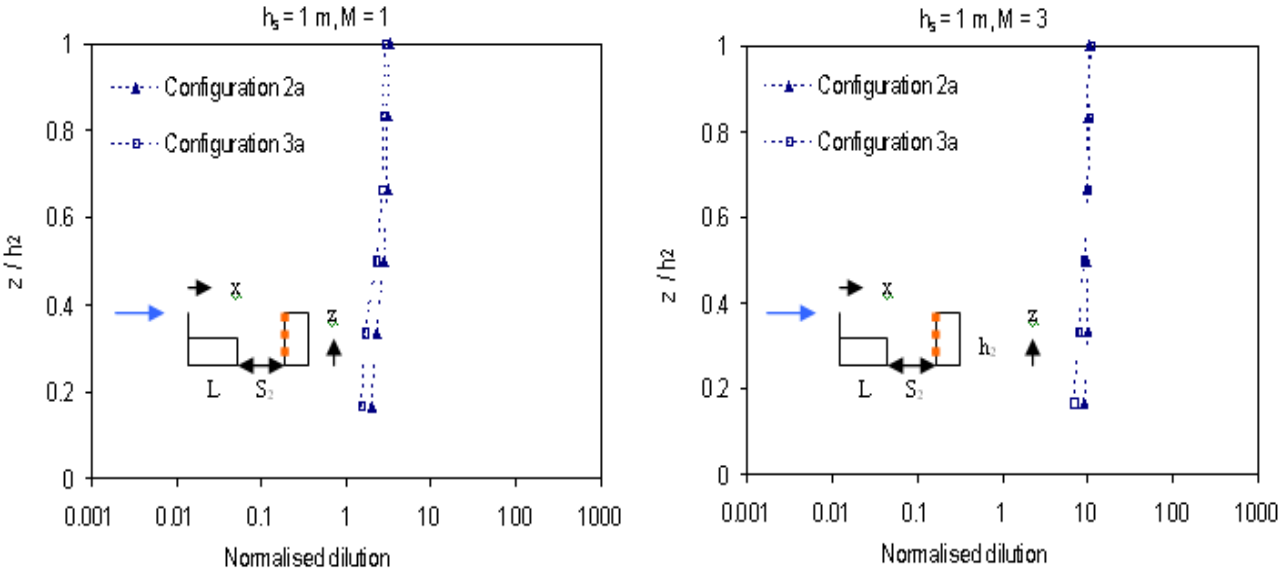


a) b)

Figure E5. Normalised dilution on windward wall of downstream building: a) M = 1; b) M = 3

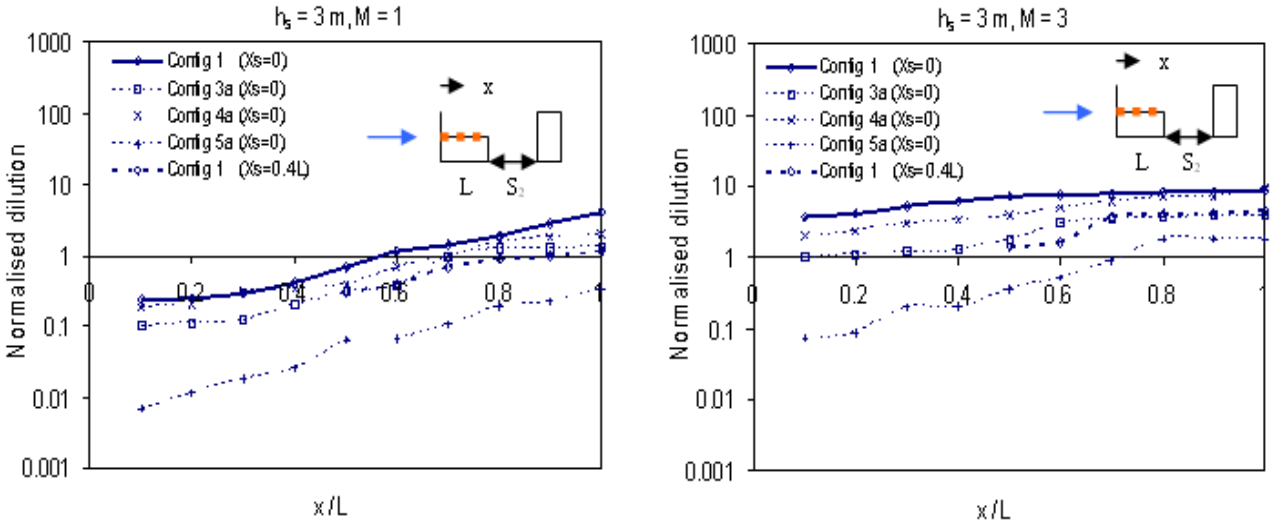


a) b)

Figure E6. Normalised dilution on rooftop of emitting building ($B_1$): a) M = 1; b) M = 3

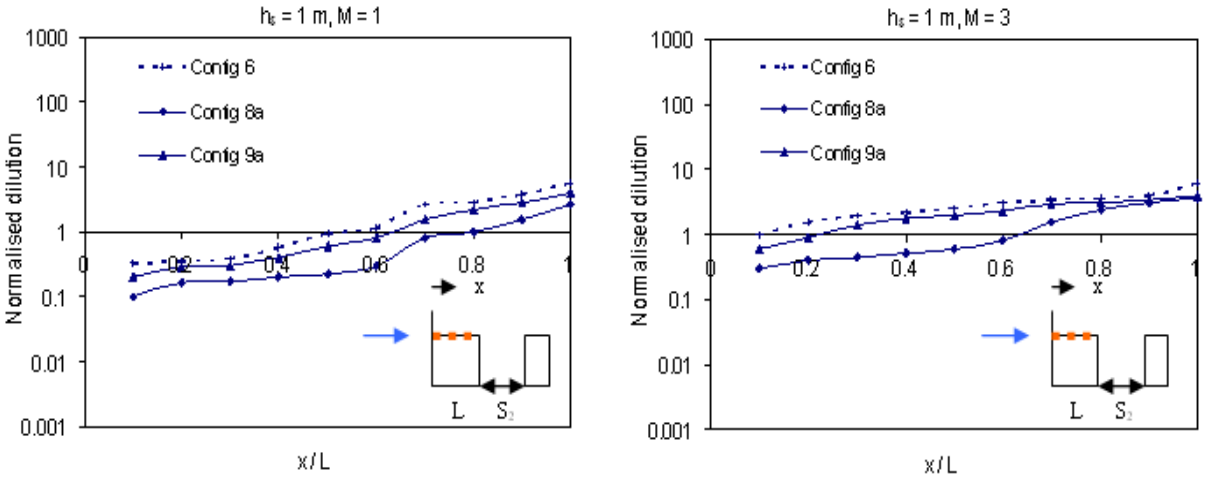


a) b)

Figure E7. Normalised dilution on rooftop of $B_6$ for: a) M = 1; b) M = 3

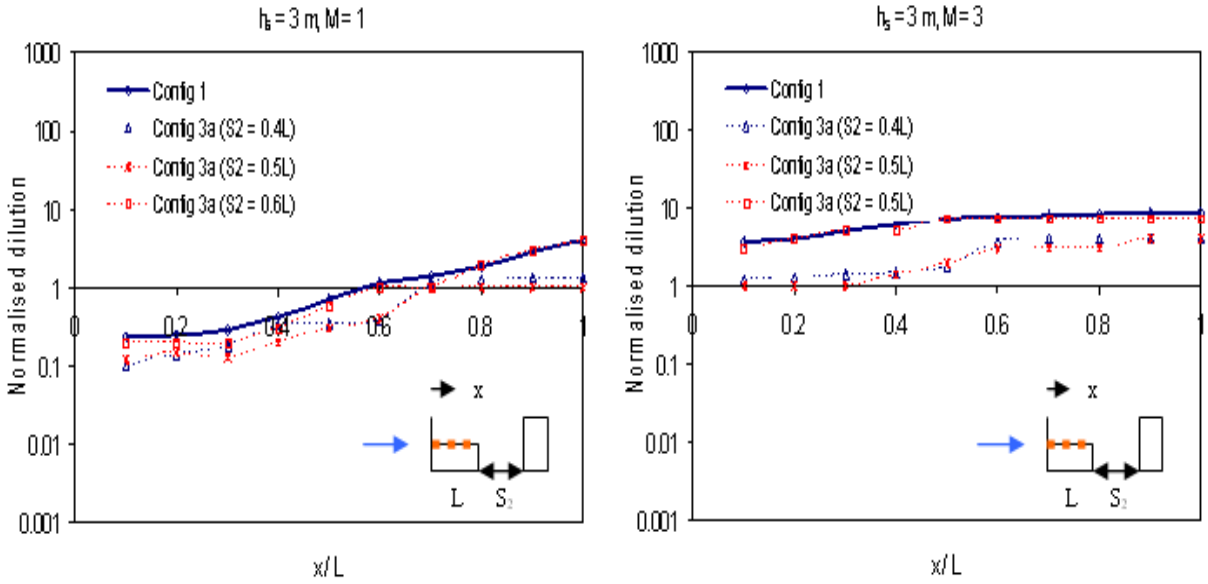


a) b)

Figure E8. Normalised dilution on rooftop of $B_1$ for: a) M = 1; b) M = 3

A Building placed upstream and downstream of the emitting building

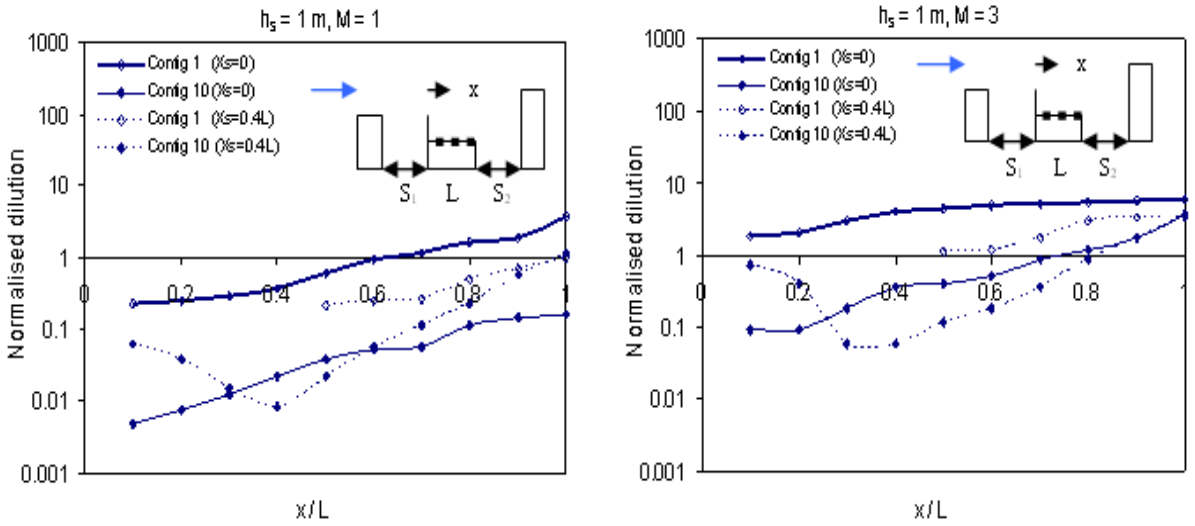


a) b)

Figure E9. Normalised dilution on rooftop of $B_1$ for $S_1 = S_2 = 0.4L$: a) M = 1; b) M = 3

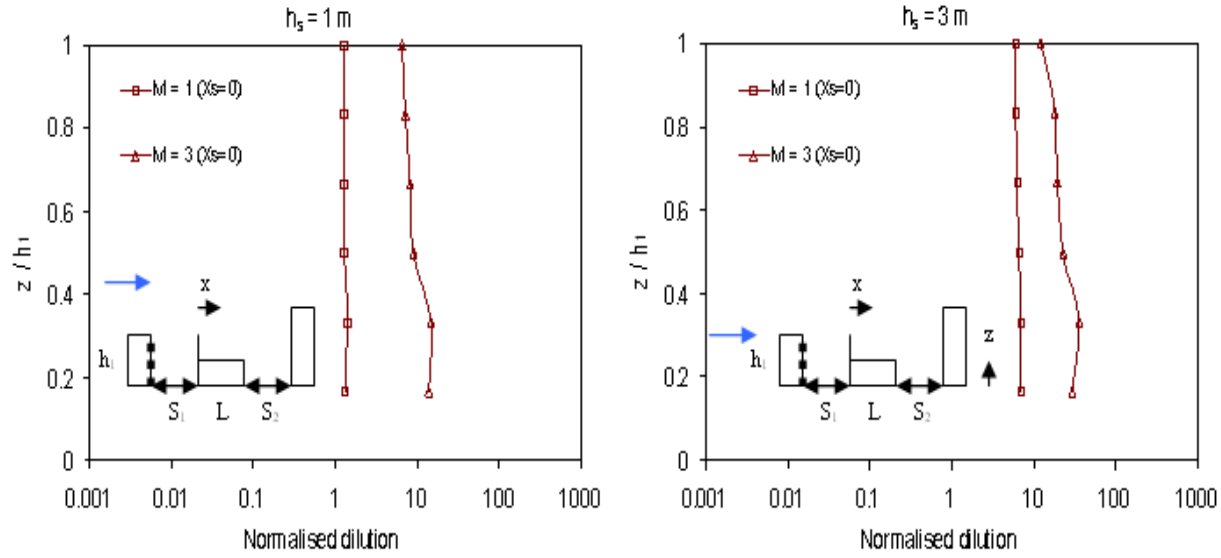


a) b)

Figure E10. Normalised dilution on leeward wall of $B_2$ for $S_1 = S_2 = 0.4L$: a) $h_s$ = 1 m; b) $h_s$ = 3 m

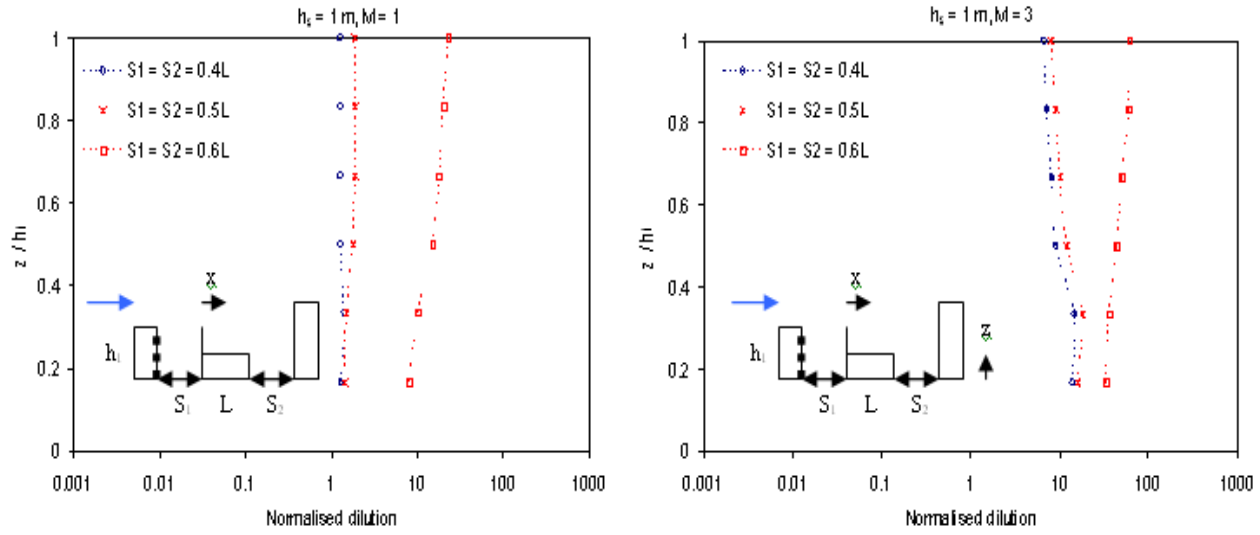


a) b)

Figure E11. Normalised dilution on leeward wall of upstream building ($B_2$) for Configuration 10 at $X_s = 0$: a) M = 1; b) M = 3

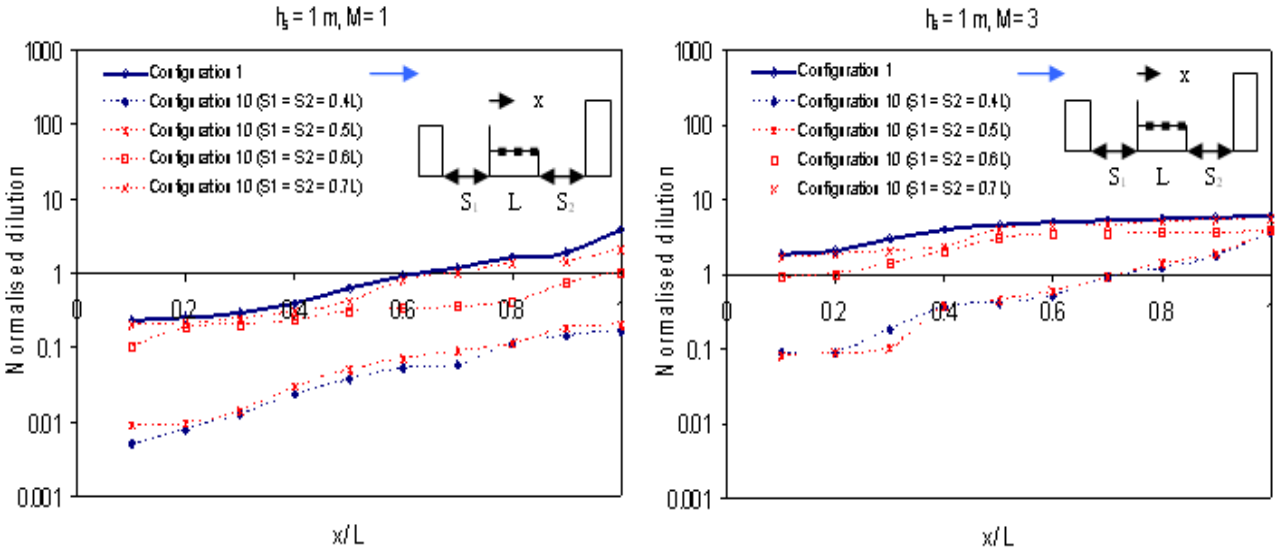


a) b)

Figure E12. Normalised dilution on rooftop of $B_1$ for Configuration 10 at $X_s = 0$: a) M = 1; b) M = 3

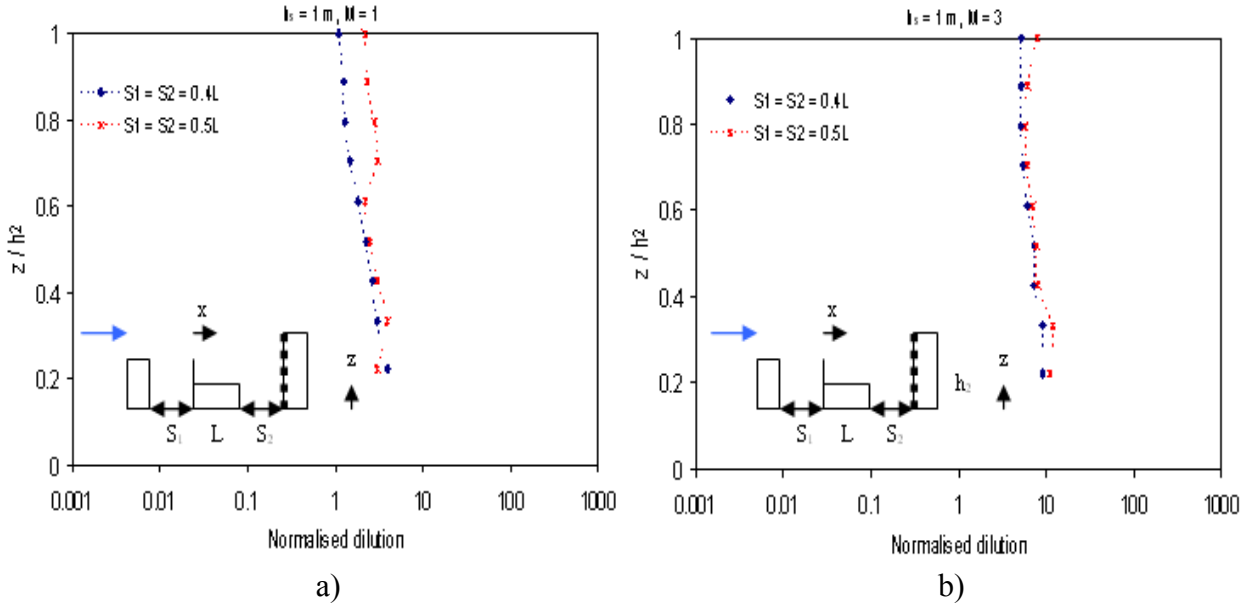


Figure E13. Normalised dilution on windward wall of $B_5$ for Configuration 10 at $X_s = 0$: a) M = 1; b) M = 3

# Appendix F

# Additional results for the application of rectified ASHRAE 2007 approach

This appendix presents results for application of the rectified ASHRAE 2007 approach which was previously explained in Chapter 6. The results consist of application of the rectified approach to present studies (Figures F1 to F6) and previous studies (Figure F7 to F10).

Application to present study

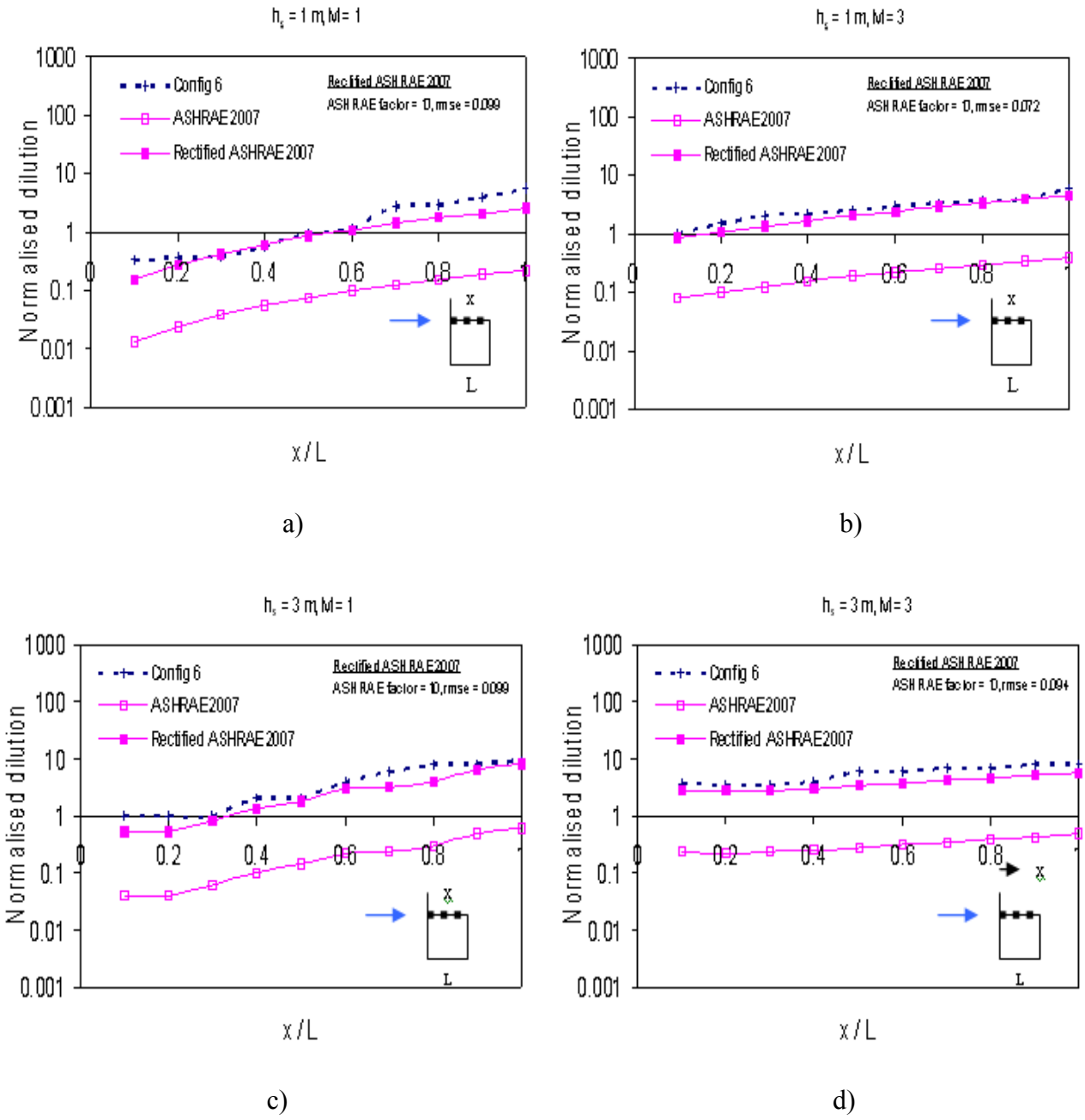


Figure F1. Normalised dilution on rooftop of $B_6$ for $X_s = 0$: a) $h_s = 1$ m, $M = 1$; b) $h_s = 1$ m, $M = 3$; c) $h_s = 3$ m, $M = 1$; d) $h_s = 3$ m, $M = 3$

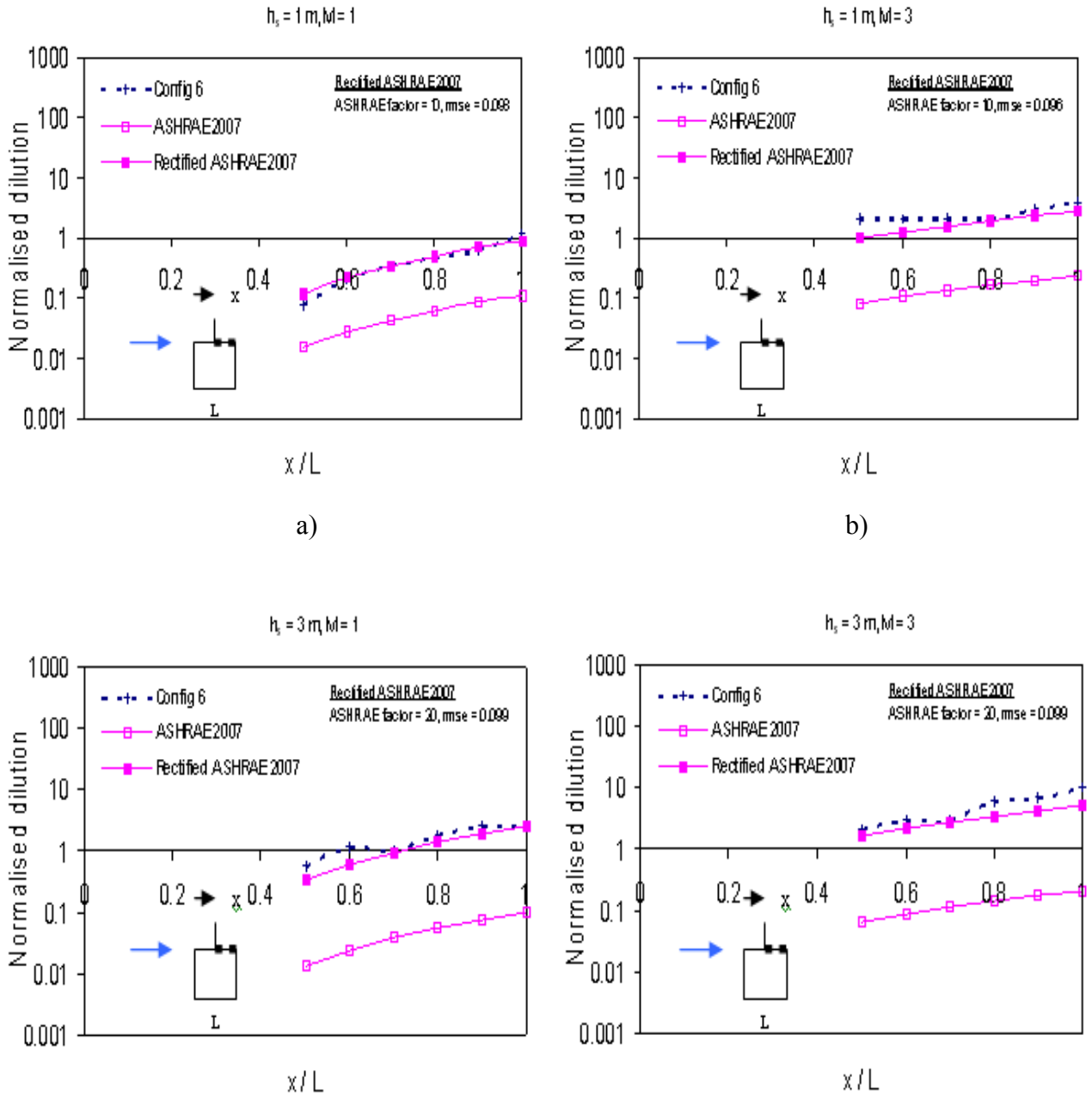


Figure F2. Normalised dilution on rooftop of $B_6$ for $X_s = 0.4L$: a) $h_s = 1$ m, $M = 1$; b) $h_s = 1$ m, $M = 3$; c) $h_s = 3$ m, $M = 1$; d) $h_s = 3$ m, $M = 3$

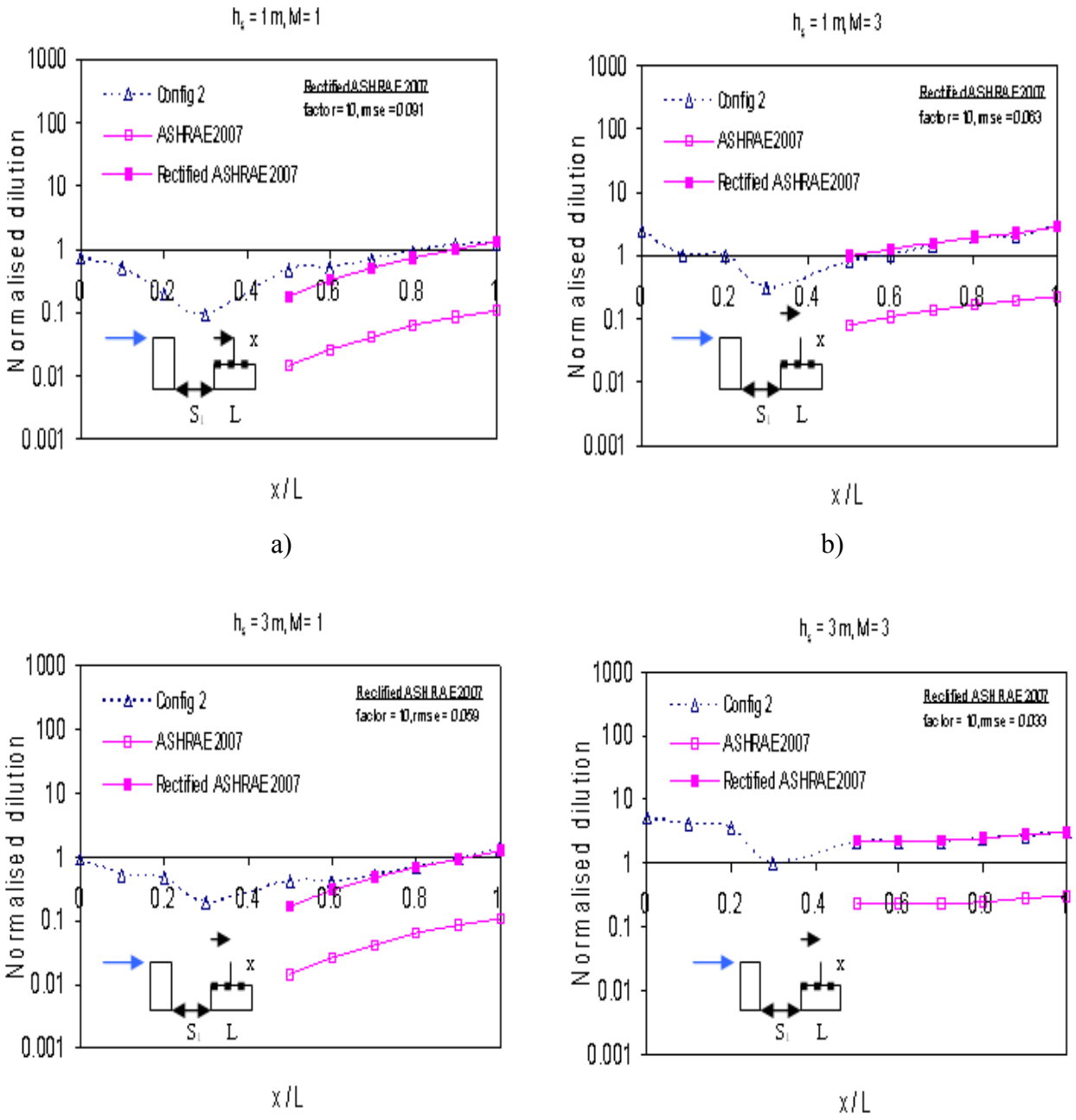


Figure F3. Normalised dilution on rooftop of $B_1$ for $X_s = 0.4L$: a) $h_s = 1$ m, $M = 1$; b) $h_s = 1$ m, $M = 3$; c) $h_s = 3$ m, $M = 1$; d) $h_s = 3$ m, $M = 3$

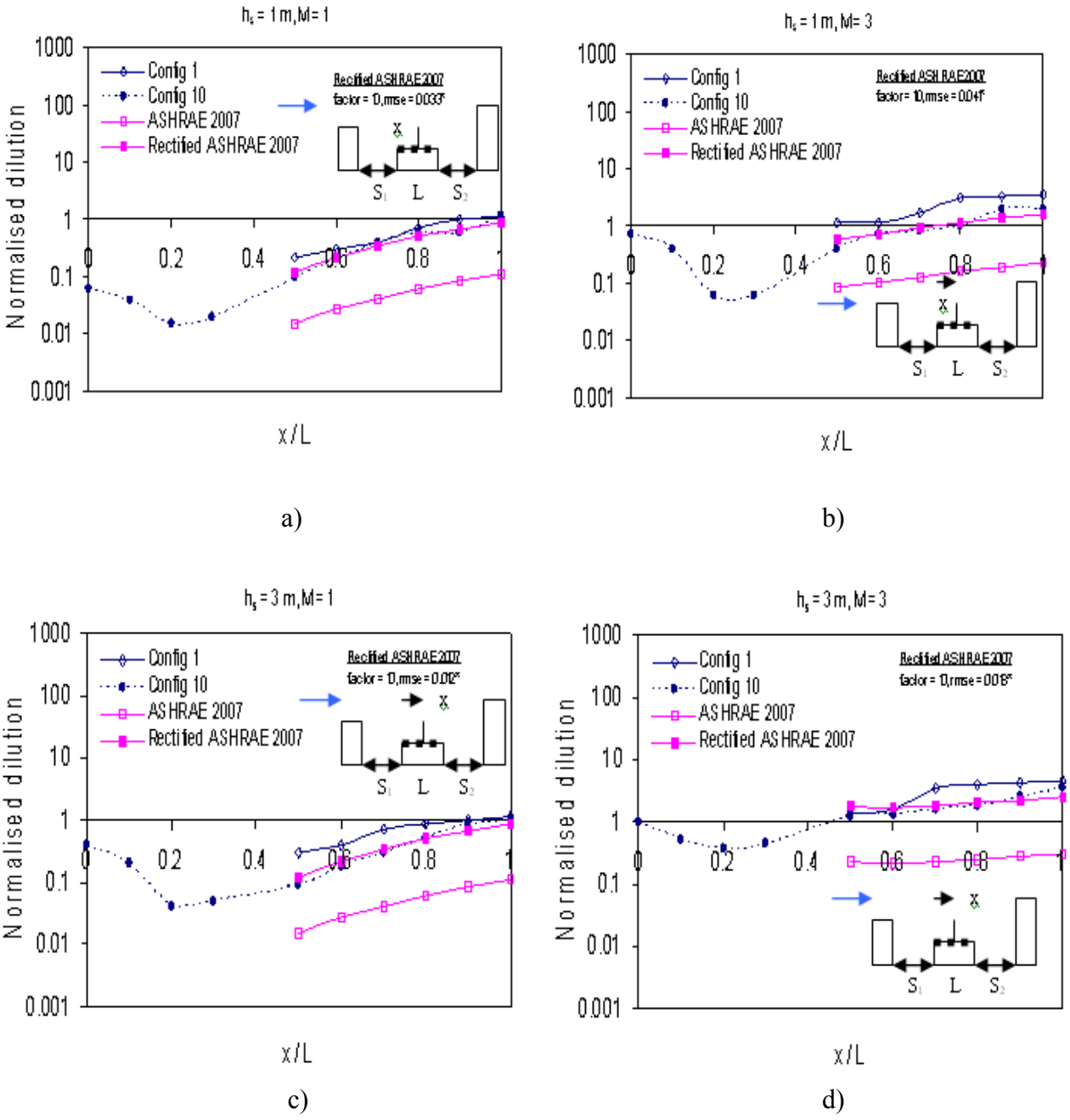


Figure F4. Normalised dilution on rooftop of $B_1$ for $X_s = 0.4L$ and $S_1 = S_2 = 0.4L$: a) $h_s$ = 1 m, M = 1; b) $h_s$ = 1 m, M = 3; c) $h_s$ = 3 m, M = 1; d) $h_s$ = 3 m, M = 3 (*rmse was evaluated using the wind tunnel data and rectified ASHRAE, only for receptors downwind of stack (6 receptor))

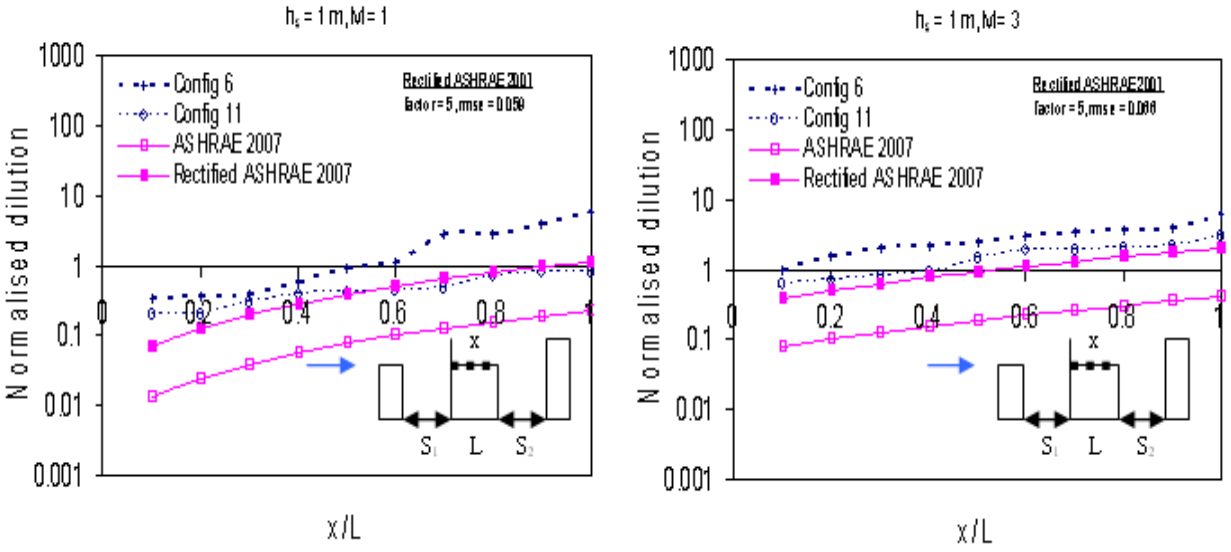


a) b)

Figure F5. Normalised dilution on rooftop of $B_6$ for $X_s = 0$ and $S_1 = S_2 = 0.4L$: a) M = 1; b) M = 3

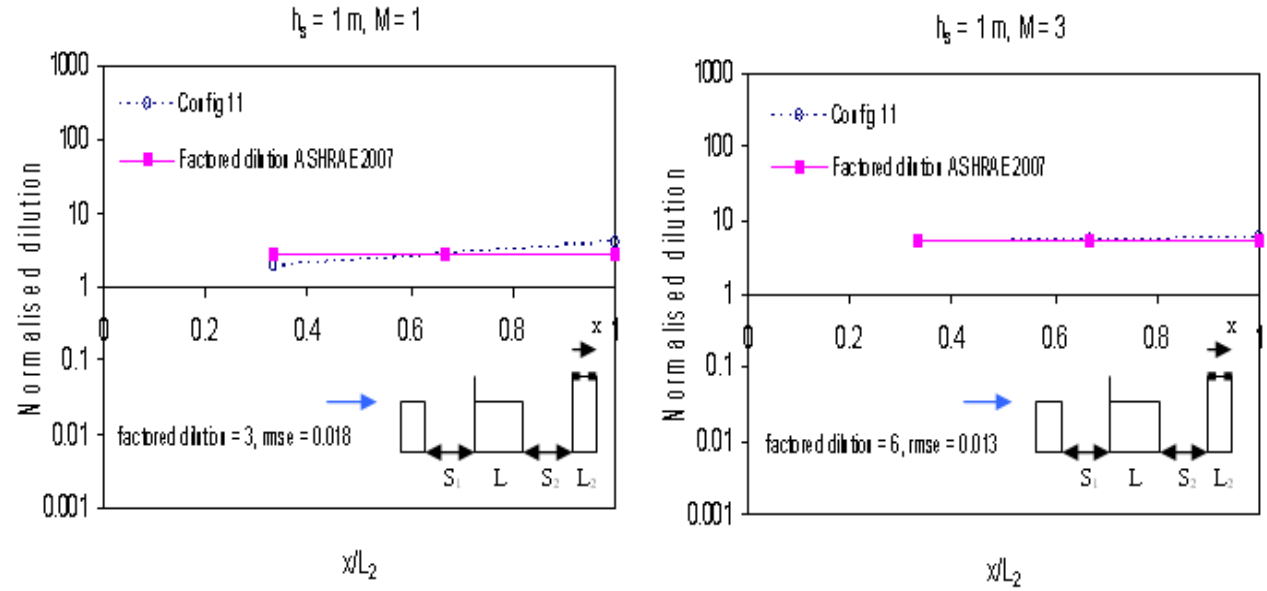


a) b)

Figure F6. Normalised dilution on rooftop of $B_5$ for $X_s = 0$ and $S_1 = S_2 = 0.4L$: a) M = 1; b) M = 3

Application to previous studies

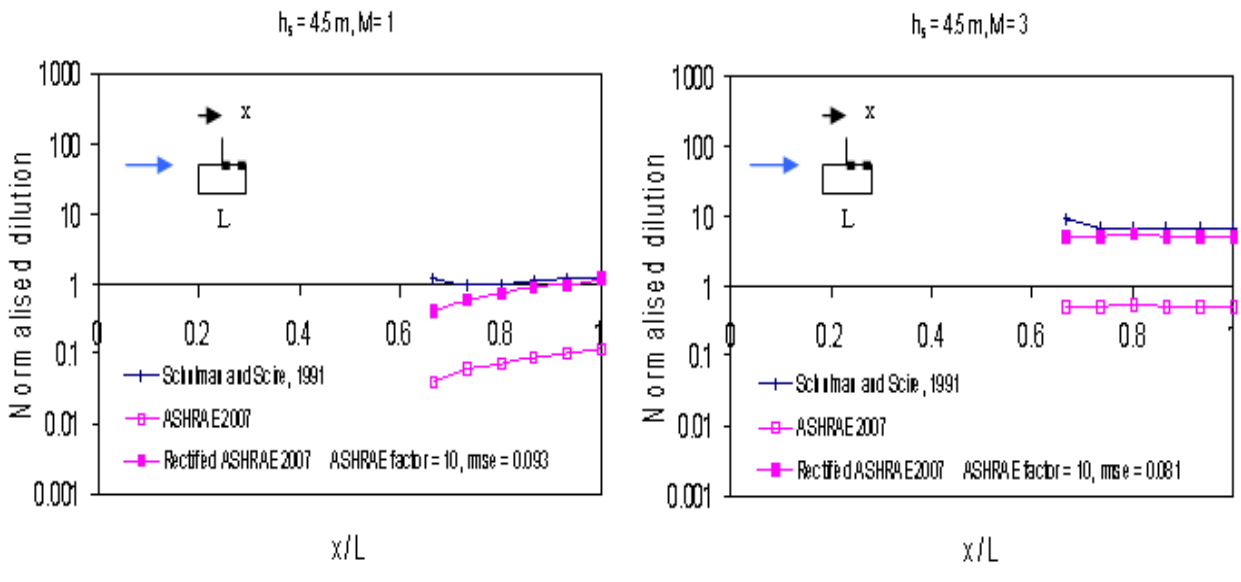


Figure F7 Rectified ASHRAE model applied to the wind tunnel data from Schulman and Scire, 1991 for the flat roofed low-rise building for $X_s$ = 0.6L: a) M = 1; b) M = 3

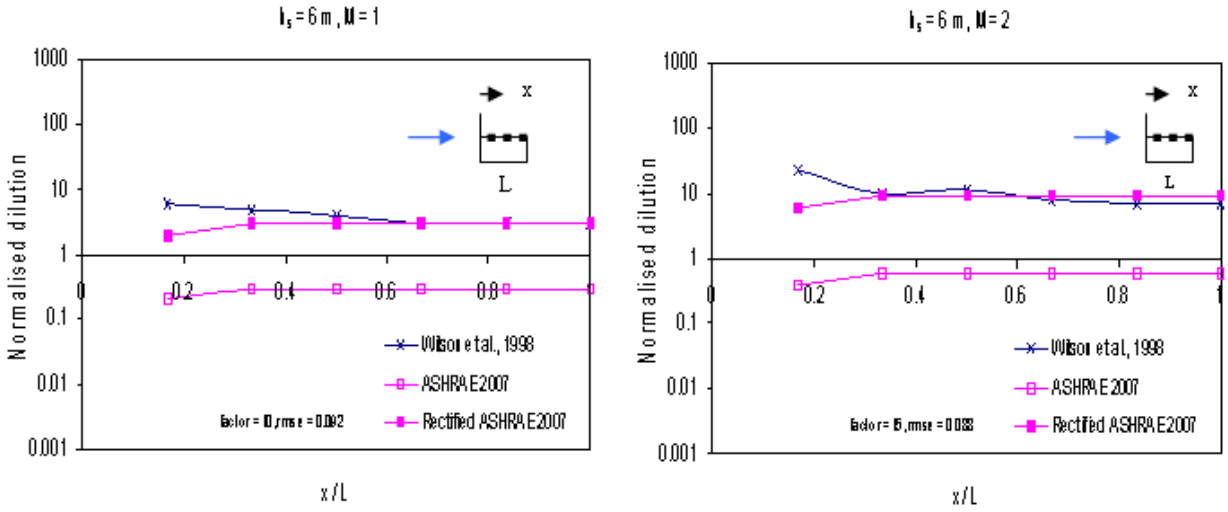


Figure F8 Validation with wind tunnel data from Wilson et al., 1998 for the flat roofed low-rise building for $X_s$ = 0: a) M = 1; b) M = 2

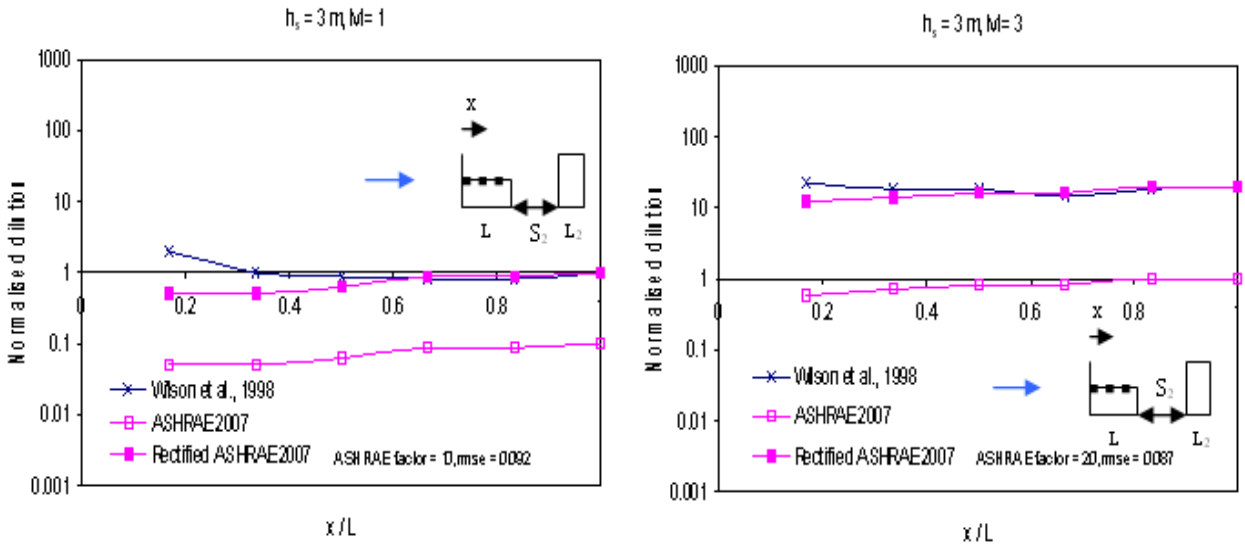


a) b)

Figure F9 Validation with wind tunnel data from Wilson et al., 1998 for the flat roofed low-rise emitting building for $X_s = 0$: a) M = 1; b) M = 3

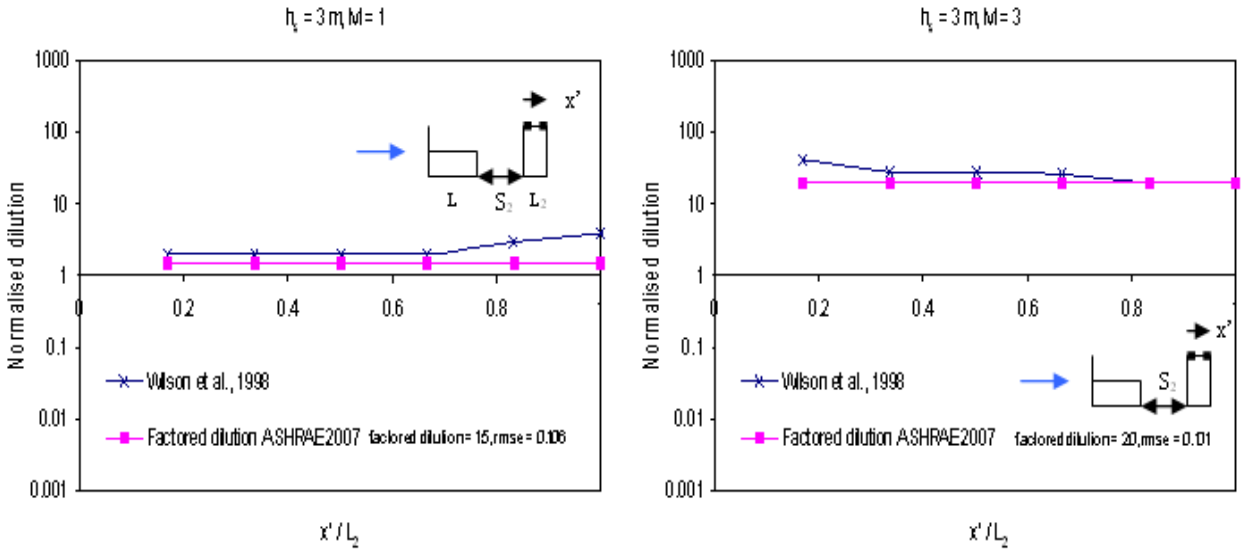


a) b)

Figure F10 Validation with wind tunnel data from Wilson et al., 1998 for the flat roofed low-rise downstream building for $X_s = 0$: a) M = 1; b) M = 3